frontiers | Research Topics

Aphids as plant pests: From biology to green control technology

Edited by
Julian Chen, Leonardo Abdiel Crespo Herrera
and Frédéric Francis

Published in
Frontiers in Plant Science
Frontiers in Physiology

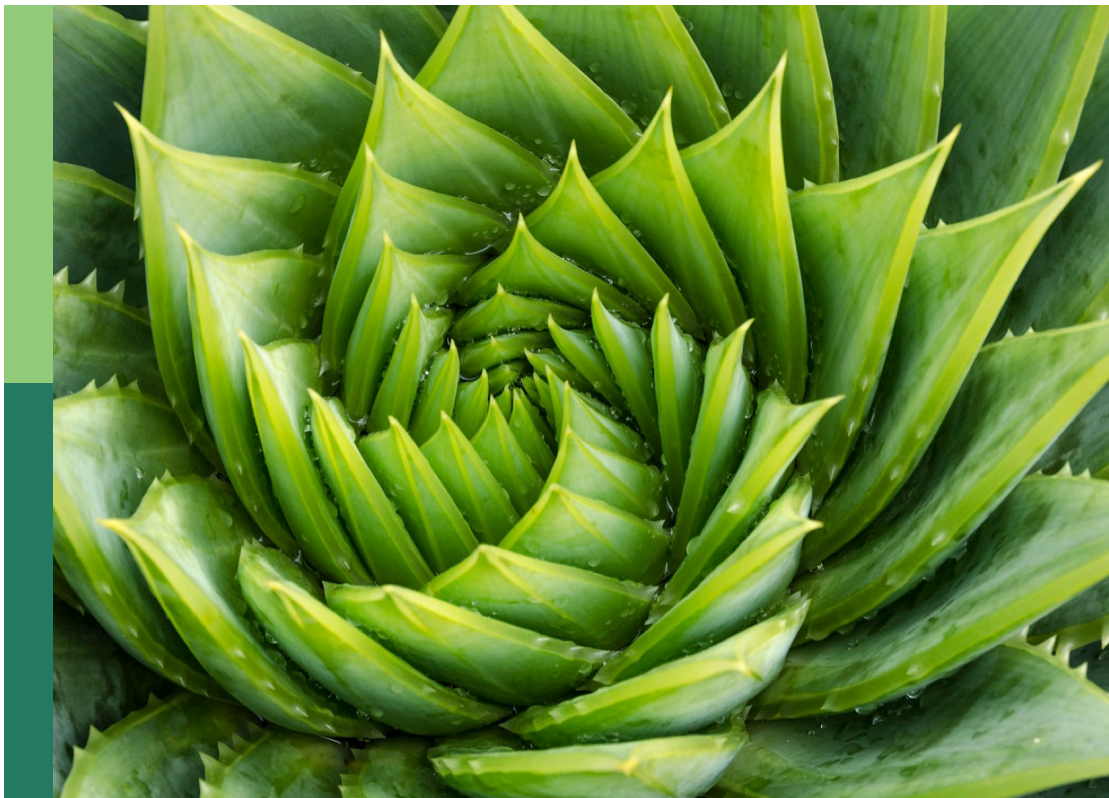

ISSN 1664-8714
ISBN 978-2-8325-4294-1
DOI 10.3389/978-2-8325-4294-1

About Frontiers

Frontiers is more than just an open access publisher of scholarly articles: it is a pioneering approach to the world of academia, radically improving the way scholarly research is managed. The grand vision of Frontiers is a world where all people have an equal opportunity to seek, share and generate knowledge. Frontiers provides immediate and permanent online open access to all its publications, but this alone is not enough to realize our grand goals.

Frontiers journal series

The Frontiers journal series is a multi-tier and interdisciplinary set of open-access, online journals, promising a paradigm shift from the current review, selection and dissemination processes in academic publishing. All Frontiers journals are driven by researchers for researchers; therefore, they constitute a service to the scholarly community. At the same time, the *Frontiers journal series* operates on a revolutionary invention, the tiered publishing system, initially addressing specific communities of scholars, and gradually climbing up to broader public understanding, thus serving the interests of the lay society, too.

Dedication to quality

Each Frontiers article is a landmark of the highest quality, thanks to genuinely collaborative interactions between authors and review editors, who include some of the world's best academicians. Research must be certified by peers before entering a stream of knowledge that may eventually reach the public - and shape society; therefore, Frontiers only applies the most rigorous and unbiased reviews. Frontiers revolutionizes research publishing by freely delivering the most outstanding research, evaluated with no bias from both the academic and social point of view. By applying the most advanced information technologies, Frontiers is catapulting scholarly publishing into a new generation.

What are Frontiers Research Topics?

Frontiers Research Topics are very popular trademarks of the *Frontiers journals series*: they are collections of at least ten articles, all centered on a particular subject. With their unique mix of varied contributions from Original Research to Review Articles, Frontiers Research Topics unify the most influential researchers, the latest key findings and historical advances in a hot research area.

Find out more on how to host your own Frontiers Research Topic or contribute to one as an author by contacting the Frontiers editorial office: frontiersin.org/about/contact

Aphids as plant pests: From biology to green control technology

Topic editors

Julian Chen — Institute of Plant Protection, Chinese Academy of Agricultural Sciences, China

Leonardo Abdiel Crespo Herrera — International Maize and Wheat Improvement Center, Mexico

Frédéric Francis — University of Liège, Belgium

Citation

Chen, J., Herrera, L. A. C., Francis, F., eds. (2024). *Aphids as plant pests: From biology to green control technology*. Lausanne: Frontiers Media SA.

doi: 10.3389/978-2-8325-4294-1

Table of contents

frontiers | Frontiers in Plant Science

TYPE Editorial
PUBLISHED 08 January 2024
DOI 10.3389/fpls.2023.1337558

OPEN ACCESS

EDITED AND REVIEWED BY
Peng Chen,
Anhui University, China

*CORRESPONDENCE
Julian Chen
chenjulian@caas.cn

RECEIVED 13 November 2023
ACCEPTED 13 December 2023
PUBLISHED 08 January 2024

CITATION
Chen J (2024) Editorial: Aphids as plant pests: from biology to green control technology. *Front. Plant Sci.* 14:1337558. doi: 10.3389/fpls.2023.1337558

Editorial: Aphids as plant pests: from biology to green control technology

Julian Chen*

State Key Laboratory for Biology of Plant Diseases and Insect Pests, Institute of Plant Protection, Chinese Academy of Agricultural Sciences, Beijing, China

KEYWORDS

aphid, endosymbiont, natural enemies, plant resistance to aphid, chemical ecology, green control method, IPM (integrated pest management)

Editorial on the Research Topic
Aphids as plant pests: from biology to green control technology

The Research Topic "*Aphids as Plant Pests: From Biology to Green Control Technology*" was edited by Professor Julian Chen from the Institute of Plant Protection, Chinese Academy of Agricultural Sciences; Professor Leonardo A. Crespo-Herrera from International Maize and Wheat Improvement Center (CIMMYT); and Professor Frederic Francis from the University of Liege, as guest editors during 2022 and 2023.

The aim and objective of the Research Topic was to bring together high-quality articles from researchers working on the area of aphids (Hemiptera: Aphidoidea), which are the most important and destructive plant pests. The Research Topic includes material on interactions between aphids and plants, the natural enemies and endosymbionts of aphids. The focus of each of the articles and reviews targets different aspects of the relevant biology and ecology, molecular-level issues, and interactions with agricultural factors, including novel strategies for green control of these insect pests and alternatives to chemical control.

This Research Topic has been produced in collaboration with *Frontiers in Plant Science*. We announced and published the Research Topic on July 14, 2022, and manuscript submissions ended on January 14, 2023. A total of 17 manuscripts were submitted, of which 10 articles were accepted, consisting of one review and nine original research articles. All accepted articles have been published in Open Access form. Additionally, we aim to put together a free Research Topic of all published manuscripts to provide an up-to-date and comprehensive overview of the latest research progress in the field. The main findings on aphids can be summarized under the following categories: from identification to forecasting, and potential global distribution in the context of climate change; the population dynamics of aphid and their symbionts; molecular biology for development, metabolism, and host adaptation; and management techniques, e.g., RNAi, ecological and biological control, and integrated pest management (IPM).

1 From identification to forecasting, and projections of potential distribution

Manual identification and quantitative analysis of trap catches are necessary in classical collection methods. Machine learning, image recognition, and artificial intelligence are useful methods for the identification of food-contaminating beetle species (Wu et al., 2019). Batz et al. proved that such methods could be used for small insect pests: specifically, for systematic monitoring of aphids, automated identification, and intelligent forecasting.

Climate change impacts crop production and the interaction of biotic and abiotic stresses, posing considerable threats to sustainable food security (Wang et al., 2022; Robles-Zazueta et al., 2023). Warming of the climate affects biological invasions by shifting interactions between plants and herbivores (Lu et al., 2013); this highlights the importance of assessments of the effects of climate warming on the population distributions of pests and their natural enemies. Lian et al. analyzed key environmental factors affecting both the survival and the potential distribution of *Lipaphis erysimi*, an important vegetable aphid, and its dominant predatory natural enemy, the hoverfly *Eupeodes corollae*, based on the MaxEnt model and using data on the geographical distribution of historical occurrences. Their data will be beneficial for pest-monitoring and for early warning and biological control systems.

2 Population dynamics of aphids and symbionts

A suction trap is useful method of surveying migration in small insect pests, such as aphids. Wheat aphids, in particular, are migrant pests. Using data from suction traps, Li et al. analyzed the migration patterns of the wheat aphid species *Sitobion miscanthi*, *Rhopalosiphum padi*, and *Schizaphis graminum* in the northern plains of the wheat-growing region of China during the period 2018 to 2020. Aphid migration trajectories changed over the years, as simulated by the NOAA HYSPLIT model. The facultative bacterial symbionts of migrant wheat aphids were investigated with specific PCR and amplicon sequencing. The dominant infection strains (*Serratia symbiotica*, *Hamiltonella defensa*, and *Regiella insercticola*) were identified from *S.miscanthi*, *R. padi*, and the diversity of the bacterial community varied across wheat aphid species and migrant populations.

3 Molecular biology for development, metabolism, and host adaptation

Omics approaches, i.e., transcriptomes, proteomes, secretomes, and so on, are useful methods of understanding insect development, metabolism, and host adaptation.

Taking the horned gall aphid *Schlechtendalia chinensis* as a test target, Wei et al. combined data from morphological observations of male aphids using SEM, high-throughput transcriptome sequencing, and weighted gene co-expression network analysis; they identified gene co-expression modules and hub genes correlated with body size traits and speculated that the male aphid degrades its own substances via autophagy and apoptosis in order to sustain life activities, resulting in body size reduction after molting.

In aphids with piercing–sucking mouth parts, salivary glands and their secretions play an important role in the feeding process. The identification of saliva proteins is an important step in understanding the adaptation of aphids to host plants (Zhang et al., 2017; Zhang et al., 2022; Zhang et al., 2023). Zhang et al. selected *Pseudoregma bambucicola*, a severe bamboo pest, as the target of their analysis; this aphid species feeds on stalks of bamboos by degrading hard bamboo cell walls. Using salivary transcriptome, secretome, and proteome analyses, they detected some secretory proteins homologous to known aphid effectors in *P. bambucicola*. Although plant cell wall-degrading enzymes were identified, most of them were expressed at low levels in the aphid salivary glands. These results imply that symbiotic bacteria of *P. bambucicola* may help the aphid adapt to a specific habitat.

Aphids and their primary symbiont, *Buchnera aphidicola*, form a stable and mutually beneficial relationship that plays an important role in providing the necessary nutrients to the host aphid (Li et al., 2023). Based on the genome sequence of the wheat aphid *Siotobion miscanthi* and its primary symbiont *Buchnera*, which the authors had previously studied, Li et al. identified a metabolic relay gene, ilvA, linking the aphid and *Buchnera* in the isoleucine synthesis pathway, with higher levels of expression observed in the aphid bacteriocytes. This gene is also conserved in different aphid genomes. The function of ilvA is important in aphid development and reproduction, as evaluated through RNAi.

4 Management techniques

4.1 RNAi

RNA interference (RNAi) targeting an insect-specific gene is an important method of evaluating gene function and plays a role in pest management. For aphid gene knockdown, RNAi is usually conducted using molecules of double-stranded RNA (dsRNA) via an artificial diet or plant-mediated expression. Zhang et al. identified and characterized a novel potential RNAi target gene (*SmDSR33*) encoding a salivary protein in grain aphids (*Sitobion miscanthi*). Through plant-mediated RNAi, transgenic wheat lines expressing dsRNA for targeted silencing of *SmDSR33* were developed, and were found to significantly reduce aphids' fecundity, survival, and feeding behavior. *SmDSR33*, an essential salivary protein gene, could be exploited as an effective RNAi target through plant-mediated RNAi for aphid control in wheat.

4.2 Ecological and biological control

Infochemicals are important cues in the interactions of plants, herbivores and their natural enemies. Some herbivore-induced

plant volatiles (HIPVs) are key components in attracting natural enemies, which is also beneficial for the development of techniques for ecological and biological control. Xu et al. examined an orchard ecosystem, including *Vitex negundo* (Lamiaceae), an indigenous plant species in northern China; the cotton aphid *Aphis gossypii*; and the predatory ladybug *Harmonia axyridis*. The candidate active HIPVs mediated by the aphid, including sclareol, eucalyptol, nonanal, and a-terpineol, may attract *H. axyridis*, indicating a potential avenue for improving biological control of aphids in orchards.

Agrosystem biodiversity benefit pest management: based on the natural enemy hypothesis, a complex environment favors natural enemies, e.g., banker plant systems using non-pest arthropod species as alternative prey. In order to select the right banker plants in IPM programs, it is necessary to acquire a deep understanding of the indirect interactions between the target pest and alternative prey, as mediated by biocontrol agents. Wang et al. established and studied a banker plant system, including a banker plant (*Vicia faba*), an alternative prey (*Megoura japonica*), and a predator (*Harmonia axyridis*), to control the target pest (*Myzus persicae*) on pepper. The presence of the alternative prey was able to increase *H. axyridis* population and provide benefits for the targeted aphid control.

4.3 IPM

Integrated pest management (IPM) is an environmentally sustainable approach that involves using a combination of practices and control methods to manage a pest at low cost with minimal use of chemical pesticides. The demonstration of technologies providing effective control is important in the evaluation of pest management systems. Uyi et al. targeted *Melanaphis sorghi*, a serious pest of the sorghum plant in the southern USA, and investigated the effects of host plant resistance (DKS37-07) deploy pesticide application, and biological control of natural enemies on *M. sorghi* in five sorghum production locations in four states in the southeastern USA. The integration of these three components is central to the development of *M. sorghi* management.

Author contributions

JC: Writing – original draft, Writing – review & editing.

Funding

The author(s) declare financial support was received for the research, authorship, and/or publication of this article. This research was supported by National Key R&D Program of China (2023YFD1400800).

Conflict of interest

The author declares that the research was conducted in the absence of any commercial or financial relationships that could be construed as a potential conflict of interest.

Publisher's note

References

Li, Q., Fan, J., Chen, Y., Hou, M., and Chen, J. (2023). ilvE as a potential RNAi target to inhibit amino acid synthesis to control the wheat aphid *Sitobion miscanthi*. *Entomologia Generalis* 43 (1), 177–185.

Lu, X., Siemann, E., Shao, X., Wei, H., and Ding, J. (2013). Climate warming affects biological invasions by shifting interactions of plants and herbivores. *Global Change Biol.* 19, 2339–2347.

Robles-Zazueta, C., Crespo-Herrera, L., Piñera-Chavez, F., Rivera-Amado, C., and Aradottir, G. (2023). Climate change impacts on crop breeding: Targeting interacting biotic and abiotic stresses for wheat improvement. *Plant Genome*, e20365.

Wang, B., Hof, A., and Ma, C. (2022). Impacts of climate change on crop production, pests and pathogens of wheat and rice. *Front. Agr. Sci. Eng.* 9 (1), 4–18.

Wu, L., Liu, Z., Bera, T., Ding, H., Langley, D., Jenkins-Barnes, A., et al. (2019). A deep learning model to recognize food contaminating beetle species based on elytra fragments. *Comput. Electron. Agric.* 166, 105002.

Zhang, Y., Fan, J., Francis, F., and Chen, J. (2017). Watery saliva secreted by the grain aphid, *Sitobion avenae* stimulates aphid resistance in wheat. *J. Agric. Food Chem.* 65 (40), 8798–8805.

Zhang, Y., Fu, Y., Liu, X., Francis, F., Fan, J., Liu, H., et al. (2023). SmCSP4 from aphid saliva stimulates salicylic acid-mediated defence responses in wheat by interacting with transcription factor TaWKRY76. *Plant Biotechnol. J.* 221, 2389–2407.

Zhang, Y., Liu, X., Francis, F., Xie, H., Fan, J., Wang, Q., et al. (2022). The salivary effector protein Sg2204 in the greenbug *Schizaphis graminum* suppresses wheat defense and is essential for enabling aphid feeding on host plants. *Plant Biotechnol. J.* 20, 2187–2201.

frontiers | Frontiers in Plant Science

TYPE Original Research
PUBLISHED 15 September 2022
DOI 10.3389/fpls.2022.1006225

OPEN ACCESS

EDITED BY
Julian Chen,
Institute of Plant Protection (CAAS), China

REVIEWED BY
Faten Momen,
National Research Centre, Egypt
Xiang-Shun Hu,
Northwest A&F University, China

*CORRESPONDENCE
Osariyekemwen Uyi
osariyekemwen.uyi@uniben.edu

SPECIALTY SECTION
This article was submitted to Sustainable and Intelligent Phytoprotection, a section of the journal Frontiers in Plant Science

RECEIVED 29 July 2022
ACCEPTED 19 August 2022
PUBLISHED 15 September 2022

CITATION
Uyi O, Lahiri S, Ni X, Buntin D, Jacobson A, Reay-Jones FPF, Punnuri S, Huseth AS and Toews MD (2022) Host plant resistance, foliar insecticide application and natural enemies play a role in the management of *Melanaphis sorghi* (Hemiptera: Aphididae) in grain sorghum.
Front. Plant Sci. 13:1006225.
doi: 10.3389/fpls.2022.1006225

Host plant resistance, foliar insecticide application and natural enemies play a role in the management of *Melanaphis sorghi* (Hemiptera: Aphididae) in grain sorghum

Osariyekemwen Uyi[1,2]*, Sriyanka Lahiri[3], Xinzhi Ni[4], David Buntin[5], Alana Jacobson[6], Francis P. F. Reay-Jones[7], Somashekhar Punnuri[8], Anders S. Huseth[9] and Michael D. Toews[1]

[1]Department of Entomology, University of Georgia, Tifton, GA, United States, [2]Department of Zoology and Entomology, Faculty of Natural and Agricultural Sciences, University of the Free State, Bloemfontein, South Africa, [3]Department of Entomology, Gulf Coast Research and Education Center, University of Florida, Wimauma, FL, United States, [4]Crop Genetics and Breeding Research Unit, USDA-ARS, Tifton, GA, United States, [5]Department of Entomology, University of Georgia, Griffin, GA, United States, [6]Department of Entomology and Plant Pathology, Auburn University, Auburn, AL, United States, [7]Department of Plant and Environmental Sciences, Clemson University, Pee Dee Research and Education Center, Florence, SC, United States, [8]College of Agriculture, Family Sciences and Technology, Fort Valley State University, Fort Valley, GA, United States, [9]Department of Entomology and Plant Pathology, North Carolina State University, Raleigh, NC, United States

The invasive *Melanaphis sorghi* (Theobald; =*Melanaphis sacchari* Zehntner) is a serious pest of sorghum production in the southern USA. Demonstration of technologies that provide effective control is key to management of this pest. Here, we investigated the effect of host plant resistance (resistant cultivar: DKS37-07 and susceptible cultivar: DKS53-53) and a single foliar insecticide (flupyradifurone: Sivanto Prime) application on *M. sorghi* infestations and the role of natural enemy populations in grain sorghum production across five locations in four states in southeastern USA. Foliar insecticide application significantly suppressed *M. sorghi* infestations on both the resistant and susceptible sorghum cultivars across all locations. Planting the host plant resistant cultivar (DKS37-07) significantly reduced aphid infestation across all locations. Plant damage ratings did not vary widely, but there was generally a positive association between aphid counts and observed plant damage, suggesting that increasing aphid numbers resulted in corresponding increase in plant damage. Planting a host plant resistant cultivar and foliar insecticide application generally preserved grain yield. Both sorghum hybrids supported an array of different life stages of natural enemies (predators [lady beetle larvae and adults; hoverfly larvae and lacewing larvae] and parasitoids [a braconid and aphelinid]) for both the sprayed and non-sprayed treatments. We found a strong and significant positive relationship between the natural enemies and the *M. sorghi* infestation. Results suggest that planting a host plant resistant

cultivar and the integration of natural enemies with insecticide control methods in the management of *M. sorghi* is central to the development of an effective pest management strategy against this invasive pest.

KEYWORDS

invasive species, aphid, insect pest management, insecticide application, natural enemy

Introduction

Melanaphis sorghi (Theobald) which was until recently known as *Melanaphis sacchari* Zehntner in previous literature (Nibouche et al., 2021), is an invasive multivoltine piercing and sucking pest of sugarcane, *Saccharum officinarum* (L.), and sorghum, *Sorghum bicolor* (L.) in Asia, Africa, Oceania, Central, South and North America (Sharma and Nwanze, 1997; Singh et al., 2004). *Melanaphis sorgi* was first detected on the Florida peninsula on the southeastern coast of the United States in 1977 and consequently only achieved a minor pest status in sugarcane production (Denmark, 1988; Mondor et al., 2006). Following the detection of a new haplotype of *M. sorghi* in Texas and Louisiana in 2013 (Harris-Shultz et al., 2017; Medina et al., 2017; Nibouche et al., 2018), the pest became a significant economic pest of sorghum (Bowling et al., 2016) and has since spread to 25 states in the southern United States, thus infesting all sorghum-production regions (Peterson et al., 2018; EDDMapS, 2020). As of the time, this aphid was originally misidentified as the sugarcane aphid, *Melanaphis sacchari*, until a recent study (Nibouche et al., 2021) based on morphological and molecular evidence revised its name to *M. sorghi*.

The rapid invasion success of *M. sorghi* may be partly due to its narrow host range (Armstrong et al., 2015;Haar et al., 2019; Harris-Shultz and Ni, 2021), capacity for dispersal (Bowling et al., 2016) and its potential to occupy a wide range of climatic conditions and ecosystems (Singh et al., 2004; Bowling et al., 2016; Souza and Davis, 2020), including disturbed ecosystems and agroecosystems where the preferred hosts are abundant (Singh et al., 2004; Bowling et al., 2016; Haar et al., 2019; Gordy et al., 2021; Harris-Shultz and Ni, 2021). *Melanaphis sorghi* can survive low temperatures (around 0°C) but does not undergo diapause, nor sexual reproduction in the United States (Bowling et al., 2016; Michaud et al., 2016). Populations overwinter on Johnson grass, *Sorghum halepense* (L.) and giant miscanthus, *Miscanthus sinensis* × *Miscanthus sacchariflorus* Greef & Deuter ex Hodkinson & Renvoize, in southern Alabama and Georgia (Haar et al., 2019; Harris-Shultz and Ni, 2021). Hot and dry weather conditions promote rapid population increases (Bowling et al., 2016) and hot weather events may further reduce the current doubling time of 4–13 days (Singh et al., 2004; Bayoumy et al., 2016; Brewer et al., 2017; Gordy et al., 2021). This may consequently lead to range expansion and rapid population increases that can limit grain yield in susceptible sorghum varieties and other economically important host crops.

In many states in southern United States, *M. sorghi* has become an important economic pest, causing significant yield loss in grain sorghum (Bowling et al., 2016; Peña-Martinez et al., 2016; Brewer et al., 2017; Szczepaniec, 2018; Lahiri et al., 2021), which translates into severe economic losses for farmers (Bowling et al., 2016). For example, the Louisiana sorghum industry suffered losses of approximately $7.7 million in 2013 due to *M. sorghi* (Kerns et al., 2015), while Georgia growers decreased the area planted to grain sorghum by nearly 60% from 2015 to 2017 due to severe infestations (Bostick et al., 2020). In Texas, annual economy-wide losses totaled $169.83 million in economic output including a direct loss of $78.57 million to farms and farm related industries (Zapata et al., 2018). At high densities, feeding by nymphs and adults of *M. sorghi* cause physiological stress in grain sorghum which causes chlorosis, leaf wilt and necrosis (Singh et al., 2004; Bowling et al., 2016). Feeding by *M. sorghi* also results in the production of copious amounts of honeydew, which promotes the growth of sooty mold on leaves, impeding photosynthesis of affected sorghum plants (Singh et al., 2004; Bowling et al., 2016). Further, sooty mold accumulation can clog grain sorghum harvest equipment (Singh et al., 2004; Bowling et al., 2016). Damage caused by *M. sorghi* decreases or stops grain sorghum growth, reducing crop yield by more than 50% and can kill susceptible grain sorghum plants (Bowling et al., 2016; Brewer et al., 2017; Gordy et al., 2019; Haar et al., 2019; Wilson et al., 2020; Lahiri et al., 2021).

Recent efforts focused on the development of economic thresholds (ET) as an integral tool to limit *M. sorghi* population growth provide decision support on insecticide timing within the framework of integrated pest management (IPM; Knutson et al., 2016; Gordy et al., 2019). Gordy et al. (2019) identified a range of 19–132 aphids per leaf as estimated ETs and suggested that a 40 aphid per leaf threshold across the range of cultivar., environmental, and market conditions in their study, however, this threshold needs revision for use on resistant sorghum cultivars. Previous studies demonstrate that knowledge of economic thresholds coupled with the use of aphid resistant sorghum varieties, insecticidal seed treatments, in-furrow or foliar insecticide sprays coupled with manipulation of planting date and nitrogen levels provide the basis for a comprehensive IPM

program to manage *M. sorghi* in grain sorghum (Sharma et al., 2013; Armstrong et al., 2015; Etheridge et al., 2018; Szczepaniec, 2018; Haar et al., 2019; Paudyal et al., 2019; Seiter et al., 2019; Wilson et al., 2020; Lahiri et al., 2021; Lytle and Huseth, 2021; Pekarcik and Jacobson, 2021). Further evaluation of factors including insecticide application and host plant resistance influencing *M. sorghi* infestations and resulting yield losses is necessary to improve IPM strategies. The use of resistant cultivars provides a baseline of protection against *M. sorghi* by suppressing population growth rates, limiting injury and improving grain yield, however, the performance of these varieties is geographically variable (Lahiri et al., 2021; Pekarcik and Jacobson, 2021). Application of foliar insecticides such as flupyradifurone (Sivanto Prime, Bayer CropScience, Research Triangle Park, NC, United States) clearly suppress *M. sorghi* populations (Lahiri et al., 2021; Pekarcik and Jacobson, 2021), but the efficacy of foliar application may vary by weather conditions or geographic locations (Lahiri et al., 2021). Hence, continuous studies on the influence of host plant resistance and foliar insecticide application across locations are needed. These studies could potentially show how to improve the efficacy of natural enemies of *M. sorghi* in the management of this pest.

Knowledge of the non-target impacts of insecticides used for *M. sorghi* can enable growers to make informed decisions about insecticide selection that decrease aphid infestation while preserving the abundance and activities of natural enemies. Several studies have recorded a multiplicity of predators and parasitoids in sorghum production systems in southern United States suggesting that natural enemies may play a role in suppressing *M. sorghi* population, especially at low densities (Singh et al., 2004; Hewlett et al., 2019; Maxson et al., 2019; Lytle and Huseth, 2021). Despite the fact that previous studies documented more than 47 arthropod species feeding on *M. sorghi* (Singh et al., 2004; Lytle and Huseth, 2021), not much is known about the role of natural enemies on *M. sorghi* in grain sorghum systems in the southeastern USA due to prolific aphid reproduction rate, and low natural enemies in the sorghum field at the initial aphid infestation (but see Lytle and Huseth, 2021). Understanding the role of insect natural enemies in grain sorghum systems that incorporate foliar insecticide sprays and host plant resistance across multiple locations in the United States is crucial to refining our IPM strategies in managing this pest. The objective of this study was to investigate the efficacy of combining host plant resistance and foliar insecticidal application using two commercial grain sorghum cultivars (susceptible cultivar: DKS53-53 and resistant cultivar: DKS37-07) across five locations, in four southeastern states in the United States. A second objective of this study was to determine if predators and parasitoids play some role in managing *M. sorghi* populations in grain sorghum systems that combine host plant resistance and foliar insecticide application within the context of IPM.

Materials and methods

Study locations and agronomic practices

Between April and August 2018, large plot field experiments utilizing grain sorghum were conducted at Tift Co., Georgia (31.5120° N, −83.6434° W), Pike Co., Georgia (33.1779° N, −84.4090° W), Moore Co., NC (35.1840° N, −79.6779° W), Barbour Co., Alabama (32.4224° N, −85.8907° W), and Darlington Co., South Carolina (34.3650° N, −80.0088° W). At each trial location, cooperators followed state Cooperative Extension recommended agronomic practices to achieve a 5,406 kg/ha yield goal. After spreading the recommended amounts of dry fertilizer, the fertilizer was incorporated using a field cultivator and then seedbed preparation was accomplished with a one-pass ripper bedder with the subsoil shank set to a depth of 50.8 cm for breaking the hardpan under the rows. A total of eight adjacent plots (11 m by 30.5 m per plot) were delineated and planted using a vacuum planter in early to mid-May. Plots were laid out on 0.9 m row centers at a planting density of 247,105 seeds per ha and a depth of 3.8-cm. A total of four plots received an *M. sorghi* susceptible grain sorghum cultivar., DKS53-53 (DeKalb®, Monsanto Company, St. Louis, MO, United States), while the remaining four plots received an *M. sorghi* resistant cultivar., DKS37-07. Sorghum seeds were treated with fluxofenin (Concep III, Syngenta Crop Protection, Greensboro, NC) to permit application of S-metolachlor (Dual Magnum, Syngenta Crop Protection) at 1.17 L/ha behind the planter for enhanced weed control. One month after planting, all plots received atrazine (AAtrex 4l, Syngenta Crop Protection) at 2.63 L/ha to provide additional weed suppression.

Insecticide treatment

Mean number of *M. sorghi* across all plots were summarized weekly. When the aphid population across the entire trial reached 50 aphids per bottom leaf, a rescue insecticide treatment was initiated in two plots planted with resistant cultivar and two plots planted with susceptible cultivar. Those plots received a one-time application of flupyradifurone (Sivanto Prime, Bayer CropScience, Rhein, Germany) at 0.36 L/ha, administered using a self-propelled sprayer equipped with hollow cone nozzles (model TXVS-8, TeeJet Technologies, Spraying Systems Co., Glendale Heights, IL). Applications were delivered in a spray volume of 93.5 L/ha.

Insect sampling and plant health assessment

Melanaphis sorghi abundance and plant condition were assessed weekly. Weekly assessments started 4 weeks after planting and continued until the grain reached the hard dough stage in mid-August of 2018 at all locations for up to 8 weeks. *Melanaphis*

sorghi (regardless of age) and natural enemies were sampled from a single lower and upper leaf from six randomly selected plants per plot. To avoid edge effects, plants were sampled from the center two rows. All nymphs, alate, and apterous adult aphids were aggregated into a single count per leaf. Exact aphid numbers were counted when the density was below 50, and when densities were above 50, the number of aphids were estimated. We recorded the presence and number of beneficial insects spanning 11 taxa that are known predators of *M. sorghi* (Singh et al., 2004; Bowling et al., 2016; Lytle and Huseth, 2021). We identified parasitoid wasps [*Lysiphlebus testaceipes* (Cresson; Hymenoptera: Braconidae) and *Aphelinus* sp. (Hymenoptera: Aphelinidae)] by characterizing aphid mummies.

To simultaneously account for aphid abundance and duration of infestations, aphid counts were converted to cumulative insect days (CID) on a per plot basis following the methods of Ruppel (1983). Briefly, aphid days were calculated for each sampling interval as the mean density of two consecutive sample dates multiplied by the length of the interval between the dates in days. These values accumulated over the entire sampling period in each year, providing a cumulative estimate of aphid infestation intensity for each plot. On a per plot basis, plant condition (or aphid damage) of six randomly selected plants was characterized on a scale of 1–9 following the methods of Sharma et al. (2013). Briefly, this scale provides a standardized method to describe *M. sorghi* infestations based on the number of leaves showing damage symptoms and honeydew/sooty mold accumulation.

Harvest

When the grain dried in the field to a moisture content of 15% or less, the center two rows from each plot were harvested using a self-propelled combine. Depending on location, harvest generally commenced in late August to early October. Grain yield in each location and moisture content were measured on the combine. For comparison purposes, all plots were adjusted to a common 14% moisture content and extrapolated to kg of grain per ha.

Data analysis

At each location, experiments were organized in a factorial arrangement of treatments nested in a randomized complete block design. Treatments were cultivar (DKS53-53 vs. DKS37-07) and insecticide application (sprayed vs. unsprayed). The experimental unit receiving treatments (cultivar and insecticide treatment) was an individual grain sorghum plot measuring 11 m by 30.5 m. Responses averaged across individual plots included aphid counts per leaf, cumulative insect days (CID)—an index of crop protection which simultaneously account for the severity and duration of aphid infestation as described by Ruppel (1983), counts of natural enemies on each of 6 random plants per plot, and plant damage estimates. Plant damage ratings at Barbour Co. were not recorded. Following square root transformation of CID and damage rating data, the effects of sorghum hybrids and foliar insecticide application on CID and damage rating was analyzed using a Generalized Linear Model (GLZ; assuming normal distribution with an identity link function). When the overall results were significant in the GLZ analysis, the difference among the treatments was compared using the sequential Bonferroni test. The effect of sorghum cultivar (DKS37-07 vs. DKS53-53) and insecticide application on sorghum yield was evaluated using univariate General Linear Model analysis of variance (GLM ANOVA). When the overall results were significant in a two-way analysis, the differences among the treatments were compared using the Tukey's Honest Significant Difference (HSD) test. We pooled yield data across all four locations and analyzed the overall effect of cultivar and insecticide treatment on grain sorghum yield, using GLM ANOVA. Regression analysis between number of *M. sorghi* and plant damage rating was only performed for the sprayed and non-sprayed susceptible sorghum cultivar (DKS53-53), because *M. sorghi* numbers and damage rating on the resistant hybrid was very low. Natural enemy counts were mostly zeros across locations, hence we pooled the data across all study locations and represented it as pie charts according to sorghum cultivar and insecticide application. Irrespective of sorghum cultivar and insecticide application, we combined all-natural enemy data (extremely very low) and performed regression analysis on the relationship between the number of *M. sorghi* and natural enemy's abundance. Except for the regression analyses that were performed using Microsoft Excel and GENSTAT 9.0 (VSN International, Hemel Hempstead, United Kingdom), all other analyses were performed using IBM SPSS Statistical software version 20.0 (SPSS, Chicago, IL, United States).

Results

Cumulative insect days

Melanaphis sorghi infestation as indicated by CID was significantly influenced by sorghum cultivar and foliar insecticide application across study locations. Specifically, there were differences at Tift Co., GA (sorghum cultivar: $\chi^2 = 228.35$, $p = 0.001$; insecticide application: $\chi^2 = 220.86$, $p = 0.001$; interaction: $\chi^2 = 95.72$, $p = 0.001$), Pike Co., GA (sorghum cultivar: $\chi^2 = 12.59$, $p = 0.001$; insecticide application: $\chi^2 = 470.31$, $p = 0.001$; interaction: $\chi^2 = 6.82$, $p = 0.009$) and Moore Co., NC (sorghum hybrid: $\chi^2 = 28.75$, $p = 0.001$; insecticide application: $\chi^2 = 131.22$, $p < 0.001$; interaction: $\chi^2 = 38.44$, $p = 0.001$; Figures 1A–C). In Tift Co., *M. sorghi* infestation was 2-fold and 3-fold higher for non-sprayed (relative to sprayed) resistant cultivar (DKS37-07) and susceptible cultivar (DKS53-53), respectively (Figure 1A). In Pike Co., CID values was 20- and 13-fold higher for non-sprayed (relative to sprayed) resistant cultivar (DKS37-07) and susceptible cultivar (DKS53-53), respectively (Figure 1B). At Moore Co., CID was 2- and 10-fold higher for non-sprayed resistant cultivar (DKS37-07) and susceptible cultivar (DKS53-53), respectively (Figure 1C).

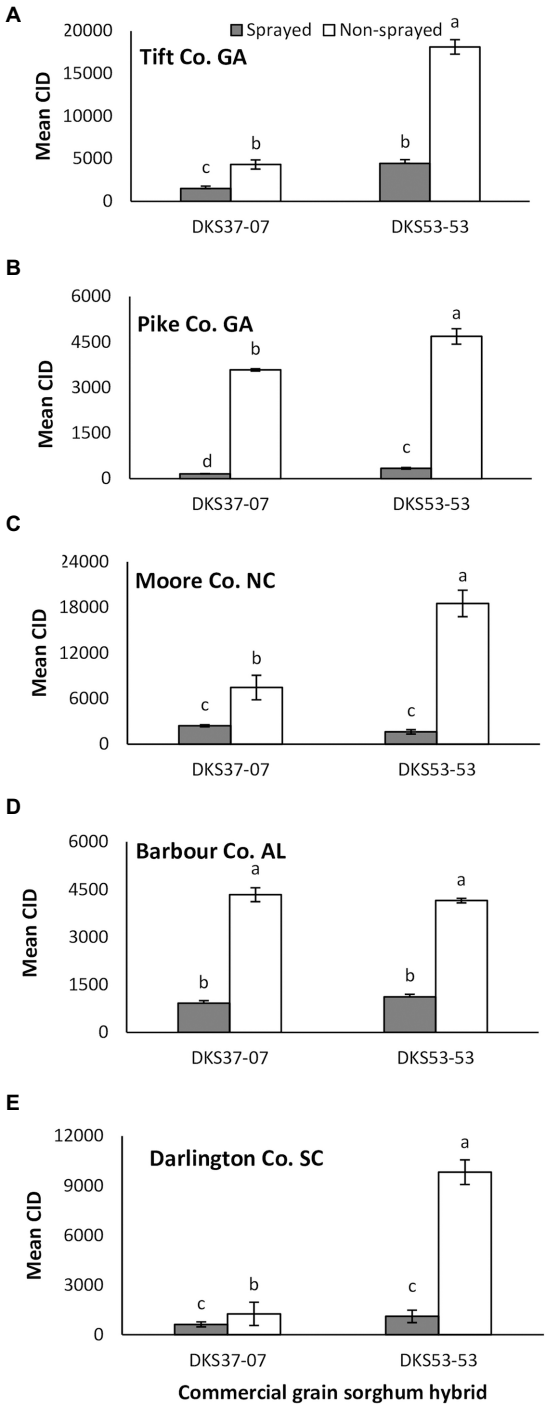

FIGURE 1
Mean (±SE) cumulative insect days (CID) in flupyradifurone sprayed and non-sprayed grain sorghum cultivars planted at Tift and Pike Co. GA, Moore Co. NC, Barbour Co. AL and Darlington Co., SC in 2018. Means capped with different letters are significantly different (sequential Bonferroni test, $p<0.05$) among all four treatments. Note that y-axis scales are different on each figure.

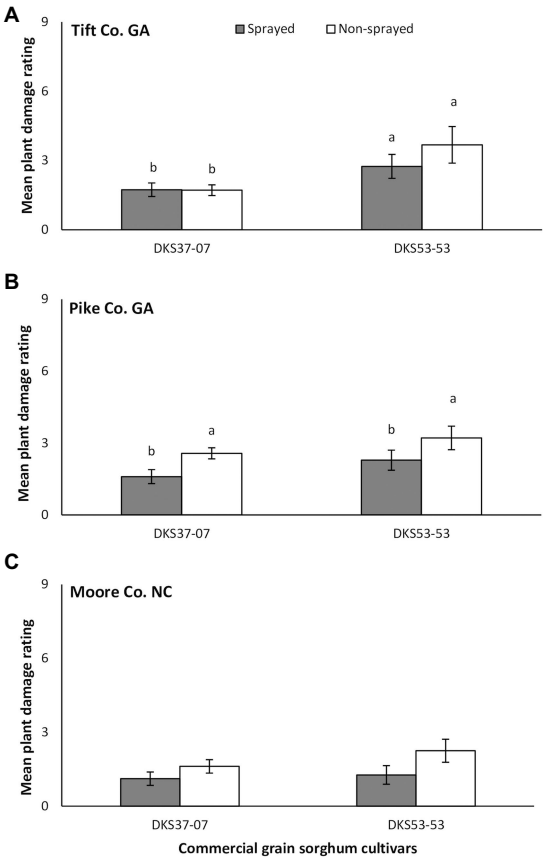

FIGURE 2
Mean (±SE) plant damage rating in flupyradifurone sprayed and non-sprayed grain sorghum cultivars planted at Tift and Pike Co. GA and Moore Co. NC. Means capped with different letters are significantly different (sequential Bonferroni test, $p<0.05$) among all four treatments.

Irrespective of foliar insecticide application, the resistant cultivar (DKS37-07) significantly reduced *M. sorghi* infestation compared to the susceptible cultivar (DK53-53) in Tift, Pike, and Moore Counties (Figures 1A–C). Cumulative insect days was not significantly influenced by sorghum cultivar but differed according to foliar insecticide application in Barbour Co., AL (sorghum cultivar: $\chi^2 = 0.002$, $p = 0.965$; insecticide application: $\chi^2 = 169.62$, $p = 0.001$; interaction: $\chi^2 = 0.626$, $p = 0.429$; Figure 1D); where CID was higher on non-sprayed plots for both sorghum cultivars. Finally, CID was significantly higher in non-sprayed sorghum plots and on susceptible sorghum cultivar in Darlington Co., SC (sorghum cultivar: $\chi^2 = 57.32$, $p = 0.001$; insecticide application: $\chi^2 = 142.86$, $p = 0.001$; interaction: $\chi^2 = 12.042$, $p = 0.001$; Figure 1E).

Plant damage rating

In Tift Co., a significant difference in plant damage rating was detected between sorghum hybrids and there was always more damage to the susceptible cultivar compared to the resistant cultivar ($\chi^2 = 9.05$, $p = 0.003$), but damage did not differ as a function of foliar insecticide application ($\chi^2 = 0.853$, $p = 0.356$; Figure 2A). There was no significant interaction between sorghum cultivar and insecticide

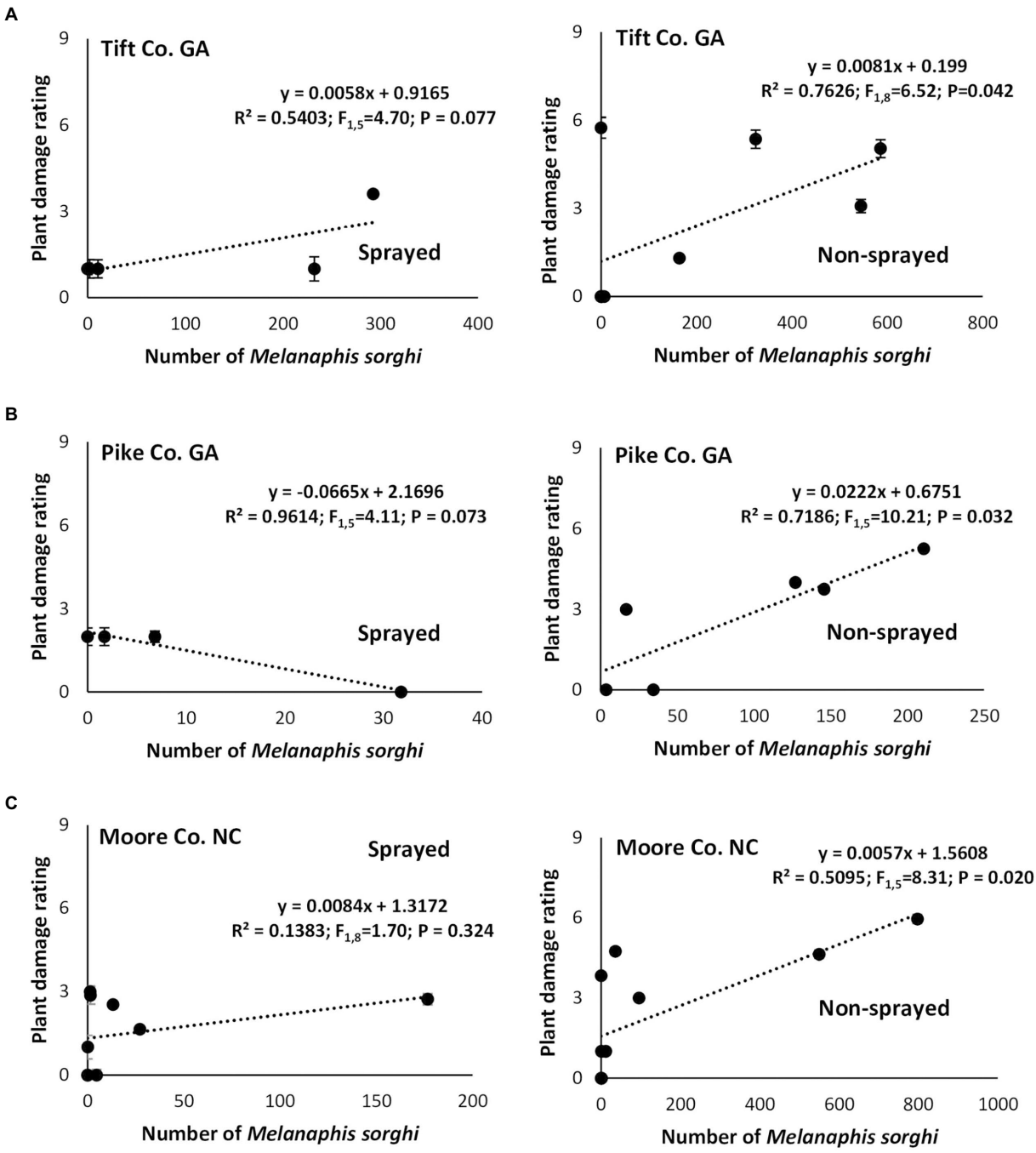

FIGURE 3
Relationship between mean weekly *Melanaphis sorghi* counts and corresponding plant damage rating in flupyradifurone sprayed and non-sprayed susceptible sorghum cultivar (DKS53-53) at Tift Co. **(A)**, Pike Co. GA **(B)**, and Moore Co. NC **(C)** in 2018.

application ($\chi^2 = 0.924$, $p = 0.336$). Plant damage rating did not vary as a function of sorghum cultivar ($\chi^2 = 1.882$, $p = 0.170$) but was greater on the non-sprayed (compare to sprayed) susceptible and resistant sorghum cultivars ($\chi^2 = 3.850$, $p = 0.05$) in Pike Co. (Figure 2B). There was no significant interaction between sorghum cultivar and insecticide application ($\chi^2 = 0.002$, $p = 0.965$). In Moore Co., there was no significant effect of sorghum cultivar ($\chi^2 = 0.384$, $p = 0.536$), foliar insecticide application ($\chi^2 = 2.676$, $p = 0.102$) or interaction between sorghum cultivar and insecticide application ($\chi^2 = 0.763$, $p = 0.382$) on plant damage rating (Figure 2C).

In Tift Co., irrespective of foliar insecticide application, linear regression analysis showed positive relationships between the number of *M. sorghi* and the resulting plant damage ratings, however, only the non-sprayed treatment showed a significant association (Figure 3A). In Pike Co., a non-significant negative relationship between the number of *M. sorghi* and plant damage

rating was evident on the sprayed susceptible sorghum cultivar while the non-sprayed susceptible sorghum cultivar had a significant strong linear relationship between the number of *M. sorghi* and plant damage rating (Figure 3B). Finally, in Moore Co., a non-significant weak relationship between the number of *M. sorghi* and plant damage rating was evident in the sprayed susceptible sorghum cultivar while the non-sprayed susceptible sorghum cultivar had a significant positive linear relationship between the number of *M. sorghi* and plant damage rating (Figure 3C).

Sorghum yield

Overall, grain sorghum yield was not significantly influenced by sorghum cultivar and foliar insecticide application when data from all four locations where pooled (cultivar: $F_{1,61} = 1.31$; $p = 0.257$; insecticide application: $F_{1,61} = 3.38$; $p = 0.071$; interaction: $F_{1,61} = 0.68$; $p = 0.415$), however, differences were detected in individual locations. In Tift Co., the resistant cultivar out yielded the susceptible cultivar ($F_{1,20} = 581.60$; $p = 0.001$), but did not differ as a function of foliar insecticide application ($F_{1,20} = 0.616$, $p = 0.442$; Figure 4A). There was no significant interaction between sorghum cultivar and insecticide application ($F_{1,20} = 0.624$, $p = 0.446$). Sorghum yield did not vary as a function of sorghum cultivar ($F_{1,4} = 3.73$, $p = 0.126$) but was significantly influenced by foliar insecticide application ($F_{1,4} = 27.48$, $p = 0.006$); with the sprayed treatment demonstrating evidently higher yield compared to non-sprayed for both sorghum cultivars in Pike Co. (Figure 4B). There was no significant interaction between sorghum hybrid and insecticide application nor the interaction of both factors ($F_{1,4} = 1.12$, $p = 0.352$). In Moore Co., there was a significant effect of sorghum cultivar ($F_{1,20} = 10.37$, $p = 0.004$) on sorghum yield with the susceptible hybrid producing higher yield compared to the resistant hybrid (Figure 4C). There was no effect of foliar insecticide application ($F_{1,20} = 3.27$, $p = 0.088$) on sorghum yield, but there was a significant interaction between sorghum cultivar and insecticide application ($F_{1,20} = 7.76$, $p = 0.011$). In Barbour Co., sorghum productivity did not vary as a function of sorghum cultivar ($F_{1,4} = 0.61$, $p = 0.479$) but was significantly influenced by foliar insecticide application ($F_{1,4} = 33.19$, $p = 0.004$); with the sprayed treatment demonstrating evidently higher yield compared to non-sprayed for both sorghum cultivars (Figure 4D). There was no significant interaction between sorghum cultivar and insecticide application ($F_{1,4} = 1.04$, $p = 0.313$).

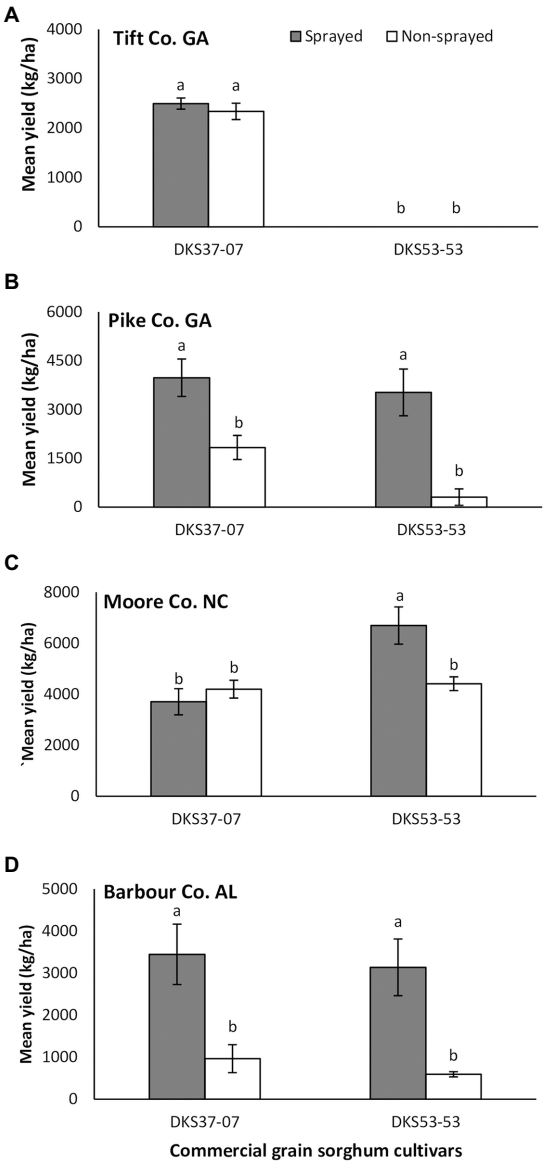

FIGURE 4
Mean (±SE) grain yield (kg/ha) as a function of sorghum cultivar and flupyradifurone foliar application at Tift Co., Pike Co. GA, Moore Co. NC and Barbour Co. AL. Means capped with different letters are significantly different ($p<0.05$; Turkey's test) among all four treatments. Note that y-axis scales are different on each figure.

Natural enemy abundance and association

The two sorghum cultivars (DKS37-07 and DKS53-53) supported an array of different predator and parasitoid life stages (larvae and adults) in both the sprayed and non-sprayed treatments (Figures 5, 6). Seven species of adult and larvae of lady beetles [*Coccinella septempunctata* (L.), *Hippodamia convergens* (Guérin-Méneville), *Hippodamia sinuate* (Mulsant), *Coleomegilla maculata* (DeGeer), *Scymnus loewii* (Mulsant), *Cycloneda sanguinea* (L.)] and *Harmonia axyridis* (Pallas; Coleoptera: Coccinellidae), four species of lacewing larvae [*Hemerobius* sp. (Neuroptera: Hemerobiidae), *Ceraeochrysa valida* (Banks), *Chrysopa quadripunctata* Burmeister, and *Chrysoperla plorabunda* (Fitch; Neuroptera: Chrysopidae)], and two parasitoid taxa [*Lysiphlebus testaceipes* (Cresson;

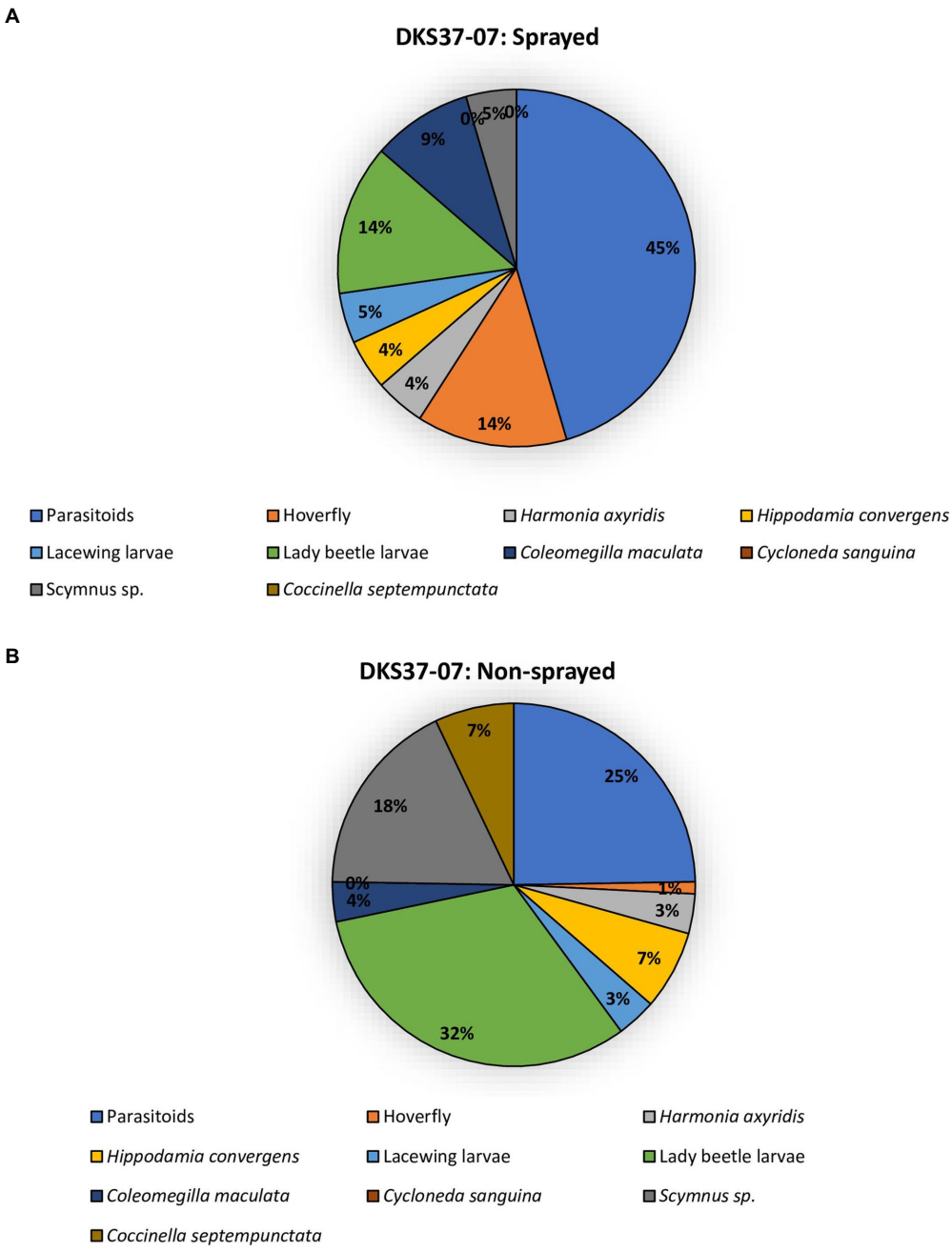

FIGURE 5
Percentage of natural enemies observed on resistant sorghum cultivar (DKS37-07) that was flupyradifurone sprayed **(A)** or non-sprayed **(B)** using the pooled data from all locations.

Hymenoptera: Braconidae) and *Aphelinus* sp] were recorded for both sprayed and non-sprayed plots of both cultivars (Figures 5, 6). In the foliar insecticide sprayed resistant sorghum hybrid, parasitoids accounted for 45% of the total natural enemy number while lady beetle larvae and *Allograpta obliqua* larvae represented 14% each of the total natural enemies found (Figure 5A). Lady beetle larvae (32%) and parasitoids (25%) were more abundant on the non-sprayed resistant sorghum cultivar (Figure 5B). In the sprayed susceptible sorghum cultivar., parasitoids accounted for 87% of the total natural enemy composition while lady beetle larvae represented 5% of the total natural enemies found (Figure 6A). Lady beetle larvae (56%) and parasitoids (20%) were more abundant on the non-sprayed susceptible sorghum cultivar (Figure 6B).

Linear regression analysis showed a significant positive relationship between the number of *M. sorghi* and number of adult predators in Tift, Pike and Moore Counties (Figures 7A–D) except for Barbour, Co., AL. Similarly, a significant positive relationship

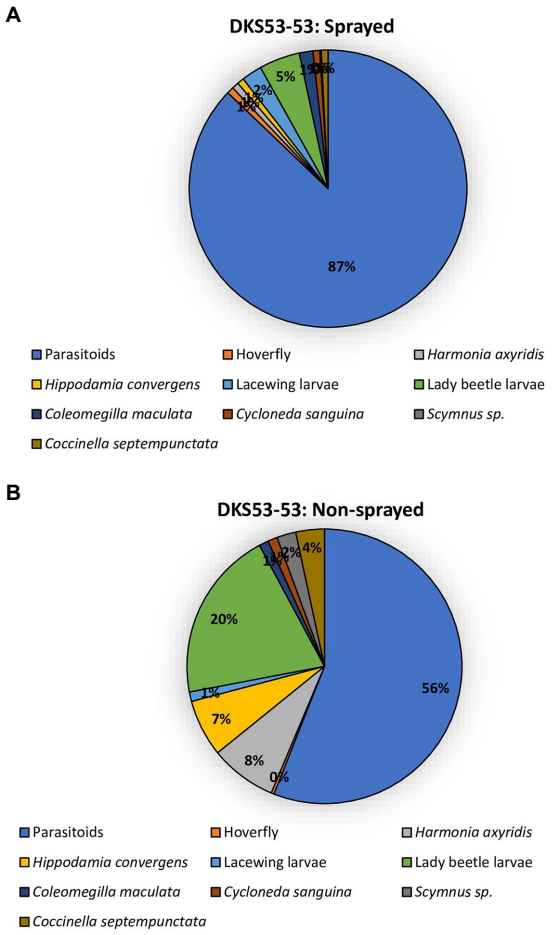

FIGURE 6
Percentage of natural enemies observed on susceptible sorghum cultivar (DKS53-53) that was flupyradifurone sprayed **(A)** or non-sprayed **(B)** using the pooled data from all locations.

between the number of *M. sorghi* and number of larval predators was evident in all four study locations (Figures 7E–H). Finally, there was a significant positive relationship between the number of *M. sorghi* and parasitoids numbers and mummified aphids (Figures 8A–D).

Discussion

We documented the benefits of combining aphid resistant sorghum cultivar and a single foliar insecticide application of flupyradifurone to suppress *M. sorghi* infestation and reduce yield loss in four locations in southeastern United States. Although within-season plant damage ratings did not vary widely, planting resistant cultivar and foliar application preserved grain yield across locations except under extreme aphid pressure at the Tift Co. study location. Our study also documented a positive association between aphid infestations and the number of natural enemies suggesting that natural enemies do play a role in the integrated pest management of *M. sorghi*. This finding is important because it shows that even a highly efficacious insecticide application may not preserve yield; an integrated approach is necessary.

Identification of environmental factors that drive infestation intensity on a spatio-temporal scale across the invasive range of the pest is key to advancing our understanding of the population ecology of this invasive pest and such studies should be the focus of future research. The mean CID were significantly lower in the insecticide sprayed plots, and on the resistant cultivar (DK37-07) across all locations except Barbour Co., AL where relatively light aphid pressure was observed. The suppression of *M. sorghi* population in this study confirms the reliability of the use of host pant resistance and flupyradifurone application to manage *M. sorghi* across a wide geographic area in the invasive range of the pest in the United States (Szczepaniec, 2018; Lahiri et al., 2021). Tift Co., GA and Moore Co., NC had higher infestations compared to other locations. Changes in weather conditions such as temperature and frequency of rainfall events as well as the presence or absence of natural enemies may influence the severity of *M. sorghi* infestation across spatial scales (Szczepaniec, 2018; Seiter et al., 2019; Souza and Davis, 2020; Wilson et al., 2020). As has been demonstrated by a previous study (Lahiri et al., 2021), differences in CID between sorghum cultivars were most evident when CID was very high compared to locations where CID was low. In southeastern USA grain sorghum, *M. sorghi* infestation intensity often varies among locations and years (Haar et al., 2019; Lahiri et al., 2021).

Across study locations, host plant resistance and the application of flupyradifurone did not significantly influence plant injury except in Tift Co. where the resistant cultivar (DKS37-07) suffered considerably less damage compared to the susceptible cultivar (DKS53-53). Although plant damage ratings did not vary widely in the study, there was generally a positive association between aphids counts and observed plant damage suggesting that increasing aphid numbers resulted in corresponding increase in plant damage.

The lack of significant differences between grain sorghum cultivars and between insecticide treatments, in the overall grain yield (when data from all locations were pooled) shows the importance of location variation in these kinds of experiments (e.g., Lahiri et al., 2021), and further buttress the need for an areawide approach in integrated pest management in sorghum. However, grain sorghum data from individual locations differed either according to sorghum cultivar or insecticide application. Preserved grain yield in plots treated with flupyradifurone application across all locations (except Tift Co.) confirm the findings of previous authors who worked on *M. sorghi* in southeastern United States (e.g., Haar et al., 2019; Lahiri et al., 2021; Pekarcik and Jacobson, 2021). Yields were significantly greater in Moore Co., NC compared to the other study sites. We reason that this difference may be due to a multiplicity of factors including but not limited to rainfall, soil type, weather conditions and other environmental conditions that could

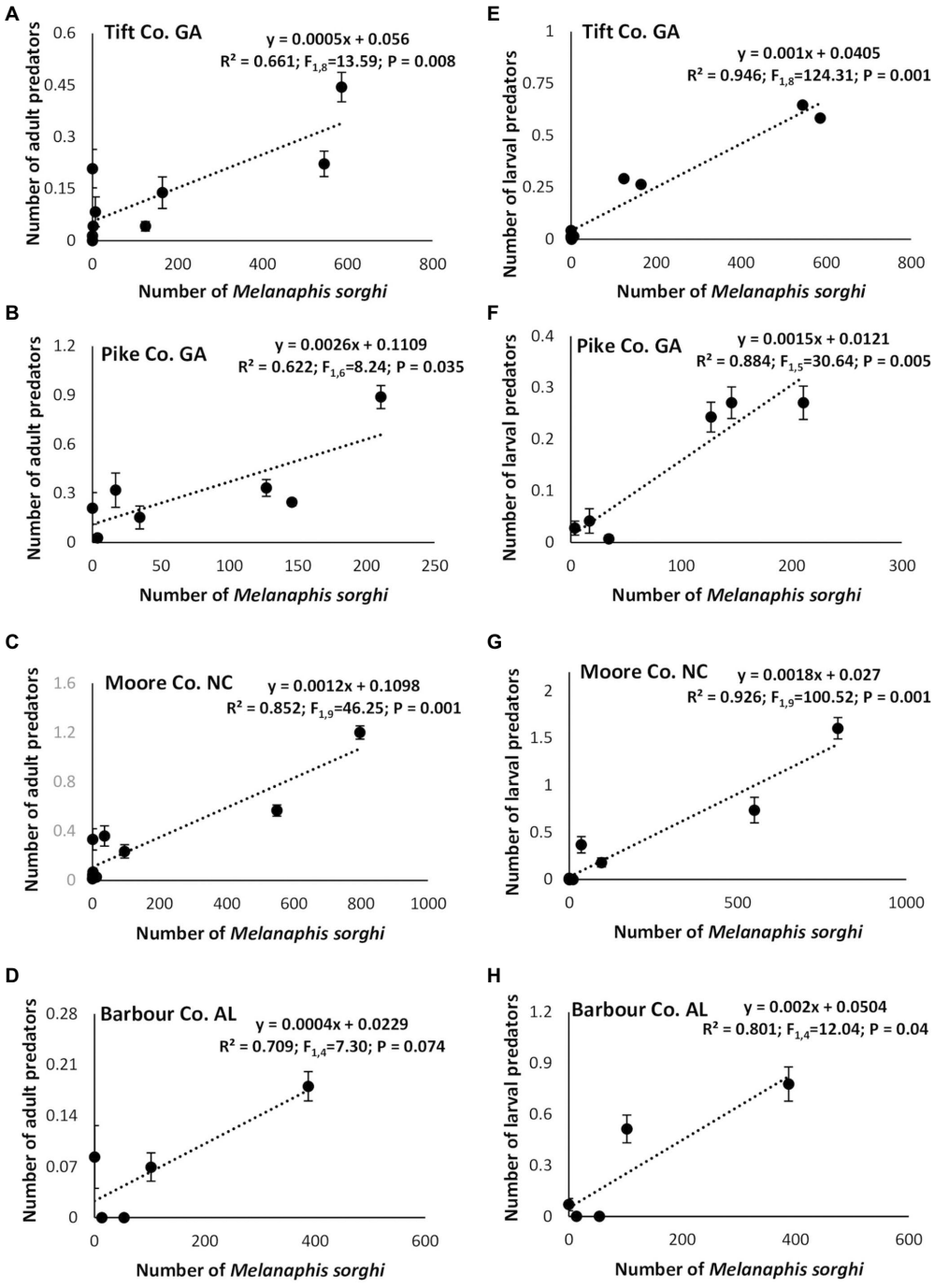

FIGURE 7
Relationships between mean (±SE) weekly *Melanaphis sorghi* counts and adult **(A–D)** or larval **(E–H)** predators across cultivars, insecticide treatment and locations.

influence *M. sorghi* infestation intensity. Host plant resistance had a positive effect on grain yield in Tift and Moore Counties; in Moore Co., no foliar application was required to achieve greater than 500 kg/ha yield in the resistant cultivar (DKS37-07). Yield loss is the cumulative effect of all stresses during the growing year. Aphids represent a major source of stress and can explain some yield results, but other factors such as plant disease, water stress and even bird damage prior to harvest could have suppressed yield potential. In Tift Co., complete yield loss was recorded in experimental plots planted with the susceptible grain sorghum cultivar (DKS53-53) irrespective of insecticide treatment. Studies reporting 100% yield loss in susceptible grain sorghum cultivars grown under intense pressure are not uncommon in the literature (see Brewer et al., 2017; Lahiri et al., 2021).

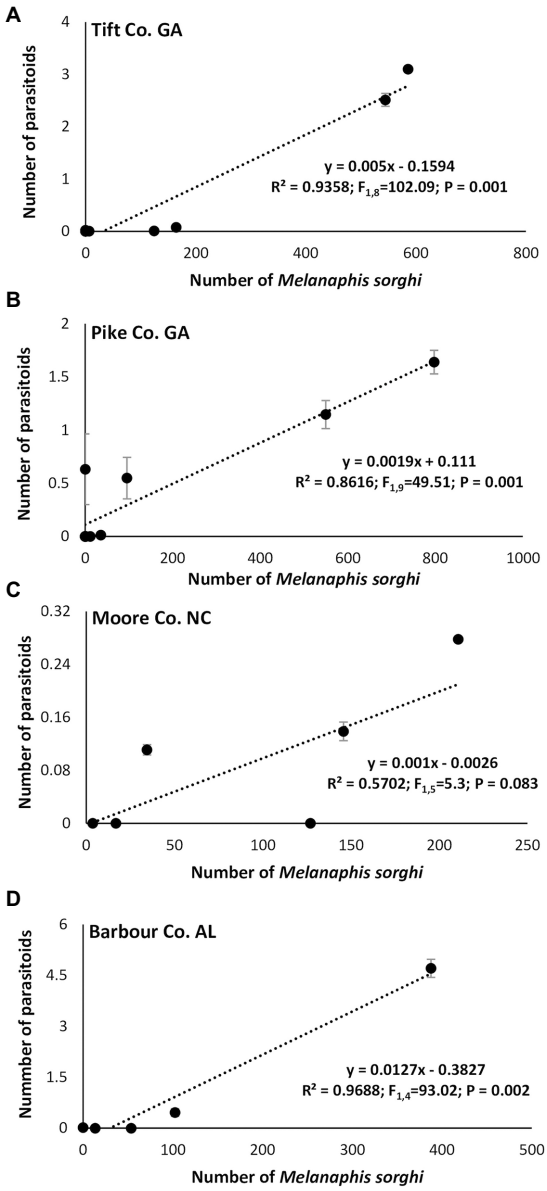

FIGURE 8
Relationship between mean weekly *Melanaphis sorghi* and parasitoids observed across hybrids, insecticide treatment, and locations.

In addition to using host plant resistance and foliar insecticide application as an effective management tool in *M. sorghi* infestation as described in this current study, we also found that the two sorghum cultivars (DKS37-07 and DKS53-53) supported an array of different life stages of natural enemies (predators and parasitoids) for both the sprayed and non-sprayed treatments. Studies suggest that natural enemies maybe utilized in the *M. sorghi* and grain sorghum system to reduce pest damage and yield loss (Szczepaniec, 2018; Lahiri et al., 2021). Our findings suggest that predators may be more abundant in resistant sorghum (DKS37-07) compared to the susceptible cultivar (DKS53-53). Predators of *M. sorghi* reported in this current study (*C. septempunctata*, *H. convergens*, *H. sinuate*, *C. maculata*, *S. loewii*, *C. sanguinea*, and *H. axyridis*; *Hemerobius* sp., *C. valida*, *C. quadripunctata*, and *C. plorabunda*; *A. obliqua*, *P. clavatus*, and *E. americanus*) have been reported from the invasive range of *M. sorghi* in southeastern United States (Szczepaniec, 2018; Lytle and Huseth, 2021). For both resistant and susceptible cultivars, parasitoids (*L. testaceipes* and *Aphelinus* sp.) were more abundant in the sprayed treatments suggesting that foliar insecticide applications may not have any serious negative effects on the populations of the parasitoids encountered in this study. We hypothesized that the changes in natural enemy populations between sprayed and unsprayed could be a simple reflection of fewer aphids resulting in fewer natural enemies. Differences in predators and parasitoids species abundance or composition are not uncommon because factors including but not limited to weather conditions and prey or host availability can cause their population to spatio-temporally vary (Varenhorst and O'Neal, 2012; Whalen et al., 2016; Lytle and Huseth, 2021).

The strong and significant positive relationship between the natural enemies (larval predators, adults predators and parasitoids numbers) and *M. sorghi* infestation suggests that flupyradifurone application may not have significant negative effects on natural enemy populations. Lytle and Huseth (2021), who studied the impact of insecticide sprays on *M. sorghi* and natural enemy populations in grain sorghum system in North Carolina, also reported that foliar insecticidal treatments did not negatively impact natural enemy populations. The authors showed that by 22 and 29 days after spraying, there were no differences in natural enemy abundance in any treatments including the untreated control.

These findings suggest that the combination of host plant resistance and foliar insecticide application and the presence of natural enemies significantly suppressed *M. sorghi* population and in parts increased yield in grain sorghum. The integration of natural enemies with other conventional control methods in the management of *M. sorghi* comprise an effective integrated pest management strategy against this invasive pest. Our results provide some new insights into the role of natural enemies and other conventional control methods that can enable more informed decisions for growers that are concerned with the balance between insecticide application and biological control for lasting and sustained pest suppression in the *M. sorghi* and grain sorghum system. Given the importance of sorghum and the expansion of sorghum planted areas, in the United States [United States Department of National Agricultural Statistics Services (USDA-NASS), 2017], studies that integrate planting dates with the use of natural enemies and other conventional control approaches could further identify or refine strategies that limit this pest.

Data availability statement

The original contributions presented in the study are included in the article/supplementary material, further inquiries can be directed to the corresponding author.

Author contributions

SL, XN, and MT conceptualized the study. MT, SL, XN, DB, AJ, FR-J, SP, and AH collected data and critically reviewed and amended the manuscript. OU and SL performed data analyses. OU wrote the manuscript. All authors contributed to the article and approved the submitted version.

Funding

This research was supported by a None-Assistance Cooperative Agreement (NACA) 58-6048-6-021 from an areawide pest management project entitled "Area-Wide Pest Management of the Invasive Sugarcane Aphid in Grain Sorghum," which was awarded to the ARS Research Project 6648-21220-018-00D entitled "Genetic Improvement of Maize and Sorghum for Resistance to Biotic and Abiotic Stresses" and the Alabama Agricultural Experiment Station.

Acknowledgments

The authors acknowledge technical assistance related to planting and plot maintenance from David Griffin and technical assistance collecting the data from Sarah Hobby, Apurba Barman, Lauren Perez, Amanda Lytle, and Penny Tapp. Bayer CropScience, Dow Agrosciences, DuPont, Monsanto, and Syngenta AG donated seed and crop protection chemicals used in these trials. Mention of trade names or commercial products in this publication is solely for the purpose of providing specific information and does not imply recommendation or endorsement by the USDA-ARS or any of the participating land grant institutions.

Conflict of interest

The authors declare that the research was conducted in the absence of any commercial or financial relationships that could be construed as a potential conflict of interest.

Publisher's note

All claims expressed in this article are solely those of the authors and do not necessarily represent those of their affiliated organizations, or those of the publisher, the editors and the reviewers. Any product that may be evaluated in this article, or claim that may be made by its manufacturer, is not guaranteed or endorsed by the publisher.

References

Armstrong, J. S., Rooney, W. L., Peterson, G. C., Villenueva, R. T., Brewer, M. J., and Sekula-Ortiz, D. (2015). Sugarcane aphid (Hemiptera: Aphididae): host range and sorghum resistance including cross-resistance from greenbug sources. *J. Econ. Entomol.* 108, 576–582. doi: 10.1093/jee/tou065

Bayoumy, M. H., Ramaswamy, P., and Michaud, J. P. (2016). Comparative life histories of greenbugs and sugarcane aphids (Hemiptera: Aphididae) co-infesting susceptible and resistant sorghums. *J. Econ. Entomol.* 109, 385–391. doi: 10.1093/jee/tov271

Bostick, N. M., LaForest, J. H., Bargeron, C. T., Culbreath, A. K., Brenneman, T. B., Schmidt, J. M., et al. (2020). Assessment of consensus-based scouting for management of sugarcane aphid (Heteroptera: Aphididae) in Georgia. *J. Entomol. Sci.* 55, 1–13. doi: 10.18474/0749-8004-55.1.1

Bowling, R. D., Brewer, M. J., Kerns, D. L., Gordy, J., Seiter, N., Elliott, N. E., et al. (2016). Sugarcane aphid (Hemiptera: Aphididae): a new pest on sorghum in North America. *J. Integr. Pest Manag.* 7, 1–13. doi: 10.1093/jipm/pmw011

Brewer, M. J., Gordy, J. W., Kerns, D. L., Woolley, J. B., Rooney, W. L., and Bowling, R. D. (2017). Sugarcane aphid population growth, plant injury, and natural enemies on selected grain sorghum hybrids in Texas and Louisiana. *J. Econ. Entomol.* 110, 2109–2118. doi: 10.1093/jee/tox204

Denmark, H. A. (1988). Sugarcane aphids in Florida. Florida Department of Agriculture & consumer services, division of plant industry. *Entomol. Circ.* 302:2.

EDDMapS (2020). Early Detection & Distribution Mapping system. The University of Georgia—Center for Invasive Species and Ecosystem Health. Available at: http://www.eddmaps.org/ (Accessed March 30, 2020).

Etheridge, B., Gore, J., Catchot, A. L., Cook, D. R., Musser, F. R., and Larson, E. J. (2018). Influence of temperature on the efficacy of foliar insecticide sprays against sugarcane aphid (Hemiptera: Aphididae) populations in grain sorghum. *J. Econ. Entomol.* 112, 196–200. doi: 10.1093/jee/toy315

Gordy, J. W., Brewer, M. J., Bowling, R. D., Buntin, G. D., Seiter, N. J., Kerns, D. L., et al. (2019). Development of economic thresholds for sugarcane aphid (Hemiptera: Aphididae) in susceptible grain sorghum hybrids. *J. Econ. Entomol.* 112, 1251–1259. doi: 10.1093/jee/toz028

Gordy, J. W., Seiter, N. J., Kerns, D. L., Reay-Jones, F. P. F., Bowling, R. D., Way, M. O., et al. (2021). Field assessment of aphid doubling time and yield of sorghum susceptible and partially resistant to sugarcane aphid (Hemiptera: Aphididae). *J. Econ. Entomol.* 114, 2076–2087. doi: 10.1093/jee/toab135

Haar, P. J., Buntin, G. D., Jacobson, A., Pekarcik, A., Way, M. O., and Zarrabi, A. (2019). Evaluation of tactics for management of sugarcane aphid (Hemiptera: Aphididae) in grain sorghum. *J. Econ. Entomol.* 112, 2719–2730. doi: 10.1093/jee/toz215

Harris-Shultz, K., and Ni, X. (2021). A sugarcane aphid (Hemiptera: Aphididae) "super-clone" remains on U.S. sorghum and Johnsongrass and feeds on giant Miscanthus. *J. Entomol. Sci.* 56, 43–52. doi: 10.18474/0749-8004-56.1.43

Harris-Shultz, K., Ni, X., Wadl, P. A., Wang, X., Wang, H., Huang, F., et al. (2017). Microsatellite markers reveal a predominant sugarcane aphid (Homoptera: Aphididae) clone is found on sorghum in seven states and one territory of the USA. *Crop. Sci.* 57, 2064–2072. doi: 10.2135/cropsci2016.12.1010

Hewlett, J. A., Szczepaniec, A., and Eubanks, M. D. (2019). The effects of sugarcane aphid density in sorghum on predation by lady beetles and lacewings. *Biol. Control* 129, 171–177. doi: 10.1016/j.biocontrol.2018.10.015

Kerns, D., Brown, S., Beuzelin, J., and Guidry, K. M. (2015). Sugarcane aphid: a new invasive pest of sorghum. *Louisiana Agric.* 58, 12–14.

Knutson, A., Bowling, R., Brewer, M. J., Bynum, E., and Porter, P. (2016). The sugarcane aphid: management guidelines for grain and forage sorghum in Texas. Lubbock (TX): Texas A&M AgriLife extension publication ENTO-035. Available at: http://lubbock.tamu.edu/files/2016/05/ENTO-035_Sugarcane_Aphid-Management_2016.pdf (Accessed July 5, 2021).

Lahiri, S., Ni, X., Buntin, G. D., Punnuri, S., Jacobson, A., Reay-Jones, F. P. F., et al. (2021). Combining host plant resistance and foliar insecticide application to manage, *Melanaphis sacchari* (Hemiptera: Aphididae) in grain sorghum. *Int. J. Pest Manag.* 67, 10–19. doi: 10.1080/09670874.2019.1660830

Lytle, A. J., and Huseth, A. S. (2021). Impact of foliar insecticide sprays on *Melanaphis sacchari* (Hemiptera: Aphididae) and natural enemy populations in grain sorghum. *Crop Prot.* 149:105764. doi: 10.1016/j.cropro.2021.105764

Maxson, E. L., Brewer, M. J., Rooney, W. L., and Woolley, J. B. (2019). Species composition and abundance of the natural enemies of sugarcane aphid, *Melanaphis sacchari* (Zehnter) (Hemiptera: Aphididae), on sorghum in Texas. *Proc. Entomol. Soc. Wash.* 121, 657–680. doi: 10.4289/0013-8797.121.4.657

Medina, R. F., Armstrong, S. J., and Harrison, K. (2017). Genetic population structure of sugarcane aphid, *Melanaphis sacchari*, in sorghum, sugarcane, and Johnsongrass in the continental USA. *Entomol. Exp. Appl.* 162, 358–365. doi: 10.1111/eea.12547

Michaud, J. P., Whitworth, R. J., Schwarting, H., McCornack, B., and Zukoff, S. (2016). *Sorghum Insect Management*. Manhattan, KS: Kansas State University Research and Extension MF742. Available at: http://entomology.k-state.edu/extension/publications/ (Accessed July 29, 2021).

Mondor, E. B., Tremblay, M. N., and Messing, R. H. (2006). Morphological and ecological traits promoting aphid colonization of the Hawaiian islands. *Biol. Invasions* 9, 87–100. doi: 10.1007/s10530-006-9010-z

Nibouche, S., Costet, L., Holt, J. R., Jacobson, A., Pekarcik, A., Sadeyen, J., et al. (2018). Invasion of sorghum in the Americas by a new sugarcane aphid (*Melanaphis sacchari*) superclone. *PLoS One* 13:e0196124. doi: 10.1371/journal.pone.0196124

Nibouche, S., Costet, L., Medina, R. F., Holt, J. R., Sadeyen, J., Zoogones, A.-S., et al. (2021). Morphometric and molecular discrimination of the sugarcane aphid, *Melanaphis sacchari*, (Zehntner, 1897) and the sorghum aphid, *Melanaphis sorghi* (Theobald, 1904). *PLoS One* 16:e0241881. doi: 10.1371/journal.pone.0241881

Paudyal, S., Armstrong, J. S., Harris-Shultz, K. R., Wang, H., Giles, K. L., Rott, P. C., et al. (2019). Evidence of host plant specialization among the U.S. sugarcane aphid (Hemiptera: Aphididae) genotypes. *Trends Entomol.* 15, 47–58.

Pekarcik, A. J., and Jacobson, A. L. (2021). Evaluating sugarcane aphid, *Melanaphis sacchari* (Hemiptera: Aphididae), population dynamics, feeding injury, and grain yield among commercial sorghum varieties in Alabama. *J. Econ. Entomol.* 114, 757–768. doi: 10.1093/jee/toab013

Peña-Martinez, R., Muñoz-Viveros, A. L., Bujanos-Mu~niz, R., Luevano-Borroel, J., Tamayo-Mejia, F., and Cortez-Mondaca, E. (2016). Sexual forms of sorghum aphid complex *Melanaphis sacchari*/*sorghi* in Mexico. *Southwest. Entomol.* 41, 127–132. doi: 10.3958/059.041.0114

Peterson, G. C., Armstrong, J. S., Pendleton, B. B., Stelter, M., and Brewer, M. J. (2018). Registration of RTx3410 through RTx3428 sorghum germplasm resistant to sugarcane aphid [*Melanaphis sacchari* (Zehntner)]. *J. Plant Regist.* 12, 391–398. doi: 10.3198/jpr2018.02.0007crg

Ruppel, R. F. (1983). Cumulative insect-days as an index of crop protection. *J. Econ. Entomol.* 76, 375–377. doi: 10.1093/jee/76.2.375

Seiter, N. J., Miskelley, A. D., Lorenz, G. M., Joshi, N. K., Studebaker, G. E., and Kelley, J. P. (2019). Impact of planting date on *Melanaphis sacchari* (Hemiptera: Aphididae) population dynamics and grain sorghum yield. *J. Econ. Entomol.* 112, 2731–2736. doi: 10.1093/jee/toz230

Sharma, H. C., and Nwanze, K. F. (1997). "Insect pests of sorghum: biology, extent of losses, and economic thresholds" in *Plant Resistance to Insects in Sorghum*. eds. H. C. Sharma, F. Singh and K. F. Nwanze (International Crops Research Institute for the Semi-Arid Tropics: Patancheru, India), 9–23.

Sharma, H. C., Sharma, S. P., and Munghate, R. S. (2013). Phenotyping for resistance to the sugarcane aphid *Melanaphis sacchari* (Hemiptera: Aphididae) in *sorghum bicolor* (Poaceae). *Int. J. Trop. Ins. Sci.* 33, 227–238. doi: 10.1017/S1742758413000271

Singh, B. U., Padmaja, P. G., and Seetharama, N. (2004). Biology and management of the sugarcane aphid, *Melanaphis sacchari* (Zehntner) (Homoptera: Aphididae), in sorghum: a review. *Crop Prot.* 23, 739–755. doi: 10.1016/j.cropro.2004.01.004

Souza, M. F., and Davis, J. A. (2020). Potential population growth of *Melanaphis sacchari* (Zehntner) (Hemiptera: Aphididae) under six constant temperatures on grain sorghum (Sorghum bicolor L.). *Fla. Entomol.* 103, 116–123. doi: 10.1653/024.103.0419

Szczepaniec, A. (2018). Interactive effects of crop variety, insecticide seed treatment, and planting date on population dynamics of sugarcane aphid (*Melanaphis sacchari*) and their predators in late-colonized sorghum. *Crop Prot.* 109, 72–79. doi: 10.1016/j.cropro.2018.03.002

United States Department of National Agricultural Statistics Service [USDA-NASS] (2017). Acreage Agricultural Statistics Board. Available at: https://usda.mannlib.cornell.edu/usda/current/Acre/Acre-06-30-2017.pdf (Accessed July 5, 2021).

Varenhorst, A. J., and O'Neal, M. E. (2012). The response of natural enemies to selective insecticides applied to soybean. *Environ. Entomol.* 41, 1565–1574. doi: 10.1603/EN12068

Whalen, R. A., Herbert, D. A., Malone, S., Kuhar, T. P., Brewster, C. C., and Reisig, D. D. (2016). Effects of diamide insecticides on predators in soybean. *J. Econ. Entomol.* 109, 2014–2019. doi: 10.1093/jee/tow173

Wilson, B. E., Reay-Jones, F. P. F., Lama, L., Mulcahy, M., Reagan, T. E., Davis, J. A., et al. (2020). Influence of sorghum cultivar, nitrogen fertilization, and insecticides on infestations of the sugarcane aphid (Hemiptera: Aphididae) in the southern United States. *J. Econ. Entomol.* 113, 1850–1857. doi: 10.1093/jee/toaa121

Zapata, S. D., Dudensing, R., Sekula, D., Esparza-Dıaz, G., and Villanueva, R. (2018). Economic impact of the sugarcane aphid outbreak in South Texas. *J. Agric. Appl. Econ.* 50, 104–128. doi: 10.1017/aae.2017.24

frontiers | Frontiers in Plant Science

TYPE Original Research
PUBLISHED 25 November 2022
DOI 10.3389/fpls.2022.1019693

OPEN ACCESS

EDITED BY
Julian Chen,
Institute of Plant Protection, Chinese Academy of Agricultural Sciences, China

REVIEWED BY
Mónica Asunción Hurtado Ruiz,
University of Jaume I, Spain
Wen Xie,
Insitute of Vegetables and Flowers, Chinese Academy of Agricultural Sciences, China

*CORRESPONDENCE
Shihao Zhou
zsh88200939@126.com

†These authors have contributed equally to this work

SPECIALTY SECTION
This article was submitted to Sustainable and Intelligent Phytoprotection, a section of the journal Frontiers in Plant Science

RECEIVED 15 August 2022
ACCEPTED 14 November 2022
PUBLISHED 25 November 2022

CITATION
Lian Y, Wang A, Peng S, Jia J, Yang X, Li J, Yang S, Zheng R and Zhou S (2022) Potential global distribution area projections of the aphid *Lipaphis erysimi* and its predator *Eupeodes corollae* in the context of climate change. *Front. Plant Sci.* 13:1019693. doi: 10.3389/fpls.2022.1019693

Potential global distribution area projections of the aphid *Lipaphis erysimi* and its predator *Eupeodes corollae* in the context of climate change

Yuyang Lian[1,2†], Aqiang Wang[1,2†], Sihua Peng[1†], Jingjing Jia[3†], Xiaofeng Yang[1†], Jinlei Li[2], Shuyan Yang[1], Rongjiao Zheng[2] and Shihao Zhou[1,2*]

[1]Sanya Nanfan Research Institute of Hainan University, Sanya, Hainan, China, [2]Key Laboratory of Germplasm Resources Biology of Tropical Special Ornamental Plants of Hainan Province, College of Forestry, Hainan University, Haikou, Hainan, China, [3]Institute of Plant Protection, Hainan Academy of Agricultural Sciences (Research Center of Quality Safety and Standards for Agricultural Products of Hainan Academy of Agricultural Sciences), Haikou, Hainan, China

Climate change affects the population distribution of pests and their natural enemies, and predicting these effects is necessary for pest monitoring and green control. *Lipaphis erysimi* is an important vegetable pest, and its natural enemy, the *Eupeodes corollae* Fabricius has a strong predatory effect on the *L. erysimi*. To assess the spread trends of *L. erysimi* and its natural enemy, the hoverfly, *E. corollae* under current (1970-2000) and future climates (2041-2060), based on the MaxEnt model, this paper uses data on the geographical distribution of the historical occurrence of *L. erysimi* and *E. corollae* to speculate on their potential distribution areas worldwide and analyze the key environmental factors affecting the survival and spread of both. The results showed that the Representative Concentration Pathway (RCP) 2.6 and RCP4.5 climatic conditions are favorable for the spread of *L. erysimi*, the RCP8.5 climatic conditions are unfavorable for the spread of *L. erysimi*, and all three future climatic conditions are unfavorable for the spread of *E. corollae*. The highest fitness of *L. erysimi* was found at the annual average temperature of 18 °C and the annual average precipitation of 900 mm, while the highest fitness of *E. corollae* was found at the annual average temperature of 10 °C and the lowest temperature in the coldest month of 0 °C. This study can provide a reference basis for monitoring and early warning and biological control of *L. erysimi*.

KEYWORDS

***Lipaphis erysimi*, *Eupeodes corollae* Fabricius, Suitable area, Climate factor, MaxEnt**

Introduction

Lipaphis erysimi (Kaltenbach) (Homoptera: Aphididae) mainly harms cruciferous crops such as radish, rape, and cabbage, and is particularly harmful to Brassica crops such as mustard and rape (Rana, 2005). It was first discovered in the United States by Davis (1914) and is now widely distributed worldwide. *L. erysimi* are reproduce quickly and usually cluster in groups on the young stems and abaxial surface of leaves to feed on sap, seriously affecting the growth and development of vegetables, the secreted honeydew can cause sooty blotch, prevent the leaves from photosynthesis. In addition, *L. erysimi* can act as a mediating insect to transmit a variety of plant viruses, resulting in slow growth, yellowing and wilting of leaves, and even death of the entire plant (Koramutla et al., 2016). Rape is one of the major oil crops in the world, and the *L. erysimi*'s damage has caused huge losses to the economy (Chattopadhyay et al., 2005). The larvae of *Eupeodes corollae* Fabricius (Diptera: Syrphidae) are an important predatory natural enemy of *L. erysimi* (He et al., 1990), they feed heavily and are the dominant species in many locations, making them ideal for control of the *L. erysimi* (Pekas et al., 2020).

Global warming has become one of the main features of today's climate change, and the Earth's climate is expected to become hotter and more humid in the coming century than it is today (Barreca, 2012). Insects are sensitive to environmental changes because of their small size, thin body walls, rapid heat exchange with the environment, and poor ability to self-regulate body temperature (Yamamura et al., 2006). Temperature and humidity are important factors affecting the growth, development, survival, and reproduction of individual insects and populations, and adaptation to temperature and humidity is a key condition necessary for insects to carry out their life activities (Khaliq et al., 2014). The maximum and minimum temperatures of 27.37°C and 14.62°C, maximum and minimum relative humidity of 95.28% and 62.28%, respectively, were detected at the peak of *L. erysimi* occurrence, and the population density of *L. erysimi* decreased with the increase of humidity (Reza et al., 2004). The developmental starting temperatures for eggs, the first instar larvae, the second instar larvae, the third instar larvae, and pupae of the *E. corollae* are 9.69°C, 12.39°C, 6.97°C, 2.03°C, and 2.35°C, respectively, and temperatures above 30°C result in mass mortality of larvae and failure of pupae to fledge (Dong et al., 2004). The fledge rate can reach 90% when the soil humidity is 75%-90%, and lower than 60% will remarkably reduce the fledge rate (Li et al., 1996). Temperature and humidity are crucial to the population dynamics of *L. erysimi* and *E. corolla*. Therefore, we selected *E. corolla* as predatory natural enemies of *L. erysimi* to study the changes of their potential distribution area in different climatic conditions.

Ecological niche models are based on ecological niche theory, which analyzes known species distribution data and their associated environmental variables to predict the potential distribution of species (Sillero, 2011; Yackulic et al., 2013). The maximum entropy (MaxEnt) ecological niche model is a machine learning modeling approach based on the maximum entropy principle that uses only data related to environmental variables and habitat suitability to simulate species ecological niche, and estimates the distribution of potential fitness zones of specie's by determining the maximum entropy distribution constrained by environmental variables (Elith et al., 2011; Warren and Seifert, 2011), the output of which is a distribution map reflecting different fitness levels of species (Zhao et al., 2022b). MaxEnt's principle-based algorithm can obtain the most uniform potential distribution of species and can provide highly accurate predictions compared to other prediction models, even when species distribution data are small or incomplete. In addition, the output of the MaxEnt model combined with GIS can describe the weight of each environmental factor affecting the expected distribution of species, so that the dominant environmental parameters affecting species distribution can be obtained (Phillips et al., 2006; Pearson et al., 2007; Liu et al., 2018). Dong et al. (2022) used the MaxEnt model to predict the change of potential suitable areas of *Bactrocera dorsalis* (Hendel). The results showed that the suitable areas for *B. dorsalis* will increase, and the range will likely expand northward from existing locations in the future. Using MaxEnt to predict the distribution of *Bactrocera correcta*, it was concluded that its potential suitable areas include India and neighboring countries in Asia, pacific islands, and North Australia, Central and South America, central Africa. Water vapor pressure and solar radiation were the most influential variables for *B. correcta*, the rising temperature could lead increasing of suitable area slightly (Zhang et al., 2022b). How will the potential global distribution areas of *L. erysimi* and *E. corollae* change under future climates? What are the key environmental factors for the survival and dispersal of both? Is it possible to introduce the *E. corollae* for biological control in areas with serious *L. erysimi* damage? These questions are not yet clear. Therefore, we used the MaxEnt model and Arc GIS to construct an ecological niche model to analyze the potential distribution areas of *L. erysimi* and its natural enemy, *E. corollae* under current (1970-2000) and future climates (2041-2060) in our study to clarify the weights of different environmental variables on the ecological distribution of both, and to determine the key environmental parameters for the survival and dispersal of both. This study will provide theoretical and data support for the monitoring and early warning of *L. erysimi* and its biological control.

Materials and methods

Collection and screening of geographic distribution data

A total of 707 *L. erysimi* and 26173 *E. corollae* geographic coordinates of historical occurrence were obtained by visiting

the GBIF (https://www.gbif.org/) (Beck et al., 2014) and CABI (https://www.cabi.org/) (Pasiecznik et al., 2005) websites. To avoid overfitting, we created a 2 km × 2 km raster, took only one coordinate point data in each raster, and removed duplicate points and coordinate points on the sea surface (Welch and Harwood, 2014). Finally, we filtered 570 *L. erysimi* and 9775 *E. corollae* coordinates data and saved them in ".CSV" format.

Climate data acquisition and screening

The current 19 environmental variables data (Table 1) used in this study were obtained from the WorldClim (https://www.worldclim.org) (Fick and Hijmans, 2017) database, which was released in January 2020 and spans the period 1970-2000 with a precision of 2.5 arc-minutes. Using the knife cut method in MaxEnt 3.4.4 (Phillips and Dudík, 2008) software to rank the contribution of environmental factors, and then using SPSS 26.0 to analyze the correlation between environmental factors, when the absolute value of the correlation between two ecological factors was greater than or equal to 0.8, only one representative environmental factor will be kept (Li et al., 2022), meanwhile, the heat map for correlation analysis of environmental factors in *L. erysimi* (Figure 1) and *E. corollae* (Figure 2) was constructed. Finally, we removed the nine environmental variables factors for the *L. erysimi* (Bioclimatic (Bio) 6, Bio7, Bio9, Bio10, Bio11, Bio13, Bio14, Bio16) and the nine environmental variables for the *E. corollae* (Bio4, Bio7, Bio9, Bio10, Bio11, Bio12, Bio13, Bio17), and obtained 11 *L. erysimi* (Bio1, Bio2, Bio3, Bio4, Bio5, Bio8, Bio12, Bio15, Bio17, Bio18, Bio19) and 11 environmental variable factors of *E. corollae* (Bio1, Bio2, Bio3, Bio5, Bio6, Bio8, Bio14, Bio15, Bio16, Bio18, Bio19).

In this study, environmental date from three GHG emission scenarios, Representative Concentration Pathway (RCP) 2.6, RCP4.5 and RCP8.5, were selected to project the future climate suitability areas for the *L. erysimi* and *E. corollae* under future climate conditions. Three future scenarios were obtained from the WorldClim. These bioclimatic variables ran in the model were selected from Coupled Model Intercomparison Project Phase 6 (CMIP6), and their accuracy was 2.5 arc-minutes. RCP 2.6 reveals carbon dioxide emissions could peak globally in 2020 and start to decline in 2080. It also shows that the atmospheric concentration would peak in the middle of the century, followed by a steady decline. In the RCP 4.5, emissions will peak in the middle of the century and then rapidly decline over the next 30 years. The emissions will stabilize to be half of what the levels were in the year 2000. Carbon dioxide concentration will continue to increase according to current trends, but will stabilize and the rate of increased emissions will not be as rapid as previously expected. Serving as the antithesis of RCP 2.6, RCP 8.5 serves as the worst case scenario for the future of emissions. In this RCP, emissions continue to drastically increase throughout the century – predominantly during early and middle parts of the current century. By 2100, the emissions will have stabilized, but will rest at 30 gigatonnes of carbon as opposed to the eight gigatonnes in 2000 (Van Vuuren et al., 2011).

TABLE 1 Climate and environment variables.

Variables	Bioclimatic variables	Original resolutions	Online sources
Bio1	Annual average temperature (°C)	2.5 minutes	WorldClim
Bio2	Monthly mean temperature difference between day and night (°C)		
Bio3	Ratio of diurnal temperature difference to annual temperature difference (%)		
Bio4	Seasonal variance of temperature (°C)		
Bio5	Maximum temperature in the warmest month (°C)		
Bio6	Lowest temperature in the coldest month (°C)		
Bio7	Annual variation range of temperature (°C)		
Bio8	Average temperature in the wettest quarter (°C)		
Bio9	Average temperature in the driest quarter (°C)		
Bio10	Average temperature of the warmest quarter (°C)		
Bio11	Average temperature in the coldest quarter (°C)		
Bio12	Average annual precipitation (mm)		
Bio13	Precipitation in the wettest month (mm)		
Bio14	Precipitation in the driest month (mm)		
Bio15	Seasonal variation coefficient of precipitation (%)		
Bio16	Precipitation in the wettest quarter (mm)		
Bio17	Precipitation in the driest quarter (mm)		
Bio18	Precipitation in the warmest quarter (mm)		
Bio19	Precipitation in the coldest quarter (mm)		

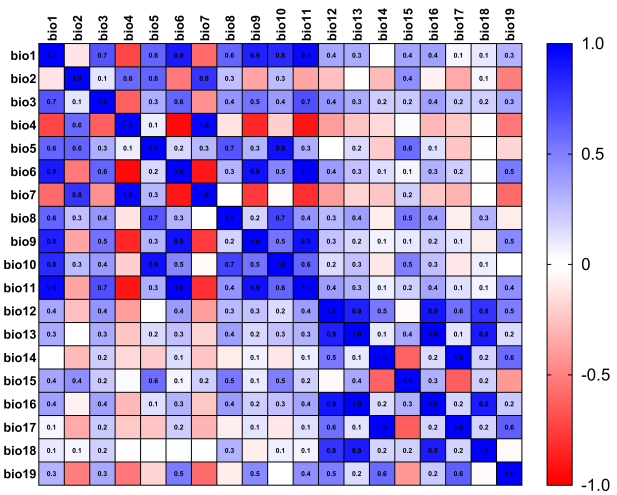

FIGURE 1
Heat map for correlation analysis of environmental factors in *L. erysimi*.

Model construction and evaluation

First, we imported the filtered bioclimatic variable data (1970-2000) for the current GHG emission scenario into the MaxEnt model, and then imported the geographic distribution data of *L. erysimi* and *E. corollae* into the model separately, and randomly selected 75% of the data as the training set for the experiment, and the remaining 25% of the coordinate data as the test set, with a number of iterations of 10. MaxEnt software settings are as follows: check "Create response curves" and "Do jackknife to measure variable importance"; "out format" option select "Logistic", check "Random seed"; set "Random test percentage" to 25, check "Write plot data", the rest keep the default settings. The raster files were reclassified using the Spatial Analyst option of the Arc toolbox in ArcMap 10.8 software, and the distribution areas were set to four gradients (Welch and Harwood, 2014): Unsuitable area (0-0.2), Low suitable area (0.2-0.4), Moderately suitable area (0.4-0.6), and Highly suitable area (0.6-1).

In this study, the area under the receiver operating characteristic curve (AUC) (Fielding and Bell, 1997) was used as a measure of model prediction accuracy and the interval

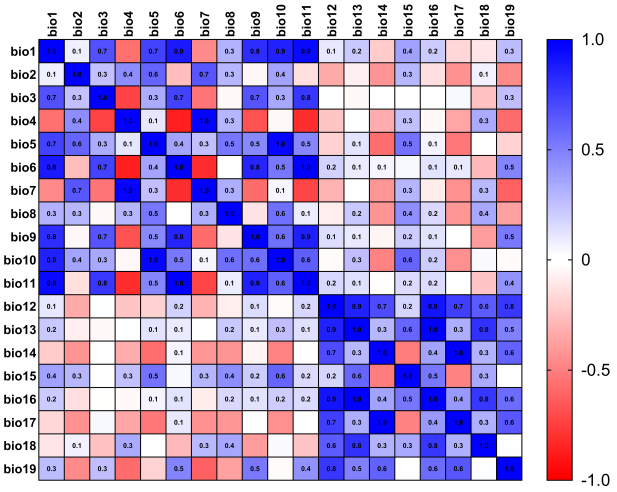

FIGURE 2
Heat map for correlation analysis of environmental factors in *E. corollae*.

ranges from 0.5 to 1. 0.5 corresponds to a completely random prediction, in the range of 0.5-0.7 indicates poor accuracy of the prediction results, in the range of 0.7-0.9 indicates moderate accuracy of the prediction results, and when the prediction results are greater than 0.9, it indicates very high accuracy of the prediction results (Barry and Elith, 2006).

3 Results

Model performance evaluation

The MaxEnt model was constructed using the geographic distribution data of *L. erysimi* and *E. corolla* and the screened environmental variable data, and the performance of the MaxEnt model was evaluated using the mean values of AUCs obtained after 10 iterations of the model. The mean values of all AUCs were calculated to be greater than or equal to 0.8 (Table 2), which indicated that the model had a good performance and could predict the potential distribution areas of *L. erysimi* and *E. corolla* more accurately.

Potential distribution area changes of *L. erysimi* under current and future climate conditions

The potential distribution areas of *L. erysimi* under current and future climatic conditions are shown in Figure 3 and Table 3. Under current climatic conditions, the highly suitable area of *L. erysimi* is mainly distributed in western Europe, China Taiwan, southern coastal areas of China, eastern United States, northern Myanmar, and northern India, covering 1.67×10^5 km^2 or 1.15% of the total area; The moderately suitable area is mainly distributed in southwestern Europe, eastern and southern China, eastern United States, southeastern South America, and northern India, with an area of 7.48×10^5 km^2, accounting for 5.15% of the total area; The low suitable area is widely distributed in Europe, America, Africa, Asia, and Australia, accounting for 14.25% of the total area. Under the RCP2.6, the area of highly suitable area of *L. erysimi* increased, the area of moderate and low suitable area decreased, and the total suitable area decreased by 7.58×10^4 km^2. Under both the RCP4.5 and RCP8.5, the area of high and low suitable area of *L. erysimi* decreased, while the area of moderately suitable area increased, and the total suitable area increased by 9.10×10^3 km^2 under the RCP4.5 and decreased by 2.22×10^4 km^2 under the RCP8.5. This indicates that the expansion of *L. erysimi* will be inhibited under the RCP8.5, while the expansion of *L. erysimi* will be promoted under the RCP2.6 and RCP4.5.

Changes in the potential distribution area of *E. corollae* under current and future climatic conditions

The potential distribution areas of *E. corollae* under current and future climatic conditions are shown in Figure 4 and Table 4. Under current climatic conditions, the highly suitable area of *E. corollae* is mainly distributed in China Taiwan, northern India, and northern Myanmar, with an area of 3.69×10^3 km^2, accounting for 0.03% of the total area; The moderately suitable area is mainly distributed in central Europe and eastern Asia, with scattered distribution in coastal areas of America, with an area of 7.85×10^5 km^2, accounting for 5.41% of the total area; The low suitable area is distributed in northeastern Europe, western North America, southern South America, southeastern China, eastern United States, and southern Australia, with an area of 9.80×10^5 km^2, accounting for 6.75% of the total area. Under all three future climatic conditions, the area of the highly suitable area of *E. corollae* was significantly reduced (by more than 65%) compared with the current climatic conditions, and the total suitable area was reduced by 1.29×10^4 km^2, 1.78×10^4 km^2 and 1.25×10^4 km^2, indicating that all three future climatic conditions were unfavorable for the expansion of *E. corollae*.

Influence of environmental variables on the distribution of *L. erysimi* and *E. corollae*

The knife-cut test can show the magnitude of the contribution of environmental variables to the gain in the distribution of *L. erysimi* and *E. corollae*, and the correlation analysis of environmental variables using the knife-cut method yielded the results of the effect of environmental variables on the distribution of *L. erysimi* (Figure 5) and *E. corollae* (Figure 6). In

TABLE 2 Area under the receiver operating characteristic curve.

Species	AUC	Current	2050s		
			RCP2.6	RCP4.5	RCP8.5
Lipaphis erysimi	Testing data	0.886	0.883	0.883	0.885
Eupeodes corollae Fabricius	Testing data	0.802	0.800	0.802	0.801

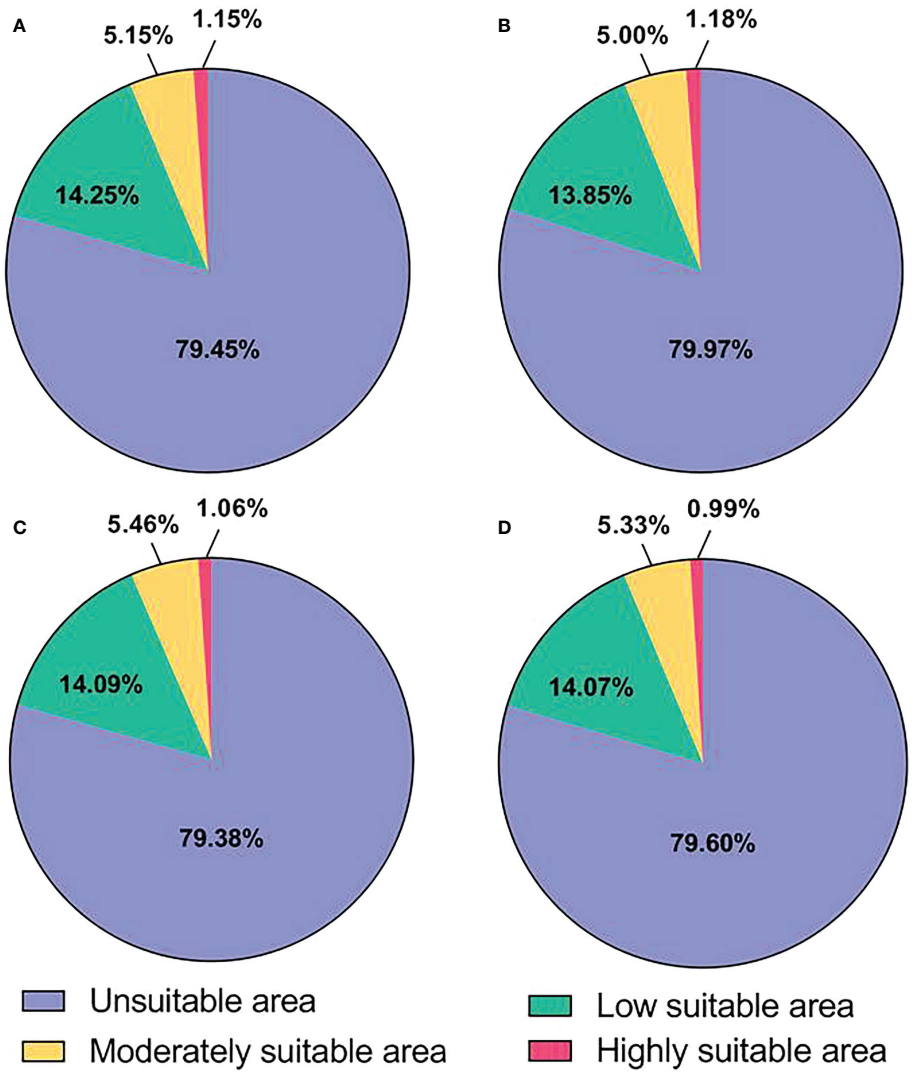

FIGURE 3
Proportion of suitable area for *L. erysimi*. **(A)**, Current climatic conditions. **(B)**, RCP2.6 climatic conditions. **(C)**, RCP4.5 climatic conditions. **(D)**, RCP8.5 climatic conditions.

L. erysimi, the model gains of Bio1 (Annual average temperature) and Bio12 (Annual average precipitation) were 0.8 and 0.68, respectively, with high regularization gains, which contributed more to the distribution gain of *L. erysimi*. In *E. corollae*, Bio1 (Annual average temperature) and Bio6 (Lowest temperature in the coldest month) had the highest model gains of 0.59 and 0.56, respectively, indicating that these two variables had the greatest influence on the distribution of *E. corolla*.

The response curves of the dominant environmental variables showed that *L. erysimi* had no suitableness when the annual average temperature was below 0°C and above 29°C, and its suitableness was highest when the annual average temperature was around 18°C (Figure 7A). The highest suitableness was found when the annual average precipitation reached 1000 mm, and then declined with increasing annual average precipitation. Since the standard error of the response curve is large when the annual average precipitation more than 4000 mm, it does not be consider (Figure 7B). The response curves of the annual average temperature and the lowest temperature in the coldest month were consistent in the *E. corolla*, both increasing and then decreasing, with the highest suitableness at the annual average temperature around 10°C (Figure 7C) and the highest suitableness at the lowest temperature in the coldest month around 0°C (Figure 7D).

TABLE 3 The regions and area of suitable area for *L. erysimi*.

	Highly suitable area	Moderately suitable area	Low suitable area
Current (Total area is 2.98×10^6 km^2)	Eastern United States, Eastern Brazil, Eastern Uruguay, Western Germany, Western Netherlands, Western Denmark, Ireland, United Kingdom, France, Western Georgia, Belgium, Northern India, Northern Myanmar, Eastern Coast of Vietnam, Southern Coast of China, China Taiwan, Korea, Southern Japan (1.67×10^5 km^2)	Eastern United States, Eastern Brazil, Eastern Argentina, Eastern Germany, Eastern Netherlands, Eastern Denmark, Western Poland, Western Ukraine, Uruguay, Southern Sweden, Northern Italy, United Kingdom, France, Czech Republic, Hungary, Romania, Bulgaria, Northern Turkey, Georgia, Northern India, Nepal, Northern Myanmar, Bangladesh, Vietnam, Southeastern China, North Korea, South Korea, Japan, Southeastern Australia, Northern New Zealand (7.48×10^5 km^2)	Southern North America, Northern and Eastern South America, Southern and Eastern Africa, Western and Central Europe, Southeastern Asia, Eastern Australia (2.07×10^6 km^2)
RCP2.6 (Total area is 2.91×10^6 km^2)	Eastern United States, Eastern Brazil, Eastern Uruguay, Western Germany, Western Netherlands, Western Denmark, Ireland, United Kingdom, France, Western Georgia, Belgium, Northern India, Northern Myanmar, Eastern Coast of Vietnam, Southern Coast of China, China Taiwan, Southern Japan (1.71×10^5 km^2)	Eastern United States, Eastern Brazil, Eastern Argentina, Eastern Germany, Eastern Netherlands, Eastern Denmark, Western Poland, Western Ukraine, Uruguay, Southern Sweden, Northern Italy, United Kingdom, France, Czech Republic, Hungary, Romania, Bulgaria, Northern Turkey, Georgia, Northern India, Nepal, Northern Myanmar, Bangladesh, Vietnam, Southern China Coast, South Korea, Japan, Southeastern Australia, Northern New Zealand (7.26×10^5 km^2)	Southern North America, Northern and Eastern South America, Southern and Eastern Africa, Western and Central Europe, Southeastern Asia, Eastern Australia (2.01×10^6 km^2)
RCP4.5 (Total area is 3.00×10^6 km^2)	Eastern United States, Eastern Brazil, Eastern Uruguay, Western Germany, Western Netherlands, Western Denmark, Ireland, United Kingdom, France, Belgium, Northern India, Northern Myanmar, Eastern Coast of Vietnam, Southern Coast of China, China Taiwan, Southern Japan (1.53×10^5 km^2)	Eastern United States, Eastern Brazil, Eastern Argentina, Eastern Germany, Eastern Netherlands, Eastern Denmark, Western Poland, Western Ukraine, Uruguay, Southern Sweden, Northern Italy, United Kingdom, France, Czech Republic, Hungary, Romania, Bulgaria, Northern Turkey, Georgia, Northern India, Nepal, Northern Myanmar, Vietnam, Southeastern China, North Korea, South Korea, Japan, Southeastern Australia, Northern New Zealand (7.93×10^5 km^2)	Southern North America, Northern and Eastern South America, Southern and Eastern Africa, Western and Central Europe, Southeastern Asia, Eastern Australia (2.04×10^6 km^2)
RCP8.5 (Total area is 2.96×10^6 km^2)	Eastern United States, Eastern Brazil, Western Germany, Western Netherlands, Western Denmark, Ireland, United Kingdom, Southeastern France, Belgium, Northern India, Northern Myanmar, Eastern Coast of Vietnam, Southern Coast of China, China Taiwan, Southwestern Korea, Southern Japan (1.44×10^5 km^2)	Eastern United States, Eastern Brazil, Eastern Argentina, Eastern Germany, Eastern Netherlands, Eastern Denmark, Western Poland, Western Ukraine, Uruguay, Southern Sweden, Northern Italy, United Kingdom, France, Czech Republic, Hungary, Romania, Bulgaria, Northern Turkey, Georgia, Northern India, Nepal, Northern Myanmar, Vietnam, Southeastern China, North Korea, South Korea, Japan, Southeastern Australia, Northern New Zealand (7.74×10^5 km^2)	Southern North America, Northern and Eastern South America, Southern and Eastern Africa, Western and Central Europe, Southeastern Asia, Eastern Australia (2.04×10^6 km^2)

The curves show the mean response of the 10 replicate MaxEnt runs. Red indicates the average value and blue indicates ± SD.

Discussion

The highly and moderately suitable areas of *L. erysimi* under current climatic conditions in our study were mainly distributed at 15°-65°N and 15°-55°S, and are distributed in the Americas, Europe, Asia, and Australia, with concentrations in China, the United States, France, India, and so on, which is generally consistent with the reported distribution of *L. erysimi* (Patel et al., 2004; Desneux et al., 2006; Adhab and Schoelz, 2015; Bai et al., 2022). It proves the reliability of the prediction software used in our study. The area of highly suitable area of *L. erysimi* increased in the United States and India and decreases in Korea under the RCP2.6. The area of highly suitable area of *L. erysimi* increased in India and decreased in the United States and Korea under the RCP4.5. The area of highly suitable area of *L. erysimi* in France was reduced under the RCP8.5. The range and area of highly suitable area of *E. corollae* under the current climate conditions are smaller than that of *L. erysimi*, mainly distributed in 23.5-65°N and 30-55°S. The area of highly suitable area of *E. corollae* decreases remarkably under the three future climate conditions. China Taiwan, changes from a highly suitable area to a moderately suitable area, and the area of highly suitable area in northern India and northern Myanmar decreases. India is the third largest producer of rapeseed mustard, accounting for 19.8% of global acreage and 9.8% of total production, and damage by *L. erysimi* can result in up to 90% yield loss (Palial et al., 2022). Most of India is suitable for *L. erysimi* under current climatic conditions, and the suitable area for *L. erysimi* in India will increase under the RCP2.6 and RCP4.5. Whereas, *E. corollae* only be suitable in a small area in northern India, and its suitable area will decrease in future climatic conditions, which may increase the difficulty of using *E. corollae* for biological control of *L. erysimi* in India. Zhang et al. (2022a) Predicting the distribution of the Asian Longhorned Beetle, *Anoplophora glabripennis* (Coleoptera: Cerambycidae) and its natural enemies in China. The results showed that the Northern China (e.g., Xinjiang, Gansu, and Inner Mongolia), where *A. glabripennis* causes more serious damage, is also a

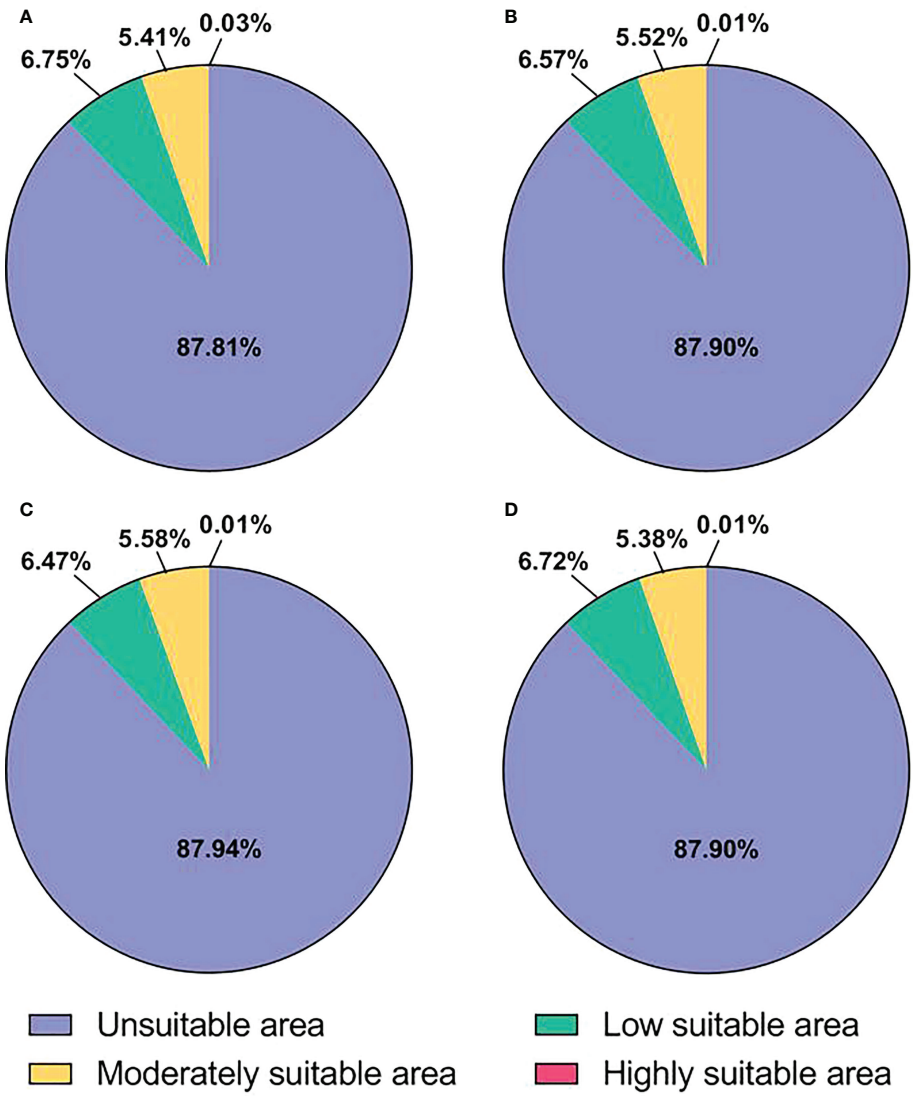

FIGURE 4
Proportion of suitable area for *E. corollae*. **(A)**, Current climatic conditions. **(B)**, RCP2.6 climatic conditions. **(C)**, RCP4.5 climatic conditions. **(D)**, RCP8.5 climatic conditions.

potential suitable area for *Dastarcus helophoroides* and *Dastarcus major*, which provides a potential strategy for the management of *A. glabripennis*. In our study, the suitable area of *E. corollae* in Western Europe, southern China, eastern United States, Japan, and Korea partially overlap with those of the *L. erysimi*, it is speculated that the use of *E. corollae* for *L. erysimi* control in these areas may present a good effect.

Environmental variables act on species distributions at spatial scales that vary in size, and at relatively large scales, species interactions are often weakened and climatic variables play a major role (Hortal et al., 2010). Insects are poikilotherm, and temperature is crucial to their development. The distribution of insects and the number of generations in different regions can be inferred by measuring the developmental temperature and effective accumulation temperature of insects. In addition, humidity is closely related to insect life activities such as pupation, fledging, and evaporation of water from insects (Eberle et al., 2022). The two most critical environmental variables affecting the potential geographic distribution of *L. erysimi* in our study were Bio1 (Annual average temperature) and Bio12 (Annual average precipitation), and the two most critical environmental variables affecting the potential geographic distribution of *E. corollae* were Bio1 (Annual average temperature) and Bio6

TABLE 4 The regions and area of suitable area for *E. corollae*.

	Highly suitable area	Moderately suitable area	Low suitable area
Current (Total area is 1.76×10^6 km^2)	Northern India, Eastern Nepal, Northern Myanmar, China Taiwan, China, Southern Japan (3.69×10^3 km^2)	Eastern United States, Western Canada, Southern Chile, Iceland, Ireland, United Kingdom, France, Germany, Belgium, Netherlands, Denmark, Poland, Ukraine, Georgia, Czech Republic, Hungary, Romania, Bulgaria, Greece, Italy, Norway, Southern Sweden, Southern Finland, Northern Spain, Northern Portugal, Northern India, Nepal, Northern Myanmar, Southeastern China, South Korea, Japan (7.85×10^5 km^2)	Northwestern and Southeastern North America, Southern South America, Eastern and Southern Europe, Southeastern Asia, Southern Australia (9.80×10^5 km^2)
RCP2.6 (Total area is 1.75×10^6 km^2)	Northern India, Northern Myanmar, Central Japan (1.13×10^3 km^2)	Eastern United States, Western Canada, Southern Chile, Iceland, Ireland, United Kingdom, France, Germany, Belgium, Netherlands, Denmark, Poland, Ukraine, Georgia, Czech Republic, Hungary, Romania, Bulgaria, Greece, Italy, Norway, Southern Sweden, Southern Finland, Northern Spain, Northern Portugal, Northern India, Nepal, Northern Myanmar, Southeastern China, South Korea, Japan (8.01×10^5 km^2)	Northwestern and Southeastern North America, Southern South America, Eastern and Southern Europe, Southeastern Asia, Southern Australia (9.53×10^5 km^2)
RCP4.5 (Total area is 1.75×10^6 km^2)	Northern India, Northern Myanmar, Central Japan (1.13×10^3 km^2)	Eastern United States, Western Canada, Southern Chile, Iceland, Ireland, United Kingdom, France, Germany, Belgium, Netherlands, Denmark, Poland, Ukraine, Georgia, Czech Republic, Hungary, Romania, Bulgaria, Greece, Italy, Norway, Southern Sweden, Southern Finland, Northern Spain, Northern Portugal, Northern India, Nepal, Northern Myanmar, Southeastern China, South Korea, Japan (8.10×10^5 km^2)	Northwestern and Southeastern North America, Southern South America, Eastern and Southern Europe, Southeastern Asia, Southern Australia (9.39×10^5 km^2)
RCP8.5 (Total area is 1.76×10^6 km^2)	Northern India, Northern Myanmar, Central Japan (1.26×10^3 km^2)	Eastern United States, Western Canada, Southern Chile, Iceland, Ireland, United Kingdom, France, Germany, Belgium, Netherlands, Denmark, Poland, Ukraine, Georgia, Czech Republic, Hungary, Romania, Bulgaria, Greece, Italy, Norway, Southern Sweden, Southern Finland, Northern Spain, Northern Portugal, Northern India, Nepal, Northern Myanmar, Southeastern China, South Korea, Japan (7.80×10^5 km^2)	Northwestern and Southeastern North America, Southern South America, Eastern and Southern Europe, Southeastern Asia, Southern Australia (9.74×10^5 km^2)

(Lowest temperature in the coldest month). The suitableness of *L. erysimi* was the highest when the annual average temperature was 10°C-20°C. The suitableness of *L. erysimi* was the highest when the annual average precipitation was 1000 mm, and then decrease with the increase of annual average precipitation. Studies have shown that the optimum temperature of *L. erysimi* is at or below 20°C. Cloudy and cold weather is helpful to the development of *L. erysimi* (Singh et al., 2007). The occurrence of *L. erysimi* is severe in dry weather and the number of *L. erysimi* is inversely proportional to relative humidity when humidity is high (Mishra and Kanwat, 2018), the predicted results of our study are consistent with this result. The two most critical environmental variables influencing the distribution of *E. corollae* are both temperatures, with the highest suitableness at the annual average temperature of 10°C and the lowest temperature in the coldest month of 0°C, and *E. corollae* has been found to maintain egg production and predation at temperatures as low as 12°C (Moerkens et al., 2021), but no studies on the predatory performance of *E. corollae* at low temperatures have been reported, and it is speculated that conditions of 10°C-15°C may be conducive to the predation, development, and reproduction of *E. corollae*.

The MaxEnt ecological niche model has some limitations in that it only analyzes the influence of abiotic factors on species distribution, while in reality species distribution is also influenced by biotic factors (Wang et al., 2019). *L. erysimi*

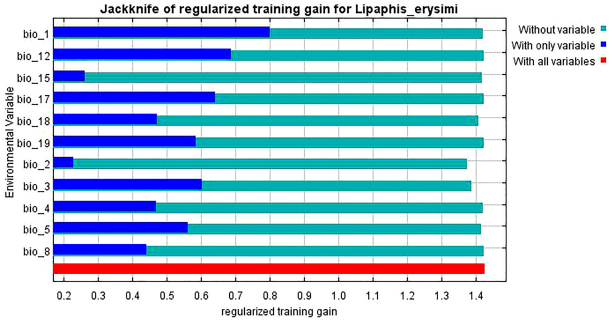

FIGURE 5
Evaluation of environmental variables affecting the distribution of *L. erysimi* by Jackknife test.

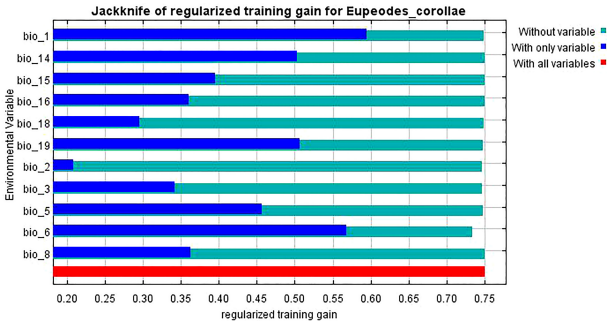

FIGURE 6
Evaluation of environmental variables affecting the distribution of *E. corollae* by Jackknife test.

often follows seedlings dispersed by anthropogenic transfer, thus the actual distribution range is larger than predicted (Zhao et al., 2022a). In addition, if there is excessive humidity in the field or continuous rainfall, the aphids will be washed away and die in large numbers by the rain, leading to a reduction in the population density of *E. corollae* due to lack of food (Putra and Yasuda, 2006).

In conclusion, this study used the geographic distribution data of the historical occurrence of *L. erysimi* and *E. corollae* to project their potential distribution areas under current and future climates based on the MaxEnt model, and analyzed the key environmental factors affecting the survival and spread of both, concluding that RCP2.6 and RCP4.5 will be favorable for the survival and spread of *L. erysimi*, but will inhibit the spread of the natural enemy *E. corolla*; Low temperatures favor the predation of *E. corollae* but also promote the occurrence of *L. erysimi*; High humidity reduces population densities of *L. erysimi* and *E. corolla*; Therefore, we should fully consider

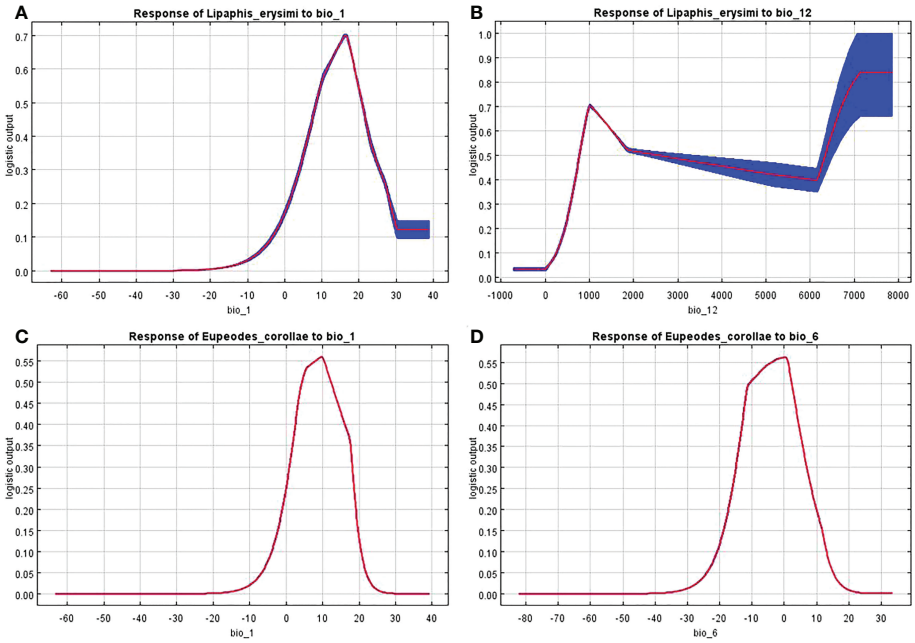

FIGURE 7
Response curve of distribution probability of *L. erysimi* and *E. corollae* to bioclimatic factors. **(A)**, Response curve of *L. erysimi* to Bio1. **(B)**, Response curve of *L. erysimi* to Bio12. **(C)**, Response curve of *E. corollae* to Bio1. **(D)**, Response curve of *E. corollae* to Bio6.

the temperature and humidity in the field when using *E. corolla* to control *L. erysimi* and develop a scientific and reasonable control strategy. This study can provide theoretical and data support for the monitoring and early warning and biological control of *L. erysimi*.

Data availability statement

The original contributions presented in the study are included in the article/supplementary material. Further inquiries can be directed to the corresponding author.

Author contributions

YL, AW, SP, JJ, XY and SZ participated in the study design and analysis of the manuscript. JL, SY and RZ participated in the study design and helped to draft the manuscript. Supervision and financial support by SZ, revised and processed. All authors contributed to the article and approved the submitted version.

Funding

This study was supported by Hainan Major Science and Technology Project (ZDKJ201901). Hainan Province Science and Technology Special Fund (ZDYF2022XDNY163).

Conflict of interest

The authors declare that the research was conducted in the absence of any commercial or financial relationships that could be construed as a potential conflict of interest.

Publisher's note

All claims expressed in this article are solely those of the authors and do not necessarily represent those of their affiliated organizations, or those of the publisher, the editors and the reviewers. Any product that may be evaluated in this article, or claim that may be made by its manufacturer, is not guaranteed or endorsed by the publisher.

References

Adhab, M. A., and Schoelz, J. E. (2015). Report of the turnip aphid, *Lipaphis erysimi* (Kaltenbach 1843) from Missouri, USA. *J. Plant Prot. Sci.* 55, 327–328. doi: 10.1515/jppr-2015-0035

Bai, P. H., Hu, R. R., Bian, D. B., Liu, B. S., Li, N., and Hu, C. F. (2022). Laboratory toxicity evaluation of *Vitex negundo* extracts on *Lipaphis erysimi*. *Tianjin Agric. Sci.* 28, 57–60. doi: 10.3969/j.issn.1006-6500.2022.S.014

Barreca, A. I. (2012). Climate change, humidity, and mortality in the united states. *J. Environ. Econ Manage.* 63, 19–34. doi: 10.1016/j.jeem.2011.07.004

Barry, S., and Elith, J. (2006). Error and uncertainty in habitat models. *J. Appl. Ecol.* 43, 413–423. doi: 10.1111/j.1365-2664.2006.01136.x

Beck, J., Böller, M., Erhardt, A., and Schwanghart, W. (2014). Spatial bias in the GBIF database and its effect on modeling species' geographic distributions. *Ecol. Inform.* 19, 10–15. doi: 10.1016/j.ecoinf.2013.11.002

Chattopadhyay, C., Agrawal, R., Kumar, A., Singh, Y. P., Roy, S. K., Khan, S. A., et al. (2005). Forecasting of *Lipaphis erysimi* on oilseed brassicas in India–a case study. *Crop Prot.* 24, 1042–1053. doi: 10.1016/j.cropro.2005.02.010

Davis, J. J. (1914). New or little known species of aphididae. *Can. Entomol.* 46, 226–236. doi: 10.4039/Ent46226-7

Desneux, N., Rabasse, J. M., Ballanger, Y., and Kaiser, L. (2006). Parasitism of canola aphids in France in autumn. *J. Pest Sci.* 79, 95–102. doi: 10.1007/s10340-006-0121-1

Dong, K., Dong, Y., and Luo, Y. Z. (2004). Studies on the developmental zero temperature and effective accumulated temperature of *Syrphus corollae* fabricius. *J. Yunnan Agric. Univ.* 19, 177–178+198. doi: 10.16211/j.issn.1004-390x (n).2004.02.013

Dong, Z., He, Y., Ren, Y., Wang, G., and Chu, D. (2022). Seasonal and year-round distributions of *Bactrocera dorsalis* (Hendel) and its risk to temperate fruits under climate change. *Insects* 13, 550. doi: 10.3390/insects13060550

Eberle, S., Schaden, L. M., Tintner, J., Stauffer, C., and Schebeck, M. (2022). Effect of temperature and photoperiod on development, survival, and growth rate of mealworms, *Tenebrio molitor*. *Insects* 13, 321. doi: 10.3390/insects13040321

Elith, J., Phillips, S. J., Hastie, T., Dudík, M., Chee, Y. E., and Yates, C. J. (2011). A statistical explanation of MaxEnt for ecologists. *Divers. Distrib.* 17, 43–57. doi: 10.1111/j.1472-4642.2010.00725.x

Fick, S. E., and Hijmans, R. J. (2017). WorldClim 2: new 1-km spatial resolution climate surfaces for global land areas. *Int. J. climatol.* 37, 4302–4315. doi: 10.1002/joc.5086

Fielding, A. H., and Bell, J. F. (1997). A review of methods for the assessment of prediction errors in conservation presence/absence models. *Environ. Conserv.* 24, 38–49. doi: 10.1017/S0376892997000088

He, J. L., Sun, X. Q., Gui, L. M., and Ye, W. J. (1990). A preliminary study on the biology of *Eupeodes corollae* fabricius in shanghai. *J. Shanghai Agric. Univ.* 8, 221–228+234.

Hortal, J., Roura- Pascual, N., Sanders, N. J., and Rahbek, C. (2010). Understanding (insect) species distributions across spatial scales. *Ecography.* 33, 51–53. doi: 10.1111/j.1600-0587.2009.06428.x

Khaliq, A. M., Javed, M., Sohail, M., and Sagheer, M. (2014). Environmental effects on insects and their population dynamics. *J. Entomol. Zool Stud.* 2, 1–7.

Koramutla, M. K., Aminedi, R., and Bhattacharya, R. (2016). Comprehensive evaluation of candidate reference genes for qRT-PCR studies of gene expression in mustard aphid, *Lipaphis erysimi* (Kalt). *Sci. Rep.* 6, 1–10. doi: 10.1038/srep25883

Li, Z., Liu, Y., and Zeng, H. (2022). Application of the MaxEnt model in improving the accuracy of ecological red line identification: A case study of zhanjiang, China. *Ecol. Indic.* 137, 108767. doi: 10.1016/j.ecolind.2022.108767

Li, G. T., Zhang, F. S., and Gao, J. F. (1996). Observation on the biological characteristics of *Eupeodes corollae* fabricius. *J. Jilin Agric. Univ.* 18, 154–157. doi: 10.13327/j.jjlau.1996.s1.051

Liu, Y., Zhou, K., and Xia, Q. (2018). A MaxEnt model for mineral prospectivity mapping. *Nat. Resour. Res.* 27, 299–313. doi: 10.1007/s11053-017-9355-2

Mishra, S. K., and Kanwat, P. M. (2018). Seasonal incidence of mustard aphid, *Lipaphis erysimi* (Kalt) and its major predator on mustard and their correlation with abiotic factors. *J. Entomol. Zool Stud.* 6, 831–836.

Moerkens, R., Boonen, S., Wäckers, F. L., and Pekas, A. (2021). Aphidophagous hoverflies reduce foxglove aphid infestations and improve seed set and fruit yield in sweet pepper. *Pest Manage. Sci.* 77, 2690–2696. doi: 10.1002/ps.6342

Palial, S., Kumar, S., Atri, C., Sharma, S., and Banga, S. S. (2022). Antixenosis and antibiosis mechanisms of resistance to turnip aphid, *Lipaphis erysimi* (Kaltenbach) in *Brassica juncea-fruticulosa* introgression lines. *J. Pestic. Sci.* 95, 749–760. doi: 10.1007/s10340-021-01418-8

Pasiecznik, N. M., Smith, I. M., Watson, G. W., Brunt, A. A., Ritchie, B., and Charles, L. M. F. (2005). CABI/EPPO distribution maps of plant pests and plant diseases and their important role in plant quarantine. *Bull. Oepp.* 35, 1–7. doi: 10.1111/j.1365-2338.2005.00815.x

Patel, S. R., Awasthi, A. K., and Tomar, R. K. S. (2004). Assessment of yield losses in mustard (*Brassica juncea* l.) due to mustard aphid (*Lipaphis erysimi* kalt.) under different thermal environments in Eastern central India. *Appl. Ecol. Environ. Res.* 2, 1–15. doi: 10.15666/aeer/02001015

Pearson, R. G., Raxworthy, C. J., Nakamura, M., and Townsend Peterson, A. (2007). Predicting species distributions from small numbers of occurrence records: a test case using cryptic geckos in Madagascar. *J. Biogeogr.* 34, 102–117. doi: 10.1111/j.1365-2699.2006.01594.x

Pekas, A., Craecker, D. I., Boonen, S., Wäckers, F. L., and Moerkens, R. (2020). One stone; two birds: concurrent pest control and pollination services provided by aphidophagous hoverflies. *Biol. Control.* 149, 104328. doi: 10.1016/j.biocontrol.2020.104328

Phillips, S. J., Anderson, R. P., and Schapire, R. E. (2006). Maximum entropy modeling of species geographic distributions. *Ecol. Modell.* 190, 231–259. doi: 10.1016/j.ecolmodel.2005.03.026

Phillips, S. J., and Dudík, M. (2008). Modeling of species distributions with maxent: new extensions and a comprehensive evaluation. *Ecography.* 31, 161–175. doi: 10.1111/j.0906-7590.2008.5203.x

Putra, N. S., and Yasuda, H. (2006). Effects of prey species and its density on larval performance of two species of hoverfly larvae, *Episyrphus balteatus* de geer and *Eupeodes corollae* fabricius (Diptera: Syrphidae). *Appl. Entomol. Zool.* 41, 389–397. doi: 10.1303/aez.2006.389

Rana, J. S. (2005). Performance of *Lipaphis erysimi* (Homoptera: Aphididae) on different brassica species in a tropical environment. *J. Pestic. Sci.* 78, 155–160. doi: 10.1007/s10340-005-0088-3

Reza, M. D. W., Biswas, A. K., and Roy, K. (2004). Seasonal abundance of *Lipaphis erysimi* (Kalt.) population on mustard. *Uttar. Pradesh J. Zoology.* 24, 129–132.

Sillero, N. (2011). What does ecological modelling model? a proposed classification of ecological niche models based on their underlying methods. *Ecol. Modell.* 222, 1343–1346. doi: 10.1016/j.ecolmodel.2011.01.018

Singh, R., Singh, D., and Rao, V. U. M. (2007). Effect of abiotic factors on mustard aphid (*Lipaphis erysimi* kalt.) on Indian brassica. *Indian J. Agric. Sci.* 41, 67–70.

Van Vuuren, D. P., Edmonds, J., Kainuma, M., Riahi, K., Thomson, A., Hibbard, K., et al. (2011). The representative concentration pathways: an overview. *Clim. Change.* 109, 5–31. doi: 10.1007/s10584-011-0148-z

Wang, R., Yang, H., Luo, W., Wang, M., Lu, X., Huang, T., et al. (2019). Predicting the potential distribution of the Asian citrus psyllid, *Diaphorina citri* (Kuwayama), in China using the MaxEnt model. *PeerJ.* 7, e7323. doi: 10.7717/peerj.7323

Warren, D. L., and Seifert, S. N. (2011). Ecological niche modeling in maxent: the importance of model complexity and the performance of model selection criteria. *Ecol. Appl.* 21, 335–342. doi: 10.1890/10-1171.1

Welch, K. D., and Harwood, J. D. (2014). Temporal dynamics of natural enemy–pest interactions in a changing environment. *Biol. Control.* 75, 18–27. doi: 10.1016/j.biocontrol.2014.01.004

Yackulic, C. B., Chandler, R., Zipkin, E. F., Royle, J. A., and Nichols, J. D. (2013). Presence-only modelling using MAXENT: when can we trust the inferences? *Methods Ecol. Evol.* 4, 236–243. doi: 10.1111/2041-210x.12004

Yamamura, K., Yokozawa, M., Nishimori, M., Ueda, Y., and Yokosuka, T. (2006). How to analyze long-term insect population dynamics under climate change: 50-year data of three insect pests in paddy fields. *Popul. Ecol.* 48, 31–48. doi: 10.1007/s10144-005-0239-7

Zhang, Y., Hughes, A. C., Zhao, Z., Li, Z., and Qin, Y. (2022b). Including climate change to predict the global suitable area of an invasive pest: *Bactrocera correcta* (Diptera: Tephritidae). *Glob. Ecol. Conserv.* 34, e02021. doi: 10.1016/j.gecco.2022.e02021

Zhang, Q. C., Wang, J. G., and Lei, Y. H. (2022a). Predicting distribution of the Asian longhorned beetle, anoplophora glabripennis (Coleoptera: Cerambycidae) and its natural enemies in China. *Insects* 13, 687. doi: 10.3390/insects13080687

Zhao, Q., Gao, X. Y., Cai, B., Chen, C., and Wei, J. F. (2022a). Potential distribution of *Diatraea saccharalis* in China based on max ent model. *Plant Quarantine* 36, 77–82. doi: 10.19662/j.cnki.issn1005-2755.2021.00.032

Zhao, Y., Wang, J. G., Chen, C., Mao, Q. Y., Huang, H. C., Cai, H., et al. (2022b). Study on the potential distribution area of *Diaphorina citri* (Kuwayama) in yunnan based on max ent niche model. *J. Yunnan Agric. Univ. (Natural Science).* 37, 61–68. doi: 10.12101/j.issn.1004-390X(n).202012003

frontiers | Frontiers in Plant Science

TYPE Original Research
PUBLISHED 12 December 2022
DOI 10.3389/fpls.2022.1083848

OPEN ACCESS

EDITED BY
Julian Chen,
Institute of Plant Protection (CAAS), China

REVIEWED BY
Javad Karimi,
Ferdowsi University of Mashhad, Iran
Yanhui Lu,
Zhejiang Academy of Agricultural Sciences, China

*CORRESPONDENCE
Su Wang
wangsu@ipepbaafs.cn
Shu Li
lishu@ipepbaafs.cn

SPECIALTY SECTION
This article was submitted to Sustainable and Intelligent Phytoprotection, a section of the journal Frontiers in Plant Science

RECEIVED 29 October 2022
ACCEPTED 21 November 2022
PUBLISHED 12 December 2022

CITATION
Wang J, Yang Y, Li Y, Jin Z, Desneux N, Han P, Wang S and Li S (2022) Direct and indirect effects of banker plants on population establishment of *Harmonia axyridis* and aphid control on pepper crop. *Front. Plant Sci.* 13:1083848. doi: 10.3389/fpls.2022.1083848

Direct and indirect effects of banker plants on population establishment of *Harmonia axyridis* and aphid control on pepper crop

Jie Wang[1,2], Yajie Yang[1], Yuanxi Li[2], Zhenyu Jin[3], Nicolas Desneux[4], Peng Han[5], Su Wang[1]* and Shu Li[1]*

[1]Institute of Plant Protection, Beijing Academy of Agriculture and Forestry Sciences, Beijing, China, [2]Department of Entomology, College of Plant Protection, Nanjing Agricultural University, Nanjing, China, [3]Forewarning and Management of Agricultural and Forestry Pest, Hubei Engineering Technology Center and College of Agriculture, Yangtze University, Jingzhou, China, [4]Université Côte d'Azur, INRAE, CNRS, UMR ISA, Nice, France, [5]Yunnan Key Laboratory of Plant Reproductive Adaptation and Evolutionary Ecology /Institute of Biodiversity, School of Ecology and Environmental Sciences, Yunnan University, Kunming, China

Banker plant systems increase biological pest control by supporting populations of natural enemies, i.e., using non-pest arthropod species as alternative prey. However, the presence of alternative prey does not always result in improved control of the target pest species owing to the complexity of biotic interactions. To increase the effectiveness of banker plants in IPM programs, a fine understanding of the indirect interactions between target aphid and alternative prey mediated by biocontrol agents is necessary. In this study, we first established a banker plant system, banker plant (*Vicia faba*)–alternative prey (*Megoura japonica*)–predator (*Harmonia axyridis*), to control the target pest (*Myzus persicae*) on pepper. We found that *M. japonica* strongly preferred faba bean as a host plant and posed no risk to *Solanaceous* crops. *Harmonia axyridis* adults had no significant predation preference for the alternative prey. In the short term, the interaction direction of the two aphid species depended on the relative initial density and the timescale. *Harmonia axyridis* showed a stronger negative effect on *M. persicae* than that on *M. japonica*. In the long term, the presence of alternative prey, *M. japonica*, enhanced the control effect of *H. axyridis* to *M. persicae* with initial density of 100–500 aphids per plant. The presence of the alternative prey could proliferate the population of *H. axyridis*, with from 0.2- to 2.1-fold increase of *H. axyridis* eggs. Overall, we put forward a strategy for setting the initial density of alternative prey of the banker plant system to target the high and low density of aphids, which highlighted the importance of indirect interactions in designing a proper banker plant system.

KEYWORDS

aphid, banker plants, IPM, indirect interaction, population quantitative relationship

Introduction

Conservation biological control (CBC) could enhance the survival, longevity, and fecundity of natural enemies by habitat management to increase their effectiveness in pest control (Gurr et al., 2017). The key to an effective CBC is an early colonization and establishment of natural enemies in crops, when pest populations are still at low densities (Symondson et al., 2002). Different types of functional plants have been proposed to support natural enemies, increasing the efficiency and sustainability of biological control of pests (Xie et al., 2012; Zhao et al., 2017; Hatt et al., 2018; Hatt et al., 2019b; Damien et al., 2020). As an important form of CBC, banker plant system could preserve populations of beneficial arthropods in crops by providing alternative prey/hosts and could provide an on-farm refuge for spontaneous populations for sustainably effective pest control (Frank, 2010; Huang et al., 2011; Li et al., 2015). The use of banker plant systems has been increasingly investigated and developed for greenhouse and field crops (Zheng et al., 2017; Xu et al., 2020; Chen et al., 2022). However, research studies mainly focus on the establishment of the banker plant system (Wang et al., 2020; Wang et al., 2021), and further research is needed to understand the quantitative relationship among trophies when the banker plant system applied to pest control (Li et al., 2020).

The population dynamic of species in ecosystem not only depends on the direct feeding behavior in food web (Symondson et al., 2002) but also on the indirect interaction among species (Montoya et al., 2009; Zhang et al., 2019). In agroecosystem, preys without direct resource competition could have indirect interaction mediated by shared natural enemies (van Veen et al., 2006; Frost et al., 2016; Holt and Bonsall, 2017). These interactions affect the predator's predation in the short term (Desneux and O'Neil, 2008; Jaworski et al., 2013) and even direct the predator and prey population dynamics in the long term (e.g., apparent competition, Holt, 1977; Jaworski et al., 2015; Desneux et al., 2019). Understanding how pests, alternative prey, and natural enemy interact in complex managed environments is essential to the pest management in agriculture (Chailleux et al., 2014). When the banker plant system is used to control the target pests in the field, there is no direct resource competition between the alternative prey and the target pests. Whether the indirect interaction mediated by the shared natural enemies affects the population dynamics is still uncovered.

Depending on the temporal or spatial scale, the behavior of prey, and the quality and density of prey, the natural enemy–mediated indirect interactions can take different forms, such as apparent competition, mutualism, amensalism, and commensalism (Chaneton and Bonsall, 2000; Chailleux et al., 2014). Natural enemy–mediated indirect interactions contribute to pest population dynamics, and insufficient efforts have been made to generate predictions that would facilitate the use of indirect interactions in biological control in different spatial scales (Chailleux et al., 2014). On a large scale, maintaining a high level of biodiversity has been proved to promote the growth of natural enemies of pests and improve the control of target pests (Karp et al., 2018). Small-scale experiments show that natural enemies benefit from mixed food by alternative prey (Liu et al., 2006; Messelink et al., 2008). Many studies have also shown that alternative prey/food can help natural enemy populations establish in crops before pest arrival (Gurr et al., 2016; Jaworski et al., 2019; Sanchez et al., 2021). Whereas alternative prey could induce a decrease in pest densities in crops through indirect interactions with a shared natural enemy (i.e., apparent competition) (Liu et al., 2006; Desneux and O'Neil, 2008), generalist predators are widely used as biocontrol agents to regulate populations of pest in agriculture (Symondson et al., 2002; van Lenteren, 2012). When the alternative prey is applied to pest biological control programs, it is necessary to clarify the indirect interactions induced by the generalist predators (Chailleux et al., 2014; Costa and Anjos, 2020).

This study aims to identify the quantitative relationship among trophies when the banker plant system applied to pest control. Targeting the widely distributed and important pest of protected vegetables, *Myzus persicae* (Aparicio et al., 2020; Wang et al., 2022), we explored the interactions when the *Harmonia axyridis* banker plant system was applied to *M. persicae* control. We hypothesized that (1) *Harmonia axyridis* adults do not show predation preference for the two aphid species; (2) the direction, sign, and strength of the indirect interactions mediated by shared predator between the two aphid species depends on the relative initial density and time; (3) the alternative prey, *M. japonica*, preserve populations of *H. axyridis* and provide sustainably effective pest control in caged study.

Materials and methods

Insects and plants

Initial colonies of the green peach aphid (*Myzus persicae*), the bean aphid (*Megoura japonica*), and the harlequin ladybird (*Harmonia axyridis*) were collected from Beijing Noah Organic Farm (116°59′E, 40°6′N), Beijing, China. The aphids, *M. persicae*, was reared on *Capsicum annuum* var. Zhongjiao 105 (Institute of Vegetables and Flowers, CAAS), and *M. japonica* was reared on *Vicia faba* var. Kexi (Sichuan Kexi Seed Co., Ltd.). The ladybeetle *H. axyridis* was reared in cages (35 × 35 × 55 cm) made of nylon mesh net and aluminum alloy frames. They were fed *ad libitum* with *M. japonica* reared on faba bean plants. All colonies were kept at 25 ± 2°C, 60 ± 5% relative humidity (RH), 16-hour light: 8-h dark (L16:D8-h) photoperiod in the insectary of the Institute of Plant Protection, Beijing Academy of Agriculture and Forestry Sciences (BAAFS). The culture environment was regulated using an automatic environmental management system (LT-100, Suntech, Beijing, China).

The tomato, eggplant, and pepper seedlings were grown in plastic trays (54 × 28 × 6 cm, 21 plants per tray) and transplanted individually in plastic pots once they reached 15 cm in height.

All plants were cultured individually in plastic pots (H = 25 cm, D = 15 cm) with commercial substrate (Pindstrup®) at 25 ± 2°C, 60 ± 5% RH, and L16:D8-h photoperiod. The tomato, eggplant, and pepper plants reaching 30–35 cm in height with five to seven fully expanded true leaves, and faba bean plants with five to seven fully expanded true leaves were used for experiments.

Evaluating *Megoura japonica* fitness on faba bean

Newborn nymph (<12 h) of *Megoura japonica* were placed individually on the back of faba bean leaves in plastic Petri dish (H = 1.5 cm, D = 5 cm). The leaves bases were covered with absorbent cotton to moisturize. Dishes were kept in the laboratory at 25 ± 2°C, 60 ± 5% RH, and L16:D8 h. The leaves were replaced every 2 days. Development and survival data were recorded daily. The presence of an exuvium was used as the criterion for molting to the next developmental stage. After the emergence of adults, the number of newborn nymphs was recorded and the nymphs were removed from the dishes daily until the death of the adult. One hundred newborn nymphs were used for the life table study (n = 100).

Host specificity of *Megoura japonica*

A choice experiment was conducted to evaluate the host specificity of *M. japonica* to the faba bean and three *Solanaceous* vegetables (tomato, eggplant, and pepper). One 2.5-cm (in diameter) leaf disc of each plant was placed on the wet filter paper with an equal distance between them to form a square in a plastic Petri dish (H = 1.5 cm, D = 9 cm). Thirty third-instar nymphs of *M. japonica* were released onto the center of the filter paper. Dishes were kept in the laboratory at 25 ± 2°C, 60 ± 5% RH, and L16:D8 h. The number of *M. japonica* on each leaf disc (treatment) was counted at 3, 6, 12, and 24 h after the release of aphids into the Petri dish. The position of different leaf discs was determined randomly and rotated in each replication. The experiment was a randomized complete block design and replicated 16 times (n = 16).

A survival experiment was conducted to determine survival or development of *M. japonica* on different host plants (faba bean, tomato, eggplant, and pepper). Ten fourth-instar nymphs of *M. japonica* were introduced to the head of the potted plant with five to seven fully expanded true leaves. Each plant was placed randomly at an interval of 3 m in a greenhouse. The greenhouse was maintained at 26 ± 2°C, 70 ± 10% RH, and L16:D8 h. The number of *M. japonica* that survived on each plant of different host plants was recorded at 24, 48, 72, and 96 h. Each treatment (host plant) was replicated 10 times (n = 10).

Predation preference of *Harmonia axyridis* to *Myzus persicae* and *Megoura japonica*

On the basis of the daily predation of *H. axyridis* adults on *M. persicae* and *M. japonica*, we set five levels of prey complex. The total number of preys per dish remained constant at 180. The ratios tested of *M. persicae* and *M. japonica* were 180:0, 120:60, 90:90, 60:120, and 0:180. In each experimental unit, third-instar nymphs of *M. persicae* and *M. japonica* were randomly chosen from the stock colony reared in the laboratory and carefully transferred onto a Petri dish (9 cm in diameter) using a fine brush for 1 h of acclimatization, after which one newly hatched (< 24 h) adult of *H. axyridis* was added to the center of the dish. Male and female *H. axyridis* were tested separately. All adults suffered starving for 24 h before being used in preference experiments. The experiments were conducted in the laboratory (25 ± 1°C, 65 ± 5% RH, and L16:D8 h). After 24 h, each prey type consumed by the predator was counted. Ten replicates were prepared for each prey complex (n = 10).

Interaction between two aphids when the application of banker plant system

In greenhouse, we studied the dynamic relationship, interaction direction, sign, and strength of the predator (*H. axyridis*), alternative prey (*M. japonica*), and target pest (*M. persicae*) when banker plant system applied to *M. persicae* control using a 2 x 2 factorial design (Figure 1). The first three-level treatment varied the alternative prey density (0, 200, and 400 per plant). The second three-level treatment varied the target pest density (100, 300, and 500 per plant) in the microcosms. One potted pepper and faba bean were set oppositely in a microcosm (35 × 35 × 55 cm). Third-instar nymphs of *M. persicae* and *M. japonica* were randomly chosen from the colonies reared in the laboratory and released on the pepper and faba bean plant, respectively. After 1 day of acclimatization, one pair newly hatched (<24 h) adults of *H. axyridis* was released. Population dynamics of the three insect species were monitored 39 days following the introduction of predators. Adults and nymphs of *H. axyridis*, *M. persicae*, and *M. japonica* were counted on all leaves every 3 days. Plants were fertilized and watered to avoid any abiotic stress. Each treatment was repeated 15 times (n = 15).

Data analysis

According to Özgökçe et al. (2018), the life table raw data were analyzed using the computer program TWOSEX-MSChart (Chi, 2017b) based on the age-stage, two-sex life table theory

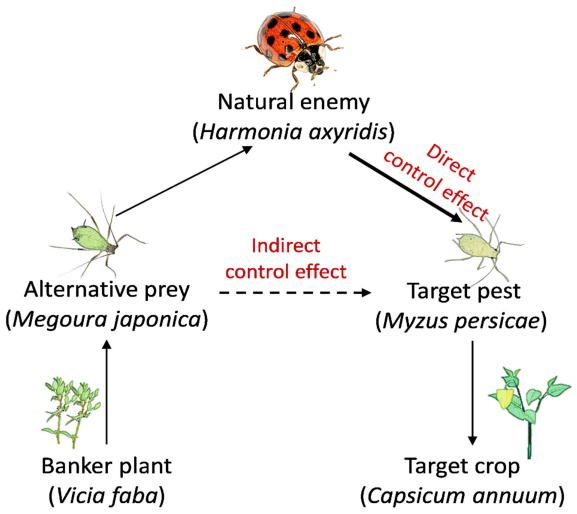

FIGURE 1
The scheme of the interaction of the predator (*Harmonia axyridis*), alternative prey (*Megoura japonica*), and target pest (*Myzus persicae*) when the banker plant system applied to biological aphid control on pepper.

(Chi and Liu, 1985; Chi, 1988). The variances and standard errors of the developmental time, fecundity, longevity, and population parameters were estimated using the bootstrap technique (Efron and Tibshirani, 1993) with 100,000 resampling. The bootstrap routine is embedded in the TWOSEX program. The difference between treatments was examined by using paired bootstrap test (Efron and Tibshirani, 1993).

The data obtained from the host specificity experiments did not follow normal distribution (Shapiro–Wilk test, $P< 0.05$) and/or homoscedasticity (Bartlett's test, $P< 0.05$), and Friedman test and Kruskal–Wallis test was used to compare the differences among treatments for the choice rate of *M. japonica* on different plants in laboratory choice experiments and number of *M. japonica* colonizing on different plants in greenhouse, respectively.

Manly's model was used to estimate the predation preference of *H. axyridis* to *M. japonica* and *M. persicae* at different prey ratios. Manly (1973) equation:

$$\beta j = \frac{\ln(r_j/A_j)}{\sum_{i=1}^{n}\ln(r_i/A_i)}$$

A_i was the number of individuals of a given prey type i available for predation by *H. axyridis* (= total number of prey available for predation) and r_i was the number of a prey type i that has not been attacked. The number of prey types was $n = 2$ and $\beta_j = 1/n$ when prey was chosen randomly.

The Wilcoxon signed-rank test of two related samples in non-parametric test was used to compare the predation preference of *H. axyridis*, and the Mann–Whitney U-test of two independent samples was used to compare the difference in predation preference between male and female adults ($P< 0.05$).

To differentiate long-term from short-term interactions between preys, the data were divided into two time periods. Short-term interactions were assessed on days 0–9 and long-term interactions on days until the end of experiments according to the predation pressure in the system.

Log response ratios (RRs) were used separately for each aphid species as a measure of the strength of the negative impact of predation, and mean ratios of the log abundance of the two aphid species were used as a measure of the symmetry of the impact of predation on each aphid species (Gelman and Hill, 2007). The impacts of predation at each treatment level were compared with the control (no alternative prey, *M. japonica*). Log RRs was also used to estimate the log-proportional difference between the mean of a particular treatment level and that of a control (Hedges et al., 1999). For each experiment, the mean ratios of log abundance at each treatment level of different sampling days were tested for significant differences from the control without alternative prey using *t*-test.

A delta correction (RRΔ) and its variance [var (RRΔ)] were used on the basis of the standard deviation (SD), sample size (N), and mean (X) of the treatment (T) and control (C) following Lajeunesse (2015):

$$\mathrm{RR}^{\Delta} = \ln\frac{\overline{X_T}}{\overline{X_C}} + \frac{1}{2}\left[\frac{(\mathrm{SD_T})^2}{N_T\bar{X}_T^2} - \frac{(\mathrm{SD_C})^2}{N_C\bar{X}_C^2}\right]$$

$$\mathrm{var(RR\Delta)} = \left[\frac{(\mathrm{SD_T})^2}{N_T\bar{X}_T^2} + \frac{(\mathrm{SD_C})^2}{N_C\bar{X}_C^2}\right] + \frac{1}{2}\left[\frac{(\mathrm{SD_T})^4}{N_T^2\bar{X}_T^4} + \frac{(\mathrm{SD_C})^4}{N_C^2\bar{X}_C^4}\right]$$

As the ladybird abundance data did not follow normal distribution (Shapiro–Wilk test, $P< 0.05$) and/or homoscedasticity (Bartlett's test, $P< 0.05$), Kruskal–Wallis test was used to compare the differences among treatments. All statistical analyses were performed using SPSS 25.0 (SPSS Inc., Chicago, IL, USA).

Results

Megoura japonica fitness on faba bean

The developmental times, longevity, reproductive periods, and fecundity of *M. japonica* on faba bean are shown in Table 1. The developmental time periods of the pre-adult and adult stage were 5.63 ± 0.08 days and 15.03 ± 0.95 days, respectively. The longevity and reproductive periods were 19.02 ± 0.99 days and 9.14 ± 0.53 days, respectively. The fecundity was 44.09 ± 3.34 offspring (Table 1).

TABLE 1 The developmental, longevity, and fecundity of *Megoura japonica* fed on faba bean.

Parameters	Development stage	n	Mean ± SE
Developmental time (days)	First instar	100	1.00 ± 0.02
	Second instar	100	1.12 ± 0.02
	Third instar	95	1.41 ± 0.03
	Fourth instar	90	2.12 ± 0.03
	Pre-adult	90	5.63 ± 0.08
	Adult	90	15.03 ± 0.95
Longevity (days)	Adult	90	19.02 ± 0.99
Reproductive period (days)	Adult	90	9.14 ± 0.53
Fecundity (offspring)	Adult	90	44.09 ± 3.34

Host specificity of *Megoura japonica*

Megoura japonica significantly preferred faba bean leaf disc in the laboratory choice experiments (3H: $X^2 = 39.146$, $P< 0.001$; 6H: $X^2 = 33.064$, $P< 0.001$; 12H: $X^2 = 39.992$, $P< 0.001$; 24H: $X^2 = 30.157$, $P< 0.001$). The number of *M. japonica* chose faba bean increased over time, whereas the number of *M. japonica* on eggplant, pepper, and tomato decreased rapidly over time (Figure 2A). *Megoura japonica* developed better on the faba bean plants than that on the *Solanaceae* crops. The population size of the bean aphid on faba bean plants reached the 3.5 times of the initial value after 96 h, whereas the population size on eggplant, pepper, and tomato decreased significantly (24H: $X^2 = 29.431$, $P< 0.001$; 48H: $X^2 = 33.056$, $P< 0.001$; 72H: $X^2 = 37.981$, $P< 0.001$; 96H: $X^2 = 37.956$, $P< 0.001$). Although the number of *M. japonica* on tomato plants was significantly higher than that on eggplant and pepper at 24 h, they almost went extinction on eggplant, pepper, and tomato at 72 h, indicating that those plants were unsuitable hosts for *M. japonica* (Figure 2B).

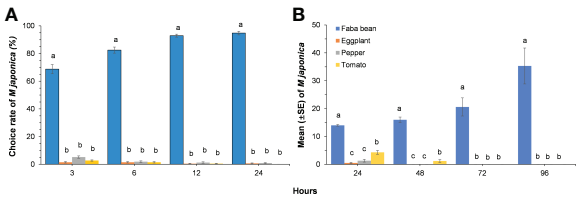

FIGURE 2
The choice rate of *Megoura japonica* on different plants over time in laboratory choice experiments **(A)** and mean (± SE) of *Megoura japonica* colonizing on different plants in greenhouse **(B)**. Means capped with different letters in the same sampling time are significantly different ($P < 0.05$; Friedman test for choice rate and Kruskal–Wallis test for mean of *M. japonica*) among treatments.

Predation preference

Predation preference of *H. axyridis* strongly depended on prey relative abundance with a disproportionately high predation on the most abundant prey (Figures 3A, C). On the basis of the analyses of Manly's Beta values (β_j), predation preference did not change across various *M. persicae* and *M. japonica* relative prey ratios (Figures 3B, D). Female *H. axyridis* consumed a slightly higher number of prey than male, but Manly's Beta values were no significant difference between genders (60:120 *M. persicae*:*M. japonica*, $P = 0.560$; 90:90 *M. persicae*:*M. japonica*, $P = 0.845$; 120:60 *M. persicae*:*M. japonica*, $P = 0.46$).

Interactions between aphids in short term

When the initial density of *M. persicae* is low (100 aphids per plant) (i.e., the initial density of *M. persicae* is less than that of *M. japonica*.), the density of *M. persicae* is significantly different at the same time ($X^2 = 22.182$, $P< 0.001$) but no interaction between time ($X^2 = 2.431$, $P = 0.051$). The density of *M. persicae* was significantly higher than that of the control on the sixth and ninth days (6 days: $X^2 = 25.068$, $P< 0.001$; 9 days: $X^2 = 24.227$, $P< 0.001$; Figure 4A). When the initial density of *M. persicae* is medium (300 aphids per plant), the density of *M. persicae* among treatments is significantly different at the same time ($X^2 = 6.357$, $P = 0.002$). In addition, the density of *M. persicae* was significantly higher than that of the control on the ninth day (3 days: $X^2 = 2.638$, $P = 0.267$; 6 days: $X^2 = 5.439$, $P = 0.066$; 9 days: $X^2 = 6.145$, $P = 0.046$; Figure 4B). With higher initial density of *M. persicae* (500 aphids per plant), no significant difference was found among treatments ($X^2 = 0.392$, $P = 0.676$) and sampling times (3 days: $X^2 = 0.383$, $P = 0.826$; 6 days: $X^2 = 0.127$, $P = 0.939$; 9 days: $X^2 = 1.127$, $P = 0.569$; Figure 4C).

Predator-mediated interaction intensity on *Myzus persicae*

On the basis of the density of *M. persicae* in control without alternative prey, the effect of *H. axyridis* on *M. persicae* varied from positive to negative with the increase of the initial density of *M. persicae*, and the positive effect increased as the initial density of the alternative prey, *M. japonica* (Figure 5). The negative impact of predation for *M. persicae* weakened with time at low initial density (Figure 5A). At intermediate and higher initial density, the negative impact of predation on the target prey *M. persicae* weakened with time and initial density of alternative prey (Figures 5B, C).

The log abundance of *M. persicae* and *M. japonica* was significantly different among treatments (Figures 5D–F). On day

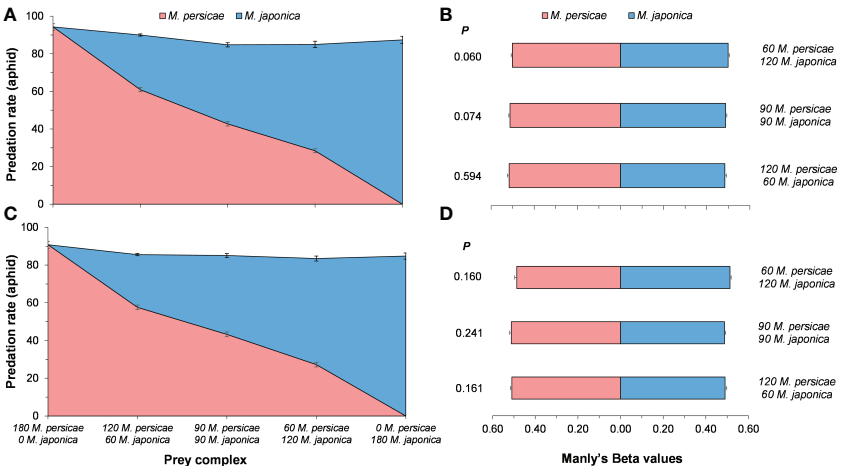

FIGURE 3
Mean (± SE) of consumed *Myzus persicae* and *Megoura japonica*, predation preference of female **(A, B)** and male **(C, D)** *Harmonia axyridis* in various prey complex. Wilcoxon signed-rank test of two related samples in non-parametric test was used to compare the predation preference of *H. axyridis*.

3, the mean ratio of treatments with higher initial density of *M. persicae* (500:200 *M. persicae*:*M. japonica* and 500:400 *M. persicae*:*M. japonica*) were marginally greater than 1 (Figures 5D–F). Whereas the treatments with higher initial density of *M. persicae* on day 3 were significantly greater than that of the control (100:200 *M. persicae*:*M. japonica*, $P < 0.000$; 100:400 *M. persicae*:*M. japonica*, $P < 0.001$; Figure 5D). With the increase of time, the mean ratio of the log abundance of *M. persicae* and *M. japonica* was lower than 1 (Figures 5D–F). This indicated that different initial density of alternative prey had a more significant negative impact on *M. persicae* than that on *M. japonica*. Moreover, the treatments with lower initial density of *M. persicae* on days 6 and 9 were significantly greater than that of the control (Figures 5D–F). The mean ratio of treatment (300:200 *M. persicae*:*M. japonica*, 0.73 ± 0.01) on day 9 was significantly lower than that of the control (0.98 ± 0.02, $t = -2.45$, $P = 0.01$).

Effect of banker plant on *Myzus persicae* population dynamics

Overall, a higher number of *M. persicae* were registered throughout the duration of the experiment with than that without alternative prey (Figure 6). At low initial density, the population of *M. persicae* in control decreased and subsided on the 18th day. Whereas the population of *M. persicae* in treatments with alternative prey increased and then decreased, reaching the peak on the ninth day, which was 1.7 times of the initial density (Figure 6A). The population of *M. persicae* in control at intermediate and higher initial density decreased and subsided before the treatments with *M. japonica* (Figures 6B, C).

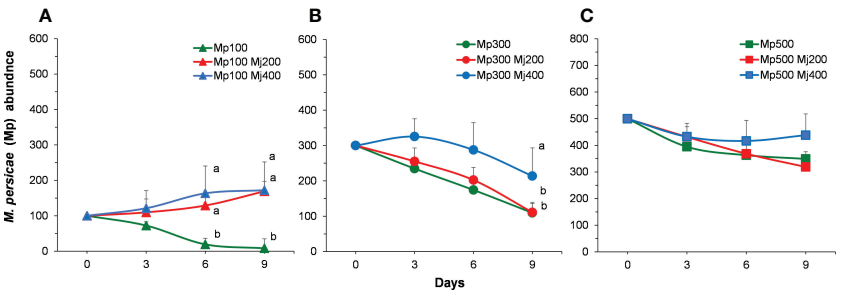

FIGURE 4
Population abundance of *Myzus persicae* (Mp) in different treatments with the initial density of *M. persicae* is 100 **(A)**, 300 **(B)**, and 500 **(C)**. Mj, *Megoura japonica*. Different letters next to the curves indicate significant differences among treatments (P<0.05).

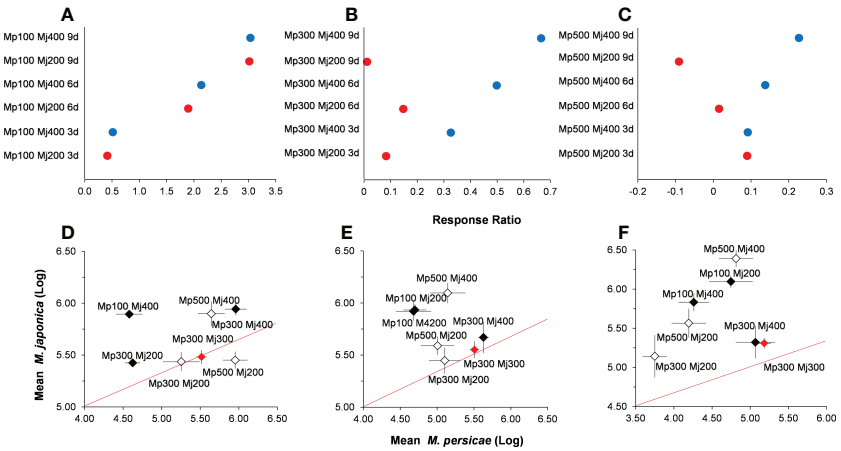

FIGURE 5
Relationships among the relative abundance of *Myzus persicae* (Mp) and *Megoura japonica* (Mj) in different treatments for log response ratios with the initial density of *M. persicae* is 100 **(A)**, 300 **(B)**, and 500 **(C)**, and sampling after 3 **(D)**, 6 **(E)**, and 9 **(F)** days.

Effect of the banker plant system on *Harmonia axyridis* abundance

Harmonia axyridis was sustained by the alternative prey and varied with different initial density in the system (Figure S1). The predator egg abundance was positively related to the total initial density of aphids (F= 42.893, df =11,133, P< 0.001; Figure S2A). In addition, the total initial density of aphids positively affected the hatching rate and net reproductive rate of *H. axyridis* egg (F = 7.673, df =11,133, P=0.006; Figure S2B; F= 31.824, df =11,133, P< 0.001; Figure S2C).

Discussion

The banker plant system, integrating the essence of augmentative and CBC, has been widely used to aid establishment, development, and dispersal of beneficials employed in pest biological control (Parolin et al., 2012; Miller et al., 2018; Wang et al., 2021; Ardanuy et al., 2022). However, the size of the founder population of the banker plant system has received little attention despite their importance in biological control efficacy and adoption (Sanchez et al., 2021). In this study, we explored the dynamic relationship and interaction degree of the predator (*H. axyridis*), alternative prey (*M. japonica*), and target pest (*M. persicae*). We found that the interaction direction of the two aphids depends on the relative initial density and time. *Harmonia axyridis* showed a stronger negative effect on *M. persicae* than that on *M. japonica*. *Megoura japonica* with different initial densities had different effects on the proliferation of *H. axyridis*. During the whole experimental period, the presence of alternative prey, *M. japonica*, enhanced the control effect of *H. axyridis* to *M. persicae* with initial density of 100–500 aphids per plant.

Alternative prey generally has been shown to enhance predator densities and to have a negative effect on the population of another

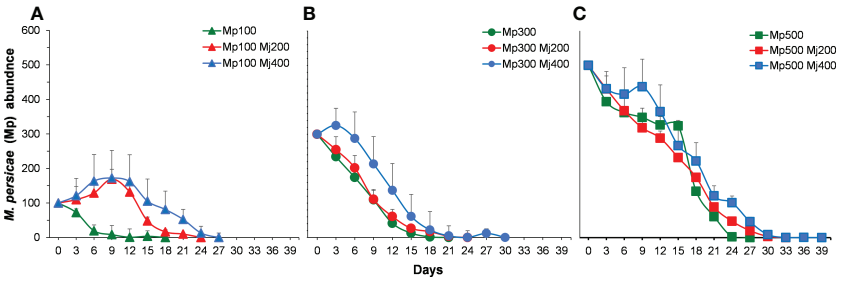

FIGURE 6
Population abundance of *Myzus persicae* (Mp) in different treatments through the whole term with the initial density of *M. persicae* is 100 **(A)**, 300 **(B)**, and 500 **(C)**. Mj, *Megoura japonica*.

prey species, resulting in increased biocontrol services on target pests in agroecosystems (Desneux and O'Neil, 2008; Eubanks and Finke, 2014; Ramirez and Eubanks, 2016; Wang et al., 2021). When alternative prey and target pests co-existed, the spatial location of the two prey species may reduce the efficiency of indirect interactions, especially likely when the alternative prey is provided by using mulch or banker plants (Chailleux et al., 2014). Therefore, understanding how alternative prey and beneficials interact when banker plant was used is essential for pest management programs. On the timescale of this study, the interaction direction of the two aphids is related to the relative initial density and time. *Harmonia axyridis* showed a stronger negative effect on *M. persicae* than that on *M. japonica*. However, the highest hatching rate of *H. axyridis* eggs is 26.12%, which indicates that intraguild predation (IGP) may occur in the system. Previous experience of cannibalism did not increase further cannibalism frequency of *H. axyridis* (Ovchinnikov et al., 2019). Some studies have shown that intraspecific predation would negatively affect the predator numerical response, resulting in different forms indirect interactions (Holt and Lawton, 1994; Liu et al., 2006). Conversely, supplementing non-prey food resources, such as floral resources (e.g., marigold), could reduce IGP of *H. axyridis* in agroecosystems (Liang et al., 2022).

Predators could affect the colonization and abundance of a single prey by direct predation (i.e., consumptive effects) and by altering prey activity, behavior, and development (i.e., non-consumptive effects) (Orrock et al., 2008). Moreover, predator's habit (e.g., predation preference) could also modify the strength, the direction, and the symmetry of indirect interactions among preys (Holt and Bonsall, 2017). If the predator has no preference, then the indirect interaction mediated by shared predator among preys would change from negative to positive due to the predator satisfaction or prey switching (Abrams and Matsuda, 1996; Jaworski et al., 2015). As predator preference leads to apparent competition, a critical first step was to establish if there was predator preference between the two prey species (Jaworski et al., 2013; Emery and Mills, 2020). Our results indicated that *H. axyridis* adults show no preference for the two aphid species when their densities varied in a short period (i.e., 24 h).

The RRs could quantify the effect size of predation prey individually in proportion to their abundance in the controls. This also served as an initial indicator of potential asymmetrical effects between the two aphid species (Desneux et al., 2019; Emery and Mills, 2020). We found that the interaction direction and intensity of *H. axyridis* predation on the two aphids in the system were related to the relative initial density of the two aphid species and timescales. The negative effect of *H. axyridis* on *M. persicae* was stronger than that of *M. japonica* in the short term (9 days). In addition, consistent with the results of the study by Abrams and Matsuda (1996), we found that the interaction direction between the two aphid species changed with different initial density ratio. The *t*-test of the mean ratios of the log abundance of two preys could be used to test for asymmetry in comparison with the mean ratios of the control treatments (Emery and Mills, 2020). Nevertheless, we used the *t*-test with control without alternative prey and found that the effect of *H. axyridis* on *M. persicae* changed from positive to negative with the increase of the initial density of *M. persicae*, and the positive effect increased with the increase of the initial density of *M. japonica*.

The asymmetric interaction between the two aphids mediated by *H. axyridis* may be related to the predation rate on different aphids or the asymmetric non-consumption effect of prey (Emery and Mills, 2020). We found that, although the initial density of *M. persicae* is high, the alternative prey generally trended to upward and the *M. persicae* shows a downward trend in the long term. Although *H. axyridis* adults did not show predation preference in Petri dishes, we do not take in consideration the effect of living plants on predation preference. Studies have shown that plant morphology impacts the activity and prey availability of predatory ladybugs (Grevstad and Klepetka, 1992). According to the experimental observation, *Myzus persicae* is the apical meristem scattered in pepper plants, whereas *M. japonica* are evenly distributed in faba bean plants, which may lead to differences in predation on different aphids, causing the asymmetric effect of *H. axyridis* impact on two aphids. Although the literature on short-term interaction has received less attention, it may have negative effects on biological control (Bompard et al., 2013; Chailleux et al., 2014; Blubaugh et al., 2018; Emery and Mills, 2020). Our study confirmed that the existence of alternative prey did not affect the control effect of *H. axyridis* on *M. persicae*.

Studies on indirect interaction mediated by shared natural enemies mainly focused on two pests on one plant (Liu et al., 2006; Bompard et al., 2013; Jaworski et al., 2015), leading to a hard discrimination between indirect interactions and resource competition (Bompard et al., 2013). Noonburg and Byers (2005) showed that the negative competitive impact of invasive species on native species is more likely to be apparent competition than resource competition. Meanwhile, Jones et al. (2009) stated that the effect of resource competition is higher than that of apparent competition in ecosystem. In our research, two preys apparently do not experience resource competition, but only indirect interaction mediated by shared predators. If natural enemies can quickly gather in habitat patches containing two preys with high density, then short-term apparent competition will also appear, and its mechanism is controlled by spatial effects (Holt and Lawton, 1994). However, we failed to test spatial effects in this study. In addition, the environmental factors (e.g., fertilizer application and climate warming) could also modulate natural enemy-mediated indirect interactions between pests, which could trigger multiple indirect bottom-up effects and increase both interspecific competition and overall biocontrol service (Han et al., 2019; Han et al., 2020; Han et al., 2022).

The establishment of biological control agents in the banker plant system is a probabilistic event that depends on the size of the founder population and the banker plant species (Sanchez et al., 2021). Compared with other studies in which mix-stage

predators were introduced (Messelink et al., 2008; Bompard et al., 2013; Jaworski et al., 2015; Han et al., 2020), only one pair of *H. axyridis* adults was released. Allee effects had been suggested, which led to the decline of the suitability of predator population in the banker plant system (Sanchez et al., 2021). Therefore, the possible Allee effects may account for the differences in the effect of banker the plant system on *H. axyridis* abundance. Moreover, the timely replacement of banker plant may enhance the establishment of biological control agents in the banker plant system. Studies have proved that early planting and timely replanting of functional plants (e.g., repellent plants) in crops would ensure a more effective and suitable pest control (Hatt et al., 2019a; Wang et al., 2022).

Studies have shown that it is difficult to distinguish the negative effects of experiments from the operational problems related to complex experimental design, and it is difficult to detect the strongly apparent competition effect through experiments (Chaneton and Bonsall, 2000). Consequently, apparent competition and mutualism can be methodologically dissected in this food web when the banker plant system was applied to aphid control. This work adds to the previous literature on indirect food web interactions and the potentially indirect benefits of the banker plant system in pest management programs (Chailleux et al., 2014). On the basis of the co-effects of different initial density of alternative prey on target pest and the proliferation of predator, *H. axyridis*, we put forward two strategies for pest biological control. When the density of target prey is low, higher density of alternative prey in the banker plant system could enhance population buildup of beneficials without affecting the control effect on pest. When the density of target prey is high, lower density of alternative prey could directly support population of beneficials and facilitate indirectly the potential negative effect (i.e., apparent competition) on target pest in the ecosystem. Overall, we put forward a strategy for setting the initial density of alternative prey of the banker plant system to target the high and low density of aphids, which highlighted the importance of indirect interactions in designing a proper banker plant system.

Data availability statement

The raw data supporting the conclusions of this article will be made available by the authors, without undue reservation.

Author contributions

SW, SL, and JW conceived the research. JW, SL, and YY performed the experiments. JW, SL, and SW analyzed the data. JW, SL, YY, YL, ZJ, ND, PH, and SW wrote the manuscript. All authors contributed to the article and approved the submitted version.

Funding

This study was sponsored by projects of the Youth Program of National Natural Science Foundation of China (32202372), the Beijing Key Laboratory of Environment Friendly Management on Fruit Diseases and Pests in North China, the National Natural Science Foundation of China (32001904), the Technical Innovation Program of Beijing Academy of Agriculture and Forestry Sciences (KJCX20200110), the Major Science and Technology Program of China Tobacco Corporation (11020210104LS-06), and the Beijing Technology Program (Z201100008020014).

Acknowledgments

The authors acknowledge technical assistance related to analyzing the data from Dr. Huang Ningxing from the Institute of Plant Protection, Beijing Academy of Agriculture and Forestry Sciences, and capturing theory form Dr. Jaworski Coline C. from the Department of Zoology, University of Cambridge.

Conflict of interest

The authors declare that the research was conducted in the absence of any commercial or financial relationships that could be construed as a potential conflict of interest.

Publisher's note

Supplementary material

The Supplementary Material for this article can be found online at: https://www.frontiersin.org/articles/10.3389/fpls.2022.1083848/full#supplementary-material

References

Abrams, P. A., and Matsuda, H. (1996). Positive indirect effects between prey species that share predators. *Ecology* 77 (2), 610–616. doi: 10.2307/2265634

Aparicio, Y., Gabarra, R., and Arno, J. (2020). Interactions among *Myzus persicae*, predators and parasitoids may hamper biological control in Mediterranean peach orchards. *Entomol. Gen.* 40 (3), 217–228. doi: 10.1127/entomologia/2020/0946

Ardanuy, A., Figueras, M., Matas, M., Arnó, J., Agustí, N., Alomar, Ò., et al. (2022). Banker plants and landscape composition influence colonisation precocity of tomato greenhouses by mirid predators. *J. Pest Sci.* 95, 447–459. doi: 10.1007/s10340-021-01387-y

Blubaugh, C. K., Asplund, J. S., Eigenbrode, S. D., Morra, M. J., Philips, C. R., Popova, I. E., et al. (2018). Dual-guild herbivory disrupts predator-prey interactions in the field. *Ecology* 99 (5), 1089–1098. doi: 10.1002/ecy.2192

Bompard, A., Jaworski, C. C., Bearez, P., and Desneux, N. (2013). Sharing a predator: can an invasive alien pest affect the predation on a local pest? *Popul. Ecol.* 55 (3), 433–440. doi: 10.1007/s10144-013-0371-8

Chailleux, A., Mohl, E. K., Teixeira Alves, M., Messelink, G. J., and Desneux, N. (2014). Natural enemy-mediated indirect interactions among prey species: Potential for enhancing biocontrol services in agroecosystems. *Pest Manage. Sci.* 70 (12), 1769–1779. doi: 10.1002/ps.3916

Chaneton, E. J., and Bonsall, M. B. (2000). Enemy-mediated apparent competition: empirical patterns and the evidence. *Oikos* 88 (2), 380–394. doi: 10.1034/j.1600-0706.2000.880217.x

Chen, X., Jaworski, C. C., Dai, H., Liang, Y., Guo, X., Wang, S., et al. (2022). Combining banker plants to achieve long-term pest control in multi-pest and multi-natural enemy cropping systems. *J. Pest Sci.* 95, 685–697. doi: 10.1007/s10340-021-01428-6

Chi, H. (1917). TWOSEX-MSChart: A computer program for the age-stage, two-sex life table analysis. (Taichung: National Chung Hsing University). Available at: http://140.120.197.173/Ecology/Download/ Twosex-MSChart.rar.

Chi, H. (1988). Life-table analysis incorporating both sexes and variable development rates among individuals. *Environ. Entomol.* 17 (1), 26–34. doi: 10.1093/ee/17.1.26

Chi, H., and Liu, H. (1985). Two new methods for the study of insect population ecology. *Bull. Inst. Zool. Acad. Sin.* 24 (2), 225–240.

Chi, H., You, M., Atlıhan, R., Smith, C. L., Kavousi, A., Özgökçe, M. S., et al (2020). Age-stage, two-sex life table: an introduction to theory, data analysis, and application. *Entomol. Gen.* 40 (2), 103–24. doi: 10.1127/entomologia/2020/0936

Chi, H., Güncan, A., Kavousi, A., Gharakhani, G., Atlihan, R., Özgökçe, MS., et al (2022). TWOSEX-MSChart: the key tool for life table research and education. *Entomol. Gen.* in press. doi: 10.1127/entomologia/2022/1851

Costa, M. I. S., and Anjos, L. (2020). The occurrence of apparent competition and apparent mutualism in a modeled greenhouse system with two non-competing pests and a shared biocontrol agent. *Neotrop. Entomol.* 49 (6), 874–881. doi: 10.1007/s13744-020-00820-8

Damien, M., Llopis, S., Desneux, N., van Baaren, J., and Le Lann, C. (2020). How does floral nectar quality affect life history strategies in parasitic wasps? *Entomol. Gen.* 40 (2), 147–156. doi: 10.1127/entomologia/2020/0906

Desneux, N., Kaplan, I., Yoo, H. J. S., Wang, S., and O'Neil, R. J. (2019). Temporal synchrony mediates the outcome of indirect effects between prey *via* a shared predator. *Entomol. Gen.* 39 (2), 127–136. doi: 10.1127/entomologia/2019/0824

Desneux, N., and O'Neil, R. J. (2008). Potential of an alternative prey to disrupt predation of the generalist predator, *Orius insidiosus*, on the pest aphid, *Aphis glycines*, *via* short-term indirect interactions. *Bull. Entomol. Res.* 98 (6), 631–639. doi: 10.1017/S0007485308006238

Efron, B., and Tibshirani, R. J. (1993). *An Introduction to the Bootstrap* (New York, USA: Chapman & Hall Inc).

Emery, S. E., and Mills, N. J. (2020). Effects of predation pressure and prey density on short-term indirect interactions between two prey species that share a common predator. *Ecol. Entomol.* 45 (4), 821–830. doi: 10.1111/een.12855

Eubanks, M. D., and Finke, D. L. (2014). Interaction webs in agroecosystems: beyond who eats whom. *Curr. Opin. Insect Sci.* 2, 1–6. doi: 10.1016/j.cois.2014.06.005

Frank, S. D. (2010). Biological control of arthropod pests using banker plant systems: past progress and future directions. *Biol. Control* 52 (1), 8–16. doi: 10.1016/j.biocontrol.2009.09.011

Frost, C. M., Peralta, G., Rand, T. A., Didham, R. K., Varsani, A., and Tylianakis, J. M. (2016). Apparent competition drives community-wide parasitism rates and changes in host abundance across ecosystem boundaries. *Nat. Commun.* 7, 12644. doi: 10.1038/ncomms12644

Gelman, A., and Hill, J. (2007). *Data analysis using regression and multilevel/hierarchical models* (Cambridge, U. K: Cambridge University Press).

Grevstad, F. S., and Klepetka, B. W. (1992). The influence of plant architecture on the foraging efficiencies of a suite of ladybird beetles feeding on aphids. *Oecologia* 92 (3), 399–404. doi: 10.1007/BF00317466

Gurr, G. M., Lu, Z., Zheng, X., Xu, H., Zhu, P., Chen, G., et al. (2016). Multi-country evidence that crop diversification promotes ecological intensification of agriculture. *Nat. Plants* 2, 16014. doi: 10.1038/nplants.2016.14

Gurr, G. M., Wratten, S. D., Landis, D. A., and You, M. (2017). Habitat management to suppress pest populations: progress and prospects. *Annu. Rev. Entomol.* 62, 91–109. doi: 10.1146/annurev-ento-031616-035050

Han, P., Becker, C., Le Bot, J., Larbat, R., Lavoir, A. V., and Desneux, N. (2020). Plant nutrient supply alters the magnitude of indirect interactions between insect herbivores: From foliar chemistry to community dynamics. *J. Ecol.* 108 (4), 1497–1510. doi: 10.1111/1365-2745.13342

Han, P., Lavoir, A. V., Rodriguez-Saona, C., and Desneux, N. (2022). Bottom-up forces in agroecosystems and their potential impact on arthropod pest management. *Annu. Rev. Entomol.* 67, 239–259. doi: 10.1146/annurev-ento-060121-060505

Han, Z., Tan, X., Wang, Y., Xu, Q., Zhang, Y., Harwood, J. D., et al. (2019). Effects of simulated climate warming on the population dynamics of *Sitobion avenae* (Fabricius) and its parasitoids in wheat fields. *Pest. Manage. Sci.* 75 (12), 3252–3259. doi: 10.1002/ps.5447

Hatt, S., Uyttenbroeck, R., Lopes, T., Chen, J., Piqueray, J., Monty, A., et al. (2018). Effect of flower traits and hosts on the abundance of parasitoids in perennial multiple species wildflower strips sown within oilseed rape (*Brassica napus*) crops. *Arthropod. Plant Interact.* 12, 787–797. doi: 10.1007/s11829-017-9567-8

Hatt, S., Xu, Q., Francis, F., and Chen, J. (2019a). Intercropping oilseed rape with wheat and releasing *Harmonia axyridis* sex pheromone in northern China failed to attract and support natural enemies of aphids. *Biotechnol. Agron. Soc Environ.* 23 (3), 147–152. doi: 10.25518/1780-4507.17921

Hatt, S., Xu, Q., Francis, F., and Osawa, N. (2019b). Aromatic plants of East Asia to enhance natural enemies towards biological control of insect pests. A review. *Entomol. Gen.* 38 (4), 275–315. doi: 10.1127/entomologia/2019/0625

Hedges, L. V., Gurevitch, J., and Curtis, P. S. (1999). The meta-analysis of response ratios in experimental ecology. *Ecology* 80 (4), 1150–1156. doi: 10.1890/0012-9658(1999)080[1150:TMAORR]2.0.CO;2

Holt, R. D. (1977). Predation, apparent competition, and the structure of prey communities. *Theor. Popul. Biol.* 12 (2), 197–129. doi: 10.1016/0040-5809(77)90042-9

Holt, R. D., and Bonsall, M. B. (2017). Apparent competition. *Annu. Rev. Ecol. Evol. Syst.* 48, 447–471. doi: 10.1146/annurev-ecolsys-110316022628

Holt, R. D., and Lawton, J. H. (1994). The ecological consequences of shared natural enemies. *Annu. Rev. Ecol. Syst.* 25, 495–520. doi: 10.1146/annurev.es.25.110194.002431

Huang, N., Enkegaard, A., Osborne, L. S., Ramakers, P. M. J., Messelink, G. J., Pijnakker, J., et al. (2011). The banker plant method in biological control. *Crit. Rev. Plant Sci.* 30 (3), 259–278. doi: 10.1080/07352689.2011.572055

Jaworski, C. C., Bompard, A., Genies, L., Amiens-Desneux, E., and Desneux, N. (2013). Preference and prey switching in a generalist predator attacking local and invasive alien pests. PloS *One* 8 (12), e82231. doi: 10.1371/journal.pone.0082231

Jaworski, C. C., Chailleux, A., Bearez, P., and Desneux, N. (2015). Apparent competition between major pests reduces pest population densities on tomato crop, but not yield loss. *J. Pest Sci.* 88 (4), 793–803. doi: 10.1007/s10340-015-0698-3

Jaworski, C. C., Xiao, D., Xu, Q., Ramirez-Romero, R., Guo, X., Wang, S., et al. (2019). Varying the spatial arrangement of synthetic herbivore-induced plant volatiles and companion plants to improve conservation biological control. *J. Appl. Ecol.* 56 (5), 1176–1188. doi: 10.1111/1365-2664.13353

Jones, T. S., Godfray, H. C., and van Veen, F. J. (2009). Resource competition and shared natural enemies in experimental insect communities. *Oecologia* 159 (3), 627–635. doi: 10.1007/s00442-008-1247-z

Karp, D. S., Chaplin-Kramer, R., Meehan, T. D., Martin, E. A., DeClerck, F., Grab, H., et al. (2018). Crop pests and predators exhibit inconsistent responses to surrounding landscape composition. *Proc. Natl. Acad. Sci. U.S.A.* 115 (33), 7863–7870. doi: 10.1073/pnas.1800042115

Lajeunesse, M. J. (2015). Bias and correction for the log response ratio in ecological meta-analysis. *Ecology* 96 (8), 2056–2063. doi: 10.1890/14-2402.1

Liang, Y., Chen, X., Dai, H., Wang, J., Guo, X., Wang, S., et al. (2022). Flower provision reduces intraguild predation between predators and increases aphid biocontrol in tomato. *J. Pest Sci.* 95, 461–472. doi: 10.1007/s10340-021-01396-x

Li, S., Tan, X., Desneux, N., Benelli, G., Zhao, J., Li, X., et al. (2015). Innate positive chemotaxis to pollen from crops and banker plants in predaceous biological control agents: Towards new field lures? *Sci. Rep.* 5, 12729. doi: 10.1038/srep12729

Liu, C., Yan, L., Li, H., and Wang, G. (2006). Effects of predator-mediated apparent competition on the population dynamics of *Tetranychus urticae* on apples. *BioControl* 51 (4), 453–463. doi: 10.1007/s10526-005-4363-z

Li, S., Wang, J., Huang, N., Jin, Z., Wang, S., and Zhang, F. (2020). Research progress and prospect on banker plant systems of predators for biological control. *Sci. Agric. Sin.* 53 (19), 3975–3987. doi: 10.3864/j.issn.0578-1752.2020.19.011

Manly, B. F. J. (1973). A linear model for frequency-dependent selection by predators. *Res. Popul. Ecol.* 14, 137–150. doi: 10.1007/BF02518839

Messelink, G. J., van Maanen, R., van Steenpaal, S. E. F., and Janssen, A. (2008). Biological control of thrips and whiteflies by a shared predator: Two pests are better than one. *Biol. Control* 44 (3), 372–379. doi: 10.1016/j.biocontrol.2007.10.017

Miller, P., Tracey, L., and Rebek, E. J. (2018). Banker plants for aphid biological control in greenhouses. *J. Integr. Pest Manage.* 9, 1–8. doi: 10.1093/jipm/pmy002

Montoya, J. M., Woodward, G., Emmerson, M. C., and Sole, R. V. (2009). Press perturbations and indirect effects in real food webs. *Ecology* 90 (9), 2426–2433. doi: 10.1890/08-0657.1

Noonburg, E. G., and Byers, J. E. (2005). More harm than good: when invader vulnerability to predators enhances impact on native species. *Ecology* 86 (10), 2555–2560. doi: 10.1890/05-0143

Orrock, J. L., Grabowski, J. H., Pantel, J. H., Peacor, S. D., Peckarsky, B. L., Sih, A., et al. (2008). Consumptive and nonconsumptive effects of predators on metacommunities of competing prey. *Ecology* 89 (9), 2426–2435. doi: 10.1890/07-1024.1

Ovchinnikov, A. N., Belyakova, N. A., Ovchinnikova, A. A., and Reznik, S. Y. (2019). Factors determining larval cannibalistic behavior in invasive and native populations of the multicolored Asian ladybird, *Harmonia axyridis*. *Entomol. Gen.* 38 (2), 243–254. doi: 10.1127/entomologia/2019/0702

Özgökçe, M. S., Chi, H., Atlıhan, R., and Kara, H. (2018). Demography and population projection of *Myzus persicae* (Sulz.) (Hemiptera: Aphididae) on five pepper (*Capsicum annuum* L.) cultivars. *Phytoparasitica* 46 (2), 169–169. doi: 10.1007/s12600-018-0651-0

Parolin, P., Bresch, C., Poncet, C., and Desneux, N. (2012). Functional characteristics of secondary plants for increased pest management. *Int. J. Pest Manage.* 58, 369–377. doi: 10.1080/09670874.2012.734869

Ramirez, R. A., and Eubanks, M. D. (2016). Herbivore density mediates the indirect effect of herbivores on plants *via* induced resistance and apparent competition. *Ecosphere* 7 (2), e01218. doi: 10.1002/ecs2.1218

Sanchez, J. A., López-Gallego, E., Pérez-Marcos, M., and Perera-Fernández, L. (2021). The effect of banker plants and pre-plant release on the establishment and pest control of *Macrolophus pygmaeus* in tomato greenhouses. *J. Pest Sci.* 94 (2), 297–307. doi: 10.1007/s10340-020-01257-z

Symondson, W. O., Sunderland, K. D., and Greenstone, M. H. (2002). Can generalist predators be effective biocontrol agents? *Annu. Rev. Entomol.* 47, 561–594. doi: 10.1146/annurev.ento.47.091201.145240

van Lenteren, J. C. (2012). The state of commercial augmentative biological control: plenty of natural enemies, but a frustrating lack of uptake. *BioControl* 57, 1–20. doi: 10.1007/s10526-011-9395-1

van Veen, F. J. F., Morris, R. J., and Godfray, H. C. (2006). Apparent competition, quantitative food webs, and the structure of phytophagous insect communities. *Annu. Rev. Entomol.* 51, 187–208. doi: 10.1146/annurev.ento.51.110104.151120

Wang, J., Li, S., Fang, Y., Zhang, F., Jin, Z., Desneux, N., et al. (2022). Enhanced and sustainable control of *Myzus persicae* by repellent plants in organic pepper and eggplant greenhouses. *Pest Manage. Sci.* 78 (2), 428–437. doi: 10.1002/ps.6681

Wang, J., Li, S., Yang, J., Guo, M., Dai, H., Ramirez-Romero, R., et al. (2021). The fitness of mass rearing food on the establishment of *Chrysopa pallens* in a banker plant system under fluctuating temperature conditions. *Insects* 12 (11), 1014 doi: 10.3390/insects12111014

Wang, Y., Yao, F., Soares, M. A., Basiri, S. E., Amiens-Desneux, E., Campos, M. R., et al. (2020). Effects of four non-crop plants on life history traits of the lady beetle *Harmonia axyridis*. *Entomol. Gen.* 40 (3), 243–252. doi: 10.1127/entomologia/2020/0933

Xie, H., Chen, J., Cheng, D., Zhou, H., Sun, J., Liu, Y., et al. (2012). Impact of wheat-mung bean intercropping on English grain aphid (Hemiptera: Aphididae) populations and its natural enemy. *J. Econ. Entomol.* 105 (3), 854–859. doi: 10.1603/ec11214

Xu, Q., Wang, S., Li, S., and Hatt, S. (2020). "Conservation biological control in organic greenhouse vegetables," in *Integrative biological control progress in biological control*. Eds. Y. Gao, H. M. Hokkanen and I. Menzler-Hokkanen (Cham, Switzerland: Springer). doi: 10.1007/978-3-030-44838-7_8

Zhang, Y., Fan, J., and Fu, Y. (2019). Plant-mediated interactions between two cereal aphid species: promotion of aphid performance and attraction of more parasitoids by infestation of wheat with phytotoxic aphid *Schizaphis graminum*. *J. Agric. Food Chem.* 67 (10), 2763–2773. doi: 10.1021/acs.jafc.8b06150

Zhao, J., Guo, X., Tan, X., Desneux, N., Lucia, Z., Zhang, F., et al. (2017). Using *Calendula officinalis* as floral resource to enhance aphid and thrips suppression by the flower bug *Orius sauteri* (Hemiptera: Anthocoridae). *Pest Manage. Sci.* 73, 515–520. doi: 10.1002/ps.4474

Zheng, X., Lu, Y., Zhu, P., Zhang, F., Tian, J., Xu, H., et al. (2017). Use of banker plant system for sustainable management of the most important insect pest in rice field in China. *Sci. Rep.* 7, 45581. doi: 10.1038/srep45581

frontiers | Frontiers in Plant Science

TYPE Original Research
PUBLISHED 09 January 2023
DOI 10.3389/fpls.2022.1100394

OPEN ACCESS

EDITED BY
Qingli Shang,
Jilin University, China

REVIEWED BY
Chuanwang Cao,
Independent researcher, China
Shaoying Wu,
Hainan University, China
Anna-Maria Botha-Oberholster,
Stellenbosch University, South Africa

*CORRESPONDENCE
Frédéric Francis
frederic.francis@uliege.be
Lanqin Xia
xialanqin@caas.cn

SPECIALTY SECTION
This article was submitted to Sustainable and Intelligent Phytoprotection, a section of the journal Frontiers in Plant Science

RECEIVED 16 November 2022
ACCEPTED 21 December 2022
PUBLISHED 09 January 2023

CITATION
Zhang J, Li H, Zhong X, Tian J, Segers A, Xia L and Francis F (2023) Silencing an aphid-specific gene *SmDSR33* for aphid control through plant-mediated RNAi in wheat. *Front. Plant Sci.* 13:1100394. doi: 10.3389/fpls.2022.1100394

Silencing an aphid-specific gene *SmDSR33* for aphid control through plant-mediated RNAi in wheat

Jiahui Zhang[1,2], Huiyuan Li[1,2], Xue Zhong[1,2], Jinfu Tian[1,2], Arnaud Segers[2], Lanqin Xia[1,3]* and Frédéric Francis[2]*

[1]Institute of Crop Sciences, Chinese Academy of Agricultural Sciences (CAAS), Beijing, China, [2]Functional and Evolutionary Entomology, Gembloux Agro-Bio Tech, University of Liege, Gembloux, Belgium, [3]National Nanfan Research Institute (Sanya), Chinese Academy of Agricultural Sciences/Hainan Yazhou Bay Seed Laboratory, Sanya, Hainan, China

Grain aphid (*Sitobion miscanthi*) is one of the most dominant and devastating insect pests in wheat, which causes substantial losses to wheat production each year. Engineering transgenic plants expressing double strand RNA (dsRNA) targeting an insect-specific gene has been demonstrated to provide an alternative environmentally friendly strategy for aphid management through plant-mediated RNA interference (RNAi). Here we identified and characterized a novel potential RNAi target gene (*SmDSR33*) which was a gene encoding a putative salivary protein. We then generated stable transgenic wheat lines expressing dsRNA for targeted silencing of *SmDSR33* in grain aphids through plant-mediated RNAi. After feeding on transgenic wheat plants expressing *SmDSR33*-dsRNA, the attenuated expression levels of *SmDSR33* in aphids were observed when compared to aphids feeding on wild-type plants. The decreased *SmDSR33* expression levels thus resulted in significantly reduced fecundity and survival, and decreased reproduction of aphids. We also observed altered aphid feeding behaviors such as longer duration of intercellular stylet pathway and shorter duration of passive ingestion in electroneurography assays. Furthermore, both the surviving aphids and their offspring exhibited decreased survival rates and fecundity, indicating that the silencing effect could be persistent and transgenerational in grain aphids. The results demonstrated that *SmDSR33* can be selected as an effective RNAi target for wheat aphid control. Silencing of an essential salivary protein gene involved in ingestion through plant-mediated RNAi could be exploited as an effective strategy for aphid control in wheat.

KEYWORDS

wheat (*Triticum aestivum* L), grain aphid (*Sitobion miscanthi*), RNA interference (RNAi), salivary protein, aphid control

Introduction

Aphids are the most destructive agricultural insect pests, which cause potential yield losses of common wheat (*Triticum aestivum* L) by sap-sucking and virus transmission (Xia et al., 2012; Sun et al., 2019). The grain aphid (*Sitobion miscanthi*) is one of the most devastating wheat aphids that causes substantial damage to wheat, which was previously misidentified as *Sitobion avenae* (Zhang et al., 2013; Yu et al., 2014; Zhang et al., 2022a). Currently, neurotoxic insecticides are still the predominant measure for aphid management. However, intensive use of pesticides can cause aphid resistance and harmfulness to non-target organisms, which leads to environmental issues (Sanahuja et al., 2011). Limited aphid resistance germplasm has significantly hampered the process of conventional breeding projects (Crespo-Herrera et al., 2019). Therefore, it is imperative to search for effective and practical strategies for aphid management in wheat.

RNA interference (RNAi) has been recognized as one of the most potential technologies for pest control. Transgenic plant-mediated RNA interference (RNAi), which provides a protective and environmentally friendly strategy for aphid management, has been proven to be a practicable method in recent years (Price and Gatehouse, 2008). For example, interference of structural sheath protein (SHP) encoding gene in grain aphids by feeding on transgenic barely plants effectively reduce their survival and reproduction rates. Knock-down of *shp* strongly affect feeding behavior and the transgenerational effect can last for the next seven generations (Abdellatef et al., 2015). The dsRNA-transgenic *Arabidopsis* plants with the cuticular protein gene impaired the fecundity of *Myzus persicae* (Bhatia and Bhattacharya, 2018). Transgenic wheat plants expressing *SaZFP*-dsRNA decreased the survival and fecundity significantly in *S. avenae* with effects also observed on offspring (Sun et al., 2019). Plastid-expressed dsRNAs can be efficiently applied for sap-sucking pest control. Aphids feeding on transplastomic plants exhibited significant mortality, decreased aphid fecundity, and reduced weight of survivors (Dong et al., 2022).

As sap-sucking insects, aphids secrete gel saliva during stylet penetration and watery saliva during sap sucking (Khan and Naveed, 2022). Aphid salivary protein plays a pivotal role in the interaction between pest and host plants (Pan et al., 2015). ApC002 was first discovered in *Acyrthosiphon pisum* and has been proven to play a critical role in the foraging and feeding process of pea aphid (Mutti et al., 2008). Transient expression of salivary proteins in *Nicotiana benthamiana*, such as Mp10, Mp42, Mp56, Mp57, and Mp58, caused reduced virulence and fecundity of green peach aphids (Bos et al., 2010; Elzinga et al., 2014; Rodriguez et al., 2014). *M. persicae* salivary proteins Mp1, Mp2, Mp55, and MpMIIF1 were verified to inhibit host plant defense responses and facilitate green peach aphid performance on host plants (Pitino and Hogenhout, 2013; Elzinga et al., 2014; Naessens et al., 2015). Overexpression of salivary proteins Me10 and Me23 enhanced potato aphid infestation and fecundity (Atamian et al., 2013). Knockdown of the transcript of effector protein Armet by RNA interference impeded the feeding behavior of pea aphids. Overexpression of *Armet* in *N. benthamiana* was shown to activate plant-pathogen interactions and induce salicylic acid-mediated defense in plants, but had no detectable effects on aphid performance (Wang et al., 2015b; Cui et al., 2019). Expression of bird cherry-oat aphid candidate effector Rp1 in transgenic barley plants significantly promoted aphid fecundity and suppressed plant defense responses (Escudero-Martinez et al., 2020). Besides, transient overexpression of salivary effectors Sm9723 and Sg2204 in tobacco inhibited cell death and suppressed plant defense responses. Silencing *Sm9723* through a nanocarrier-mediated dsRNA delivery system significantly decreased the survival rates and fecundity of aphids and affected feeding behavior. Similarly, *Sg2204*-silenced aphids exhibited a strong wheat defense response and negatively impacted aphid survival rate, fecundity, and feeding behavior. The aphid performance on host plants was significantly reduced when silencing the homologs of *Sg2204* from four other aphid species (Zhang et al., 2022a; Zhang et al., 2022b). These results implied that the genes encoding salivary proteins in aphids are potential candidates for aphid control in plants though plant-mediated RNAi.

Here, we isolated a novel putative salivary protein encoding gene, *SmDSR33*, in grain aphid based on our previous transcriptomic profiling. We found that feeding on transgenic wheat plants expressing *SmDSR33*-dsRNA decreased the survival rate and the fecundity significantly in grain aphids. The surviving aphids exhibited a silencing effect and induced a transgenerational effect on their offspring.

Materials and methods

Plants and insects

Plants: the hexaploid wheat variety *Triticum aestivum* L. cv Zhengmai 7698 (ZM7698) was used in this study. A total of 30-35 wild-type and transgenic wheat plant seeds were sown in pots and were cultured in a climate chamber at 22°C under a 16-h photoperiod, and with a relative humidity of 40%-60%.

Insects: grain aphids, *S. miscanthi* were reared on two-leaf stage aphid susceptible wheat seedlings in a controlled chamber with similar conditions than for plant growing. Apterous adult grain aphids from a single clonal lineage were reared on wheat seedlings in a continuous culture for 24 hours to produce synchronized nymphs. After that, the adults were removed, and the offspring were used in subsequent experiments. All

experiments were carried out in a climate chamber under the above-mentioned conditions.

Isolation and characterization of *SmDSR33*

Total RNA of pooled adults was extracted by using TransZol Up (TransGen Biotech, Beijing, China). cDNA was synthesized by using FastKing RT Kit (Tiangen, Beijing, China). The full length of the *SmDSR33* gene was obtained using TransStart® FastPfu DNA Polymerase (TransGen Biotech, Beijing, China) following the instructions. The DNA amplification products were sequenced by the Institute of Crop Sciences (Institute of Crop Sciences, Chinese Academy of Agricultural Sciences, Beijing, China). The theoretical isoelectric point (pI) and molecular weight (MW) of SmDSR33 were calculated through ExPASy (https://web.expasy.org/compute_pi/). The transmembrane region and putative signal peptide were predicted using TMHMM (http://www.cbs.dtu.dk/services/TMHMM/) and SignalP (http://www.cbs.dtu.dk/services/SignalP/), respectively. The counterparts of *SmDSR33* of other aphid species were obtained by the Basic Local Alignment Search Tool (BLAST) against the aphidbase database (http://bipaa.genouest.org/is/aphidbase/). Phylogenetic trees of *SmDSR33* in twelve aphid species were constructed using the nucleotide acid sequences as a matrix *via* MEGA X software (www.megasoftware.net). The branch strength was analyzed by using the maximum likelihood method and performing 100 bootstrap replications.

Vector construction and wheat transformation

To amplify the 439 bp *SmDSR33* target sequence, specific primers were designed. A 320 bp fragment of GFP were selected as a control in the aphid bioassay experiment. The amplified PCR products were recovered and inserted at inverted repetitions into the *Spe*I/*Eco*RV and *Sac*I/*Hpa*I sites of the pEasy-Blun-Zero-AdhI vector to construct the hairpin RNAi, Bzero-DSR33-adhI-DSR33. The vector of Bzero-DSR33-adhI-DSR33 was digested by *Ssp* I and *BsrG* I to obtain the expression cassette. The latter was recovered for bombardment. The RNAi fragment was driven by the maize Ubi promoter. Bombardment-mediated transformation was applied to immature embryos isolated from ZM7698. Somatic embryos were induced in tissue culture on medium, and whole plants were then regenerated and selected. Healthy seedlings were transplanted to soil to grow until maturity.

Southern blot analysis

The CTAB method was used to extract genomic DNA from young T_3 plant leaf tissues as described by Sambrook et al. (1989). The restriction enzyme was used to digest 35 μg of genomic DNA overnight. The products were fractionated for 12-16 h at 60 V on a 0.8% agarose gel in 1×TBE buffer. The Hybond-N^+ membranes were used for blotting (Amersham, UK). The digoxigenin (DIG) High Prime DNA Labeling and Detection Starter Kit I (Roche, Germany) was used for prehybridization, hybridization, washing, and detection of the membranes. The primer sets SmDSR33S-F/R were used to synthesized DNA probes (Supplementary Table 1).

Quantitative real-time PCR

For the expression level of *SmDSR33* at different development stages, total RNAs of grain aphids were isolated from the four nymphs and adults reared on susceptible wheat. For the expression level of *SmDSR33* in aphids fed with different transgenic wheat and wild-type plants, the adult aphids were collected and used for total RNA extraction and further experiments.

The cDNA was synthesized following conventional procedures. A quantitative real-time PCR (qRT-PCR) assay was carried out using the SYBRH Green Real-time PCR Master Mix (Tiangen, Beijing, China) in an ABI 7300 Real Time PCR system. The aphid *Actin* gene and ribosomal protein S27 A (*Rps27*) gene were selected as internal controls, and *SmDSR33* specific primers were designed for normalization (Supplementary Table 1). All qRT-PCR experiments were performed in triplicate. The relative gene expression of each target gene was calculated by using the mean value of the reference genes through the $2^{-\Delta\Delta CT}$ method (Livak and Schmittgen, 2001).

Aphid bioassays

A single clonal lineage of apterous adult grain aphids was reared on wheat seedlings in cages for 24 hours to produce nymphs. The newborn nymphs produced during the period of 24 hours were transferred to fresh transgenic wheat plants.

T_3 homozygous wheat plants with *SmDSR33*-dsRNA expression were selected to evaluate the effects on aphid survival and fecundity. At the 3-4 leaf stage, 20 neonatal first instar nymphs of *S. miscanthi* were placed on the leaf of each plant. The mortality of aphids was recorded every day. Ten plants from each line were used in every experiment. The experiment was repeated three times.

Life cycle parameters were calculated as follows: the net reproductive rate, $R_0 = \Sigma l_x \cdot m_x$, the mean generation time, $T = \Sigma x l_x m_x / \Sigma L_x m_x$ the intrinsic rate of increase, $r_m = (lnR_0)/T$, and the finite rate of increase, $\lambda = e^{r_m}$. In the equations, l_x is the surviving rate to a specific age x , and m_x is the number of new-born nymphs produced by per live adult for a specific age x (Biondi et al., 2013).

Electrical penetration graph technique analysis

The Giga-8 DC EPG amplifier (EPG-Systems, Wageningen, Netherlands) and a Faraday cage was used to record the probing and feeding behaviors of apterous adult aphids on wheat. Firstly, synchronous adult aphids were inoculated on 33-592 transgenic plants and control plants for two days, respectively. Then, the aphid was starved for 2 h. After that, water-soluble silver conductive paint was used to attach each aphid to a flexible gold wire (18 μm diameter×2 cm length) through the dorsal thorax individually. The aphids were placed onto the adaxial side of a leaf from transgenic and wild-type wheat plants at the three-leaf stage, and the opposite ends of the gold wires (2 mm in diameter×3 cm length) were connected to copper wire with conducting silver glue, which was connected to a DC amplifier. The plant electrode was inserted into the soil. Under light conditions, the EPG signal of each individual was continuously monitored for 8 h. We monitored 12 behavioral recordings for each treatment. The software Stylet+a (EPG-Systems) was used to analyze EPG signals. According to the method described by Tjallingii (Tjallingii, 1985; Tjallingii, 1994), the different waveforms were correlated with feeding behavior. Non-probing (np) waveform, which reflects stylet external to wheat leaf tissue. Pathway phase contains two waveforms, waveform C, which reflects the intercellular stylet pathway, potential drops (pd), which reflects intracellular punctures during intercellular pathway. Waveform G (xylem phase) is the only waveform that reflects active sap ingestion from xylem elements. Phloem phase can be divided into two phases: E1 always occurs at the start of the phloem phase and reflects saliva secretion into the sieve element, E2 reflects passive phloem sap ingestion. EPG data was analyzed using the EPG-Excel data workbook provided by Sarria et al. (2009).

Statistical analysis

The two-tailed Student's *t*-test was used to evaluate the differences between wild-type and transgenic wheat lines. For all comparisons, significance (*P* value) was calculated at the 1% or 5% level. The standard error of the mean (SEM) for each treatment was calculated using three biological replicates. For the EPG experiments, means and standard errors of variables were calculated from recordings per individual aphid, and differences were analyzed by Student's *t*-test. All data represents means ± SEM.

Results

Characterization of *SmDSR33* gene in grain aphids

We identified a candidate gene *SmDSR33*, which encoding a putative salivary protein in grain aphid, based on transcriptomic profiling and dsRNA feeding assay (Wang et al., 2015a). The full-length cDNA sequence of *SmDSR33* was 534 bp in length, encoding a 177 amino acid putative salivary protein. The SmDSR33 protein was predicted to have an Mw of 19.376 kDa and a pI of 6.26, possess a signal secretion peptide with a predicted cleavage site between amino acid residues 20 and 21 and have one predicted transmembrane helix, suggesting that SmDSR33 was a secreted protein (Figure 1A, Supplementary Figure S1).

To clarify the evolutionary relationships of this gene in different insect species, sequences of *SmDSR33* counterparts in pea aphid (*A. pisum*), soybean aphid (*Aphis glycines*), cotton aphid (*A. gossypii*), Russian wheat aphid (*Diuraphis noxia*), sugarcane aphid (*Melanaphis sacchari*), black cherry aphid (*M. cerasi*), peach aphid (*M. persicae*), banana aphid (*Pentalonia nigronervosa*), corn aphid (*Rhopalosiphum maidis*), bird cherry-oat aphid (*Rhopalosiphum padi*), and yellow sugarcane aphid (*Sipha flava*) were obtained by BLAST against aphidbase database and NCBI. The phylogenetic tree of *SmDSR33* was constructed *via* MEGA X software. Phylogenetic analysis demonstrated *SmDSR33* was more closely related to its orthologs in the pea aphid (*A. pisum*) (Figure 1B).

We the used qRT-PCR to investigate the *SmDSR33* expression level in grain aphids at different developmental stages. Results revealed that *SmDSR33* transcription was accumulated throughout the developmental phases at different levels (Figure 1C). The *SmDSR33* expression pattern peaked in the adult aphid and was about 1.6-fold higher compared to first instar nymphs.

Wheat plants expressing *SmDSR33*-dsRNA induce *SmDSR33* silencing in aphids upon feeding

To investigate the function of *SmDSR33*, a 439 bp fragment of *SmDSR33* gene was selected as a template for RNAi target (Figure 2A). We used BLAST against the NCBI database to evaluate the specificity of the *SmDSR33* fragment. At the nucleotide acid level, no continuous three 21-nt matches were detected between the selected 439 bp fragment and aphid natural

10.3389/fpls.2022.1100394

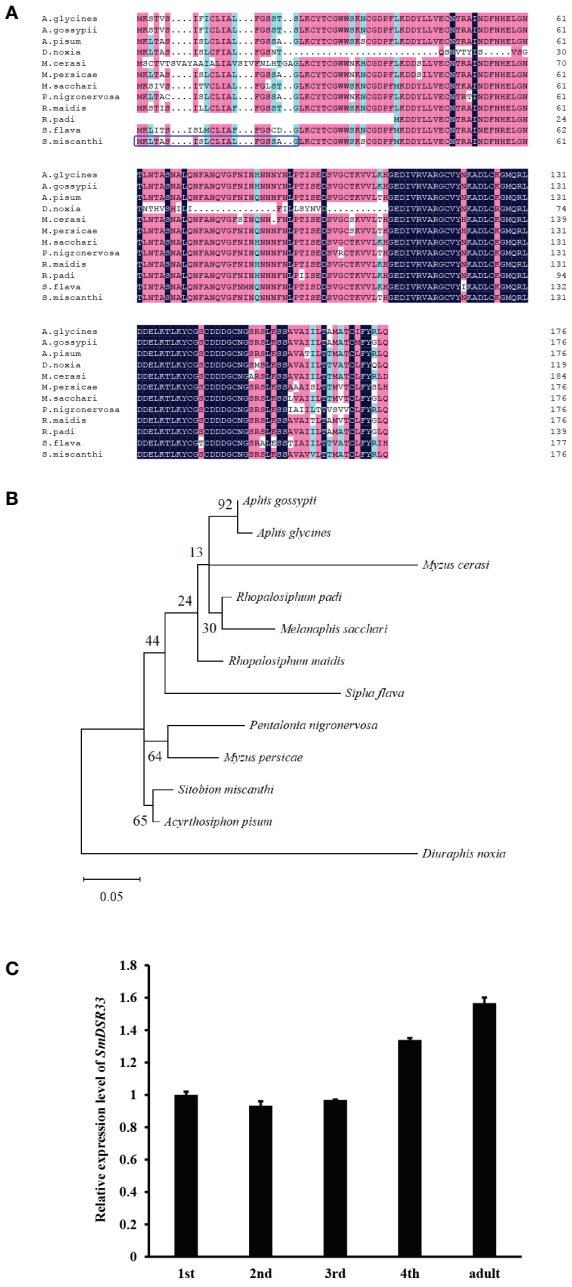

FIGURE 1
Characterization of SmDSR33. **(A)** Multiple sequence alignment of SmDSR33 protein and orthologs from other aphid species. The deduced amino acid sequences from eleven aphid species include *Acyrthosiphon pisum* (NM_001163178.1), *Aphis glycines* (AG000929-RA), *Aphis gossypii* (XM_027996540.1), *Diuraphis noxia* (XM_015509488.1), *Melanaphis sacchari* (XM_025349621.1), *Myzus cerasi* (Mca00769.t1), *Myzus persicae* (XM_022311485.1), *Pentalonia nigronervosa* (g3912.t1), *Rhopalosiphum maidis* (XM_026949227.1). *Rhopalosiphum padi* (Rpa07522.t1), and *Sipha flava* (XM_025560312.1). Black shades indicate identical amino acids. Pink shades indicate similar amino acid, and blue shades include the sequences with identical and similar residues. Signal peptide of SmDSR33 is highlighted with blue box. **(B)** Phylogenetic tree of SmDSR33 and its homologs from other aphid species constructed with the maximum likelihood method. Bootstrap supporting values (1000 replicates) are shown at the branch nodes. **(C)** The expression profile of *SmDSR33* in grain aphid at different development stages. The expression profiles of *SmDSR33* at different developmental stages of grain aphids fed on wheat. Values and error bars represent the mean and SEM of three independent biological replicates, each with a pool of 15 individual aphids.

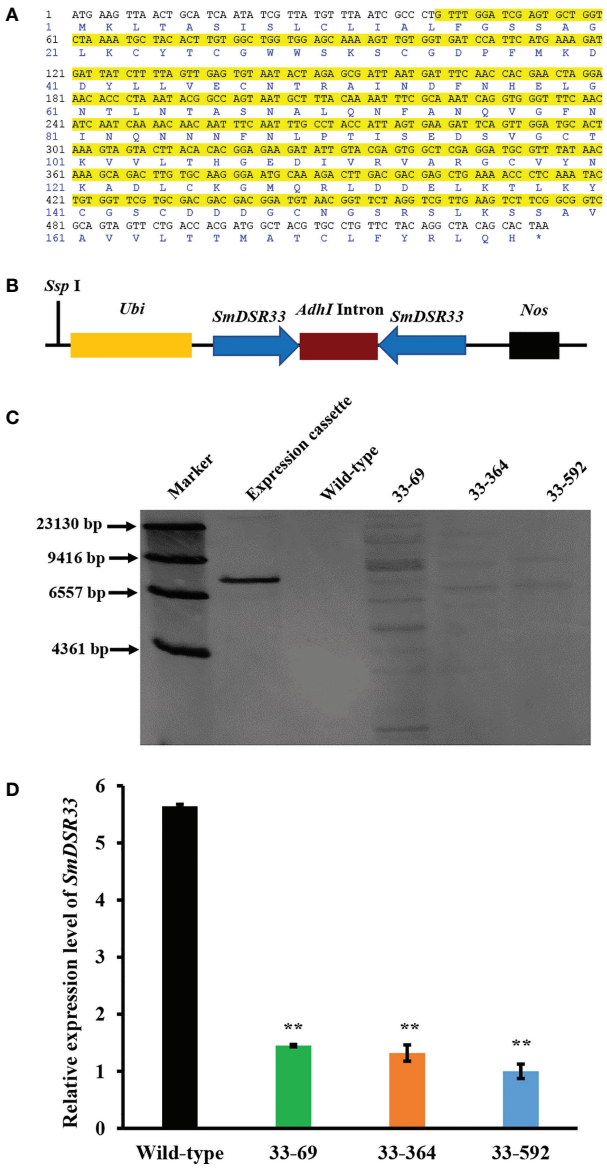

FIGURE 2
RNAi induced silencing of *SmDSR33* gene in wheat. **(A)** The encoding sequence of SmDSR33 and its deduced amino acid sequence. The sequences selected for construction of the RNAi vector are highlighted in yellow. **(B)** A schematic show of the *SmDSR33* expression cassette and position of *Ssp I* restriction enzyme. **(C)** Southern blot analysis of the transgenic wheat lines. Genomic DNA was digested with *Ssp*I and hybridized with a *SmDSR33* gene fragment with the expression cassette digested with *Ssp* I as a positive control. **(D)** Relative expression levels of *SmDSR33* of grain aphid fed on wild-type and transgenic wheat lines. The expression level of *SmDSR33* in the adult aphids fed on wild-type and different transgenic wheat lines after inoculation of one-day-old newborn nymphs, respectively. Values and error bars represent the mean and SEM of three independent biological replicates, each with a pool of 15 surviving individual aphids (Student's *t*-test, ** $P<0.01$).

enemies or humans (data not shown), which implied that the selected *dsSmDSR33* fragment would not pose potential risks to non-target organisms (Bachman et al., 2013). Then, the RNAi vector harboring *SmDSR33*-hairpin DNA was constructed (Figure 2B). After transformed into wheat immature embryos of wheat variety cv ZM 7698, we obtained 8 independent transgenic wheat lines, among which, we randomly selected 3 of them for further analysis. Southern blot analysis indicated that the expression cassette of *SmDSR33*-dsRNA had been successfully integrated into the wheat genome with two to twelve copies (Figure 2C).

To further investigate whether the expression of the target *SmDSR33* gene in aphids was inhibited when feeding on transgenic wheat plants. The individual synchronous one-day-old nymphs were transferred to wild-type and transgenic wheat plants, respectively. The relative expression levels of *SmDSR33*

were detected in adult aphids. The relative expression levels of *SmDSR33* in grain aphids decreased significantly upon feeding on three transgenic wheat lines ($P< 0.01$, Figure 2D).

Fitness of the aphids fed on *SmDSR33*-dsRNA expressing transgenic wheat lines

Fitness parameters including life cycle and mortality of aphids upon feeding on different transgenic lines were further investigated to evaluate the silencing impact of *SmDSR33*. The mortality rates of aphids fed on transgenic wheat lines significantly increased when compared to that of aphis fed on wild-type plants at 9 days after feeding (DAF), reaching more than 60% at 18 DAF (Figure 3A). We also monitored the development duration of aphids from the nymphal to imago stage. The adult preoviposition period (APOP) and the total preoviposition period (TPOP) of aphids showed no significant difference between host plant lines (Figure 3B). The aphid longevity fed on transgenic wheat lines was significantly shorter than on wild-type plants. Similarly, the adult longevity and reproductive period of aphids significantly decreased than wild-type ($P<0.01$) (Figure 3C). Consequently, in comparison with the wild-type plants, the aphid total production significantly decreased when fed on all three transgenic wheat lines ($P <0.01$) (Figure 3D), and the daily fecundity of aphids fed on 33-592 transgenic line decreased at a significant level ($P <0.01$) (Figure 3D).

All of the population parameters, including the net reproductive rate (R_0), mean generation time (T), the intrinsic rates of increase (r_m) and doubling times of the population (DT), showed differences between grain aphids fed on transgenic lines

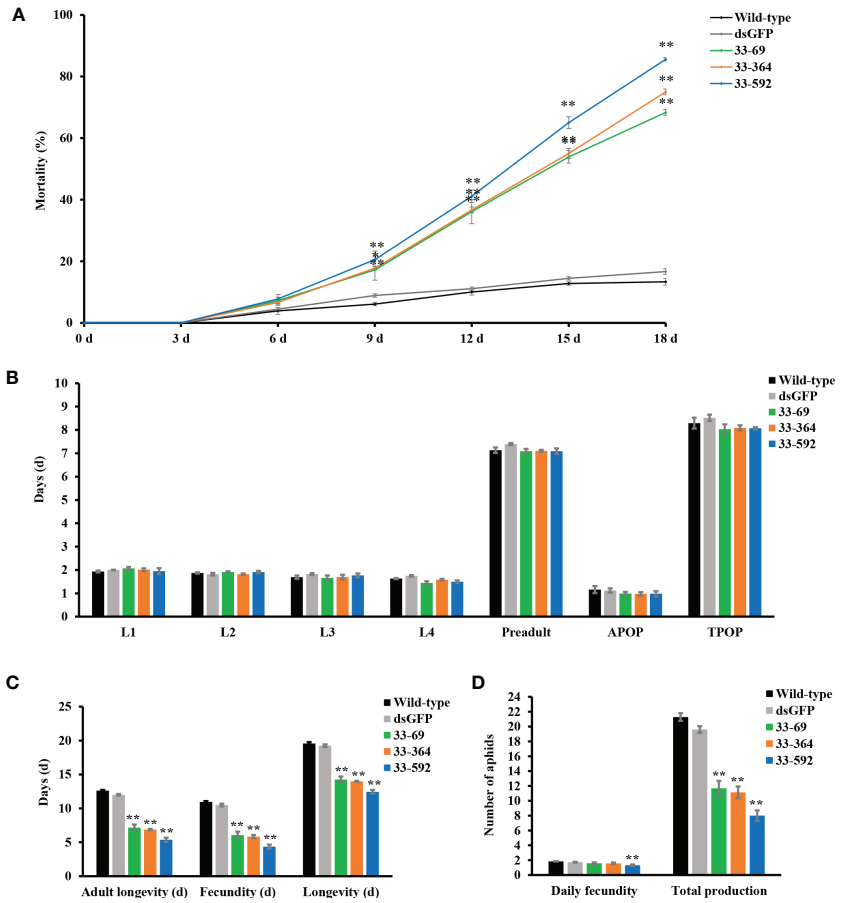

FIGURE 3
Fitness analysis of aphids fed on transgenic plants. **(A)** Mortality of aphids fed on wild-type and transgenic wheat lines. The mortality of aphids fed on wild-type and *dsSmDSR33* expression transgenic wheat lines. Twenty synchronous one-day-old nymphs were put into clip cages individually on transgenic and wild-type wheat plants. All experiments were repeated three times. Values and bars represent the mean ± SEM (Student's *t*-test, * $P<0.05$, ** $P<0.01$). **(B)** The longevity of different stages, adult preoviposition period (APOP) and total preoviposition period (TPOP) of aphids fed on transgenic lines and wild-type control. **(C)** The adult longevity, fecundity and the total longevity of aphids fed on transgenic wheat lines and wild-type control. **(D)** The reproduction of aphids fed on transgenic wheat lines and the wild-type control. All experiments were repeated three times, each with 20 synchronous one-day-old nymphs. Values and bars represent the mean ± SEM (Student's *t*-test, * $P<0.05$, ** $P<0.01$).

and those on wild-type plants (Table 1). For example, the net reproductive rates (R_0) of aphids were significantly lower when fed on transgenic wheat lines. The mean generation time (T) of aphids fed on 33-592 line was significantly decreased than wild-type (P <0.01) (Table 1).

Feeding behavior of aphids feeding on transgenic wheat plants

To investigate the feeding behavior of aphids, transgenic wheat line 33-592 was selected to perform electropenetrography (EPG) assays. As shown in Figures 4A-F, there was no difference between the aphids fed on *SmDSR33* and *dsGFP* wheat plants at time point of first probe activity. The number of non-probing (np) waveforms of *SmDSR33*-silenced aphids fed on 33-592 line was significantly higher than on wild-type plants. Furthermore, the total duration of np waveforms and C phases of *SmDSR33*-silenced aphids was significantly increased compared to control. Finally, there was no difference in the duration of E1 waveforms, but did of phloem ingestion (E2) with a significant reduction for aphids on control plants. These results indicated that the feeding behavior of grain aphids was affected after *SmDSR33* silencing.

Feeding on transgenic lines induces transgenerational silencing of *SmDSR33* in aphids

Newborn nymphs produced in a parallel experiment were used to investigate potential transgenerational RNAi effects of *SmDSR33*. The expression levels of *SmDSR33* in the offspring of aphids fed on transgenic and wild-type plants was investigated subsequently. *SmDSR33* expression in grain aphids was suppressed in their offspring fed on wild-type plants (Figure 5). Aphid relative expression levels reached 77.71%, 70.04%, 74.63%, and 61.80% of control level in successive first to fourth generations (Figure 5A). Even after switching to wild-type plants, aphid offspring still exhibited higher mortality rates (Figure 5B).

Discussion

Aphids are phloem-feeding insects that secrete saliva effectors into plant cells to enable successful feeding (Wang et al., 2015b). Salivary proteins play important roles in the interaction of aphids with plants (Yang et al., 2018; Zhang et al., 2021). Engineering transgenic plants expressing dsRNA for insect pest management is an effective strategy in agricultural practice (Ghag, 2017). Plant-mediated RNAi has been recognized as one of the most promising technologies to engineer insect-resistant crops, especially for wheat aphid control, which has great significance for food security, human health, and the agroecosystem in a global context (Sun et al., 2019; He, 2022).

Here, we identified a novel potential RNAi target gene (*SmDSR33*) from grain aphid, which had a high mortality due to the silencing of *SmDSR33* in grain aphid *via* artificial diet feeding assays (Wang et al., 2015a). *SmDSR33* was predicted as a gene encoding a secreted putative salivary protein which had a signal peptide and one predicted transmembrane helix (Figure 1A, Figure S1). This result is in accordance with previous studies on salivary effectors. For example, ApC002 was predicted to be a signal peptide for an extracellular protein and the cleavage site was predicted between residues 23 and 24 (Mutti et al., 2008). A signal secretion peptide with cleavage sites either between Ala20 and Gln21 (SignalP) or between Ser22 and Arg23 (PSORT) was predicted in Armet (Wang et al., 2015b). A secretory signal peptide at the N-terminal of the protein ACYPI006346 was predicted, with the predicted cleavage site between residues 19 and 20 (Pan et al., 2015). The signal peptide of Sm9723 was constituted of the first 21 amino acids and the cleavage site was predicted between residues 21 and 22 (Zhang et al., 2022a). The signal peptide of Sg2204 was constituted of the first 25 amino acids and the cleavage site was predicted between residues 25 and 26 (Zhang et al., 2022b).

We then obtained stable transgenic wheat lines expressing dsRNA of *SmDSR33* in grain aphids. Significantly decreased fecundity, survival, and reproduction rates of aphids fed on transgenic wheat plants were observed than that of wild-type

TABLE 1 Life table parameters of grain aphids fed on wild-type and different transgenic wheat lines.

Parameters	Wild-type	33-69	33-364	33-592
R_0	21.27 ± 0.52	11.32 ± 1.08**	10.86 ± 0.73**	7.94 ± 0.77**
T	14.49 ± 0.30	13.40 ± 0.19*	13.38 ± 0.16*	12.57 ± 0.26**
r_m	0.21 ± 0.01	0.18 ± 0.01*	0.18 ± 0.01*	0.16 ± 0.01*
λ	1.24 ± 0.01	1.20 ± 0.01*	1.20 ± 0.01*	1.18 ± 0.01*
DT	3.29 ± 0.08	3.86 ± 0.16*	3.91 ± 0.15*	4.25 ± 0.23*

All data are expressed as means ± SEM based on 3 repeated experiments. R_0, net reproductive rate; r_m, the intrinsic rate of increase; λ, the finite rate of increase; T, the mean generation time; DT, Doubling time (day). Student's t-test, n=3, *P<0.05, **P<0.01.

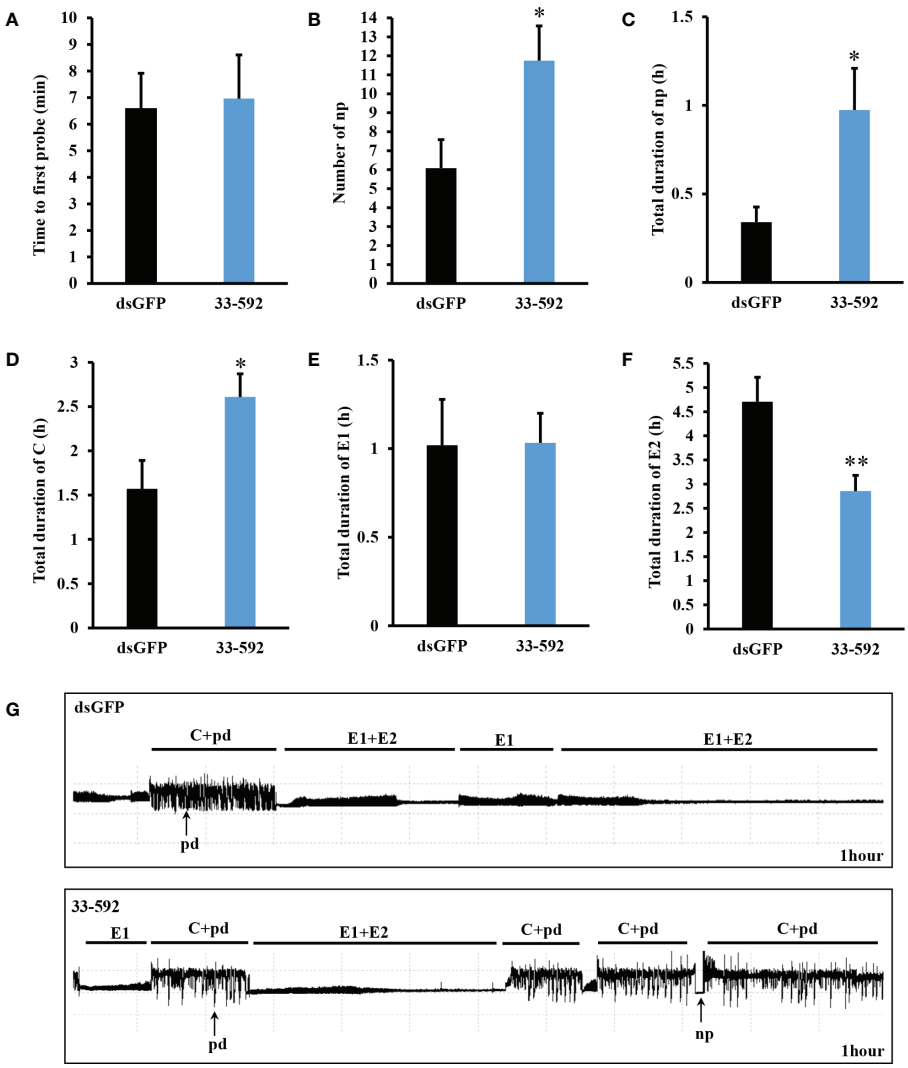

FIGURE 4
Effects of *SmDSR33* silencing on feeding behavior of grain aphid based on EPG recordings. **(A–F)** Representative parameters of aphid feeding behavior. Non-probing (np), stylet probing **(C)**, intracellular stylet puncture (pd), phloem salivation (E1), and phloem ingestion (E2). Data shown are mean ± SEM. Asterisks above bars indicate significant differences between controls and treatments (Student's *t*-test, * $p < 0.05$; ** $p < 0.01$). **(G)** Representative EPG waveforms of grain aphids feeding on dsGFP wheat plants and 33-592 transgenic wheat plants.

plants (Figure 3). Our results are in consistent with the plant-mediated RNAi experiments targeting salivary protein and effector encoding genes in aphids. For example, silencing the salivary protein gene *C002* reduced the reproduction and survival in the pea aphid (Mutti et al., 2006; Mutti et al., 2008). Silencing salivary proteins such as Mp10, Mp42, Mp56, Mp57, and Mp58 in tobacco caused reduced virulence and fecundity of green peach aphids (Bos et al., 2010; Elzinga et al., 2014; Rodriguez et al., 2014). Silencing *Sm9723* and *Sg2204* through a nanocarrier-mediated dsRNA delivery system negatively impacted aphid survival rates and fecundity of aphids (Zhang et al., 2022a; Zhang et al., 2022b).

We found that *SmDSR33* silencing increased the total duration of non-probing waveforms and C phases and decreased the duration of phloem ingestion (E2) (Figure 4). These results indicated that *SmDSR33* affected the feeding process and behavior of grain aphids. It was shown that interference of target genes could affect the feeding behavior of aphids. Knockdown of an effector protein Armet impeded the feeding behavior of pea aphids (Wang et al., 2015b). As an important multipeptide molecule, neuropeptide F (NPF) had been discovered in numerous insect species and regulated a variety of physiological activities. The probing time and total duration of phloem activity on broad bean plants were decreased when wingless adult pea aphids were injected with NPF dsRNA (Li et al., 2018). When feeding on *A. thaliana*, *Mp1* silencing decreased the fitness of green peach aphids. However, aphid feeding ability with *Mp1* silences was still retained (Wang et al.,

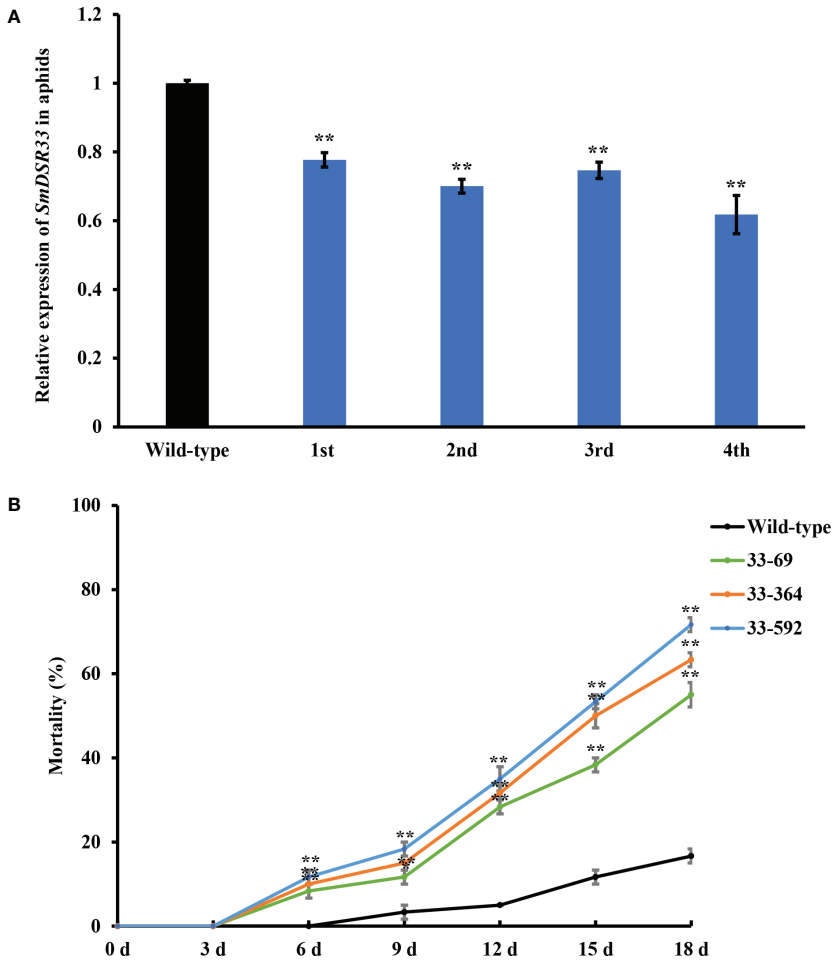

FIGURE 5
Transgenerational effect of *SmDSR33* silencing. The one-day-old newborn nymphs of aphids feeding on transgenic wheat lines were transferred to fresh wild-type wheat plants and subsequently allowed to reproduce on wild-type. **(A)** The *SmDSR33* transcript levels of adult aphids were determined in fourth successive aphid generations. **(B)** The mortality of the first generation of the offspring of aphids fed on transgenic lines at different time points after being switched to wild-type plants. Values and bars represent the mean ± SEM (Student's *t*-test, * $P<0.05$, ** $P<0.01$).

2021). Plastid-mediated RNAi was also an efficient approach for aphid control. *M. persicae* exhibited different feeding behaviors on nuclear-mediated RNAi transgenic plants and transplastomic-mediated RNAi transgenic plants (Dong et al., 2022). Feeding behavior of *S. miscanthi* and *S. graminum* were significantly impaired after knockdown of *Sm9723* and *Sg2204* (Zhang et al., 2022a; Zhang et al., 2022b).

According to previous studies on environmental RNAi, transgenerational silencing, also known as parental RNAi, in which the silencing effects of the respective target genes and survival rates could be significantly impacted in the offspring of the treated organism (Marré et al., 2016; Rechavi and Lev, 2017; Wang and Hunter, 2017). Our data showed that *SmDSR33* relative expression levels reached from 78 to 62% of control level in the following first to fourth successive generations (Figure 5). This result indicated that RNAi effect was persistent in grain aphids. This type of effect could last for several days, many weeks, few months, and even for multiple generations. With time and successive generations, the silencing effect decreased (Amdam et al., 2003; Jaubert-Possamai et al., 2007; Miller et al., 2012; Abdellatef et al., 2015). According to a previous study, parental RNAi may result from a specific dsRNA uptake mechanism or small amounts of incidentally incorporated dsRNA secondary amplification (Bucher et al., 2002). The phenomenon of telescoping generations existed in grain aphids, which means that the developing grandchildren are already carried by a parthenogenetic adult, may facilitate the transfer of siRNA/dsRNA to the subsequent generations in aphids (Abdellatef et al., 2015). Transgenerational silencing could also induce by small RNAs mediated epigenetic modifications (Castel and Martienssen, 2013). We observed the decreased silencing effect in 4th generation compared to that of 1st to 3rd generation. Our result was consistent with the study that the duration of the RNAi impact was doubled in

nymphs whose mothers had been exposed to dsRNA-producing transgenic plants (12-14 days), which indicated that the RNAi effect may persist longer in nymphs than in their mothers (Coleman et al., 2015). This could be due to the fact that the stability of dsRNA in insects may be affected by the quantities of dsRNA, the lengths of the dsRNA fragments, the activities that degrade dsRNA, and the life stages of the target species (Griebler et al., 2008; Huvenne and Smagghe, 2010; Bolognesi et al., 2012; Miller et al., 2012; Abdellatef et al., 2015). Transgenerational gene silencing exhibited significant potential in RNAi-mediated pest control, although the molecular mechanisms in insect species remained to be elucidated.

In conclusion, we not only identified and characterized a novel RNAi target gene *SmDSR33*, which is a putative salivary secretion protein in grain aphids, but also revealed that targeted silencing of *SmDSR33 via* plant-mediated RNAi significantly decreased the survival, fecundity, and total production of grain aphids, which consequently reduced aphid infestation on wheat plants. The altered feeding behavior and transgenerational RNAi silencing effects also minimized aphid infestation. As a result, our study demonstrated the significant potential of plant-mediated RNAi of an important putative salivary protein gene as a promising strategy for aphid control in crop plants in agricultural practice.

Data availability statement

The raw data supporting the conclusions of this article will be made available by the authors, without undue reservation.

Author contributions

FF and LX conceived and designed the experiments. JZ, HL, XZ, JT and AS performed the experiments. JZ analyzed the data. FF, LX and JZ wrote the manuscript. FF and LX revised the manuscript. All authors read and approved the final manuscript.

Acknowledgments

We apologize to those whose work we were unable to cite due to space and reference limitations. Part of this work is funded by the Shennong Laboratory, Zhengzhou Henan 450002, China (SN01-2022-01), the Innovation Program of Chinese Academy of Agricultural Sciences (ZDXM03, S2021ZD03) and National Engineering Laboratory of Crop Molecular Breeding. JZ was supported by the China Scholarship Council (No. 202003250096) and GSCAAS-ULg Joint PhD Program.

Conflict of interest

The authors declare that the research was conducted in the absence of any commercial or financial relationships that could be construed as a potential conflict of interest.

Publisher's note

All claims expressed in this article are solely those of the authors and do not necessarily represent those of their affiliated organizations, or those of the publisher, the editors and the reviewers. Any product that may be evaluated in this article, or claim that may be made by its manufacturer, is not guaranteed or endorsed by the publisher.

Supplementary material

The Supplementary Material for this article can be found online at: https://www.frontiersin.org/articles/10.3389/fpls.2022.1100394/full#supplementary-material

References

Abdellatef, E., Will, T., Koch, A., Imani, J., Vilcinskas, A., and Kogel, K. H. (2015). Silencing the expression of the salivary sheath protein causes transgenerational feeding suppression in the aphid *Sitobion avenae*. *Plant Biotechnol. J.* 13 (6), 849–857. doi: 10.1111/pbi.12322

Amdam, G. V., Simões, Z. L., Guidugli, K. R., Norberg, K., and Omholt, S. W. (2003). Disruption of vitellogenin gene function in adult honeybees by intra-abdominal injection of double-stranded RNA. *BMC Biotechnol.* 3 (1), 1–8. doi: 10.1186/1472-6750-3-1

Atamian, H. S., Chaudhary, R., Cin, V. D., Bao, E., Girke, T., and Kaloshian, I. (2013). In planta expression or delivery of potato aphid *Macrosiphum euphorbiae* effectors Me10 and Me23 enhances aphid fecundity. *Mol. Plant Microbe Interact.* 26 (1), 67–74. doi: 10.1094/MPMI-06-12-0144-FI

Bachman, P. M., Bolognesi, R., Moar, W. J., Mueller, G. M., Paradise, M. S., Ramaseshadri, P., et al. (2013). Characterization of the spectrum of insecticidal activity of a double-stranded RNA with targeted activity against western corn rootworm (*Diabrotica virgifera virgifera LeConte*). *Transgenic Res.* 22 (6), 1207–1222. doi: 10.1007/s11248-013-9716-5

Bhatia, V., and Bhattacharya, R. (2018). Host-mediated RNA interference targeting a cuticular protein gene impaired fecundity in the green peach aphid *Myzus persicae*. *Pest Manage. Sci.* 74 (9), 2059–2068. doi: 10.1002/ps.4900

Biondi, A., Desneux, N., Amiens-Desneux, E., Siscaro, G., and Zappalà, L. (2013). Biology and developmental strategies of the palaearctic parasitoid *Bracon nigricans* (Hymenoptera: Braconidae) on the Neotropical moth *Tuta absoluta* (Lepidoptera: Gelechiidae). *J. Economic Entomol.* 106 (4), 1638–1647. doi: 10.1603/ec12518

Bolognesi, R., Ramaseshadri, P., Anderson, J., Bachman, P., Clinton, W., Flannagan, R., et al. (2012). Characterizing the mechanism of action of double-stranded RNA activity against western corn rootworm (*Diabrotica virgifera virgifera LeConte*). *PloS One* 7 (10), e47534. doi: 10.1371/journal.pone.0047534

Bos, J. I., Prince, D., Pitino, M., Maffei, M. E., Win, J., and Hogenhout, S. A. (2010). A functional genomics approach identifies candidate effectors from the aphid species *Myzus persicae* (green peach aphid). *PloS Genet.* 6 (11), e1001216. doi: 10.1371/journal.pgen.1001216

Bucher, G., Scholten, J., and Klingler, M. (2002). Parental rnai in *tribolium* (coleoptera). *Curr. Biol.* 12 (3), R85–R86. doi: 10.1016/s0960-9822(02)00666-8

Castel, S. E., and Martienssen, R. A. (2013). RNA Interference in the nucleus: Roles for small RNAs in transcription, epigenetics and beyond. *Nat. Rev. Genet.* 14 (2), 100–112. doi: 10.1038/nrg3355

Coleman, A. D., Wouters, R. H., Mugford, S. T., and Hogenhout, S. A. (2015). Persistence and transgenerational effect of plant-mediated RNAi in aphids. *J. Exp. Bot.* 66 (2), 541–548. doi: 10.1093/jxb/eru450

Crespo-Herrera, L., Singh, R. P., Reynolds, M., and Huerta-Espino, J. (2019). Genetics of greenbug resistance in synthetic hexaploid wheat derived germplasm. *Front. Plant Sci.* 10. doi: 10.3389/fpls.2019.00782

Cui, N., Lu, H., Wang, T., Zhang, W., Kang, L., and Cui, F. (2019). Armet, an aphid effector protein, induces pathogen resistance in plants by promoting the accumulation of salicylic acid. *Philos. Trans. R Soc. Lond B Biol. Sci.* 374 (1767), 20180314. doi: 10.1098/rstb.2018.0314

Dong, Y., Wu, M., Zhang, Q., Fu, J., Loiacono, F. V., Yang, Y., et al. (2022). Control of a sap-sucking insect pest by plastid-mediated RNA interference. *Mol. Plant* 15 (7), 1176–1191. doi: 10.1016/j.molp.2022.05.008

Elzinga, D. A., De Vos, M., and Jander, G. (2014). Suppression of plant defenses by a *Myzus persicae* (green peach aphid) salivary effector protein. *Mol. Plant Microbe Interact.* 27 (7), 747–756. doi: 10.1094/MPMI-01-14-0018-R

Escudero-Martinez, C., Rodriguez, P. A., Liu, S., Santos, P. A., Stephens, J., and Bos, J. I. B. (2020). An aphid effector promotes barley susceptibility through suppression of defence gene expression. *J. Exp. Bot.* 71 (9), 2796–2807. doi: 10.1093/jxb/eraa043

Ghag, S. B. (2017). Host induced gene silencing, an emerging science to engineer crop resistance against harmful plant pathogens. *Physiol. Mol. Plant Pathol.* 100, 242–254. doi: 10.1016/j.pmpp.2017.10.003

Griebler, M., Westerlund, S. A., Hoffmann, K. H., and Meyering-Vos, M. (2008). RNA Interference with the allatoregulating neuropeptide genes from the fall armyworm *Spodoptera frugiperda* and its effects on the JH titer in the hemolymph. *J. Insect Physiol.* 54 (6), 997–1007. doi: 10.1016/j.jinsphys.2008.04.019

He, G. (2022). Engineering chloroplasts for insect pest control. *Proc. Natl. Acad. Sci. U.S.A.* 119 (22), e2205125119. doi: 10.1073/pnas.2205125119

Huvenne, H., and Smagghe, G. (2010). Mechanisms of dsRNA uptake in insects and potential of RNAi for pest control: a review. *J. Insect Physiol.* 56 (3), 227–235. doi: 10.1016/j.jinsphys.2009.10.004

Jaubert-Possamai, S., Le Trionnaire, G., Bonhomme, J., Christophides, G. K., Rispe, C., and Tagu, D. (2007). Gene knockdown by RNAi in the pea aphid *Acyrthosiphon pisum*. *BMC Biotechnol.* 7, 63. doi: 10.1186/1472-6750-7-63

Khan, S. A., and Naveed, Z. (2022). Aphid-plant interactions: How saliva of aphids modulates the plant responses. *J. Appl. Entomologist* 2 (2), 06–08.

Li, X., Qu, M. J., Zhang, Y., Li, J. W., and Liu, T. X. (2018). Expression of neuropeptide f gene and its regulation of feeding behavior in the pea aphid, *Acyrthosiphon pisum*. *Front. Physiol.* 9. doi: 10.3389/fphys.2018.00087

Livak, K. J., and Schmittgen, T. D. (2001). Analysis of relative gene expression data using real-time quantitative PCR and the 2–ΔΔCT method. *Methods* 25 (4), 402–408. doi: 10.1006/meth.2001.1262

Marré, J., Traver, E. C., and Jose, A. M. (2016). Extracellular RNA is transported from one generation to the next in *Caenorhabditis elegans*. *Proc. Natl. Acad. Sci.* 113 (44), 12496–12501. doi: 10.1073/pnas.1608959113

Miller, S. C., Miyata, K., Brown, S. J., and Tomoyasu, Y. (2012). Dissecting systemic RNA interference in the red flour beetle *Tribolium castaneum*: parameters affecting the efficiency of RNAi. *PloS One* 7 (10), e47431. doi: 10.1371/journal.pone.0047431

Mutti, N. S., Louis, J., Pappan, L. K., Pappan, K., Begum, K., Chen, M. S., et al. (2008). A protein from the salivary glands of the pea aphid, *Acyrthosiphon pisum*, is essential in feeding on a host plant. *Proc. Natl. Acad. Sci. U.S.A.* 105 (29), 9965–9969. doi: 10.1073/pnas.0708958105

Mutti, N. S., Park, Y., Reese, J. C., and Reeck, G. R. (2006). RNAi knockdown of a salivary transcript leading to lethality in the pea aphid, *Acyrthosiphon pisum*. *J. Insect Sci.* 6, 1–7. doi: 10.1673/031.006.3801

Naessens, E., Dubreuil, G., Giordanengo, P., Baron, O. L., Minet-Kebdani, N., Keller, H., et al. (2015). A secreted MIF cytokine enables aphid feeding and represses plant immune responses. *Curr. Biol.* 25 (14), 1898–1903. doi: 10.1016/j.cub.2015.05.047

Pan, Y., Zhu, J., Luo, L., Kang, L., and Cui, F. (2015). High expression of a unique aphid protein in the salivary glands of *Acyrthosiphon pisum*. *Physiol. Mol. Plant Pathol.* 92, 175–180. doi: 10.1016/j.pmpp.2015.04.006

Pitino, M., and Hogenhout, S. A. (2013). Aphid protein effectors promote aphid colonization in a plant species-specific manner. *Mol. Plant Microbe Interact.* 26 (1), 130–139. doi: 10.1094/MPMI-07-12-0172-FI

Price, D. R., and Gatehouse, J. A. (2008). RNAi-mediated crop protection against insects. *Trends Biotechnol.* 26 (7), 393–400. doi: 10.1016/j.tibtech.2008.04.004

Rechavi, O., and Lev, I. (2017). Principles of transgenerational small RNA inheritance in *Caenorhabditis elegans*. *Curr. Biol.* 27 (14), R720–R730. doi: 10.1016/j.cub.2017.05.043

Rodriguez, P. A., Stam, R., Warbroek, T., and Bos, J. I. (2014). Mp10 and Mp42 from the aphid species *Myzus persicae* trigger plant defenses in *Nicotiana benthamiana* through different activities. *Mol. Plant Microbe Interact.* 27 (1), 30–39. doi: 10.1094/MPMI-05-13-0156-R

Sambrook, J., Fritsch, E. F., and Maniatis, T. (1989). *Molecular cloning: a laboratory manual* (Ed 2nd. New York:Cold spring harbor laboratory press).

Sanahuja, G., Banakar, R., Twyman, R. M., Capell, T., and Christou, P. (2011). *Bacillus thuringiensis*: a century of research, development and commercial applications. *Plant Biotechnol. J.* 9 (3), 283–300. doi: 10.1111/j.1467-7652.2011.00595.x

Sarria, E., Cid, M., Garzo, E., and Fereres, A. (2009). Excel workbook for automatic parameter calculation of EPG data. *Comput. Electron. Agric.* 67 (1-2), 35–42. doi: 10.1016/j.compag.2009.02.006

Sun, Y., Sparks, C., Jones, H., Riley, M., Francis, F., Du, W., et al. (2019). Silencing an essential gene involved in infestation and digestion in grain aphid through plant-mediated RNA interference generates aphid-resistant wheat plants. *Plant Biotechnol. J.* 17 (5), 852–854. doi: 10.1111/pbi.13067

Tjallingii, W. (1985). Electrical nature of recorded signals during stylet penetration by aphids. *Entomologia experimentalis applicata* 38 (2), 177–186. doi: 10.1111/j.1570-7458.1985.tb03516.x

Tjallingii, W. F. (1994). Sieve element acceptance by aphids. *Eur. J. Enlomol.* 91, 47–52.

Wang, W., Dai, H., Zhang, Y., Chandrasekar, R., Luo, L., Hiromasa, Y., et al. (2015b). Armet is an effector protein mediating aphid-plant interactions. *FASEB J.* 29 (5), 2032–2045. doi: 10.1096/fj.14-266023

Wang, E., and Hunter, C. P. (2017). SID-1 functions in multiple roles to support parental RNAi in *Caenorhabditis elegans*. *Genetics* 207 (2), 547–557. doi: 10.1534/genetics.117.300067

Wang, D., Liu, Q., Li, X., Sun, Y., Wang, H., and Xia, L. (2015a). Double-stranded RNA in the biological control of grain aphid (*Sitobion avenae* f.). *Funct. Integr. Genomics* 15 (2), 211–223. doi: 10.1007/s10142-014-0424-x

Wang, Z., Lü, Q., Zhang, L., Zhang, M., Chen, L., Zou, S., et al. (2021). Aphid salivary protein Mp1 facilitates infestation by binding phloem protein 2-A1 in arabidopsis. *Biochem. Biophys. Res. Commun.* 572, 105–111. doi: 10.1016/j.bbrc.2021.07.066

Xia, L., Ma, Y., He, Y., and Jones, H. D. (2012). GM wheat development in China: current status and challenges to commercialization. *J. Exp. Bot.* 63 (5), 1785–1790. doi: 10.1093/jxb/err342

Yang, Z., Ma, L., Francis, F., Yang, Y., Chen, H., Wu, H., et al. (2018). Proteins identified from saliva and salivary glands of the Chinese gall aphid *Schlechtendalia chinensis*. *Proteomics* 18 (9), 1700378. doi: 10.1002/pmic.201700378

Yu, X., Wang, G., Huang, S., Ma, Y., and Xia, L. (2014). Engineering plants for aphid resistance: current status and future perspectives. *Theor. Appl. Genet.* 127 (10), 2065–2083. doi: 10.1007/s00122-014-2371-2

Zhang, Y., Fu, Y., Francis, F., Liu, X., and Chen, J. (2021). Insight into watery saliva proteomes of the grain aphid, *Sitobion avenae*. *Arch. Insect Biochem. Physiol.* 106 (1), e21752. doi: 10.1002/arch.21752

Zhang, Y., Liu, X., Fu, Y., Crespo-Herrera, L., Liu, H., Wang, Q., et al. (2022a). Salivary effector Sm9723 of grain aphid *Sitobion miscanthi* suppresses plant defense and is essential for aphid survival on wheat. *Int. J. Mol. Sci.* 23 (13), 6909. doi: 10.3390/ijms23136909

Zhang, Y., Liu, X., Francis, F., Xie, H., Fan, J., Wang, Q., et al. (2022b). The salivary effector protein Sg2204 in the greenbug *Schizaphis graminum* suppresses wheat defence and is essential for enabling aphid feeding on host plants. *Plant Biotechnol. J.* 20 (11), 2187–2201. doi: 10.1111/pbi.13900

Zhang, M., Zhou, Y., Wang, H., Jones, H., Gao, Q., Wang, D., et al. (2013). Identifying potential RNAi targets in grain aphid (*Sitobion avenae* f.) based on transcriptome profiling of its alimentary canal after feeding on wheat plants. *BMC Genomics* 14, 560. doi: 10.1186/1471-2164-14-560

frontiers | Frontiers in Plant Science

TYPE Original Research
PUBLISHED 11 January 2023
DOI 10.3389/fpls.2022.1098751

OPEN ACCESS

EDITED BY
Ravi Gupta,
Kookmin University, South Korea

REVIEWED BY
Roy Kirsch,
Max Planck Institute for Chemical Ecology, Germany
Guoxing Wu,
Yunnan Agricultural University, China

*CORRESPONDENCE
Gexia Qiao
qiaogx@ioz.ac.cn
Xiaolei Huang
huangxl@fafu.edu.cn

SPECIALTY SECTION
This article was submitted to Plant Proteomics and Protein Structural Biology, a section of the journal Frontiers in Plant Science

RECEIVED 16 November 2022
ACCEPTED 19 December 2022
PUBLISHED 11 January 2023

CITATION
Zhang H, Lin R, Liu Q, Lu J, Qiao G and Huang X (2023) Transcriptomic and proteomic analyses provide insights into host adaptation of a bamboo-feeding aphid.
Front. Plant Sci. 13:1098751.
doi: 10.3389/fpls.2022.1098751

Transcriptomic and proteomic analyses provide insights into host adaptation of a bamboo-feeding aphid

Hui Zhang[1,2], Ruixun Lin[1], Qian Liu[1], Jianjun Lu[1], Gexia Qiao[2]* and Xiaolei Huang[1,3]*

[1]State Key Laboratory of Ecological Pest Control for Fujian and Taiwan Crops, College of Plant Protection, Fujian Agriculture and Forestry University, Fuzhou, China, [2]Key Laboratory of Zoological Systematics and Evolution, Institute of Zoology, Chinese Academy of Sciences, Beijing, China, [3]Fujian Provincial Key Laboratory of Insect Ecology, Fujian Agriculture and Forestry University, Fuzhou, China

Introduction: Salivary glands and their secreted proteins play an important role in the feeding process of sap-sucking aphids. The determination of saliva composition is an important step in understanding host plant adaptation of aphids. Pseudoregma bambucicola is a severe bamboo pest in subtropical areas and the only aphid species that can exclusively feed on hard stalks of bamboos. How this species can penetrate and degrade hard bamboo cell walls and utilize a very specialized niche are important unanswered questions.

Methods: In this study, comprehensive analyses based on transcriptome sequencing, RT-qPCR, liquid chromatography-tandem spectrometry (LC–MS/MS) and bioinformatics were conducted on dissected salivary glands and secreted saliva of P. bambucicola to characterize the overall gene expression and salivary protein composition, and to identify putative effector proteins important for aphid-plant interactions.

Results and Discussion: Some secretory proteins homologous to known aphid effectors important for aphid–plant interactions, such as digestive enzymes, detoxifying and antioxidant enzymes and some effectors modulating plant defenses, are also detected in salivary gland transcriptome and salivary gland and/or saliva secretomes in P. bambucicola. This indicates that these effectors are probably be essential for enabling P. bambucicola feeding on bamboo host. Although several plant cell wall degrading enzymes (PCWDEs) can be identified from transcriptome, most of the enzymes identified in salivary glands showed low expression levels and they only represent a small fraction of the complete set of enzymes for degrading cellulose and hemicellulose. In addition, our data show that P. bambucicola has no its own ability to produce pectinases. Overall, our analyses indicate that P. bambucicola may lose its own ability to express and secrete key PCWDEs, and its adaptation to unique feeding habit may depend on its symbiotic bacteria.

KEYWORDS

aphid-plant interaction, transcriptome, proteome, salivary protein, secretory protein

Introduction

Aphids are one of the most important agricultural pest groups that feed on plant phloem sap *via* piercing-sucking mouthparts. Many aphids can also serve as vectors of plant viruses, causing serious economic damage to agriculture and forestry (Hooks and Fereres, 2006; Dedryver et al., 2010). During feeding, aphids puncture the plant epidermis using their specialized stylets that penetrate between cells and reach the phloem sieve tubes to ingest phloem sap. In their long-term coevolutionary history, plants have evolved a variety of defense systems against aphid feeding, and aphids have developed complex strategies to overcome plant defenses. As the first defensive barrier against herbivores, plant cell walls are dynamic extracellular structures composed of a thick layer of polysaccharides, such as cellulose, hemicellulose and pectin, and structural proteins (Anderson and Kieber, 2020). Aphids must first overcome the cell wall barrier of host plants to access nutrients. Plant cell wall-modifying enzymes present in aphid saliva are thought to help them penetrate the cell wall (Silva-Sanzana et al., 2020). This may be a common strategy among phloem-feeding insects for plant penetration, although the source of these enzymes may sometimes be unclear. For example, pectinase activity has been detected in secreted saliva of the *Schizaphis graminum* (Ma et al., 1990); Guo et al. (2006) has also detected pectinase and cellulase activities in saliva of *Sitobion avenae*; one putative cellulase gene sequence and several cellulase transcripts have been also identified from *Acyrthosiphon pisum* and two *Myzus* species, respectively (Watanabe and Tokuda, 2010; Thorpe et al., 2016), although there has been no protein-level validation; the *Nilaparvata lugens* can secrete a salivary endo-β-1,4-glucanase into rice plants that can degrade celluloses in plant cell walls, allowing its stylet to reach the phloem (Ji et al., 2017); and a salivary β-1,4-endoglucanase with cellulolytic activity found in sharpshooter *Homalodisca vitripennis* saliva can be secreted into plants during feeding (Backus et al., 2012).

Salivary gland is an important secretary tissue that play a crucial role during insect feeding. The insect gut also play an important role in host feeding and digestion process other than salivary glands. Enzymes in the gut of aphid, for example, are thought to be involved in the detoxification and degradation of various plant compounds (Cristofoletti et al., 2003; Matthews et al., 2010; Pyati et al., 2011; Anathakrishnan et al., 2014). For aphids, however, the salivary glands may be more important in their initial probing and feeding. Aphid salivary glands can secrete saliva containing a variety of enzymes and effectors that facilitate stylet penetration and modulate plant defense (Elzinga and Jander, 2013). Aphid saliva can be categorized into watery and gel saliva with different protein composition and function (Miles, 1959; Tjallingii, 2006). Gel saliva is secreted during the early stages of stylet penetrating and is involved in coagulation and formation of salivary sheath that can protect stylets from physical damage, while watery saliva is secreted during aphid feeding and injected into plant cells for digestion of nutrients and suppressing plant defense responses (Miles, 1999; Will et al., 2007; Will et al., 2013). The major components of gel saliva are expected to include plant cell wall-degrading enzymes (PCWDEs) facilitating stylet progress, as well as some proteins and peptides that can cause plant defense; the components of water saliva include Ca^{2+} binding proteins, proteases, detoxification enzymes and effector proteins (van Bel and Will, 2016). Several salivary effectors have been found to promote aphid feeding and plant defense suppression (Zhang et al., 2017). For example, the water-soluble salivary protein *C002*, first identified in pea aphid, has been shown to be essential for its successful feeding (Mutti et al., 2008), and overexpression of *MpC002* in *Myzus persicae* on *Nicotiana benthamiana* could promote aphid fecundity (Bos et al., 2010). Some other effectors such as *Me10* and *Me23* in *Macrosiphum euphorbiae*, as well as *Mp1*and *Mp2* in *M. persicae* have also been proved to enhance aphid fecundity or promote aphid colonization (Atamian et al., 2013; Pitino and Hogenhout, 2013).

The composition of salivary proteins is supposed to be a key factor limiting aphids' host range (Elzinga and Jander, 2013). Characterization of salivary components is crucial for understanding adaptation of aphids to specific host plants. Salivary proteins are generally identified by transcriptomic and/or proteomic analyses of the dissected salivary glands and/or secreted saliva (Nicholson et al., 2012; Atamian et al., 2013; van Bel and Will, 2016; Zhang et al., 2017; Dommel et al., 2020; Zhang et al., 2020). Integrated transcriptomic and proteomic analyses of salivary protein composition can help identify new salivary protein, and obtain a more accurate and comprehensive salivary protein repertoire. The salivary protein composition has been investigated by integrated omics analysis in some aphid species, such as the *A. pisum* (Carolan et al., 2011).

Among the over 5,100 aphid species, the social aphid *Pseudoregma bambucicola* is the only one exclusively feeding on hard stems of bamboos. This species is mainly distributed in subtropical Asian areas and exclusively specialized on *Bambusa* bamboos. Bamboo is known to have an enhanced mechanical hardness and highly lignified and fibrotic cell walls. The secondary wall structure of bamboo fiber shows unique multilayered structure (Preston and Singh, 1950). Moreover, the cell wall porosity of bamboo is generally lower than that of wood species (Cao et al., 2022). But how *P. bambucicola* stylet can penetrate bamboo cell walls remains largely unknown, and answering this question is crucial for understanding the mechanisms underlying high specialization of feeding niche. We need to explore this question in two aspects: on the one hand, we need to know the role of *P. bambucicola* itself in its unique feeding niche and diet specialization; on the other hand, the contribution by the symbiotic partners to host adaption in *P.*

bambucicola should also be explored in parallel. We are actively working on resolving these issues. Previous studies on the symbiotic bacterial community of *P. bambucicola* have indicated that this aphid harbours symbiotic *Pectobacterium*, which may produce PCWDEs and assist *P. bambucicola* in feeding hard bamboo stems (Charkowski et al., 2012; Liu et al., 2021; Liu et al., 2022). However, from this aphid's perspective, it is unclear what is its salivary protein composition and what role itself can play in breaking through the plant cell wall barrier during its feeding.

In this study, a comprehensive analysis based on transcriptome and liquid chromatography-tandem spectrometry (LC–MS/MS) was conducted on dissected salivary glands and secreted saliva of *P. bambucicola* to characterize the overall gene expression and salivary protein composition, and to identify putative effector proteins important for aphid-plant interactions. This study can promote our understanding for the role of salivary glands in host specialization of *P. bambucicola*, and provide insights into its adaptation to unique feeding habit.

Materials and methods

Aphid collection and sample preparation

Parthenogenetic adults of *P. bambucicola* used in this study were collected from Fuzhou, China in 2020. Paired salivary glands and guts of *P. bambucicola* were dissected in ice-cold phosphate-buffered saline solution (PBS, 10 mM NaH_2PO4, 1.8 mM KH_2PO4, 140 mM NaCl and 2.7 mM KCl, pH=7.4) using fine tweezers. The dissected tissues were quickly washed twice in PBS solution and immediately snap-frozen in liquid nitrogen, and then stored in a -80°C freezer. Approximately 200 pairs of salivary glands were used for transcriptome and proteome sequencing, respectively, and 200 pairs of salivary glands and 150 guts were also prepared for RT-qPCR for comparison of gene expression between samples. Each sample consisted of three biological replicates. Most previous studies used artificial diets to collect saliva and identified aphid salivary proteins successfully (Harmel et al., 2008; Carolan et al., 2009; Rao et al., 2013; Yang et al., 2018). However, it is difficult to rear *P. bambucicola* with traditional artificial diet as other aphids due to its unique feeding habitat. Therefore, we turned to identify injected salivary proteins by comparative proteomic analysis of fed and unfed bamboos with aphid salivary gland transcriptome data as the search database. For identification of injected salivary proteins by *P. bambucicola*, the *Bambusa multiplex* stems that had been fed continuously by over thousands of *P. bambucicola* individuals for three days were collected, with stems that had not been fed using for control. Several samples were unqualified and thus discard during the sequencing process, two bamboo samples fed and one sample unfed by *P. bambucicola* were used finally. Transcriptome and proteome sequencing were performed by Sangon Biotech (Shanghai, China) and Jingjie PTM BioLab (Hangzhou, Zhejiang, China), respectively.

For identifying all PCWDEs in *P. bambucicola* whole body, individuals of different morphs and developmental stages, including newborn 1st instar normal nymphs, newborn 1st instar soldiers, older 1st instar normal nymphs, older 1st instar soldiers, medium instar normal nymphs, viviparous adult females producing soldiers and viviparous adult females producing normal nymphs, were also collected and subjected for transcriptome sequencing.

Transcriptome sequencing and RT-qPCR analysis

The *P. bambucicola* samples across different morphs and different developmental stages and approximately 200 pairs of dissected salivary glands of *P. bambucicola* were used for RNA extraction using TRIzol Reagent (Qiagen, CA). The RNA concentration and quality were assessed by a NanoDrop spectrophotometer, gel electrophoresis and an Agilent 2100 Bioanalyzer system (Agilent Technologies, CA, USA). Qualified RNA was then used for cDNA library construction. The generated libraries were sequenced using the DNBSEQ sequencing platform. The obtained raw data was subjected to removing adapters, low quality sequences and ambiguous nucleotides (reads with more than 5% N bases). The obtained clean data was used for *de novo* assembly with the Trinity (Grabherr et al., 2011) to obtain final unigenes. Bowtie (Bowtie, RRID: SCR_005476) (Langmead and Salzberg, 2012) was used for aligning clean reads to the unigene library, and then RSEM (RSEM, RRID: SCR_013027) (Li and Dewey, 2011) was used to calculate the gene expression level of unigenes. The relative abundance of unigenes was measured by FPKM, which represents fragments per kilobase of transcript per million mapped reads. For functional annotation, all predicted unigenes were run blast against multiple public databases, including non-redundant protein (Nr) database, Nt, Swiss-Prot, Kyoto Encyclopedia of Genes and Genomes (KEGG), euKaryotic Ortholog Groups (KOG), Pfam and Gene Ontology (GO) databases.

Insects can adapt to plant defense responses by utilizing effectors from a variety of sources, such as salivary proteins, intestinal proteins and symbiotic microorganism derived functional proteins (Zhao et al., 2019). A total of 11 genes associated with aphid feeding, including five genes related to digestion and six genes related to defense, were randomly selected for detection of gene expression levels between salivary glands and guts, with the HSP70A1 (heat shock protein 70 A1-like) and MGST1 (microsomal glutathione S-transferase 1-like) used as reference genes to normalize selected genes' expression (Table S1). Primer Premier 5.0 (Premier

Biosoft, CA, USA) was used to design RT-qPCR specific primers for selected and reference genes, as shown in Table S1. cDNA was synthesized using FastKing gDNA Dispelling RT SuperMix (Tiangen, Beijing, China). RT-qPCR was performed with Green qPCR SuperMix Kit (TransGen Biotech, Beijing, China) following the manufacturer's instructions. Three biological replicates were performed on each salivary gland and intestinal tract sample, and each biological replicate was run in three technical replicates. All data were analyzed by Graphpad (GraphPad, RRID: SCR_000306) (http://graphpad.com/) version 9.0 software with unpaired t-test ($P < 0.05$).

LC-MS/MS analysis of salivary glands and saliva

The label-free LC-MS/MS quantitative proteomic analysis was performed by the Jingjie PTM BioLab. The salivary gland samples were grinded with liquid nitrogen into cell powder and transferred to 5 ml centrifuge tube. After adding four times the volume of lysis buffer (including 1% SDS and 1% protease inhibitor cocktail), the cell powder samples were boiled with a metal bath at 95°C for 10min, and were sonicated with a high intensity ultrasonic processor (Scientz, Ningbo, China). To remove cell debris, the protein solution was spun for 10 min (12000 g at 4°C) and the supernatant was pipetted into clean tubes. The protein concentration was determined using BCA Protein Assay kit (Beyotime, Shanghai, China) following the manufacturer's instructions.

For digestion, an equal amount of protein for each sample was used and lysis buffer was added to adjust to the same volume. After adding dithiothreitol (DTT) to a final concentration of 5 mM, the protein solution was incubated at 56°C for 30 min, followed by adding iodoacetamide (IAA) to 11 mM final concentration and incubating 15 min at room temperature in the dark to alkylate cysteines. The alkylated protein samples were transferred to ultrafiltration tubes, centrifuged at 12000 g for 20 min at room temperature. The protein was re-suspended in 8 M urea (Sigma) for 3 times, and then urea was also re-suspended with 100mM ammonium bicarbonate solution for 3 times. Trypsin was added for a final trypsin:protein ratio of 1:50 (w/w) and incubated overnight. The peptides were recovered by centrifugation at 12000 g for 10 min at room temperature, and then recovered again with ultrapure water. The two peptide solutions were then combined.

The peptides were dissolved with solvent A (0.1% formic acid and 2% acetonitrile in water) and then separated using the Easy-nLC 1200 ultra-high-performance liquid system. The separated peptides were ionized by injection into an NSI ion source and then analyzed by Orbitrap Exploris^{TM} 480 mass spectrometers (Exploris 480, Thermo Fisher Scientific, USA). The electrospray ionization voltage was set to 2.3 kV, and a high-resolution Orbitrap was used to detect and analyze the peptide parent ions and their secondary fragments. The primary mass spectrum range was 400-1200 m/z with the scanning resolution was set to 60000. The fixed start point of the secondary mass spectrum scan range was 110 m/z with the scanning resolution of 15000, and TurboTMT was set to Off. A data dependent scanning (DDA) program based on Cycle time was used as the data acquisition mode. Specifically, within a 1.0-s cycle period, the parent ions of the peptide were selected according to the sequence of the signal intensity from high to low, and then entered the HCD collision pool to fragment with 27% of the fragmentation energy. The secondary mass spectrometry analysis was also performed sequentially. To improve the efficient utilization of MS, the automatic gain control (AGC) was set to 100%, the signal threshold was set to 5E4 ions/s, the maximum injection time was set as Auto, and the dynamic exclusion time of tandem MS scanning was set to 20 s to avoid repeated parent ion scanning.

The resulted MS/MS data were analyzed using Maxquant search engine (version v1.6.15.0) (Prianichnikov et al., 2020) with the protein sets (22,597 sequences) of salivary gland transcriptome using as the retrieval database and an inverse decoy library used to calculate the false positive rate (FDR). The cleavage enzyme was Trypsin/P allowing up to 2 cleavages; the minimum peptide length was 7 amino acid residues; the maximum number of modifications of the peptide was set as 5; the mass tolerance of precursor ions was 20 ppm in the first search and 4.5 ppm in the main search, respectively. The mass tolerance of fragment ions is 20 ppm. Carbamidomethyl on cys was set as a fixed modification with oxidation on Met, acetylation on protein N-terminal and decarboxamidation as variable modifications. The false discovery rate (FDR) for both protein identification and peptide–spectrum matches (PSMs) identification was 1%.

For protein extraction of bamboo tissues, samples of bamboo fed and unfed by *P. bambucicola* were grinded with liquid nitrogen. The powder samples were sonicated with a high intensity ultrasonic processor (Scientz, Ningbo, China) after adding four times the volume of lysis buffer (including 10 mM dithiothreitol and 1% protease inhibitor cocktail). An equal volume of Tris-saturated phenol was then added and centrifuged for 10 min (5500 g at 4°C). The supernatant was collected in clean centrifuge tubes and five times the volume of 0.1 M ammonium acetate/methanol were added and incubated at -20°C overnight. After centrifugation at 4°C for 10 min, the supernatant was removed, and the precipitate was washed with cold methanol once and cold acetone for three times, respectively. The precipitate was redissolved with 8 M urea (Sigma), and the protein concentration was determined using BCA Protein Assay kit (Beyotime, Shanghai, China) following the manufacturer's instructions. For enzymatic digestion, an equal amount of protein for each sample was taken and adjusted to the same volume with lysis buffer. TCA was added slowly to a final concentration of 20% TCA, mixed by

vortex, and precipitated for 2h at 4°C. After centrifugation at 4500g for 5min, the supernatant was discarded and the precipitate was washed with precooled acetone for two to three times. After the precipitation was dried, TEAB was added to a final concentration of 200 mM, and the precipitation was broken up by ultrasound. Trypsin was then added at 1:50 (trypsin: protein, m/m) ratio for digestion overnight. Dithiothreitol (DTT) was added to make the final concentration of 5 mM and reduced at 56°C for 30 min. Then iodoacetamide (IAA) was added to 11 mM final concentration and incubated for 15 min at room temperature under in the dark. The subsequent LC-MS/MS analysis were then performed as described above. And the obtained MS/MS spectra data were searched separately against the salivary gland transcriptomic database and *Bambusa* protein database (including 14361 proteins) download from Nr protein database of the NCBI (accessed on April 19, 2022).

The identified salivary gland proteins, saliva proteins and bamboo proteins was annotated with multiple public databases, including Nr, KEGG, Swiss-Prot, Pfam, GO and KOG databases. Functional enrichment analysis was then conducted with the functions phyper in R software, with FDR adjust *P*-value (Qvalue) < 0.05 as the threshold.

Bioinformatic analysis

Aphid effectors are likely secreted proteins delivered into the saliva secreted by salivary glands to mediate plant defenses (Bos et al., 2010). For identification of candidate effectors, signal peptides were predicted from the amino acid sequences of dual transcriptomic-proteomic data from salivary glands as well as proteomic data from saliva using SignalP (SignalP, RRID: SCR_015644) (https://dtu.biolib.com/SignalP-6) v6.0 (Teufel et al., 2022), followed by DeepTMHMM (Hallgren et al., 2022) to identify transmembrane domains for proteins containing signal peptides. Proteins containing an N signal peptide but no transmembrane domain were regarded as candidate effectors.

The degradation of plant cell wall components requires a large repertoire of highly specialized carbohydrate-active enzymes (CAZymes) that are produced by the organism itself or its associated symbiotic microbes (Ni and Tokuda, 2013; Scully et al., 2013; Bredon et al., 2019). Firstly, Hmmscan program in the HMMER (Hmmer, RRID : SCR_005305) (http://hmmer.janelia.org/) version 3.1b2 (Eddy, 1998) was used to search amino acid sequences of transcriptome and proteome against the family specific HMM profiles of CAZymes within dbCAN HMMdb v11 to identify CAZymes and assign them to CAZy families, with an e-value cutoff 1e-3 (≤80 aa) or 1e-5 (>80 aa) and coverage above 30% as the filter threshold. CAZy families can be classified into glycoside hydrolases (GHs), glycosyltransferases (GTs), polysaccharide lyases (PLs), carbohydrate esterases (CEs), auxiliary activities (AAs) and carbohydrate-binding modules (CBMs) (Drula et al., 2022). Enzymatic activity of all identified CAZymes were detected using Hotpep (Busk et al., 2017) to determine whether they are candidate plant cell wall degrading enzymes (PCWDEs). The identified candidates were further confirmed as putative PCWDEs by reference to Tokuda (2019). The transcriptome data used for PCWDEs identification in this study include salivary gland transcriptome and whole-body transcriptome of *P. bambucicola* across different morphs and developmental stages.

Results

Transcriptome overview of SG of *Pseudoregma bambucicola*

An average of 47,326,665 bp raw reads was yielded from transcriptome of *P. bambucicola* salivary glands. After data filtering, a total of 19.47 Gb clean data was used for *de novo* assembly, resulting in 48,028 unigenes with an average length of 1,310 bp and N50 of 2,400 bp. There were 28,512 (59.37%), 24,816 (51.67%), 21,093 (43.92%), 22,891 (47.66%), 20,427 (42.53%), 20,570 (42.83%) and 13,385 (27.87%) unigenes homologous to known sequences in the Nr, Nt, SwissProt, KEGG, KOG, PFAM and GO databases, respectively. About 32,111 (66.86%) unigenes were functionally annotated in at least one of the used databases, and many of them could be annotated by multiple databases (Figure 1A). The unigenes showed the most similarity with *Sipha flava* according to the matched species distribution of annotation based on Nr database (Figure 1B).

GO function classification was conducted on predicted unigenes and showed that most of them were enriched in cellular anatomical entity, cellular process, binding, catalytic activity and metabolic process (Figure 1C). The top 20 highly-expressed unigenes include some genes associated with mitochondrial activity, genes encoding a invertebrate-type lysozyme 6, a odorant-binding protein 2, a prohormone-2, a alpha-N-acetylgalactosaminidase, a putative sheath protein and some genes encoding proteins with unknown functions (Table S2). These highly expressed genes in salivary glands such as the gene encoding putative sheath protein and genes with unknown functions were worth for further study. In addition, many homologous genes encoding salivary proteins that are known to paly an important role in aphid-plant interactions, such as some digestive enzymes, detoxifying enzymes, antioxidant enzymes and some effector proteins modulating plant defenses, were also identified in *P. bambucicola* salivary glands (Table S3). These results suggest that some salivary components are conserved across different aphids.

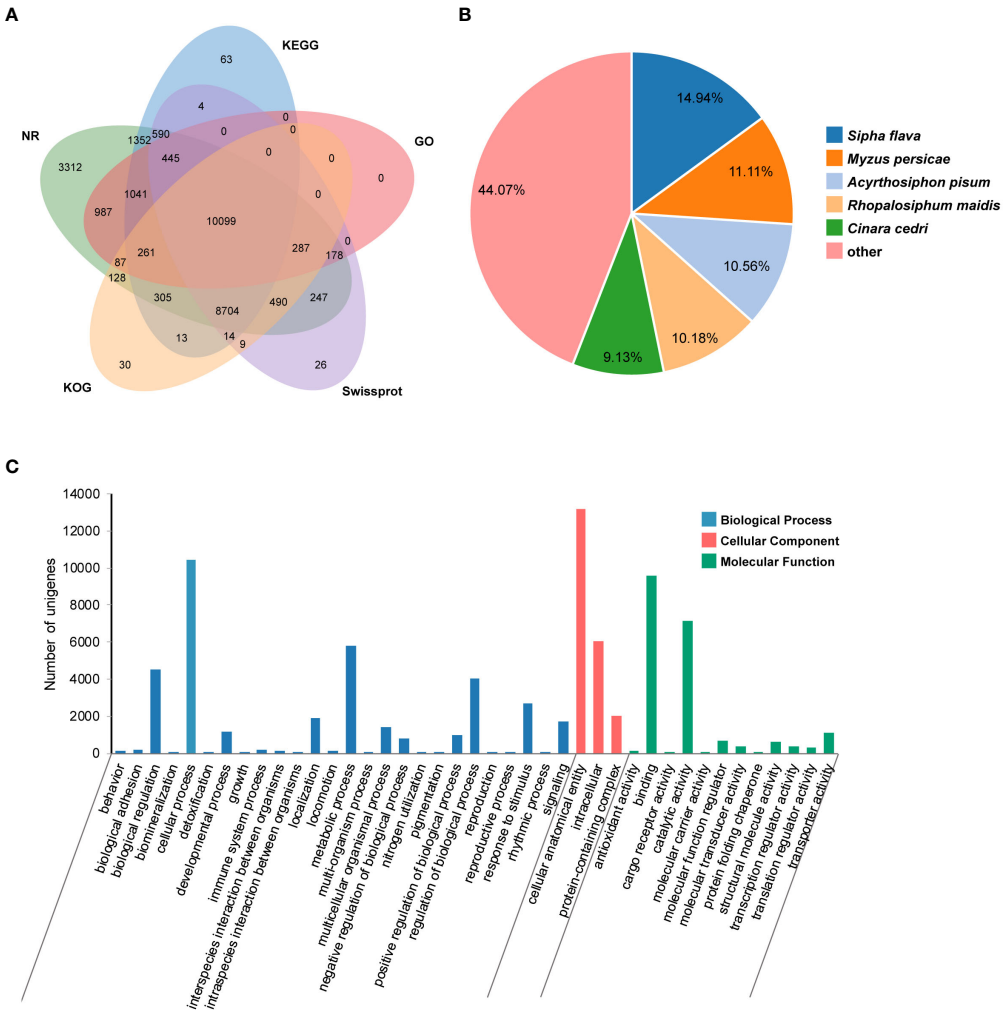

FIGURE 1
Transcriptomic annotation for *Pseudoregma bambucicola* salivary glands. **(A)** Venn diagram of annotated results *via* different databases. **(B)** Species distribution of annotation results in Nr database. Only the top five closely matched species are shown. **(C)** Gene Ontology classification of *Pseudoregma bambucicola* salivary gland unigenes.

RT-qPCR analysis of feeding–related genes

In addition to the salivary glands, guts are also important for insect feeding. To understand the relative role of salivary gland and gut in *P. bambucicola* feeding, expression levels of 11 genes, including five genes related to digestion and six genes involved in detoxification and antioxidant activities, were detected between salivary glands and guts of *P. bambucicola* by RT-qPCR. All 11 genes expressed in both salivary glands and guts. Among the five digestive-related genes, significant differences were found in the expression of beta-galactosidase-like (*GLB1*), lysosomal alpha-mannosidase (*MAN2B1*), carboxypeptidase E-like (*CPE*) and methionine aminopeptidase 1D, mitochondrial (*METAP1D*) between salivary glands and guts except the AAEL006169 (lysosomal aspartic protease), among which the *GLB1*, *MAN2B1* and *CPE* showed evidently higher expression levels in salivary glands (Figures 2A–E). For six genes involved in detoxification and antioxidant activities, the expression level of glucose dehydrogenase [FAD, quinone] (*CHDH*) in salivary glands was remarkably higher than that in guts; and superoxide dismutase [Cu-Zn] 1 (*SOD1*) also showed higher expression levels in salivary glands. Phospholipid hydroperoxide glutathione peroxidase (*GPX4*) and glutathione S-transferase-like (*GST*) were highly expressed in guts compared with salivary glands (Figures 2F–K). These results suggest that both salivary glands and guts may play important roles in digestion and detoxification in *P. bambucicola* plant feeding.

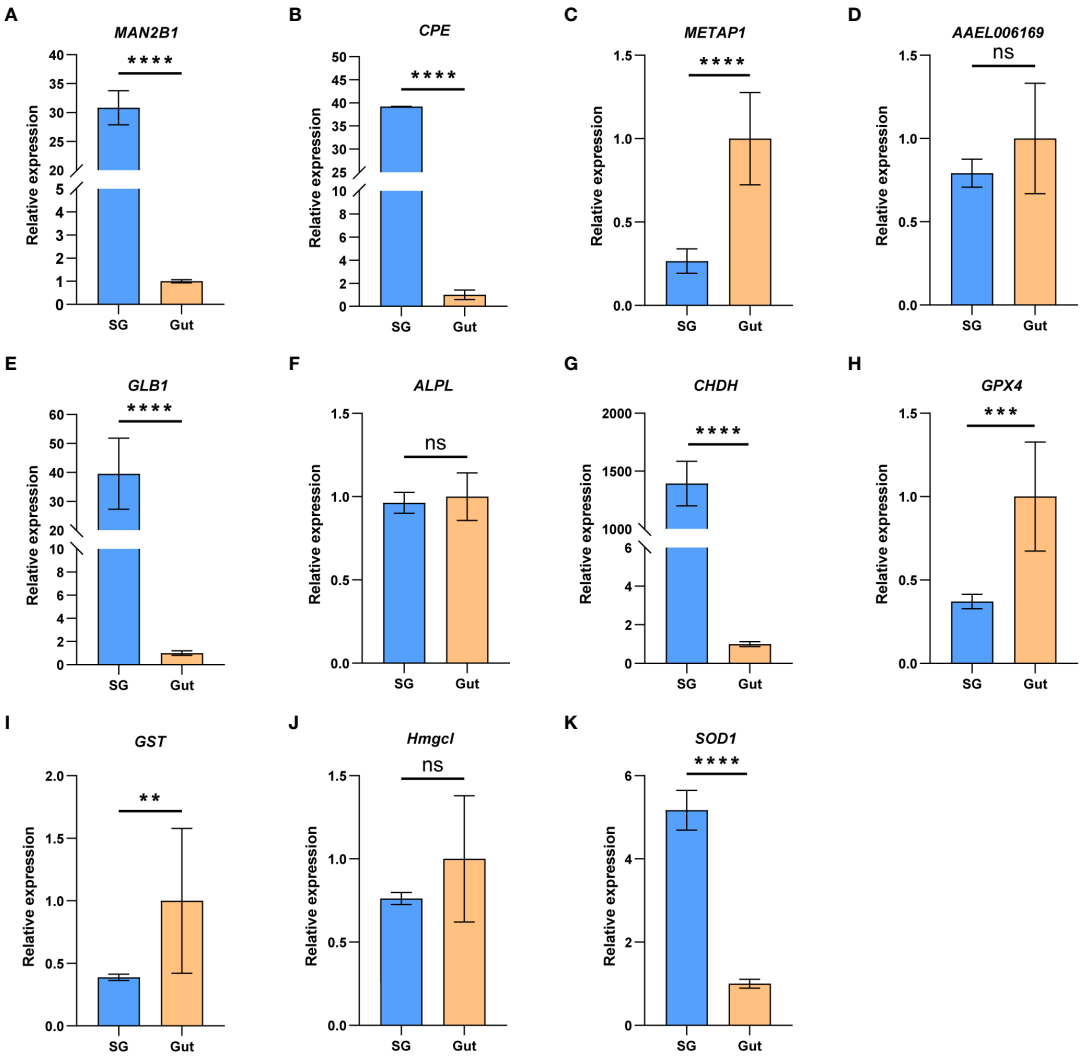

FIGURE 2
The relative gene expression of the 11 feeding-related genes between salivary glands (SG) and gut (Gut) of *Pseudoregma bambucicola* detected by RT-qPCR. **(A)** lysosomal α-mannosidase (*MAN2B1*); **(B)** carboxypeptidase E like (*CPE*); **(C)** methionine aminopeptidase-related gene (*METAP1D*); **(D)** lysosomal aspartic protease (AAEL006169); **(E)** β-galactosidase (*GLB1*); **(F)** alkaline phosphatase (*ALPL*); **(G)** glucose dehydrogenase (*CHDH*); **(H)** phospholipid hydroperoxide glutathione peroxidase (*GPX4*); **(I)** glutathione S-transferase (*GST*); **(J)** hydroxymethylglutaryl-CoA lyase (*Hmgcl*); **(K)** superoxide dismutase (*SOD1*). Heat shock protein 70 A1 and microsomal glutathione S-transferase 1 were used as internal reference genes. Asterisks above the bars indicate significant differences (**$P < 0.01$; ***$P < 0.001$; ****$P < 0.0001$). "ns" indicates not significant ($P > 0.05$).

Proteins identified from salivary gland and saliva

A total of 4793 proteins were detected from the salivary gland proteome. Of them, 3115 proteins attributed to at least one GO term, with the cellular metabolic process and organic substance metabolic process, organelle and cytoplasm, protein binding and hydrolase activity being the two most represented terms in each of the three categories, respectively (Figure S1A). Proteins without unique peptides in two of three replicates and those with an average of unique peptides less than two were filtered out, resulting in 2442 candidate proteins. All proteins were annotated with the KEGG pathway database to characterize the general metabolic functions of the salivary gland proteome, and many proteins were classified and associated with global and overview maps, signal transduction, endocrine system, translation, and transport and catabolism pathways (Figure 3A), consistent with the biological roles of salivary glands.

The raw MS/MS data of bamboo tissues unfed and fed by aphids were then analyzed and searched against the transcriptomic data of *P. bambucicola* salivary glands to identify putative salivary proteins in secreted saliva. In total,

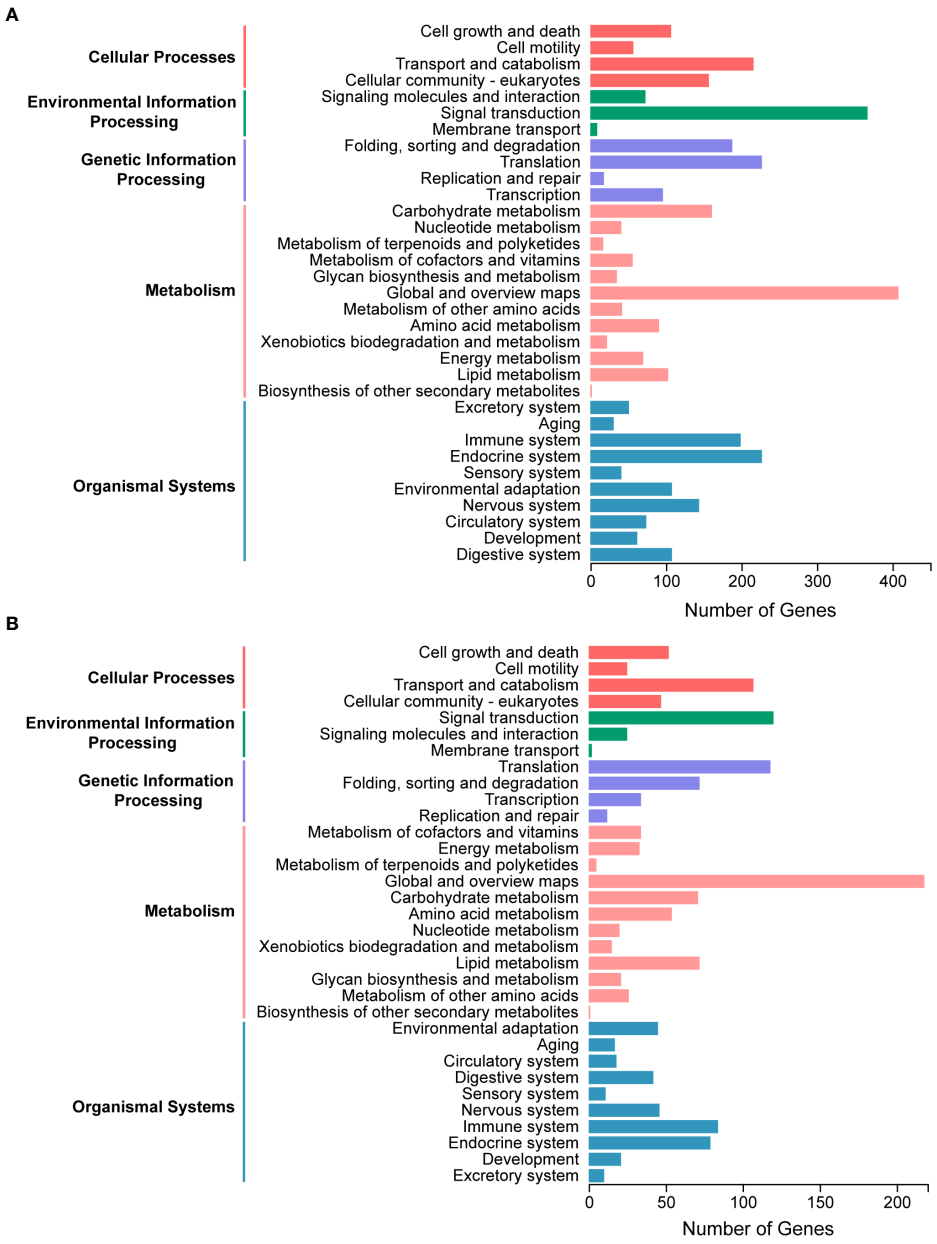

FIGURE 3
Kyoto Encyclopedia of Genes and Genomes (KEGG) pathway analysis of salivary components in *Pseudoregma bambucicola*. **(A)** Functional classification of metabolic pathways for salivary gland proteins. **(B)** Functional classification of metabolic pathways for putative saliva proteins secreted into bamboos.

3244 proteins were detected, and 1496 of them were expressed only in bamboo tissues after aphid feeding, and were regarded as aphid salivary candidates secreted into host plants. To reduce false positives, 1160 proteins with at least two unique peptides were selected for further metabolic functional analysis. The majority of proteins participated in pathways of global and overview maps, signal transduction, translation, transport and catabolism and immune system, which was generally similar to that of salivary gland proteome (Figure 3B).

KEGG pathway enrichment analysis showed that the salivary gland proteins were significantly enriched in pathways of proteasome, protein processing in endoplasmic reticulum, carbon metabolism, citrate cycle (TCA cycle), oxidative phosphorylation and protein export, while ribosome and oxidative phosphorylation were the most representative pathways for putative saliva proteins (Figure S1B, C). These results may indicate the important roles of salivary glands in protein secretion and energy metabolism.

Salivary secretory proteins

From transcriptome data of salivary glands, 1213 putative secretory proteins were predicted. Annotation against NCBI Nr database showed that 812 (66.94%) of all identified secretory proteins were functionally annotated, 359 (29.60%) proteins were annotated with unknown functions, and 42 (3.46%) proteins showed no similarity with all known sequences in the Nr database (Table S4). Functional enrichment analysis of these putative secretory proteins showed that the most enriched GO terms were structural constituent of cuticle, extracellular region and carbohydrate metabolic process, and the most enriched KEGG pathways were RNA polymerase, lysosome and other glycan degradation (Figure S2).

When we identified secreted proteins from mass spectrometry proteins, a total of 196 and 114 putative secreted effector candidates were predicted from the salivary gland and saliva proteome of *P. bambucicola*, respectively. Many of them were hypothetical proteins with unknown functions or functionally annotated proteins whose roles in aphid-plant interactions are not clear. Some candidate secretory effectors were homologous proteins also characterized in secretome of other aphid species, which had been supposed to play important roles in aphid-host interactions. For example, some detoxifying and antioxidant enzymes including glucose dehydrogenase, glutathione S-transferase, several carboxylesterases and peroxidases, were identified from salivary gland or saliva of *P. bambucicola* (Table S5). The putative salivary secretory effectors also contained some digestive enzymes such as sugar-degrading enzymes, carboxypeptidase, cathepsins, serine proteases and phospholipase, and some effectors modulating plant immunity and defense such as apolipophorin, odorant binding protein and yellow-like protein. In addition, some salivary glue proteins and cuticle proteins were also identified in both salivary gland and saliva of *P. bambucicola*, while two sheath proteins were detected only in salivary glands (Table S5). There were 44 putative secretory effectors in both salivary gland and saliva, including three salivary glue protein, a sheath protein (mucin-5AC protein), a venom serine carboxypeptidase, cathepsin L, phospholipase A-2-activating protein, odorant binding protein in addition to the above mentioned common salivary gland protein and several cuticle proteins. These putative secretory effectors may help promote aphid stylet penetration, digestion and detoxification activities, or contribute to suppression or activation of plant defense responses.

Plant cell wall degrading enzymes

The PCWDEs from the transcriptome of whole body and salivary glands were identified (Table 1, Table S6). A total of eight potential PCWDEs were identified based on salivary gland transcriptome, including four β-glucosidases, one endo-β-1,4-glucanase and three β-mannosidases. However, most of genes encoding PCWDEs showed very low expression levels (Figure 4A, Table 1). We did not identify any transcripts with potential pectinase activity, indicating that the *P. bambucicola* may loss ability to secrete and degrade pectin. When we detected PCWDEs expressed in translational levels using the proteome data of salivary glands and secreted saliva, only one β-glucosidase and one β-mannosidase were detected at protein level in salivary gland, and no other PCWDEs were detected at protein level in the secreted saliva except for four β-glucosidases with putative cellulolytic activity. Of these, only one β-mannosidase identified from salivary gland proteome and one β-glucosidase from saliva proteome were predicted containing secretory signal. Besides, two of the four β-glucosidase transcripts identified in the proteome of secreted saliva were not full-length and so it is uncertain whether they contain secretory signal or not.

To obtain more complete PCWDEs in *P. bambucicola*, PCWDEs from whole-body transcriptome across different morphs and developmental stages of *P. bambucicola* were also identified. A total of three β-glucosidases, one endo-β-1,4-glucanase and one β-mannosidase were identified, among which β-glucosidase 1, the endo-β-1,4-glucanase 1 and beta-mannosidase 1 were found in both the whole-body and salivary gland (Table 1, Table S6). Except for two glucosidases (β-

TABLE 1 Plant cell wall-degrading enzymes (PCWDEs) candidates identified from the whole body and salivary gland transcriptomes of *Pseudoregama bambucicola*.

Enzyme name	EC number	CAZy family	Number of PCWDEs		Potential secreted PCWDEs	
			Whole body	Salivary glands	Whole body	Salivary glands
Cellulases						
β-Glucosidase	3.2.1.21	GH1	3	4	1	1
Endo-β-1,4-glucanase	3.2.1.4	GH9	1	1	1	1
Hemicellulases						
β-Mannosidase	3.2.1.25	GH2	1	3	1	3

EC number, Enzyme Commission number; CAZy family, Carbohydrate-Active Enzymes family, See Table S6 for overlapping or unique identification of CAZymes between samples.

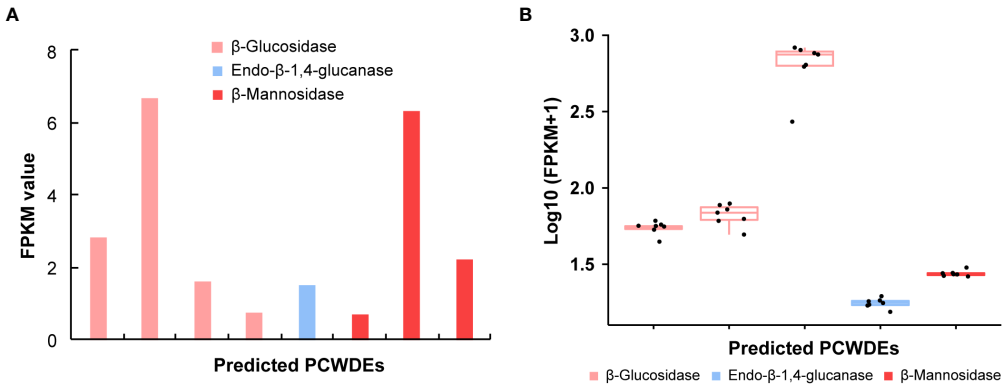

FIGURE 4
The expression patterns of genes encoding plant cell wall-degrading enzymes (PCWDEs) in different samples of *Pseudoregma bambucicola*. **(A)** The expression pattern of different PCWDEs identified from salivary glands. The bars from left to right in the histogram represent β-glucosidase 1, β-glucosidase 4, β-glucosidase 5, β-glucosidase 6, endo-β-1,4-glucanase 1, beta-mannosidase 2, beta-mannosidase 3 and beta-mannosidase 1, respectively (see Table S6 for details). **(B)** The expression pattern of PCWDEs across different morphs or developmental stages. The boxplots from left to right represent β-glucosidase 1, β-glucosidase 2, β-glucosidase 3, endo-β-1,4-glucanase 1 and beta-mannosidase 1, respectively. The black dots in each box in figure B represent *Pseudoregma bambucicola* of different morphs or developmental stages, including newborn 1st instar soldiers, older 1st instar soldiers, newborn 1st instar normal nymphs, older 1st instar normal nymphs, middle-stage normal nymphs, soldier producing adults and normal nymph producing adults.

glucosidase 2 and β-glucosidase 3) found only in whole-body, the three putative PCWDEs identified in both the whole-body and salivary gland all contained secretory signals. All predicted PCWDEs from body transcriptome of *P. bambucicola* exhibited high expression levels (with an average of FPKM > 16) (Figure 4B).

Changes of bamboo proteins in response to aphid feeding

An comparative proteomic analysis of bamboo tissues unfed and fed by aphids may reveal the changes in protein expression and plant cellular process modulated by *P. bambucicola*. A total of 171 proteins were differentially expressed between two types of bamboo tissues, with 71 of them up-regulating and 100 of them down-regulating in bamboo after being fed respectively (Table S7). The highly expressed proteins were mainly enriched in categories of non-membrane-bounded organelle, nucleolus, cell surface, hydrolase activity and maintenance of protein location in cell, while the downregulated proteins were mainly associated with vesicle, golgi apparatus, cellulose synthase activity and plant cell wall biogenesis (Figure S3).

Discussion

Aphid salivary glands can secrete saliva containing a variety of effectors that is important for aphid-plant interactions. In this study, combined transcriptomic and mass spectrometry (LC-MS/MS) analyses were conducted on salivary glands and secreted saliva of *P. bambucicola* to get a more comprehensive understanding of the salivary composition and the role of salivary glands in its successful feeding on the hard bamboo stalks. Transcriptome analysis of salivary gland components showed that many genes are abundant in binding, catalytic activity and metabolic process, and several mitochondrial genes associated with energy metabolism are especially highly expressed, suggesting that salivary glands have strong and active catalytic and energy metabolic activities. This is consistent with the biological characteristics and functions of salivary glands and salivary components. Many homologous salivary proteins important for aphid–plant interactions, such as digestive enzymes, detoxifying and antioxidant enzymes and some effectors modulating plant defenses (van Bel and Will, 2016; Zhang et al., 2017) are also detected in *P. bambucicola* salivary glands based on deduced amino acid sequences, suggesting that some similar strategies may employed by phloem-feeding aphids to overcome plant defenses.

We also detected and compared the expression of 11 genes encoding salivary proteins between salivary glands and guts, which are thought to be involved in aphid-plant interactions. The expression of transcripts for digestive enzymes including beta-galactosidase, lysosomal alpha-mannosidase, carboxypeptidase E, detoxifying enzyme glucose dehydrogenase and the antioxidant enzyme superoxide dismutase show much higher expression levels in salivary glands than in guts. Beta-galactosidase, a member of glycosyl hydrolase family that is involved in the hydrolysis of carbohydrates, has also been detected in *S. avenae*'s saliva (Rao et al., 2013). While the general role of lysosomal alpha-mannosidase in insects has been poorly characterized, a

homolog of it is also found to be highly expressed in salivary glands of *Diaphorina citri* (Wu et al., 2021), suggesting an important role in interactions between phloem-feeing insects and host plants. Carboxypeptidases are important digestive enzymes and the carboxypeptidase E is an insect neuropeptide processing enzyme regulating secretory pathway, and is required for the biosynthesis of pheromone and neuropeptide (Stone et al., 1994). The carboxypeptidase E has been assumed to be present only in brain cells producing peptidic hormones, while its high expression found in *P. bambucicola* salivary glands may imply an important role in feeding and digesting plants. During aphid feeding, plants can produce a variety of toxic chemicals and defensive compounds against aphids. While aphids also have some detoxifying enzymes for suppression of plant defenses. The glucose dehydrogenase belongs to the GMC oxidoreductase family and members of this family were shown to be present in caterpillar saliva most likely suppressing plant defenses by transcript regulation (Bede et al., 2006). Glucose dehydrogenase has been previously characterized in several other aphids, such as the *A. pisum* (Carolan et al., 2011), *Diuraphis noxia* (Nicholson et al., 2012), *S. graminum* (Zhang et al., 2022), *S. avenae* (Zhang et al., 2017), *M. euphorbiae* (Chaudhary et al., 2015), *Metopolophium dirhodum* (Rao et al., 2013) and *Schlechtendalia chinensis* (Yang et al., 2018). The dramatically overexpression of this gene in the *P. bambucicola* salivary glands may indicate that it also plays an important role in *P. bambucicola* feeding and adaption to bamboo. Superoxide dismutase can destroy toxic radicals and protect insect from the plant ROS damage and has been also reported in other aphids (Lukasik, 2007). The highly expressed superoxide dismutase in *P. bambucicola* salivary gland may involved in scavenging ROS induced by plant defense responses. Collectively, these notably highly expressed genes in salivary glands may play an important role in detoxifying phytochemicals and successful feeding on bamboo hosts. However, genes encoding the digestive enzyme methionine aminopeptidase 1D, antioxidant enzyme phospholipid hydroperoxide glutathione peroxidase, and detoxifying glutathione S-transferase expressed at higher levels in the gut than in salivary glands, suggesting the importance of guts in digestion and detoxification during plant feeding in *P. bambucicola*.

Salivary components of *P. bambucicola* were also characterized at the protein level from the dissected salivary glands and secreted saliva by LC–MS/MS analysis. Due to its special feeding habitat, it is difficult to simulate the feeding process of *P. bambucicola* and collect saliva *via* artificial diet as in other aphid species (Harmel et al., 2008; Carolan et al., 2009; Rao et al., 2013; Yang et al., 2018). As an alternative, the comparative proteomic analysis of bamboo samples unfed and fed by *P. bambucicola* may help better determine candidate proteins secreted into hosts during natural feeding process. Functional analyses of salivary gland proteins and saliva proteins reflect important roles of salivary glands in protein secretion and energy metabolism. Although 1213 transcripts are predicted to encode putative secretory proteins, only 267 secretory proteins can be detected in the salivary gland and/or saliva proteomes of *P. bambucicola* (Table S5). Consistent with previous studies (Chaudhary et al., 2015; van Bel and Will, 2016; Zhang et al., 2017; Yang et al., 2018; Zhang et al., 2020), some insect detoxification enzymes, peroxidases, digestion enzymes, effectors modulating plant defenses and salivary sheath proteins can be also detected in salivary gland and/or saliva of *P. bambucicola*. Among them, the glucose dehydrogenase, glutathione S-transferase and carboxylesterases are important detoxifying enzymes used by insects to protect against plant defensive compounds (Cox-Foster and Stehr, 1994; Yu et al., 2009; Koirala et al., 2022). Peroxidases are one of the primary antioxidative enzymes of insects and may be involved in protecting *P. bambucicola* from plant oxidative damage. Salivary sugar degrading enzymes, peptidases and proteases in insects can function as important digestive enzymes degrading plant polysaccharide and plant defense proteins (Nicholson et al., 2012; Liu et al., 2016; Zhang et al., 2017). Some digestive enzymes detected in *P. bambucicola* salivary gland or saliva secretomes have been also found in salivary gland or saliva of some aphids and other phloem-feeding insects, such as the lysosomal alpha-mannosidase (Wu et al., 2021), carboxypeptidase (Huang et al., 2020), cathepsin (Foissac et al., 2002; Zhang et al., 2017; Huang et al., 2020; Wu et al., 2021; Zhang et al., 2022), serine protease (Nicholson et al., 2012; Zhang et al., 2017) and phospholipase (Zhang et al., 2017). These putative secretory effectors may be essential for enabling *P. bambucicola* feeding on bamboo host, such as helping promote aphid stylet penetration, digestion and detoxification of toxins, or suppressing plant defenses against *P. bambucicola*. In addition, some secretory proteins homologous to known aphid effectors involved in modulating plant defenses are also detected in *P. bambucicola* salivary gland and saliva, including apolipophorins (Chaudhary et al., 2015; Zhang et al., 2017; Zhang et al., 2020), odorant binding protein (Zhang et al., 2017), protein yellow (Chaudhary et al., 2015) and some salivary sheath components (van Bel and Will, 2016; Wu et al., 2021). The high similarities in the composition of salivary secretory proteins across different aphid species may highlight their importance in aphid-plant interactions. However, whether these candidate effectors of *P. bambucicola* play conserved roles in modulating aphid-plant interactions remains to be explored. The role of potentially effector proteins of unknown function in aphid-host interaction is also worth further investigation, which may provide new insight into the mechanisms of aphid's adaption to bamboo host.

To successfully feed on the hard bamboo stalks, *P. bambucicola* must first overcome and penetrate the physical barrier of the plant cell wall. In this process, aphids require multiple PCWDEs to break down the plant cell wall polysaccharides (Silva-Sanzana et al., 2020). We identified

potential PCWDEs based on transcriptomes of whole body and salivary glands, and proteomes of salivary gland and saliva of *P. bambucicola*. Although multiple transcripts of β-glucosidases, endo-β-1,4-glucanases and β-mannosidases can be identified in salivary gland transcriptome and body transcriptome for *P. bambucicola* of different morphs and developmental stages, most of identified PCWDE candidates in salivary glands show very low expression levels. And given the multiple functions of some enzymes (such as β-glucosidases) (Watanabe and Tokuda, 2010), the activities and functions of these enzymes potentially involved in degradation of cellulose and hemicellulose need to be further verified. Moreover, it seems that this aphid can only encode a small fraction of the complete set of enzymes for degrading cellulose and hemicellulose. For example, the cellulose degradation process needs the involvement of three kinds of enzymes: the endo-β-1,4-glucanase that hydrolyse cellulose randomly, exo-β-1,4-glucanase that hydrolyse cellulose from the reducing or non-reducing end to release cellobiose, and β-glucosidase cleaving cellobiose or cello-oligosaccharides into glucose monomers (Gilbert, 2010; Watanabe and Tokuda, 2010). The *P. bambucicola* seems to lack the key exo-β-1,4-glucanase that is responsible for the intermediate steps of cellulose degradation. The same case is in the hemicellulase system where *P. bambucicola* lacks the main-chain hemicellulases, such as the xylanase and xylooligosaccharidase, while β-mannosidases are only side-chain degrading enzymes that hydrolyse the hemicellulosic oligosaccharides into monomeric sugars (Tokuda, 2019). In addition, we did not found any pectinases in either salivary gland or body samples of *P. bambucicola*. Pectinases are thought to be required for aphid stylet penetration between cells (McAllan and Adams, 1961). Pectin degradation plays an important role in the degradation of plant cell wall, which can promote the further degradation of cellulose and hemicellulose and make cell wall more easily decomposed by other enzymes (Calderón-Cortés et al., 2012). Our results suggest that *P. bambucicola* itself may not have the ability to produce pectinases, thereby failing to complete even the first step of cell wall degradation. *Via* Our findings imply that *P. bambucicola* may not be able to degrade plant cell walls on its own and may require the help of its symbiotic bacteria (Liu et al., 2021; Liu et al., 2022). Further study on functional interaction between this aphid and its dominate symbiotic bacteria is especially needed.

We also investigate the response of bamboo to *P. bambucicola* feeding by comparative proteomic analysis of bamboo tissues unfed and fed by aphids. The downregulated proteins in bamboo after being fed were mainly enriched in vesicle, golgi apparatus, plant cell wall biogenesis. These findings suggest that aphid feeding may inhibit the bamboo's normal physiological processes, such as breaking down plant cell wall and suppressing the plant cell wall synthesis activity, which may be mediated by aphid effectors secreted into host to maintain aphid's feeding.

Publisher's note

Data availability statement

The data presented in the study are deposited in the National Center for Biotechnology Information (NCBI) BioProject database under accession number PRJNA900789 (salivary gland) and PRJNA901050 (whole body), and the ProteomeXchange database with the dataset identifier PXD038131

Author contributions

XH conceptualized this study. HZ, RL, QL and JL performed the experiments and analyzed the data, XH, GQ and HZ wrote the manuscript. All authors contributed to the article and approved the submitted version

Funding

This research was supported by National Natural Science Foundation of China (Grant numbers: 31970446, 32270499).

Conflict of interest

The authors declare that the research was conducted in the absence of any commercial or financial relationships that could be construed as a potential conflict of interest.

Publisher's note

All claims expressed in this article are solely those of the authors and do not necessarily represent those of their affiliated organizations, or those of the publisher, the editors and the reviewers. Any product that may be evaluated in this article, or claim that may be made by its manufacturer, is not guaranteed or endorsed by the publisher.

Supplementary material

The Supplementary Material for this article can be found online at: https://www.frontiersin.org/articles/10.3389/fpls.2022.1098751/full#supplementary-material

References

Anathakrishnan, R., Sinha, D. K., Murugan, M., Zhu, K. Y., Chen, M.-S., Zhu, Y. C., et al. (2014). Comparative gut transcriptome analysis reveals differences between virulent and avirulent Russian wheat aphids, diuraphis noxia. *Arthropod-Plant Inte.* 8, 79–88. doi: 10.1007/s11829-014-9293-4

Anderson, C. T., and Kieber, J. J. (2020). Dynamic construction, perception, and remodeling of plant cell walls. *Annu. Rev. Plant Biol.* 71, 39–269. doi: 10.1146/annurev-arplant-081519-035846

Atamian, H. S., Chaudhary, R., Cin, V. D., Bao, E., Girke, T., and Kaloshian, I. (2013).). in planta expression or delivery of potato aphid macrosiphum euphorbiae effectors Me10 and Me23 enhances aphid fecundity. *Mol. Plant Microbe Interact.* 26, 67–74. doi: 10.1094/MPMI-06-12-0144-FI

Backus, E. A., Andrews, K. B., Shugart, H. J., Carl Greve, L., Labavitch, J. M., and Alhaddad, H. (2012). Salivary enzymes are injected into xylem by the glassy-winged sharpshooter, a vector of xylella fastidiosa. *J. Insect Physiol.* 58, 949–959. doi: 10.1016/j.jinsphys.2012.04.011

Bede, J. C., Musser, R. O., Felton, G. W., and Korth, K. L. (2006). Caterpillar herbivory and salivary enzymes decrease transcript levels of medicago truncatula genes encoding early enzymes in terpenoid biosynthesis. *Plant Mol. Biol.* 60, 519–531. doi: 10.1007/s11103-005-4923-y

Bos, J. I., Prince, D., Pitino, M., Maffei, M. E., Win, J., and Hogenhout, S. A. (2010). A functional genomics approach identifies candidate effectors from the aphid species myzus persicae (green peach aphid). *PloS Genet.* 6, e1001216. doi: 10.1371/journal.pgen.1001216

Bredon, M., Herran, B., Lheraud, B., Bertaux, J., Grève, P., Moumen, B., et al. (2019). Lignocellulose degradation in isopods: new insights into the adaptation to terrestrial life. *BMC Genom.* 20, 462. doi: 10.1186/s12864-019-5825-8

Busk, P. K., Pilgaard, B., Lezyk, M. J., Meyer, A. S., and Lange, L. (2017). Homology to peptide pattern for annotation of carbohydrate-active enzymes and prediction of function. *BMC Bioinform.* 18, 214. doi: 10.1186/s12859-017-1625-9

Calderón-Cortés, N., Quesada, M., Watanabe, H., Cano-Camacho, H., and Oyama, K. (2012). Endogenous plant cell wall digestion: a key mechanism in insect evolution. *Annu. Rev. Ecol. Evol. Syst.* 43, 45–71. doi: 10.1146/annurev-ecolsys-110411-160312

Cao, M., Ren, W., Zhu, J., Wang, H., Guo, J., Zhang, X., et al. (2022). Cell wall pore structures of bamboo evaluated using gas adsorption methods. *Holzforschung* 76, 754–754. doi: 10.1515/hf-2022-0006

Carolan, J. C., Caragea, D., Reardon, K. T., Mutti, N. S., Dittmer, N., Pappan, K., et al. (2011). Predicted effector molecules in the salivary secretome of the pea aphid (Acyrthosiphon pisum): a dual transcriptomic/proteomic approach. *J. Proteome Res.* 10, 1505–1518. doi: 10.1021/pr100881q

Carolan, J. C., Fitzroy, C. I., Ashton, P. D., Douglas, A. E., and Wilkinson, T. L. (2009). The secreted salivary proteome of the pea aphid acyrthosiphon pisum characterised by mass spectrometry. *Proteomics* 9, 2457–2467. doi: 10.1002/pmic.200800692

Charkowski, A., Blanco, C., Condemine, G., Expert, D., Franza, T., Hayes, C., et al. (2012). The role of secretion systems and small molecules in soft-rot enterobacteriaceae pathogenicity. *Annu. Rev. Phytopathol.* 50, 425–449. doi: 10.1146/annurev-phyto-081211-173013

Chaudhary, R., Atamian, H. S., Shen, Z., Briggs, S. P., and Kaloshian, I. (2015). Potato aphid salivary proteome: enhanced salivation using resorcinol and identification of aphid phosphoproteins. *J. Proteome Res.* 14, 1762–1778. doi: 10.1021/pr501128k

Cox-Foster, D. L., and Stehr, J. E. (1994). Induction and localization of FAD-glucose dehydrogenase (GLD) during encapsulation of abiotic implants in manduca sexta larvae. *J. Insect Physiol.* 40, 235–249. doi: 10.1016/0022-1910(94)90047-7

Cristofoletti, P. T., Ribeiro, A. F., Deraison, C., Rahbé, Y., and Terra, W. R. (2003). Midgut adaptation and digestive enzyme distribution in a phloem feeding insect, the pea aphid acyrthosiphon pisum. *J. Insect Physiol.* 49, 11–24. doi: 10.1016/s0022-1910(02)00222-6

Dedryver, C. A., Le Ralec, A., and Fabre, F. (2010). The conflicting relationships between aphids and men: A review of aphid damage and control strategies. *C. R. Biol.* 333, 539–553. doi: 10.1016/j.crvi.2010.03.009

Dommel, M., Oh, J., Huguet-Tapia, J. C., Guy, E., Boulain, H., Sugio, A., et al. (2020). Big genes, small effectors: pea aphid cassette effector families composed from miniature exons. *Front. Plant Sci.* 11. doi: 10.3389/fpls.2020.01230

Drula, E., Garron, M. L., Dogan, S., Lombard, V., Henrissat, B., and Terrapon, N. (2022). The carbohydrate-active enzyme database: functions and literature. *Nucleic. Acids Res.* 50, D571–D577. doi: 10.1093/nar/gkab1045

Eddy, S. R. (1998). Profile hidden Markov models. *Bioinformatics* 14, 755–763. doi: 10.1093/bioinformatics/14.9.755

Elzinga, D. A., and Jander, G. (2013). The role of protein effectors in plant–aphid interactions. *Curr. Opin. Plant Biol.* 16, 451–456. doi: 10.1016/j.pbi.2013.06.018

Foissac, X., Edwards, M. G., Du, J. P., Gatehouse, A. M. R., and Gatehouse, J. A. (2002). Putative protein digestion in a sap-sucking homopteran plant pest (rice brown plant hopper; nilaparvata lugens: Delphacidae)–identification of trypsin-like and cathepsin b-like proteases. *Insect Biochem. Mol. Biol.* 32, 967–978. doi: 10.1016/s0965-1748(02)00033-4

Gilbert, H. J. (2010). The biochemistry and structural biology of plant cell wall deconstruction. *Plant Physiol.* 153, 444–455. doi: 10.1104/pp.110.156646

Grabherr, M. G., Haas, B. J., Yassour, M., Levin, J. Z., Thompson, D. A., Amit, I., et al. (2011). Full-length transcriptome assembly from RNA-seq data without a reference genome. *Nat. Biotechnol.* 29, 644–652. doi: 10.1038/nbt.1883

Guo, G. X., Liu, Y., Yang, J. J., and Ma, X. Z. (2006). Identification, activity and function determination of several salivary enzymes secreted by macrosiphum avenae. *Acta Entomol. Sin.* 49, 768–774. doi: 10.16380/j.kcxb.2006.05.008

Hallgren, J., Tsirigos, K. D., Pedersen, M. D., Armenteros, J. J. A., Marcatili, P., Nielsen, H., et al. (2022). DeepTMHMM predicts alpha and beta transmembrane proteins using deep neural networks. *bioRxiv*. doi: 10.1101/2022.04.08.487609

Harmel, N., Létocart, E., Cherqui, A., Giordanengo, P., Mazzucchelli, G., Guillonneau, F., et al. (2008). Identification of aphid salivary proteins: a proteomic investigation of myzus persicae. *Insect Mol. Biol.* 17, 165–174. doi: 10.1111/j.1365-2583.2008.00790.x

Hooks, C. R. R., and Fereres, A. (2006).). protecting crops from non-persistently aphid-transmitted viruses: a review on the use of barrier plants as a management tool. *Virus Res.* 120, 1–16. doi: 10.1016/j.virusres.2006.02.006

Huang, H. J., Ye, Z. X., Lu, G., Zhang, C. X., Chen, J. P., and Li, (2020). J. m Identification of salivary proteins in the whitefly bemisia tabaci by transcriptomic and LC–MS/MS analyses. *Insect Sci.* 28, 1369–1381. doi: 10.1111/1744-7917.12856

Ji, R., Ye, W., Chen, H., Zeng, J., Li, H., Yu, H., et al. (2017). A salivary endo-β-1,4-glucanase acts as an effector that enables the brown planthopper to feed on rice. *Plant Physiol.* 173, 1920–1932. doi: 10.1104/pp.16.01493

Koirala, B. K. S., Moural, T., and Zhu, F. (2022). Functional and structural diversity of insect glutathione s-transferases in xenobiotic adaptation. *Int. J. Biol. Sci.* 18, 5713–5723. doi: 10.7150/ijbs.77141

Langmead, B., and Salzberg, S. L. (2012). Fast gapped-read alignment with bowtie 2. *Nat. Methods* 9 (4), 357–359. doi: 10.1038/nmeth.1923

Li, B., and Dewey, C. N. (2011). RSEM: accurate transcript quantification from RNA-seq data with or without a reference genome. *BMC Bioinf.* 12, 323. doi: 10.1186/1471-2105-12-323

Liu, Q., Zhang, H., and Huang, X. (2022). Strong linkage between symbiotic bacterial community and host age and morph in a hemipteran social insect. *Microb. Ecol*. doi: 10.1007/s00248-022-02114-5

Liu, Q., Zhang, H., Zeng, L., Yu, Y., Lin, X., and Huang, X. (2021). Coexistence of three dominant bacterial symbionts in a social aphid and implications for ecological adaptation. *Insects* 12, 416. doi: 10.3390/insects12050416

Liu, X., Zhou, H., Zhao, J., Hua, H., and He, Y. (2016). Identification of the secreted watery saliva proteins of the rice brown planthopper, nilaparvata lugens (Stl) by transcriptome and shotgun LC-MS/MS approach. *J. Insect Physiol.* 89, 60–69. doi: 10.1016/j.jinsphys.2016.04.002

Lukasik, I. (2007). Changes in activity of superoxide dismutase and catalase within cereal aphids in response to plant o-dihydroxyphenols. *J. Appl. Entomol.* 131, 209–214. doi: 10.1111/j.1439-0418.2006.01136.x

Ma, R., Reese, J. C., Black, W. C.IV, and Bramel-Cox, P. (1990). Detection of pectinesterase and polygalacturonase from salivary secretions of living greenbugs, schizaphis graminum (Homoptera: Aphididae). *J. Insect Physiol.* 36, 507–512. doi: 10.1016/0022-1910(90)90102-L

Matthews, H. J., Down, R. E., and Audsley, N. (2010). Effects of manduca sexta allatostatin and an analogue on the peach-potato aphid myzus persicae (Hemiptera: Aphididae) and degradation by enzymes in the aphid gut. *Arch. Insect Biochem. Physiol.* 75, 139–157. doi: 10.1002/arch.20376

McAllan, J. W., and Adams, J. B. (1961). The significance of pectinase in plant penetration by aphids. *Can. J. Zool.* 39, 305–310. doi: 10.1139/z61-034

Miles, P. W. (1959). Secretion of two types of saliva by an aphid. *Nature* 183, 756. doi: 10.1038/183756b0

Miles, P. W. (1999). Aphid saliva. *Biol. Rev.* 74, 41–85. doi: 10.1111/j.1469-185X.1999.tb00181.x

Mutti, N. S., Louis, J., Pappan, L. K., Begum, k., Chen, M. S., Park, Y., et al. (2008). A protein from the salivary glands of the pea aphid, acyrthosiphon pisum, is essential in feeding on a host plant. *Proc. Natl. Acad. Sci. U.S.A.* 105, 9965–9969. doi: 10.1073/pnas.0708958105

Nicholson, S. J., Hartson, S. D., and Puterka, G. J. (2012). Proteomic analysis of secreted saliva from Russian wheat aphid (Diuraphis noxia kurd.) biotypes that differ in virulence to wheat. *J. Proteomics* 75, 2252–2268. doi: 10.1016/j.jprot.2012.01.031

Ni, J., and Tokuda, G. (2013). Lignocellulose-degrading enzymes from termites and their symbiotic microbiota. *Biotechnol. Adv.* 31, 838–850. doi: 10.1016/j.biotechadv.2013.04.005

Pitino, M., and Hogenhout, S. A. (2013). Aphid protein effectors promote aphid colonization in a plant species-specific manner. *Mol. Plant Microbe Interact.* 26, 130–139. doi: 10.1094/MPMI-07-12-0172-FI

Preston, R. D., and Singh, K. (1950). The fine structure of bamboo fibres. i. optical properties and X-ray data. *J. Exp. Bot.* 1, 214–226. doi: 10.1093/JXB/1.2.214

Prianichnikov, N., Koch, H., Koch, S., Lubeck, M., Heilig, R., Brehmer, S., et al. (2020). MaxQuant software for ion mobility enhanced shotgun proteomics. *Mol. Cell. Proteomics* 19, 1058–1069. doi: 10.1074/mcp.TIR119.001720

Pyati, P., Bandani, A. R., Fitches, E., and Gatehouse, J. A. (2011). Protein digestion in cereal aphids (Sitobion avenae) as a target for plant defence by endogenous proteinase inhibitors. *J. Insect Physiol.* 57, 881–891. doi: 10.1016/j.jinsphys.2011.03.024

Rao, S. A., Carolan, J. C., and Wilkinson, T. L. (2013). Proteomic profiling of cereal aphid saliva reveals both ubiquitous and adaptive secreted proteins. *PloS One* 8, e57413. doi: 10.1371/journal.pone.0057413

Scully, E. D., Geib, S. M., Hoover, K., Tien, M., Tringe, S. G., Barry, K. W., et al. (2013). Metagenomic profiling reveals lignocellulose degrading system in a microbial community associated with a wood-feeding beetle. *PloS One* 8, e73827. doi: 10.1371/journal.pone.0073827

Silva-Sanzana, C., Estevez, J. M., and Blanco-Herrera, F. (2020). Influence of cell wall polymers and their modifying enzymes during plant-aphid interactions. *J. Exp. Bot.* 71, 3854–3864. doi: 10.1093/jxb/erz550

Stone, T. E., Li, J. P., and Bernasconi, P. (1994). Purification and characterization of the manduca sexta neuropeptide processing enzyme carboxypeptidase e. *Arch. Insect Biochem. Physiol.* 27, 193–203. doi: 10.1002/arch.940270305

Teufel, F., Almagro Armenteros, J. J., Johansen, A. R., Gíslason, M. H., Pihl, S. I., Tsirigos, K. D., et al. (2022). SignalP 6.0 predicts all five types of signal peptides using protein language models. *Nat. Biotechnol.* 40, 1023–1025. doi: 10.1038/s41587-021-01156-3

Thorpe, P., Cock, P. J. A., and Bos, J. (2016). Comparative transcriptomics and proteomics of three different aphid species identifies core and diverse effector sets. *BMC Genomics* 17, 172. doi: 10.1186/s12864-016-2496-6

Tjallingii, W. F. (2006). Salivary secretions by aphids interacting with proteins of phloem wound responses. *J. Exp. Bot.* 57, 739–745. doi: 10.1093/jxb/erj088

Tokuda, G. (2019). Plant cell wall degradation in insects: Recent progress on endogenous enzymes revealed by multi-omics technologies. *Adv. Insect Physiol.* 57, 97–136. doi: 10.1016/bs.aiip.2019.08.001

van Bel, A. J. E., and Will, T. (2016). Functional evaluation of proteins in watery and gel saliva of aphids. *Front. Plant Sci.* 7. doi: 10.3389/fpls.2016.01840

Watanabe, H., and Tokuda, G. (2010). Cellulolytic systems in insects. *Annu. Rev. Entomol.* 55, 609–632. doi: 10.1146/annurev-ento-112408-085319

Will, T., Furch, A. C. U., and Zimmermann, M. R. (2013). How phloem-feeding insects face the challenge of phloem-located defenses. *Front. Plant Sci.* 4. doi: 10.3389/fpls.2013.00336

Will, T., Tjallingii, W. F., Thönnessen, A., and van Bel, A. J. E. (2007). Molecular sabotage of plant defense by aphid saliva. *Proc. Natl. Acad. Sci. U.S.A.* 104, 10536–10541. doi: 10.1073/pnas.0703535104

Wu, Z. Z., Qu, M. Q., Chen, M. S., and Lin, J. T. (2021). Proteomic and transcriptomic analyses of saliva and salivary glands from the Asian citrus psyllid, diaphorina citri. *J. Proteomics* 238, 104136. doi: 10.1016/j.jprot.2021.104136

Yang, Z., Ma, L., Francis, F., Yang, Y., Chen, H., Wu, H., et al. (2018). Proteins identified from saliva and salivary glands of the Chinese gall aphid schlechtendalia chinensis. *Proteomics* 18, e1700378. doi: 10.1002/pmic.201700378

Yu, Q. Y., Lu, C., Li, W. L., Xiang, Z. H., and Zhang, Z. (2009). Annotation and expression of carboxylesterases in the silkworm, bombyx mori. *BMC Genomics* 10, 553. doi: 10.1186/1471-2164-10-553

Zhang, Y., Fan, J., Sun, J., Francis, F., and Chen, J. (2017). Transcriptome analysis of the salivary glands of the grain aphid, sitobion avenae. *Sci. Rep.* 7, 15911. doi: 10.1038/s41598-017-16092-z

Zhang, Y., Fu, Y., Francis, F., Liu, X., and Chen, J. (2020). Insight into watery saliva proteomes of the grain aphid, sitobion avenae. *Arch. Insect Biochem. Physiol.* 106, e21752. doi: 10.1002/arch.21752

Zhang, Y., Liu, X., Francis, F., Xie, H., Fan, J., Wang, Q., et al. (2022). The salivary effector protein Sg2204 in the greenbug schizaphis graminum suppresses wheat defence and is essential for enabling aphid feeding on host plants. *Plant Biotechnol. J.* 20, 2187–2201. doi: 10.1111/pbi.13900

Zhao, C., Zhang, P. J., Yu, L. X., and Yu, X. P. (2019). Advances in the adaption to plant defenses in phytophagous insects. *Acta Entomol. Sin.* 62, 124–132. doi: 10.16380/j.kcxb.2019.01.013

frontiers | Frontiers in Plant Science

TYPE Original Research
PUBLISHED 12 January 2023
DOI 10.3389/fpls.2022.1090559

OPEN ACCESS

EDITED BY
Julian Chen,
Institute of Plant Protection (CAAS), China

REVIEWED BY
Jia Fan,
Institute of Plant Protection (CAAS), China
Xiaolei Huang,
Fujian Agriculture and Forestry University, China
Yong Liu,
Shandong Agricultural University, China

*CORRESPONDENCE
Xiaojun Guo
guoxj@brcast.org.cn
Su Wang
anthocoridae@163.com

SPECIALTY SECTION
This article was submitted to Sustainable and Intelligent Phytoprotection, a section of the journal Frontiers in Plant Science

RECEIVED 15 November 2022
ACCEPTED 23 December 2022
PUBLISHED 12 January 2023

CITATION
Xu Q, Wu C, Xiao D, Jin Z, Zhang C, Hatt S, Guo X and Wang S (2023) Ecological function of key volatiles in *Vitex negundo* infested by *Aphis gossypii*. *Front. Plant Sci.* 13:1090559. doi: 10.3389/fpls.2022.1090559

Ecological function of key volatiles in *Vitex negundo* infested by *Aphis gossypii*

Qingxuan Xu[1], Changbing Wu[2], Da Xiao[1], Zhenyu Jin[2], Changrong Zhang[3], Séverin Hatt[4], Xiaojun Guo[1*] and Su Wang[1*]

[1]Institute of Plant Protection, Beijing Academy of Agriculture and Forestry Sciences, Beijing, China, [2]Hubei Engineering Research Center for Pest Forewarning and Management, College of Agriculture, Yangtze University, Jingzhou, China, [3]Institute of Plant Protection, Guizhou Academy of Agriculture Sciences, Guiyang, Guizhou, China, [4]Agroecology and Organic Farming, Institute of Crop Science and Resource Conservation, University of Bonn, Bonn, Germany

Herbivore induced plant volatiles (HIPVs) are key components of plant-herbivorous-natural enemies communications. Indeed, plants respond to herbivores feeding by releasing HIPVs to attract natural enemies. The present study analyses the effect of HIPVs of *Vitex negundo* (Lamiaceae), an indigenous plant species in northern China, on the predatory ladybug species *Harmonia axyridis.* Y-tube olfactometer bioassay showed that *H. axyridis* adults were significantly attracted by *V. negundo* infested by the aphid *Aphis gossypii.* We analyzed and compared volatile profiles between healthy and *A. gossypii* infested *V. negundo*, screened out the candidate active HIPVs mediated by *A. gossypii* which could attract *H. axyridis*, and tested the olfactory behavior of the candidate active compounds on *H. axyridis*. The gas chromatography-mass spectrometry analysis showed that five volatile compounds were significantly up-regulated after *V. negundo* infestation by *A. gossypii*, and five substances were significantly down-regulated in the terpenoid biosynthesis pathway. The olfactory behavior response showed that *H. axyridis* has significant preference for sclareol, eucalyptol, nonanal and α-terpineol, indicating that this chemical compounds are the important volatiles released by *V. negundo* to attract *H. axyridis*. This study preliminarily clarified that *V. negundo* release HIPVs to attract natural enemies when infected by herbivorous insects. The description of the volatile emission profile enriches the theoretical system of insect-induced volatile-mediated plant defense function of woody plants. Applications in crop protection would lie in designing original strategies to naturally control aphids in orchards.

KEYWORDS

HIPVs, indigenous plants, *Harmonia axyridis*, chemical ecology, woody plants

Introduction

Conservation biological control (CBC) takes full advantage of the surrounding environment of the target area to conserve natural enemy insects and balance the ecological relationship between natural enemies and pests (Tooker et al., 2020). How to effectively use ecological factors including landscape diversity, functional plants, and volatile organic compounds (VOCs) to improve the efficiency of natural enemy insects in biological control of pests is hotspot in CBC programs (Turlings and Ton, 2006; Gurr et al., 2017; Hatt et al., 2019). In this context, the information substance that links the communication between plants and insects, i.e. herbivore induced plant volatiles (HIPVs), have received more attention over the recent years (Li and Blande, 2017; Turlings and Erb, 2018).

As chemical signals between plants and insects, HIPVs can improve the defense ability of plant and mediate the interaction between plant and insect community to affect the behavior of insects (Song et al., 2017). HIPVs are mainly divided into terpenoids, green leaf volatiles (GLVs), nitrogen- and sulfur containing compounds (Aartsma et al., 2017; Ye et al., 2019). Terpenoids are the most abundant plant volatiles and the most common compounds induced by pests (Dicke, 2009). Among them, volatile substances such as monoterpenes and diterpenes are released after pest infection and directly participate in plant defense by attracting natural enemies to avoid further damage (Dudareva et al., 2004; Cheng et al., 2007). Studying the biosynthetic pathways of these volatile compounds helps to explore their effects on plant biological characteristics (Cagliero et al., 2020). For instance, terpenoids are released from the leaves of the hybrid *Populus trichocarpa* Torr. & A.Gray and *Populus deltoides* W.Bartram (Salicaceae) when infested by *Phyllobius piri* Linnaeus (Coleopotera: Curculionidae) (Blande et al., 2007) and terpenoids, such as (*E*)-4,8-dimethyl-1,3,7-nonatriene and 4,8,12-trimethyl-1,3,7,11-tridecatetraene, can induct defense-related genes (Arimura et al., 2001). Hence, terpenoids play an important role in tritrophic interactions and in the direct and indirect defense of plants.

HIPVs-mediated plant-insect interactions have been extensively studied in herbaceous or gramineous plants (Heil, 2014; Turlings and Erb, 2018). Findings led to designing and managing diversified cropping systems using selected functional plants and releasing selected chemical compounds known to repel insect pests and to attract their natural enemies (Khan et al., 2008; Xu et al., 2018a). In contrasts, the role of HIPV produced by woody plants in attracting pest predators in the vicinity of orchard ecosystems have been rarely considered to our knowledge.

Vitex negundo L. var. *heterophylla* (Franch.) Rehd (Lamiaceae) is a perennial shrub indigenous in northern China. It is an important nectar plant widely distributed in semi-natural habitats (Gill et al., 2018), notably in orchard surroundings. At present, few ecological studies explored its potential benefits as a non-crop plant supporting natural enemies of pests. Previously, it was showed that *V. negundo* infested by the aphid *Aphis gossypii* Glover (Hemiptera: Aphididae) significantly attracts lacewings *Chrysopa formosa* Brauer (Neuroptera: Chrysopidae) (Chen and Feng, 2014). While in their study, Chen and Feng (2014) did not identify the mechanism explaining the attraction of aphid predators to *V. negundo*, we hypothesized that volatiles released by the *V. negundo* plants mediated by *A. gossypii* are used as chemical information structuring the tri-trophic interactions between *V. negundo*, *A. gossypii* and predators. In this study, we first conducted field observations and highlighted that ladybugs were especially abundant on *V. negundo*. We then tested the olfactory behaviors of adults of the ladybug species *Harmonia axyridis* Pallas (Coleoptera: Coccinellidae) to *V. negundo* plants, analyzed the HIPV compounds mediated by the aphids *A. gossypii*, and lastly tested the olfactory behavioral responses of *H. axyridis* to the identified active compounds.

Materials and methods

Field investigation of *Vitex negundo* and peach trees in field

The occurrence dynamics of predatory natural enemies on peach trees and *V. negundo* were investigated in Changping district experimental station in Beijing, China in 2020 (116°2' E, 40°10' N). *Vitex negundo* plants were naturally growing in the direct surrounding of the investigated peach orchard. Every seven days from early May to early August (14 times in total), about two-year old *V. negundo* plants were surveyed in plots containing each 25 plants (in a 5 × 5 plant layout with 0.6 m between plants). Three plots were surveyed (i.e., 75 *V. negundo* plants in total) and 10 branches per plant were investigated. Larvae and adults (but neither eggs nor pupae) of ladybugs were recorded. *H. axyridis* was the most abundant species. Investigations of other habitats plants (*Artemisia sieversiana*, *Cosmos bipinnatus*, *Helianthus annuus*, *Vigna unguiculata*, *Zea mays* and *Anemarrhena asphodeloides*) performed as are described above. To investigate the presence of predators on peach trees, five points were selected at equidistance (i.e., 1.2 m between each point) through the diagonal of the peach orchard. Two peach trees were selected at each point, and 10 branches were selected on each peach tree to record the number of predatory ladybugs.

Laboratory test set up

Plant materials

Vitex negundo seeds were collected at the experimental station in Changping district, Beijing, China, and planted in a greenhouse (25 ± 2°C, natural light) at a density of four seeds per pot (1 gallon pot). Vermiculite, perlite, peat (Pindstrup), mixed

at a ratio of 1:1:4, were used as substrate, and each pot received 1 L of water every week. When *V. negundo* plants reached 10 leaves, plants of similar size were selected for the experiment.

Insects rearing

Harmonia axyridis and *A. gossypii* used in the experiments came from the laboratory populations maintained at the Institute of Plant Protection, Beijing Academy of Agriculture and Forestry Sciences. *H. axyridis* were reared in 30 cm × 30 cm × 50 cm cages and fed with *Megoura crassicauda* Mordvilko (Hemiptera: Aphididae) on *Vicia faba* L. (Fabaceae). After multiple generations of indoor reproduction, the newly emerged adults of *H. axyridis* were selected for subsequent experiments. *A. gossypii* were reared on *Cucumis sativus* L. (Cucurbitaceae). All insects were reared in climate chambers (Sanyo, MH351) at 26 ± 1°C, relative humidity of 45% ± 5%, photoperiod of 16L: 8D, light intensity of 800 lx.

Olfactory choice test to different treatment plants with Y-tube olfactometer

The selection preference behavior of adult *H. axyridis* to different treated *V. negundo* plants was tested by Y-tube olfactometer in insect behavior observation box. Three treatments were compared two-by-two: (i) *V. negundo* previously infested by *A. gossypii* aphids, (ii) healthy *V. negundo* plants, and (iii) a blank treatment as control. To prepare the aphid infested plants, *A. gossypii* (wingless aphids) were introduced on the leaves of *V. negundo* with a small brush at a density of 200 per pot, and the treated plants were covered with gauze. After 24 h, *A. gossypii* and their molting and honeydew were gently brushed off. The common arm of the Y-tube olfactometer was 15 cm, and the two tube arms were 10 cm. Air was introduced into the activated carbon tube by the atmospheric sampler. After passing through a long neck distillation bottle containing distilled water, the air entered the olfactometer through the rubber tube, and the airflow velocity was set to 400 mL/min. Before the experiment, adults of *H. axyridis* were starved for 24 h. Then, a single adult individual of *H. axyridis* was placed on the Y-tube main arm to observe its behavioral response. Timing started when the ladybug reached the center of the common arm tube. A choice was recorded when the ladybug crawled over the half of one of the two choice tubes and stayed in this area for more than 5 s. If no choice was made after 5 min, it was recorded as an absence of response and the individual was excluded. In the experiment, each ladybug was tested only once. After each tested ladybug, the position of the two treatments on the olfactometer arms was switched. After every five tested ladybugs, the Y-tube olfactometer was washed with alcohol and replaced by a clean olfactometer. In total, 60 male and 60 female adults were tested in each treatment comparison.

Analysis of *Vitex negundo* volatile compounds

Similarly than in the behavioral tests, infested plants were prepared by depositing *A. gossypii* aphids on *V. negundo* leaves at a density of 200 individuals per pot (four plants per pot) and brushing them off along with their molting and honeydew after 24h. After the treatment was completed, fresh leaves were collected from each group of *V. negundo* plants and put into plastic bags and quickly placed in liquid nitrogen. After grinding, the vortex was mixed evenly. 1 g (1 mL) of the powder was transferred immediately to a 20 mL head-space vial (Agilent, Palo Alto, CA, USA), containing NaCl saturated solution, to inhibit any enzyme reaction. The vials were sealed using crimp-top caps with TFE-silicone headspace septa (Agilent). At the time of SPME analysis, each vial was placed in 100°C for 5 min, then a 120 μm polydimethylsilioxan fibre (Agilent) was exposed to the headspace of the sample for 15 min at 100°C. After sampling, desorption of the VOCs from the fiber coating was carried out in the injection part of the GC apparatus (Model 8890; Agilent) at 250°C for 5 min in the splitless mode. The identification and quantification of VOCs was carried out using an Agilent Model 8890 GC and a 5977B mass spectrometer (Agilent), equipped with a 30 mm x 0.25 mm x 0.25 μm DB-5MS (5% phenyl-polymethylsiloxane) capillary column. Helium was used as the carrier gas at a linear velocity of 1.2 mL/min. The injector temperature was kept at 250°C and the detector at 280°C. The oven temperature was programmed from 40°C (3.5 min), increasing at 10°C/min to 100°C, at 7°C/min to 180°C, at 25°C/min to 280°C, hold for 5 min. Mass spectra was recorded in electron impact (EI) ionization mode at 70 eV. The quadrupole mass detector, ion source and transfer line temperatures were set, respectively, at 150, 230 and 280°C. Mass spectra was scanned in the range m/z 50-500 amu at 1 s intervals. Identification of volatile compounds was achieved by comparing the mass spectra with the data system library (NIST2.0) and linear retention index. Volatiles were tentatively identified with spectra and high-probability matches (> 85%) according to NIST mass spectral database. Each group was repeated three times.

Olfactory choice test to key volatile organic compounds with Y-Tube olfactometer

Choice tests using Y-tube olfactometers were conducted to observe the olfactory behavioral responses of *H. axyridis* to different concentrations of compounds which release was found to change significantly after *A. gossypii* infection (Table 1). The whole protocol was similar than when using entire leaves (see above), but with chemical compounds instead. Each compound was prepared in four concentrations, 1 μL/mL, 10 μL/mL, 100 μL/mL, 500 μL/mL (solid solute was μg/mL), and liquid paraffin was used as solvent. In the experimental treatment, 10 μL solution of the tested compound was added

to a rectangular filter paper (2 cm × 1 cm) and introduced into the flavor source bottle. 10 μL liquid paraffin was added to a filter paper in the other odor bottle as a control. The filter paper was changed every hour. The calculation formula of the selection rate is as follows:

$$\text{Selection rate of A arm} = \frac{\text{Select the number of adults of A}}{\text{Total number of effective selected adults}}$$

$$\text{Selection rate of B arm} = \frac{\text{Select the number of adults of B}}{\text{Total number of effective selected adults}}$$

Statistical analyses

We marked the non-selected *H. axyridis* as ineffective selection, and calculated the ratio of effective selection of *H. axyridis* in treatment or control as selection rate. Olfactory selection results were weighted, and the effect of treatments was analyzed using a non-parametric chi-square test. Difference in volatile chemical composition between infested and non-infested plants was analyzed through an Orthogonal Partial Least Squares Discriminant Analysis (OPLS-DA) performed on log2-transformed data followed by mean centering (Anal function Metabo Analyst R package OPLSR, R Core Team, 2020). Significantly regulated metabolites between groups were determined by VIP ≥ 1 and absolute fold change FC ≥ 1. VIP values were extracted from OPLS-DA results, which also contain score plots and permutation plots, generated using R package Metabo Analyst R. In order to avoid overfitting, a permutation test (200 permutations) was performed. Identified metabolites were annotated using KEGG Compound database (http://www.kegg.jp/kegg/compound/), annotated metabolites were then mapped to KEGG Pathway database (http://www.kegg.jp/kegg/pathway.html). Pathways with significantly regulated metabolites mapped were then fed into MSEA (metabolite sets enrichment analysis), and their significance was determined by hypergeometric test's p-values.

Results

Field investigation

Predatory ladybugs were the most abundant on *V. negundo* compared to the other plant species (Figure 1A), showing the superior ability of *V. negundo*, compared to the other plant species in this environment, to conserve natural enemies. During the observations, it was noticed that ladybugs colonized *V. negundo* after the plants were infested by the aphid *A. gossypii*. While *A. gossypii* also infested some other plant species (e.g. *Anemarrhena asphodeloides*), the high abundance of ladybugs on *V. negundo* suggested a specific interaction between *V. negundo*, aphids and ladybugs (Figure 1B–E).

Dynamic results based on the occurrence of predatory ladybugs on *V. negundo* and peach trees indicate that during the prophase, from early May to early June, the ladybugs concentrated on *V. negundo*. After the beginning of June, the number of ladybugs on *V. negundo* decreased, while the number of predatory ladybugs in the peach orchard increased rapidly (Figure 2).

Behavioral responses of *Harmonia axyridis* adults to plant odors

In the Y-tube olfactometer assays, compared with the blank control, male and female adults of *H. axyridis* had no significant preference for healthy *V. negundo* plants (female: $x^2 = 0.184$, P=0.668; male: $x^2 = 1.14$, P=0.286), but showed a significant preference for *V. negundo* previously infested by *A. gossypii* (female: $x^2 = 4.412$, P=0.036; male: $x^2 = 7.407$, P=0.006). Compared with healthy *V. negundo*, *H. axyridis* was more susceptible to plants previously infested by *A. gossypii* (female: $x^2 = 5.255$, P=0.022; male: $x^2 = 8.395$, P=0.004) (Figure 3; Figure 4A, B).

TABLE 1 Test compounds and their sources.

Formula	Compounds	CAS	Company	Purity
$C_8H_{10}O$	2-Phenylethanol	60-12-8	Macklin	99%
$C_9H_{18}O$	Nonanal	124-19-6	Macklin	96%
$C_{10}H_{18}O$	Eucalyptol	470-82-6	Macklin	99%
$C_{10}H_{18}O$	α-Terpineol	10482-56-1	Macklin	98%
$C_{15}H_{24}$	Valencene	4630-07-3	Macklin	75%
$C_{15}H_{24}$	(+)-Δ-Cadinene	483-76-1	Shanghai Yuanye Bio-Technology Co., Ltd.	95%
$C_{20}H_{36}O_2$	Sclareol	515-03-7	Macklin	98%
$C_{25}H_{43}NO_3$	Paraffin liquid	8042-47-5	Macklin	99%
"(+)" "Δ" indicates common symbols used to determine the spatial structure.				

10.3389/fpls.2022.1090559

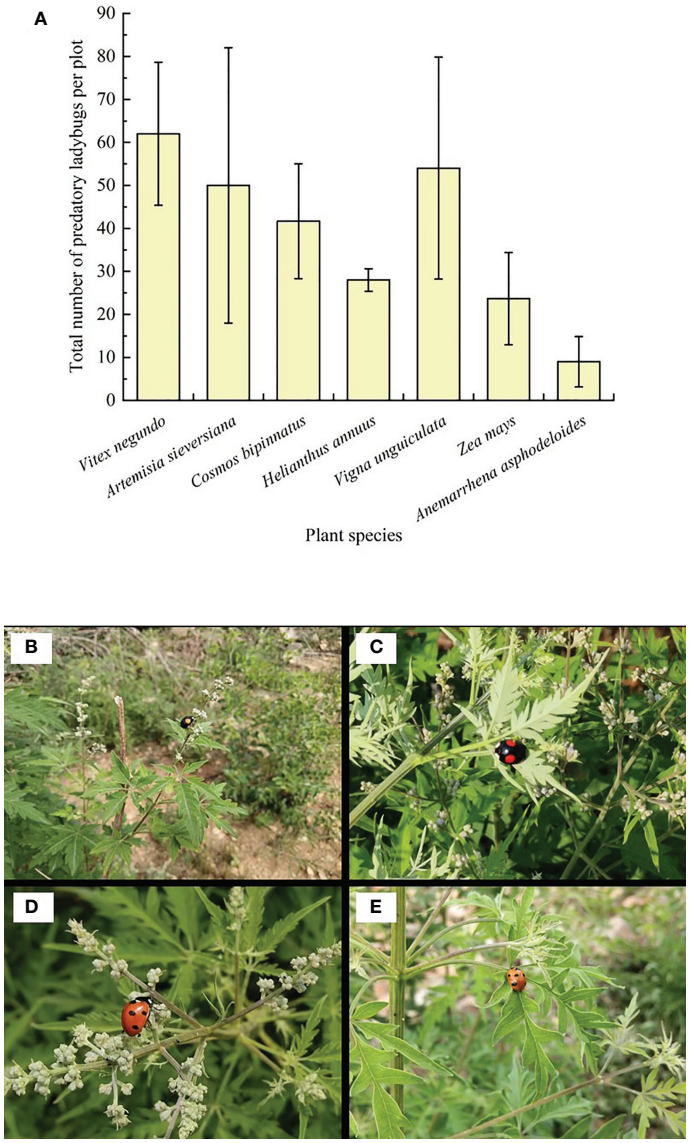

FIGURE 1
Abundance of predatory ladybugs on habitat plants and predatory ladybugs on *Vitex negundo*. Mean (± SE) per plot **(A)**, *Harmonia axyridis* **(B, C)** and *Coccinella septempunctata* **(D, E)** adults are visiting the flowers and leaves.

Analysis of *V. negundo* plant volatile compounds

A projection to orthogonal partial least squares-discriminant analysis (OPLS-DA) using the contents of all detected volatiles showed a clear separation between herbivore-infested treatments and healthy plants. The first two significant OPLS components explained 47.6% and 32.9% of the total variance, respectively (Figure 4C). The results showed that the release of isogeraniol, 2-phenylethanol, 2,6-dimethyl-1,3,5,7-octatetraene, 2,3-dihydrobenzofuran and nonanal was significantly up-regulated, the release of 43 substances was significantly down-regulated, and the release of 41 substances was not significantly changed (Figure 4D, Table 2). Terpenoids are important components of herbivore induced plant volatiles. In the biosynthesis of terpenoids, it was found that the release of eucalyptol, α-terpineol, sclareol, (+)-Δ-cadinene and valencene decreased (Figure S1, Table 2).

Behavioral response of *Harmonia axyridis* adults to volatile odorants

The results of olfactory test showed that 10 μL/mL eucalyptol and α-terpineol significantly attracted *H. axyridis* (x^2 = 4.121, P=0.042; x^2 = 13.291, P<0.001, respectively). Low concentration (1 μL/mL and 10 μL/mL) of sclareol and high concentration (100 μL/

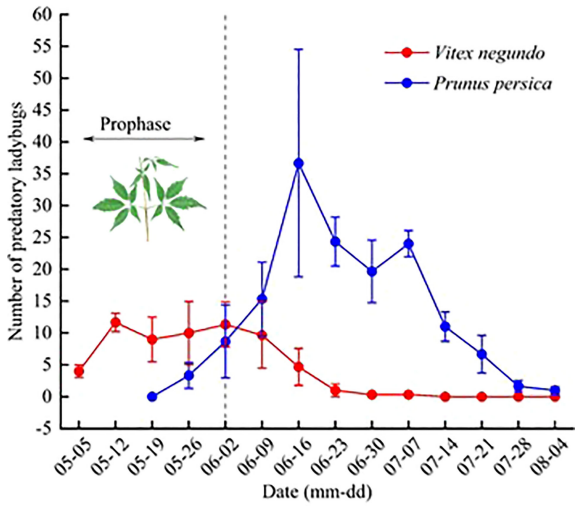

FIGURE 2
Occurrence dynamics of predatory ladybugs on *Vitex negundo* and adjacent peach trees. Note: Mean (± SE) per plot.

mL and 500 μL/mL) of nonanal also significantly attracted *H. axyridis* (x^2 = 6.377, *P*=0.012 and x^2 = 7.042, *P*=0.008; x^2 = 22.028, *P*<0.001 and x^2 = 11.239, *P*<0.001, respectively). However, 2-phenylethanol, (+)-Δ-cadinene and valencene had no significant effect on *H. axyridis* attraction at different concentrations (Figure 5).

Discussion

Non-crop habitat plants can play a role in attracting natural enemy insects, while the spill-over between the target area (e.g., crops and orchards) and non-crop habitat plants determines the effectiveness of pest control (Xie et al., 2012; Hatt et al., 2017; Xu et al., 2020). The most notable applications in crop protection are the push-pull strategies (Finch and Collier, 2000; Kleijn et al., 2011). Plant flower belt is one of the successful examples of push-pull strategy in agricultural production (Li et al., 2021). In greenhouse tomato production, *Carica papaya* L. (Caricaceae) can be used as a non-crop plant to breed *Encarsia sophia* Girault & Dodd (Hymenoptera: Aphelinidae) for the control of *Bemisia tabaci* Gennadius (Hemiptera: Aleyrodidae) (Xiao et al., 2011), while *Calendula officinalis* L. (Asteraceae) enhances the control of *Myzus persicae* Sulzer (Hemiptera: Aphididae) and *Frankliniella occidentalis* Pergande (Thysanoptera: Thripidae) by increasing the population density of *Orius sauteri* Poppius (Hemiptera: Anthocoridae) (Zhao et al., 2017) and reduces intraguild predation between predators and increases aphid biocontrol in tomato (Liang et al., 2022). In this experiment, we show that predatory ladybugs could migrate from *V. negundo* to peach orchards, and *V. negundo* release HIPVs to attract natural enemies when infected by herbivorous insects.

Plants change the characteristics of volatile organic compounds to cope with external stimuli. In response to herbivorous insect stimulation, HIPVs attract natural enemy insects (Robert et al., 2013). We showed that only the infection of *A. gossypii* can induce the attractions of *V. negundo* plant to the predator *H. axyridis*, indicating the importance of HIPVs to natural enemies in field. Moreover, the difference in content and diversity of HIPVs would account for the attractions of natural enemies (Heil, 2014; Turlings and Erb, 2018). In the present study, the release content of 2-phenylethanol and nonanal, the active ingredients attracting *H. axyridis*, increased after infested by *A. gossypii*. Structural diversity determines the complexity and diversity of plant volatile species and functions. Volatile substances with structural differences bind to specific olfactory proteins and exhibit different effects (Liu et al., 2020). Insects use a certain class of chemical information substances to achieve intraspecific information exchange (Nesbitt et al., 1979). Differences in functional groups lead to diverse chemical pheromone structures, resulting in more accurate and efficient information exchange or transfer (Liu et al., 2020). The substances that repel *M. persicae* have conjugated olefinic chemical structures (Liu et al., 2013). Diverse biological functions can also be achieved

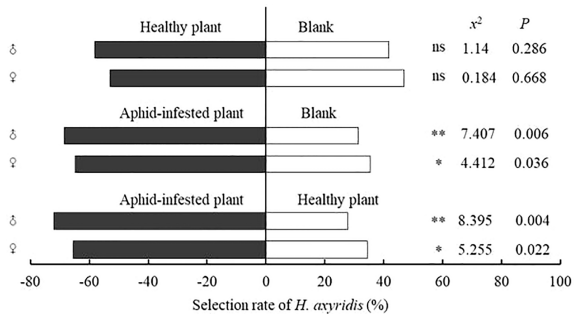

FIGURE 3
Behavioral responses of females and males of *H. axyridis* adults to different combinations in the Y-tube olfactometer assays. "*" denotes a significant difference at the *P*< 0.05 level, "**" means *P*< 0.01; "ns" indicates no significant difference.

10.3389/fpls.2022.1090559

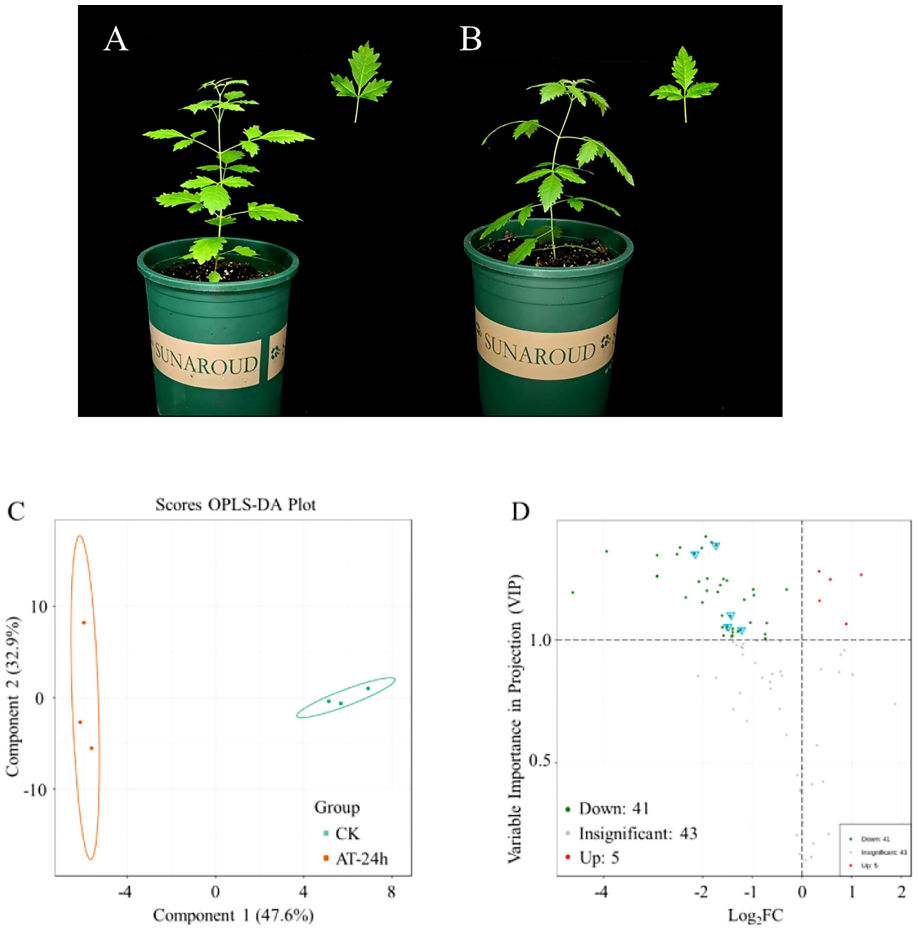

FIGURE 4
Orthogonal partial least squares-discriminant analysis (OPLS-DA) and differential material analysis of *V. negundo* plant volatile compounds. **(A, B)** *Vitex negundo* plants uninfected, and infected by *A. gossypii* during 24h. **(C)** Each point represents a sample, the samples of the same group are represented by the same color, with grouping using 95% confidence interval. **(D)** Each point represents a metabolite. When both VIP≥1 and FC≥1 double screening conditions are met, it is considered as a significantly up-regulated substance. The red point represents an up-regulated differential metabolite, and the green point represents a down-regulated differential metabolite. Gray represents a metabolite detected but not significantly different. Blue triangle marker points represent substances in terpenoid biosynthesis.

TABLE 2 Five significantly up-regulated and five down-regulated substances in terpenoid biosynthesis.

Formula	Compounds	Class I	CAS	
$C_{10}H_{18}O$	Isogeraniol	Terpenoids	5944-20-7	up-regulated
$C_8H_{10}O$	2-Phenylethanol	Alcohol	60-12-8	up-regulated
$C_{10}H_{14}$	2,6-dimethyl-1,3,5,7-octatetraene	Terpenoids	460-01-5	up-regulated
C_8H_8O	2,3-Dihydrobenzofuran	Heterocyclic compound	496-16-2	up-regulated
$C_9H_{18}O$	Nonanal	Aldehyde	124-19-6	up-regulated
$C_{10}H_{18}O$	Eucalyptol	Terpenoids	470-82-6	down-regulated
$C_{10}H_{18}O$	α-Terpineol	Terpenoids	10482-56-1	down-regulated
$C_{15}H_{24}$	Valencene	Terpenoids	4630-07-3	down-regulated
$C_{15}H_{24}$	(+)-Δ-cadinene	Terpenoids	483-76-1	down-regulated
$C_{20}H_{36}O_2$	Sclareol	Terpenoids	515-03-7	down-regulated

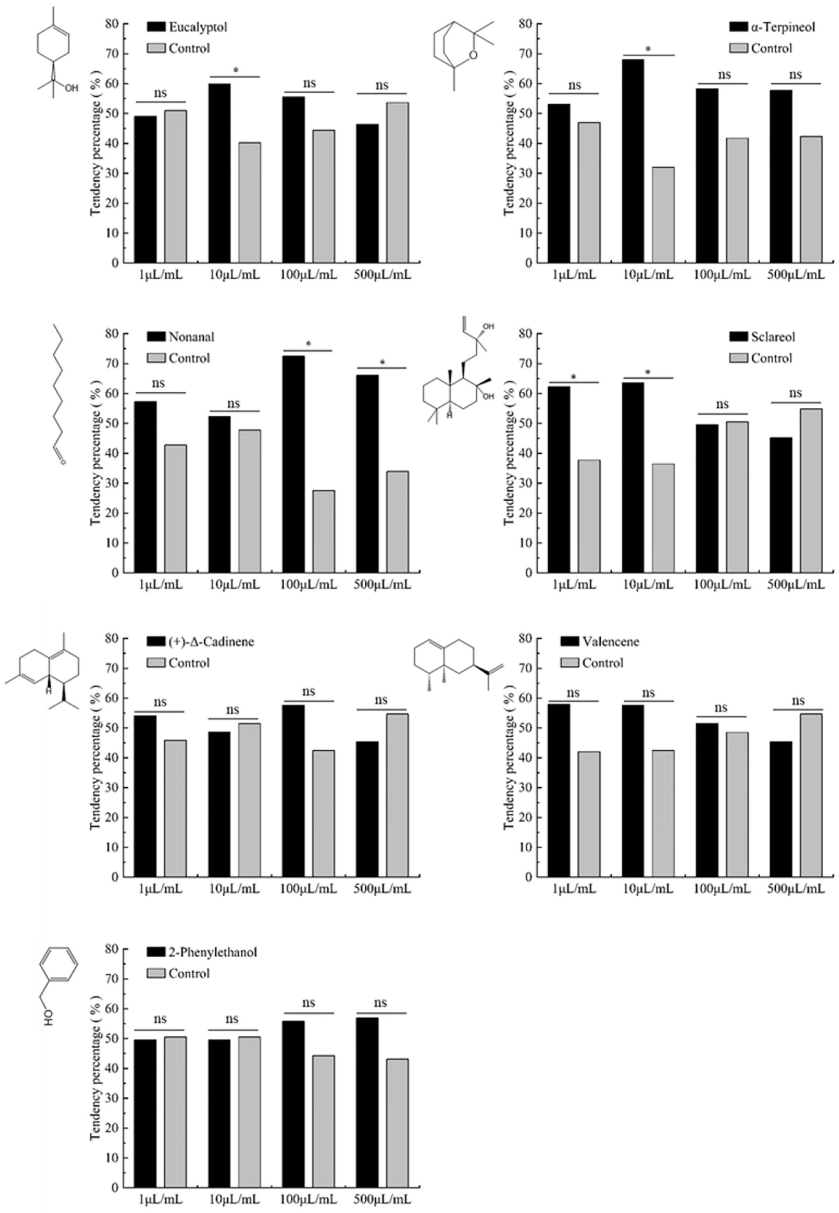

FIGURE 5
Behavioral responses of *H. axyridis* adults to key volatile compounds. Control for equal volume of paraffin liquid, Chi-square test was used between the test odor substances and the control group. "*" indicated that there was a significant difference in the preference of *H. axyridis* to the key odor substances and the control at the same concentration ($P < 0.05$) while "ns" indicated no significant difference.

by changing the length, position and spatial structure of carbon chains or double bonds (Conte et al., 1990). *Cydia pomonella* Linnaeus (Lepidoptera: Tortricidae) information substance is two double-bond of 12 carbon linear alcohol (Yang et al., 2004). The five terpenoids in this study are all composed of isoprene as the basic carbon skeleton unit. Among them, eucalyptol, α-terpineol and sclareol can directly attract *H. axyridis*, while (+)-Δ-cadinene and valencene have no significant effect on *H. axyridis*. Compared with the previous three substances, they all contain two carbon-carbon double-bonds in molecular structure. Valencene can be used as an alternative component for mosquito control (Tisgratog et al., 2018) and valencene (0.3%) showed strong repellent properties to *Tribolium castaneum* Herbst (Coleoptera: Tenebrionidae) (Guo et al., 2019), so terpenoids may exert different functions by increasing or decreasing the number of double bonds. In addition, different functional groups show different olfactory perceptions. Nonanal contains only one main carbon chain structure and only one aldehyde functional group,

which may lead to its significant attraction to *H. axyridis* at high concentrations.

The variety of plant volatiles complicates the analysis of their function. The formulations composed of MeSA and benzaldehyde can attract *Trichogramma dendrolimi* Matsumura (Hymenoptera: Trichogrammatidae), and other natural enemies (Zhao et al., 2022). Mixtures of β-pinene and limonene significantly increased the abundance of natural enemies such as *Coccinella septempunctat*a Linnaeus and *H. axyridis* (Wu et al., 2022). We found that low concentration of eucalyptol, α-terpineol and sclareol significantly attracted *H. axyridis* adults. This may be related to the reduced release of these compounds, although the effect of sclareol on natural enemy insects has rarely been reported to our knowledge. *H. axyridis* showed a significant preference for nonanal at high concentrations, which may be caused by the significant up-regulation of its release in *V. negundo*. 2-phenylethanol, (+)-Δ-cadinene and valencene have no effect on the behavior of *H. axyridis*, possibly because of its direct effect on pests or by altering plant resistance. Herbivore induced plant volatiles may only act on natural enemies or pests, and may also affect both simultaneously. For example (E)-β-Farnesene can repel aphids while attracting natural enemies (Beale et al., 2006; Xu et al., 2018b). Nonanal elicits electroantennogram response in female *Grapholita molesta* Busck (Lepidoptera: Tortricidae) (Xiang et al., 2017), and prevent *Ostrinia furnacalis* Guenée (Lepidoptera: Crambidae) from laying eggs on maize plants (Yu et al., 2020). However, in practical applications, the effect of volatile mixtures is often higher. A mixture of nonanal and (Z)-3-hexen-1-ol can significantly attract the syrphid fly *Paragus quadrifasciatus* Meigen (Diptera: Syrphidae) in the field (Yu et al., 2008), and the mixture of α-terpineole and 1,8-cineole repelled the fall armyworm *Spodoptera frugiperda* J. E. Smith (Lepidoptera: Noctuidae) (Lima et al., 2009). In recent years, a growing body of literature has shown that volatiles of plant can attract natural enemies or/and repel pests in pest management programs (Yao et al., 2021; Wang et al., 2022). That is, it is strategic to study the active substances that have attractive effects on *H. axyridis* and explore their mixed ratios for conservation biological control.

Impact of herbivory on HIPVs may depend on herbivorous insect species, density, and infection time, and external stimuli would also include soil chemical composition and temperature (Degenhardt et al., 2009; Cai et al., 2014; McCormick, 2016). For example, silicon affects HIPVs by regulating the jasmonic acid pathway, altering the mixed components of pest-induced volatiles released by rice after damage by *Capaphalocrocis medinalis* Guenée (Lepidoptera: Crambidae), and increasing attractiveness to parasitoids (Reynolds et al., 2016; Liu et al., 2017).

Genes change the release of volatiles, affecting the attractiveness of natural enemy insects (Xiao et al., 2012). Research on the regulatory genes of volatiles is a direct and effective method to verify the difference in release (Bruce et al., 2015). In addition, the behavioral responses of insects are regulated by external chemical signals, which are often identified by olfaction (Gadenne et al., 2016). Olfactory proteins in insects are very rich, which can specifically bind chemical information substances, and can also use an olfactory protein to perceive multiple signals, identify chemical signals and transmit information (Fan et al., 2011). There is a high matching specificity between queen pheromone 9-oxo-2-decenoic acid (9-ODA) and drone antennal olfactory protein *OR*11 (Wanner et al., 2007), *HoblCSP*1 and *HoblCSP*2 bind to odorants such as cinnamaldehyde (Sun et al., 2014), *HaxyOBP*13 and *HaxyOBP*14 had the highest expression in antennae and *HaxyOBP*5 could bind to methyl salicylate, nonanal and other substances (Qu et al., 2021; Qu et al., 2022). Therefore, we hypothesize that the substances with reduced release in the terpenoid biosynthetic pathway may also be key components to attract *H. axyridis*, that is, eucalyptol, α-terpineol, sclareol, (+)-Δ-cadinene and valencene may have attraction to *H.axyridis* or enhance its attractiveness. Exploring the genes regulating the synthesis and release of volatiles, analyzing the olfactory proteins involved in volatile binding and the odorant receptors involved in volatile recognition are helpful to regulate the ecological control of pests by chemical ecology methods.

Studies had showed that combining attractive synthetically produced HIPVs with functional plants which provide alternative resources to the targeted natural enemies can attract and retain efficient natural enemies in crop fields (Simpson et al., 2011; Jaworski et al., 2019). Lots of flowers play an important role in increasing fitness in predatory natural enemies (Wang et al., 2020; Fang et al., 2022). Flowers of *Perilla frutescens*, mixed with prey, have a positive effect on *H. axyridis* survival and early reproduction (Hatt and Osawa, 2019). *Vitex negundo* can provide sufficient high-quality nectar sources for bees during flowering (Su et al., 2000). And we found the visit of *H. axyridis* on *V. negundo* flowers in field. Future research could assess the fitness of nectar supporting the populations of natural enemies and evaluate the effect of *V. negundo* plantings on pest suppression in a diversity of adjacent crops. Thus, a "push and pull (i.e., nonanal)" or "attract (i.e., nonanal) and reward (i.e., *V. negundo* flowers)" strategy is a promising ecological practice to enhance conservation biological control in orchard.

Data availability statement

The raw data supporting the conclusions of this article will be made available by the authors, without undue reservation.

Author contributions

QX, CW, SW and XG conceived and designed research. QX, CW, DX, ZJ, and CZ conducted experiments and analyzed data. QX, CW and SH wrote and revised the paper. All authors contributed to the article and approved the submitted version.

Funding

This research was supported by the Youth Scientific Research Fund of Beijing Academy of Agriculture and Forestry Sciences (QNJJ202118), National Natural Science Foundation of China (ref. 32072479), and the Beijing Key Laboratory of Environment-friendly Management of Fruit Diseases and Pests in North China (BZ0432).

Conflict of interest

The authors declare that the research was conducted in the absence of any commercial or financial relationships that could be construed as a potential conflict of interest.

Publisher's note

All claims expressed in this article are solely those of the authors and do not necessarily represent those of their affiliated organizations, or those of the publisher, the editors and the reviewers. Any product that may be evaluated in this article, or claim that may be made by its manufacturer, is not guaranteed or endorsed by the publisher.

Supplementary material

The Supplementary Material for this article can be found online at: https://www.frontiersin.org/articles/10.3389/fpls.2022.1090559/full#supplementary-material

References

Aartsma, Y., Bianchi, F. J., van der Werf, W., Poelman, E. H., and Dicke, M. (2017). Herbivore-induced plant volatiles and tritrophic interactions across spatial scales. *New Phytol.* 216 (4), 1054–1063. doi: 10.1111/nph.14475

Arimura, G. I., Ozawa, R., Horiuchi, J. I., Nishioka, T., and Takabayashi, J. (2001). Plant-plant interactions mediated by volatiles emitted from plants infested by spider mites. *Biochem. Systematics Ecol.* 29 (10), 1049–1061. doi: 10.1016/S0305-1978(01)00049-7

Beale, M. H., Birkett, M. A., Bruce, T. J. A., Chamberlain, K., Field, L. M., Huttly, A. K., et al. (2006). Aphid alarm pheromone produced by transgenic plants affects aphid and parasitoid behavior. *Proc. Natl. Acad. Sci. United States America* 103, 10509–10513. doi: 10.1073/pnas.0603998103

Blande, J. D., Tiiva, P., Oksanen, E., and Holopainen, J. K. (2007). The emission of herbivore induced volatile terpenoids from two hybrid aspen (*Populus tremula* × *tremuloides*) clones under ambient and elevated ozone concentrations in the field. *Global Change Biol.* 13, 2538–2550. doi: 10.1111/j.1365-2486.2007.01453.x

Bruce, T. J. A., Aradottir, G. I., Smart, L. E., Martin, J. L., Caulfield, J. C., Doherty, A., et al. (2015). The first crop plant genetically engineered to release an insect pheromone for defence. *Sci. Rep.* 5, 11183. doi: 10.1038/srep11183

Cagliero, C., Mastellone, G., Marengo, A., Bicchi, C., Sgorbini, B., Rubiolo, P., et al. (2020). Analytical strategies for in-vivo evaluation of plant volatile emissions - a review. *Analytica Chimica Acta* 1147, 240–258. doi: 10.1016/j.aca.2020.11.029

Cai, X. M., Sun, X. L., Dong, W. X., Wang, G. C., and Chen, Z. M. (2014). Herbivore species, infestation time, and herbivore density affect induced volatiles in tea plants. *Chemoecology* 24, 1–14. doi: 10.1007/s00049-013-0141-2

Chen, R., and Feng, J. L. (2014). Study on behavioral response of different host plant and prey of *Chrysopa formosa* brauer. *Modern Agric. Sci. Technol.* (13), 128-129. doi: 10.3969/j.issn.1007-5739.2014.13.076

Cheng, A. X., Lou, Y. G., Mao, Y. B., Lu, S., Wang, L. J., and Chen, X. Y. (2007). Plant terpenoids: Biosynthesis and ecological functions. *J. Integr. Plant Biol.* 49, 179–186. doi: 10.1111/j.1744-7909.2007.00395.x

Conte, Y. L., Arnold, G., Trouiller, J., Masson, C., and Chappe, B. (1990). Identification of a brood pheromone in honeybees. *Naturwissenschaften* 77, 334–336. doi: 10.1007/BF01138390

Degenhardt, J., Hiltpold, I., Kollner, T. G., Frey, M., Gierl, A., Gershenzon, J., et al. (2009). Restoring a maize root signal that attracts insect-killing nematodes to control a major pest. *Proc. Natl. Acad. Sci. United States America* 106, 13213–13218. doi: 10.1073/pnas.0906365106

Dicke, M. (2009). Behavioural and community ecology of plants that cry for help. *Plant Cell Environ.* 32, 654–665. doi: 10.1111/j.1365-3040.2008.01913.x

Dudareva, N., Pichersky, E., and Gershenzon, J. (2004). Biochemistry of plant volatiles. *Plant Physiol.* 135, 1893–1902. doi: 10.1104/pp.104.049981

Fan, J., Francis, F., Liu, Y., Chen, J. L., and Cheng, D. F. (2011). An overview of odorant-binding protein functions in insect peripheral olfactory reception. *Genet. Mol. Res.* 10, 3056–3069. doi: 10.4238/2011.December.8.2

Fang, Y., Li, S., Xu, Q. X., Wang, J., Yang, Y. J., Mi, Y. Y., et al. (2022). Optimizing the use of basil as a functional plant for the biological control of aphids by *Chrysopa pallens* (Neuroptera: Chrysopidae) in greenhouses. *Insects* 13, 552. doi: 10.3390/insects13060552

Finch, S., and Collier, R. H. (2000). Host-plant selection by insects–a theory based on a'ppropriate/inappropriate landings' by pest insects of cruciferous plants. *Entomologia Experimentalis Applicata* 96, 91–102. doi: 10.1046/j.1570-7458.2000.00684.x

Gadenne, C., Barrozo, R. B., and Anton, S. (2016). Plasticity in insect olfaction: To smell or not to smell? *Annu. Rev. Entomology* 67, 317–333. doi: 10.1146/annurev-ento-010715-023523

Gill, B. S., Mehra, R., Navgeet,, and Kumar, S. (2018). *Vitex negundo* and its medicinal value. *Mol. Biol. Rep.* 45, 2925–2934. doi: 10.1007/s11033-018-4421-3

Guo, S. S., Wang, Y., Pang, X., Geng, Z. F., Cao, J. Q., and Du, S. S. (2019). Seven herbs against the stored product insect: Toxicity evidence and the active sesquiterpenes from *Atractylodes lancea*. *Ecotoxicology Environ. Saf.* 169, 807–813. doi: 10.1016/j.ecoenv.2018.11.095

Gurr, G. M., Wratten, S. D., Landis, D. A., and You, M. S. (2017). Habitat management to suppress pest populations: progress and prospects. *Annu. Rev. Entomology* 62, 91–109. doi: 10.1146/annurev-ento-031616-035050

Hatt, S., Lopes, T., Boeraeve, F., Chen, J., and Francis, F. (2017). Pest regulation and support of natural enemies in agriculture: experimental evidence of within field wildflower strips. *Ecol. Eng.* 98, 240–245. doi: 10.1016/j.ecoleng.2016.10.080

Hatt, S., and Osawa, N. (2019). The role of *Perilla frutescens* flowers on fitness traits of the ladybird beetle *Harmonia axyridis*. *BioControl* 64, 381–390. doi: 10.1007/s10526-019-09937-1

Hatt, S., Xu, Q., Francis, F., and Osawa, N. (2019). Aromatic plants of East Asia to enhance natural enemies towards biological control of insect pests. a review. *Entomol Gen.* 38 (4), 275–315. doi: 10.1127/entomologia/2019/0625

Heil, M. (2014). Herbivore-induced plant volatiles: targets, perception and unanswered questions. *New Phytol.* 204, 297–306. doi: 10.1111/nph.12977

Jaworski, C. C., Xiao, D., Xu, Q., Ramirez-Romero, R., Guo, X. J., Wang, S., et al. (2019). Varying the spatial arrangement of synthetic herbivore-induced plant volatiles and companion plants to improve conservation biological control. *J. Appl. Ecol.* 56 (5), 1176–1188. doi: 10.1111/1365-2664.13353

Khan, Z. R., James, D. G., Midega, C. A. O., and Pickett, J. A. (2008). Chemical ecology and conservation biological control. *Biol. control* 45, 210–224. doi: 10.1016/j.biocontrol.2007.11.009

Kleijn, D., Rundlof, M., Scheper, J., Smith, H. G., and Tscharntke, T. (2011). Does conservation on farmland contribute to halting the biodiversity decline? *Trends Ecol. Evol.* 26, 474–481. doi: 10.1016/j.tree.2011.05.009

Liang, Y. Y., Chen, X., Dai, H. J., Wang, J., Guo, X. J., Wang, S., et al. (2022). Flower provision reduces intraguild predation between predators and increases aphid biocontrol in tomato. *J. Pest Sci.* 95, 461–472. doi: 10.1007/s10340-021-01396-x

Li, T., and Blande, J. D. (2017). How common is within-plant signaling *via* volatiles? *Plant Signaling Behav.* 12, e1347743. doi: 10.1080/15592324.2017.1347743

Li, S., Jaworski, C. C., Hatt, S., Zhang, F., Desneux, N., and Wang, S. (2021). Flower strips adjacent to greenhouses help reduce pest populations and insecticide applications inside organic commercial greenhouses. *J. Pest Sci.* 94, 679–689. doi: 10.1007/s10340-020-01285-9

Lima, R. K., Cardoso, M. D., dos Santos, C. D., Moraes, J. C., Neri, D. K. P., and do Nascimento, E. A. (2009). Essential oil chemical composition from leaves of guava (*Psidium guajava* l.) and its effects on the fall armyworm *Spodoptera frugiperda* (J. e. smith 1797). (Lepidoptera: Noctuidae) behavior. *Ciencia e agrotecnologia* 33, 1777–1781. doi: 10.1590/S1413-70542009000700013

Liu, Y. B., Liu, J. F., Ma, Y., Zeng, Z. J., and He, X. J. (2020). The diversity and specificity of insect pheromones. *Chin. J. Appl. Entomology* 57, 1056–1063. doi: 10.7679/j.issn.2095-1353.2020.106

Liu, T., Li, W. Z., You, X. F., Chai, X. L., Fu, G. X., and Yuan, G. H. (2013). Repellent and anti-settling activity of common plant-derived volatiles on *Myzus persicae* (Sulzer). *Acta Tabacaria Sin.* 19, 77–84. doi: 10.3969/j.issn.1004-5708.2013.02.014

Liu, J., Zhu, J. W., Zhang, P. J., Han, L. W., Reynolds, O. L., Zeng, R. S., et al. (2017). Silicon supplementation alters the composition of herbivore induced plant volatiles and enhances attraction of parasitoids to infested rice plants. *Front. Plant Sci.* 8. doi: 10.3389/fpls.2017.01265

McCormick, A. C. (2016). Can plant-natural enemy communication withstand disruption by biotic and abiotic factors? *Ecol. Evol.* 6, 8569–8582. doi: 10.1002/ece3.2567

Nesbitt, B. F., Beevor, P. S., Hall, D. R., and Lester, R. (1979). Female sex pheromone components of the cotton bollworm, *Heliothis armigera*. *J. Insect Physiol.* 25, 535–541. doi: 10.1016/S0022-1910(79)80012-8

Qu, C., Wang, R., Che, W. N., Li, F. Q., Zhao, H. P., Wei, Y. Y., et al. (2021). Identification and tissue distribution of odorant binding protein genes in *Harmonia axyridis* (Coleoptera: Coccinellidae). *J. Integr. Agric.* 20, 2204–2213. doi: 10.1016/s2095-3119(20)63297-x

Qu, C., Yang, Z. K., Wang, S., Zhao, H. P., Li, F. Q., Yang, X. L., et al. (2022). Binding affinity characterization of four antennae-enriched odorant-binding proteins from *Harmonia axyridis* (Coleoptera: Coccinellidae). *Front. Physiol.* 13. doi: 10.3389/fphys.2022.829766

R Core Team (2020). *R: A language and environment for statistical computing* (Vienna, Austria: R Foundation for Statistical Computing). Available at: https://www.R-project.org/.

Reynolds, O. L., Padula, M. P., Zeng, R. S., and Gurr, G. M. (2016). Silicon: potential to promote direct and indirect effects on plant defense against arthropod pests in agriculture. *Front. Plant Sci.* 7. doi: 10.3389/fpls.2016.00744

Robert, C. A. M., Erb, M., Hiltpold, I., Hibbard, B. E., Gaillard, M. D. P., Bilat, J., et al. (2013). Genetically engineered maize plants reveal distinct costs and benefits of constitutive volatile emissions in the field. *Plant Biotechnol. J.* 11, 628–639. doi: 10.1111/pbi.12053

Simpson, M., Gurr, G. M., Simmons, A. T., Wratten, S. D., James, D. G., Leeson, G., et al. (2011). Attract and reward: combining chemical ecology and habitat manipulation to enhance biological control in field crops. *J. Appl. Ecol.* 48, 580–590. doi: 10.1111/j.1365-2664.2010.01946.x

Song, B. Z., Liang, Y. P., Liu, S. Z., Zhang, L. F., Tang, G. B., Ma, T., et al. (2017). Behavioral responses of *Aphis citricola* (Hemiptera: Aphididae) and its natural enemy *Harmonia axyridis* (Coleoptera: Coccinellidae) to non-host plant volatiles. *Florida Entomologist* 100, 411–421. doi: 10.1653/024.100.0202

Su, S., Chen, S., Lin, X., and Hu, F. (2000). The study of relativity of RWB to honey yield. *J. Bee* 1, 4–7.

Sun, H. Y., Guan, L., Feng, H. L., Yin, J., Cao, Y. Z., Xi, J. H., et al. (2014). Functional characterization of chemosensory proteins in the scarab beetle, *Holotrichia oblita* faldermann (Coleoptera: Scarabaeida). *PloS One* 9, e107059. doi: 10.1371/journal.pone.0107059

Tisgratog, R., Sukkanon, C., Grieco, J. P., Sanguanpong, U., Chauhan, K. R., Coats, J. R., et al. (2018). Evaluation of the constituents of vetiver oil against *Anopheles minimus* (Diptera: Culicidae), a malaria vector in Thailand. *J. Med. Entomology* 55, 193–199. doi: 10.1093/jme/tjx188

Tooker, J. F., O'Neal, M. E., and Rodriguez-Saona, C. (2020). Balancing disturbance and conservation in agroecosystems to improve biological control. *Annu. Rev. Entomology* 65, 81–100. doi: 10.1146/annurev-ento-011019-025143

Turlings, T. C. J., and Erb, M. (2018). Tritrophic interactions mediated by herbivore-induced plant volatiles: mechanisms, ecological relevance, and application potential. *Annu. Rev. Entomology* 63, 433–452. doi: 10.1146/annurev-ento-020117-043507

Turlings, T. C. J., and Ton, J. (2006). Exploiting scents of distress: the prospect of manipulating herbivore-induced plant odours to enhance the control of agricultural pests. *Curr. Opin. Plant Biol.* 9, 421–427. doi: 10.1016/j.pbi.2006.05.010

Wang, J., Li, S., Fang, Y., Zhang, F., Jin, Z. Y., Desneux, N., et al. (2022). Enhanced and sustainable control of *Myzus persicae* by repellent plants in organic pepper and eggplant greenhouses. *Pest Manage. Sci.* 78, 428–437. doi: 10.1002/ps.6681

Wang, Y. S., Yao, F., Soares, M. A., Basiri, S. E., Amiens-Desneux, E., Campos, M. R., et al. (2020). Effects of four non-crop plants on life history traits of the lady beetle *Harmonia axyridis*. *Entomol. Gen.* 40 (3), 243–252. doi: 10.1127/entomologia/2020/0933

Wanner, K. W., Nichols, A. S., Walden, K. K., Brockmann, A., Luetje, C. W., and Robertson, H. M. (2007). A honey bee odorant receptor for the queen substance 9-oxo-2-decenoic acid. *Proc. Natl. Acad. Sci. United States America* 104, 14383–14388. doi: 10.1073/pnas.0705459104

Wu, S. L., Liu, F. L., Zeng, W. A., Xiao, Z. P., Li, J. Y., Teng, K., et al. (2022). Evaluation of floral-derived volatile blend for attracting aphid parasitoids and lady beetles in the tobacco fields. *Biol. Control* 172, 104979. doi: 10.1016/j.biocontrol.2022.104979

Xiang, H. M., Ma, R. Y., Diao, H. L., Li, X. W., He, X. J., and Guo, Y. F. (2017). Peach-specific aldehyde nonanal attracts female oriental fruit moths, *Grapholita molesta* (Lepidoptera: Tortricidae). *J. Asia-Pacific Entomology* 20, 1419–1424. doi: 10.1016/j.aspen.2017.08.006

Xiao, Y. F., Chen, J. J., Cantliffe, D., Mckenzie, C., Houben, K., and Osborne, L. S. (2011). Establishment of papaya banker plant system for parasitoid, *Encarsia sophia* (Hymenoptera: Aphilidae) against *Bemisia tabaci* (Hemiptera: Aleyrodidae) in greenhouse tomato production. *Biol. Control* 58, 239–247. doi: 10.1016/j.biocontrol.2011.06.004

Xiao, Y., Wang, Q., Erb, M., Turlings, T. C. J., Ge, L., Hu, L., et al. (2012). Specific herbivore-induced volatiles defend plants and determine insect community composition in the field. *Ecol. Lett.* 15, 1130–1139. doi: 10.1111/j.1461-0248.2012.01835.x

Xie, H., Chen, J., Cheng, D., Zhou, H., Sun, J., Liu, Y., et al. (2012). Impact of wheat-mung bean intercropping on English grain aphid (Hemiptera: Aphididae) populations and its natural enemy. *J. Economic Entomology* 105 (3), 854–859. doi: 10.1603/ec11214

Xu, Q., Hatt, S., Han, Z., Francis, F., and Chen, J. (2018b). Combining e-β-farnesene and methyl salicylate release with wheat-pea intercropping enhances biological control of aphids in north China. *Biocontrol Sci. Technol.* 28 (9), 883–894. doi: 10.1080/09583157.2018.1504885

Xu, Q., Hatt, S., Lopes, T., Zhang, Y., Bodson, B., Chen, J., et al. (2018a). A push–pull strategy to control aphids combines intercropping with semiochemical releases. *J. Pest Sci.* 91, 93–103. doi: 10.1007/s10340-017-0888-2

Xu, Q., Wang, S., Li, S., and Hatt, S. (2020). "Conservation biological control in organic greenhouse vegetables," in *Integrative biological control progress in biological control*. Eds. Y. Gao, H. M. Hokkanen and I. Menzler-Hokkanen (Cham, Switzerland: Springer). doi: 10.1007/978-3-030-44838-7_8

Yang, Z. H., Bengtsson, M., and Witzgall, P. (2004). Host plant volatiles synergize response to sex pheromone in codling moth, *Cydia pomonella*. *J. Chem. Ecol.* 30, 619–629. doi: 10.1023/B:JOEC.0000018633.94002.af

Yao, C. C., Du, L. X., and Li, Y. H. (2021). Plant-to-plant communications medicated by herbivore-induced plant volatiles and the mechanisms. *Plant Prot.* 47, 1–10. doi: 10.16688/j.zwbh.2020427

Ye, M., Glauser, G., Lou, Y. G., Erb, M., and Hu, L. F. (2019). Molecular dissection of early defense signaling underlying volatile-mediated defense regulation and herbivore resistance in rice. *Plant Cell* 31, 687–698. doi: 10.1105/tpc.18.00569

frontiers | Frontiers in Plant Science

TYPE Original Research
PUBLISHED 18 January 2023
DOI 10.3389/fpls.2022.1092638

OPEN ACCESS

EDITED BY
Huipeng Pan,
South China Agricultural University, China

REVIEWED BY
Zezhong Yang,
Tianjin Academy of Agricultural Sciences, China
Tianbo Ding,
Qingdao Agricultural University, China

*CORRESPONDENCE
Julian Chen
chenjulian@caas.cn

†These authors have contributed equally to this work

SPECIALTY SECTION
This article was submitted to Plant Biotechnology, a section of the journal Frontiers in Plant Science

RECEIVED 10 November 2022
ACCEPTED 23 December 2022
PUBLISHED 18 January 2023

CITATION
Li Q, Cheng Y, Fan J and Chen JL (2023) Metabolic relay gene of aphid and primary symbiont as RNAi target loci for aphid control. *Front. Plant Sci.* 13:1092638. doi: 10.3389/fpls.2022.1092638

Metabolic relay gene of aphid and primary symbiont as RNAi target loci for aphid control

Qian Li[1,2†], Yu Cheng[2†], Jia Fan[2] and Julian Chen[2,3*]

[1]College of Bioscience and Resource Environment/Key Laboratory of Urban Agriculture (North China), Ministry of Agriculture and Rural Affairs of the People's Republic of China, Beijing University of Agriculture, Beijing, China, [2]The State Key Laboratory for Biology of Plant Diseases and Insect Pests, Institute of Plant Protection, Chinese Academy of Agricultural Sciences, Beijing, China, [3]Ministry of Agricultural and Rural Affairs -Center of Applied Biological International (MARA-CABI) Joint Laboratory for Bio-Safety, Institute of Plant Protection, Chinese Academy of Agricultural Sciences, Beijing, China

Introduction: Aphids form a stable and mutually beneficial relationship with their primary symbiont *Buchnera aphidicola*, which play an important role in providing the missing nutrients to the host aphid. Based on the genome sequence of wheat aphid *Siotobion miscanthi* and its primary symbiont *Buchnera* that we obtained in our previously study, we identified a metabolic relay gene, *ilvA*, involved in the isoleucine synthesis pathway between aphids and *Buchnera*.

Method: In this study, we identified the location and sequence structure of *ilvA* gene in aphid genome, the expression level in different instars and tissues of aphids, and the effect of reducing *ilvA* expression on the growth and development of aphids by bioinformatics analysis, quantitative PCR, RNAi and bioassay experiments.

Result: Our study showed that *ilvA* was expressed at the highest level in the 2nd instar of the aphid, while the expression of this gene was significantly higher in the aphid bacteriocytes than in other tissues. Notably, this gene is localized on the aphid sex chromosome and remains highly conserved and collinearity across different aphid genomes. Knocking down the expression of *ilvA* reduced the aphid body weight and production. However, the indices of mortality decreased slightly, but were not significantly different, compared to the control.

Discussion: The results show that the relay genes between aphids and their symbionts in the metabolism of essential nutrients have potential roles in the growth and development of aphids, meanwhile, providing target loci and new ideas for RNAi-based aphid green control strategies.

KEYWORDS

Sitobin miscanthi, Buchnera aphidicola, ilvA, metabolic relay, RNAi

1 Introduction

Aphids are important pests that cause significant economic losses in agriculture worldwide. Almost all aphids contain endosymbionts, and one of them, *Buchnera aphidicola* (hereinafter referred to as *Buchnera*), which is present in almost all aphids, provides essential nutrients to the host aphid and therefore called primary symbiont (Baumann, 2005). Additionally, aphids have a variety of secondary symbionts in their bodies, and the significance of secondary symbionts in enhancing the adaptation of aphids to adverse environments has been widely reported (De Clerck et al., 2015; Manzano-Marín et al., 2016; Li et al., 2018; Li et al., 2021). In recent years, it is worth noting the growing number of studies have shown that the function of *Buchnera* not only in providing essential amino acids to the host aphid, but also has potential effects in improving the heat tolerance of aphids (Zhang et al., 2019), revealing the differentiation process (Perreau et al., 2021; Zhang S. et al., 2021) and enhancing their resistance to drugs (Guo et al., 2020). Therefore, exploiting the close and mutually beneficial relationship between aphids and *Buchnera* may produce new ideas for developing green control strategies of aphids.

In China, the grain aphid *Sitobion miscanthi* is one of the most prevalent wheat pests and causes substantial economic losses in agriculture (Li et al., 2021). As genome sequencing technologies continuous upgrading and costs decrease, a large number of insect genomic information continues to be deciphered. Based on our previously published genome information of wheat aphid *S. miscanthi* (LF clone) (Jiang et al., 2019) and its primary symbiont *Buchnera* (Li et al., 2022), making it more convenient to study the nutrient metabolism interaction network between them. Previously, we used genomic information to identify a key relay gene *ilvE*, linking *Buchnera* to aphids in the leucine, isoleucine and valine synthesis pathways. Meanwhile, RNA interference (RNAi) experiment reveals a vital function in three essential amino acid synthesis pathways (Li et al., 2022). However, whether exist other metabolic relay genes are present in the aphid and *Buchnera* nutrient synthesis chains and can be used as candidate target genes for RNAi is still unknown.

Here, we have mined another key gene *ilvA* in the aphid-*Buchnera* relay synthesis of isoleucine pathway through the genomic information obtained in our previous work. Sequence and bioinformatics analysis showed that the *ilvA* gene was highly conserved in different aphid genomes, while the gene expression profile in different developmental stages and tissues of aphids was clarified by qPCR assay. Subsequently, the effects of *ilvA* on aphid life parameters were measured by RNAi experiments. Our results indicate that the *ilvA* gene, which links the aphid and *Buchnera* amino acid synthesis pathways, has an important effect on aphid weight and offspring, all of which suggest that *ilvA* gene can be used as candidate target for RNAi against aphids.

2 Materials and methods

2.1 Aphid rearing

The strains of *S. miscanthi* used in this study was reared on aphid-susceptible wheat seedlings (*Triticum aestivum* L) in the culture room at 20 ± 1°C with a 75% relative humidity and a light: dark photoperiod of 16: 8 hours. After 10 generations, the aphids were used for the following experiments.

2.2 Sequences, gene structure, conserved domain and synteny analysis

The gene structure and conserved domains were analyzed using NCBI Batch CDD-search, and the results were visualized by TBtools (v 1.09857) (Chen et al., 2020). Conserved motifs of the genes were analyzed by the MEME program with the following parameters: classic mode, with the number of repetitions set to zero or one per sequence and the maximum number of motifs identified set to 6. Meanwhile, the location information of gene on aphid chromosome was obtained by genome annotation file, and the results were visualized by TBtools. We downloaded the chromosome-level genome and annotations of *A. pisum* (Li et al., 2020), selected the longest representative coding sequences of each gene and translated the nucleotide sequences to amino acid sequences. Then, MCScanX v1.1 (Wang et al., 2012) was used to identify syntenic blocks of genes between *A. pisum* and the previously published chromosome-level genome of *S. miscanthi*, and the results were visualized byTBtools.

2.3 Gene expression analysis between autosome and sex chromosome

Considering that the *ilvA* gene is localized on the aphid sex chromosome, we collected newly emerged winged and wingless adult aphids for transcriptome analysis in order to understand the gene expression on the aphid autosomes and sex chromosome. Total RNA from the winged and wingless aphids were extracted with the total RNA extraction regent kit (Tianmo, Beijing, China) following the manufacturer's instructions. The quality of the RNA samples was evaluated on a 1% (w/v) agarose gel by electrophoresis and quantified by a Nanodrop 20000 spectrophotometer (DNovix, Washington, DC, United States). And enrichment of mRNA with polyA tails by Oligo (dT) magnetic beads. The obtained mRNA was then randomly interrupted with divalent cations in NEB Fragmentation Buffer, and the library was built for the following Illumina sequencing. In order to ensure the quality

and reliability of data analysis, the raw reads were filtered by removing reads with adapters, reads with unidentifiable base information (noted as N) or the low-quality reads (reads with Qphred <= 20 with more than 50% of the entire read length in number of bases). Then, fast and accurate comparison of clean reads with our published reference genome (Jiang et al., 2019) using HISAT2 software (Kim et al., 2015). The differentially expressed genes (DEGs) between the winged and wingless aphids were analyzed. Our sequence data have been deposited in the National Center for Biotechnology information's Sequence Read Archive, https://www.ncbi.nlm.nih.gov/sra (accession no. PRJNA908645).

2.4 Expression profile analysis of *ilvA* gene in aphids

ilvA was amplified by PCR from *S. miscanthi* cDNA with the specific primers listed in Table 1. The nucleotide sequence of the *ilvA* gene from *S. miscanthi* in this paper has been deposited in GenBank under accession number OQ093134. To quantify the *ilvA* transcript levels in different tissues and different developmental stages of aphids, qRT-PCR was performed with the specific primers listed in Table 1. The expression of the *ilvA* gene was normalized to the expression of the aphid housekeeping gene *NADH* (Zhang S. Y. et al., 2021). The amplification efficiency amplified with primers was 100.5 and 99.0% for *ilvA* and *NADH*. All treatments had three biological replicates, and each replicate consisted of three technical replicates.

2.5 RNAi assay and aphid bioassay experiment

The molecules of dsRNA targeting *S. miscanthi ilvA* (dsilvA) and the gene sequence of the green fluorescent protein (dsGFP), used as negative control, were synthetized according to the specific primers listed in Table 1. Meanwhile, the dsRNA and control were diluted to 500 ng/μl in an artificial diet (20% sucrose), and pure aphid artificial diet was used as the blank control. A total of 500 newly born winged adult *S. miscanthi* were picked from fresh wheat plants. After starvation for 2 hours, 15 active *S. miscanthi* were transferred into each feeding devices, and three replicate tubes were set up. After silencing, *S. miscanthi* individuals were collected at different time after treatment with dsRNA. Then, the surviving aphids were counted to calculated mortality. Additionally, the surviving aphids were used to detect RNAi efficiency by qPCR.

In addition, six aphids per 3 pairs were picked from the artificial device to perform the weight measurement. The average of these 3 pairs of weight values was calculated as one biological replicate per time point. Six biological replicates were examined. Moreover, the number of aphid production at different times of treatment was also counted. Six biological replicates were examined.

2.6 Statistical analysis

Differences in gene expression level at different time points of RNAi experiment were tested by one-way analysis of variance (ANOVA) followed by Duncan's multiple range test using SPSS version 23.0 software (IBM, Armonk, NY, United States).

3 Results

3.1 *ilvA* gene as the initiator of the isoleucine synthesis pathway in aphids

Based on our previously reported genome information of the *S. miscanthi* and its primary symbiont *Buchnera* (Jiang et al., 2019; Li et al., 2022), we found that the *Buchnera* genome contains almost all the key genes in the essential amino acid synthesis pathway, however, upstream of the aphid essential amino acid isoleucine synthesis pathway, a threonine dehydratase gene named *ilvA*, which has the function of hydrolyzing threonine to 2-oxybutanoate, is missing from the *Buchnera* genome, but present in the aphid genome (Figure 1).

TABLE 1 Primers used in this study.

Target	Primer	Sequence (5′-3′)	Reference
ilvA	*SmilvA*-F	ATGGAAGTCGAAGATCCTTTC	This study
	SmilvA-R	TCAAAGAATTTTGGGTAATGGT	
	SmilvA-q-F	CAGCCGTGTTGTCTGGTACT	
	SmilvA-q-R	TGAAGACGTCGTCTGACAGC	
dsilvA	*dsilvA*-F	TAATACGACTCACTATAGGG TCGAGGCCTGCAGGAATTTT	This study
	dsilvA -R	TAATACGACTCACTATAGGG GCCTTCCACTACGCACTTCT	
NADH	*NADH*-q-F	GATAGCTTGGGCTGGACATATAG	Zhang S. Y. et al., 2021
	NADH-q-R	CGAGGAGAACATGCTCTTAGAC	

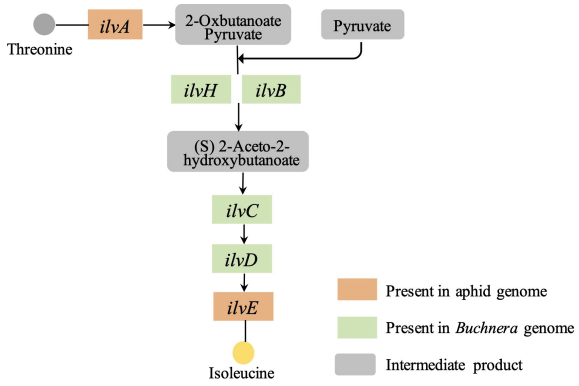

FIGURE 1
Isoleucine biosynthetic pathways in wheat aphid *S. miscanthi* and *Buchnera*.

3.2 Sequence, structure and phylogenetic analyses of *ilvA* in aphids

To verify the accuracy of genome sequencing and understand the function of the *ilvA* gene, we cloned the *ilvA* gene using specific primers (Table 1). The full-length *ilvA* gene (1272 bp) was obtained by PCR amplification, with GenBank accession number OK431491. The *ilvA* gene is localized on *S. miscanthi* chromosome 8 (SmChr_8), encoding 423 amino acids with a deduced MW of 45.4 kDa and possessing a threonine dehydratase structural domain (Figure 2). Interestingly, *S. miscanthi* chromosome 8 is derived from a sex chromosome split that is thought to be highly homozygous and conserved in different aphid genomes (sex chromosome splitting due to chromosome splicing problems during the pre-sequencing process cannot be excluded). Additionally, synteny analysis between the *S. miscanthi* and pea aphid (*A. pisum*) genomes revealed that *ilvA* is also highly conserved in terms of gene location (Figure 2A). Phylogenetic analysis showed that *ilvA* gene sequences in different insects clustered into different branches, implying that the gene is highly conserved in different insects. Domain structure and motif analysis showed that *ilvA* genes are highly conserved in Hemiptera, especially in aphids (Figures 3, 4).

3.3 Gene expression analysis of different chromosomes and selection pressure analysis of *ilvA* gene

Considering the specific location of *ilvA* on the sex chromosome of aphids, and sexually mature aphids are rarely found in *S. miscanthi*, therefore, we sequenced the transcriptomes of winged and wingless adult aphids to investigate the differences in gene expression patterns on the autosomes and sex chromosomes of *S. miscanthi*. Surprisingly, the expression of genes on autosomes was significantly higher

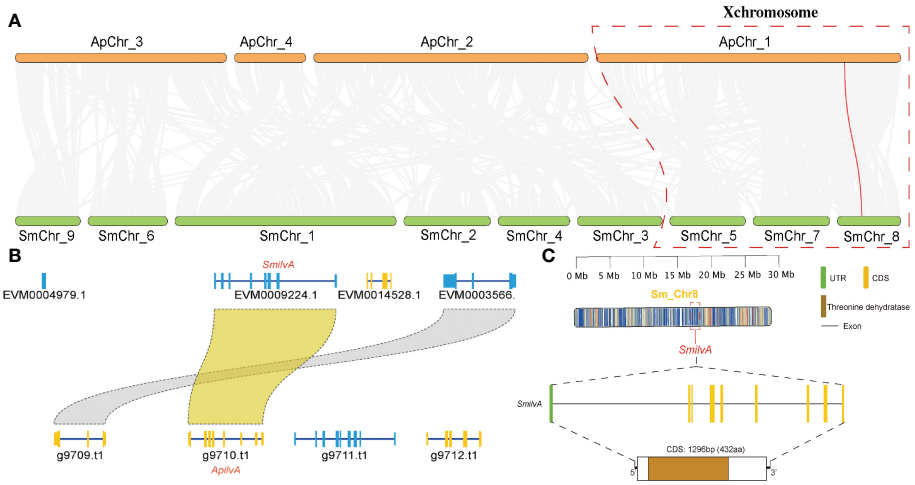

FIGURE 2
Sequence characteristics, structure and genome collinearity analysis. **(A)** Genome collinearity analysis of wheat aphid *S. miscanthi* and pea aphid *A. pisum*. Red lines represent the *ilvA* gene. **(B)** Colinearity analysis of *ilvA* gene in different aphid genomes. **(C)** Gene structure analysis of *ilvA*..

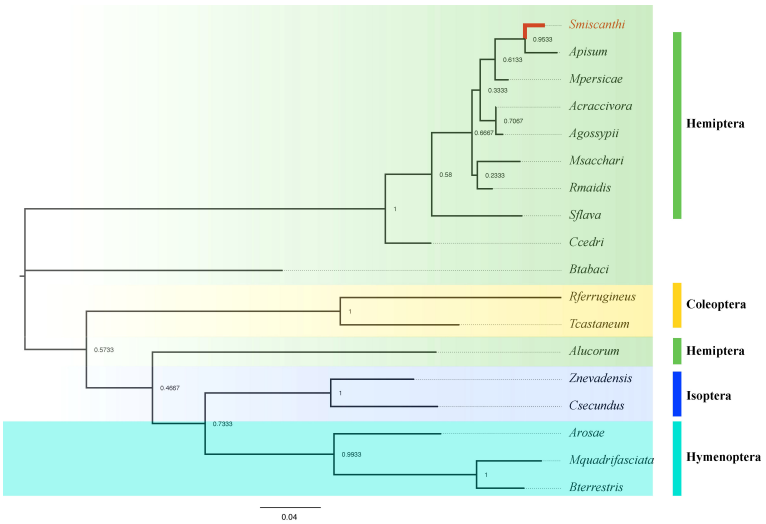

FIGURE 3
Phylogenetic analysis of *ilvA* gene in different insects.

than that on sex chromosomes in both winged and wingless adult aphids (Figure 5A). To investigate the selective pressure on genes with expression levels in winged and wingless adult aphids, we estimated Ka/Ks value for paralogous genes within the autosome and sex chromosome of *S. miscanthi*, meanwhile, we also estimated Ka/Ks value for single-copy orthologous genes for a pair of related aphid species (*S. miscanthi*/*A. pisum*). The results showed that the selection pressure on sex chromosomes was significantly higher than that on autosomes, whether it was paralogous genes on aphid chromosomes ($p < 0.0056$, Kruskal-Wallis rank sum test) or orthologous genes on different aphid chromosomes ($p < 0.0001$) (Figures 5B, C). In addition, the Ka/Ks values of *ilvA* and our previously reported *ilvE* gene in different aphids were very low, 0.166 and 0.087, respectively (Figure 5D), suggesting that these genes are under relaxed purifying selection and the function is stable in aphid genome.

3.4 Expression profile of *ilvA* at different tissues and developmental stages in *S. miscanthi*

The expression profile of *ilvA* at different tissues and developmental stages was examined using real-time PCR.

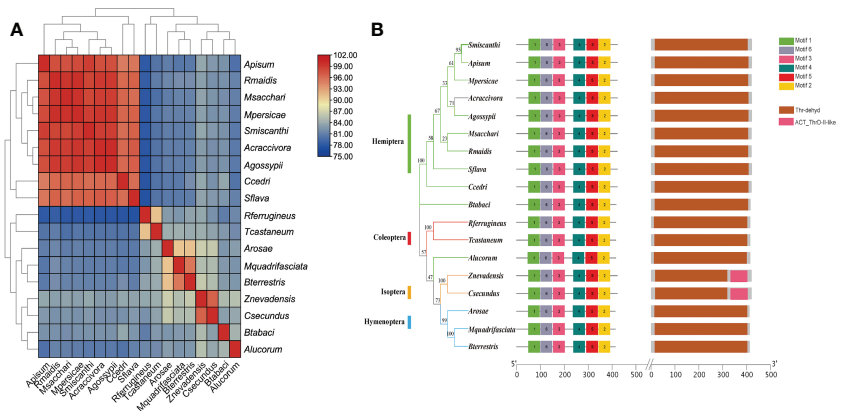

FIGURE 4
Sequence similarity, motif and domain analysis of *ilvA* gene in different insects **(A)** Sequence homology heat map analysis of *ilvA* gene in different insects. **(B)** Analysis of motifs and domains in *ilvA* gene sequence.

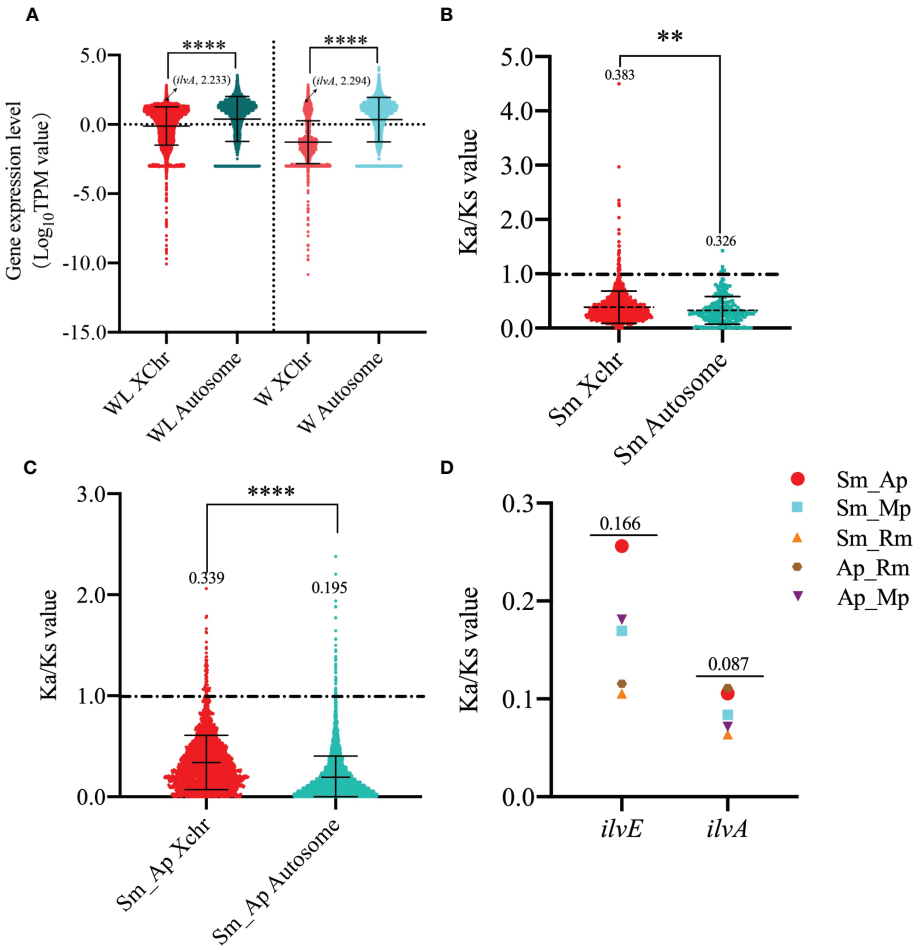

FIGURE 5
Analysis of gene expression levels and selection pressure on different type of chromosomes in winged and wingless adult aphids **(A)** Analysis of gene expression on different chromosome of winged and wingless adult aphids. **(B)** Analysis of selection pressure of different chromosome paralogous genes in *S. miscanthi*. **(C)** Analysis of selection pressure of different chromosome orthologous genes in *S. miscanthi* and *A. pisum*. **(D)** Selection pressure analysis of *ilvA* and *ilvE* orthologous genes in different aphid genomes. The "**" and "****" indicates significant differences based on the Mann-Whitney U test for two sample comparison at $P < 0.001$ and $P < 0.00001$, respectively.

Interestingly, the *ilvA* gene was expressed in all instars of aphids, with the highest expression in the 2nd instar and the lowest in the 1st instar (Figure 6A). In order to further reveal the expression specificity of *ilvA* gene in different tissues of aphids, we dissected the head, thorax, abdomen, gut, cornicle and bacteriocytes of aphids and performed the qPCR experiment. Unexpectedly, the results revealed that the expression of the *ilvA* gene was significantly higher in the bacteriocytes of aphids than in the other tissues (Figure 6B).

3.5 Effect of RNAi of *ilvA* on vital parameters of aphids

To further verify the potential function of *ilvA* in aphid development, we synthesized dsRNA *in vitro* for RNA interference experiments. As shown in Figure 7A, the expression level of *ilvA* gene decreased by 46.3% and 54.3%, respectively, after 72 h and 96 h of RNAi treatment (Figure 7A). The results showed that the synthesized dsRNA fragments could effectively interfere with the expression of *ilvA* gene. Bioassays showed that compared with feeding dsGFP and sucrose control (CK), feeding dsilvA for 24 and 48 hs had no significant effect on aphid body weight and aphid production, but decreased significantly at 72 and 96 hs (Figures 7C, D). Additionally, the indices of mortality decreased slightly, but were not significantly different in all time points, compared to the control (Figure 7B). All these results indicate that interference with the *ilvA* gene has a negative effect on the growth and development of aphids.

4 Discussion

Aphids and their primary symbiont *Buchnera aphidicola* have formed a long-term and stable symbiotic relationship. At

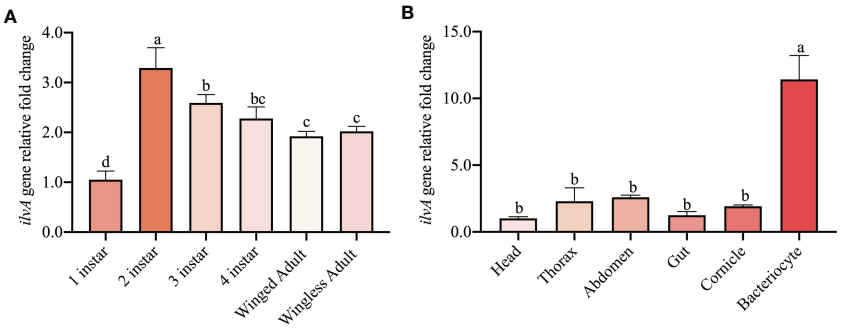

FIGURE 6
Expression of *ilvA* genes at different tissues and developmental stages in *S. miscanthi* **(A)** Expression level of *ilvA* gene in aphids at different developmental stages. **(B)** Expression level of *ilvA* gene in different tissues of aphid. Different letters above the bars indicate significant differences at $P < 0.05$.

the same time, they are considered to be typical cases in studying the coevolution relationship between insects and endosymbionts (Clark et al., 2000). Numerous studies have shown that *Buchnera* provides aphids with essential nutrients that are missing from the phloem sap of feeding host plants (Shigenobu et al., 2000). There is persuasive experimental evidence that the *Buchnera* genome provides aphids with almost all of the key genes in the essential amino acid synthesis pathway in the model insect pea aphid *A. pisum*, however, little is known about the consistency of this tight nutrient supply chain model in other aphids. Given that almost all aphids contain *Buchnera*, which plays a vital role in aphids, therefore, taking *Buchnera* as the starting point, developing a strategy to break the stable nutrient supply chain between them may become an effective new idea for green prevention and control of aphids. At present, RNA interference technology is widely used in insect gene function verification, is considered to be a new direction for the development of green biological pesticides (Bautista et al., 2009; Belles, 2010; Wuriyanghan et al., 2011; Liu et al., 2020). However, RNA interference technology cannot be effectively implemented in prokaryotes, resulting in direct silencing of aphid primary symbiont *Buchnera* gene is difficult to achieve. Therefore, it has become a new research direction to excavate and identify the relay genes between host aphid and *Buchnera* in the synthesis pathway of essential nutrients and using them as RNA interference target sites. It is gratifying that the availability

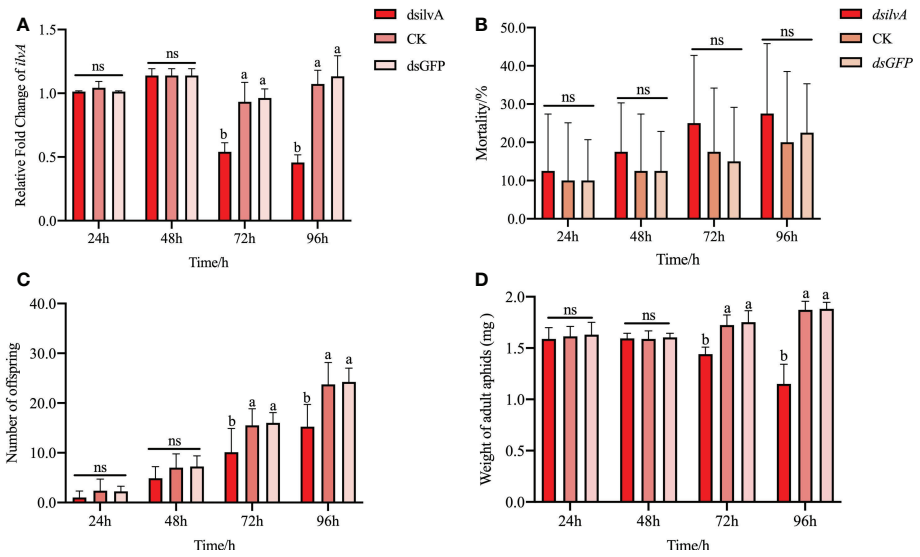

FIGURE 7
Effect of RNA interference with *ilvA* gene on life parameters of *S. miscanthi***(A)** Effect of feeding dsRNA at different times on the expression of *ilvA*. **(B)** Effect of interfering with *ilvA* at different times on the aphid mortality. **(C)** Effect of interfering with *ilvA* on offspring of *S. miscanthi*. **(D)** Effect of interfering with *ilvA* on aphid body weight of *S. miscanthi*. Different letters above the bars indicate significant differences at $P < 0.05$, while ns indicates no significant difference.

of the genomes of wheat aphid *S. miscanthi* and its primary symbiont *Buchnera* makes this work feasible.

It has been known for decades that *Buchnera* lacks some genes encoding essential amino acid biosynthesis enzymes and compensates *via* the host pea aphid *A. pisum* (Shigenobu et al., 2000; Wilson et al., 2010). Meanwhile, in our previous study, we found that a metabolic relay gene *ilvE*, a branched-chain amino acid transferase gene required for the final step in the synthesis of the three essential amino acids valine, leucine and isoleucine, was absent in the *Buchnera* genome but was present in the aphid genome (Li et al., 2022). The result was consistent with the previous studies on pea aphid genome (Wilson et al., 2010). In addition, RNAi of the *ilvE* gene significantly increased aphid mortality. Therefore, nutrient synthesis relay genes between aphids and *Buchnera* can be used as candidate targets for RNA interference. However, whether there are other metabolic relay genes in the aphid genome and have potential effect on the aphid development is still rarely reported.

In this study, combined with our previously reported genome data, we identified a threonine dehydratase gene called *ilvA* in the upstream process of isoleucine synthesis, which is absent in the *Buchnera* genome but exists in the aphid genome, and the function of the gene is to hydrolyze threonine to intermediate product 2-Oxobutanoate (Figure 1). Therefore, to further verify the function of the gene, we cloned the *ilvA* gene and obtained a complete CDS sequence. Bioinformatics analysis showed that the gene was highly conserved in sequence and location in different aphids (Figures 3, 4). Meanwhile, it is worth noting that this gene is located on the sex chromosome of aphids (Figure 2A). In recent years, with the continuous advancement of genome sequencing technology, more and more aphid genomes have been resolved (Chen et al., 2019; Roberto et al., 2020; Zhang S. et al., 2021). Related studies have reported that in different aphid genomes, sex chromosomes are highly conserved, and the selection pressure of genes on sex chromosomes of *A. pisum* is significantly higher than that of autosomes (Li et al., 2020). Moreover, the average expression level of genes on sex chromosomes of pea aphid was significantly lower than that on autosomes, which may be the reason for the significant increase of selection pressure (Jaquiery et al., 2018). In our study, we performed the transcriptome analysis of winged and wingless adult aphids and determined that the expression levels of genes on sex chromosomes were significantly lower than those on autosomes, the results are consistent with previous studies. Moreover, the selective pressure on sex chromosomes was also significantly higher than that on autosomes, whether it was paralogous gene pairs within chromosomes or orthologous gene pairs between different aphids (Figure 5). However, the expression level of *ilvA* and *ilvE* gene is much higher than the average value of other genes on sex chromosomes (Supplementary Table S1). Meanwhile, *ilvA* and *ilvE* are under low selection pressure in different aphids, which means that the function of this kind of gene in aphid is stable. In general, a lower level of gene expression may imply less important to phenotypes (Nabholz et al., 2013), and previous study implicate that the aphid sex chromosome as a less preferred location for highly expressed genes (Li et al., 2020). However, in this study, we found that although the expression level of genes on sex chromosomes is low overall, there are still some highly expressed genes, and the gene has a potential role in the synthesis of some important nutrients. This result also means that the aphid sex chromosome is still a mysterious region worthy of further study.

To investigate the expression level of the *ilvA* gene in aphids, we next determined the expression pattern of the *ilvA* in different developmental stages and tissues of *S. miscanthi* by qPCR. Our results showed that the expression of the *ilvA* gene was significantly higher in the 2rd instars of aphids than in the other instars and exhibited lowest expression level in 1st instars (Figure 3). Surprisingly, the *ilvA* gene was highly expressed in the bacteriocytes of aphids, where *Buchnera* shelters. Interestingly, the specific expression location of this gene is consistent with another synthetic relay gene *ilvE* (Li et al., 2022). Previous reports suggest that *Buchnera* plays an important role in maintaining amino acid synthesis and supply homeostasis in aphids (Wilson et al., 2010). Therefore, with the growth and development of aphids, the increasing titer of *Buchnera* may have a potential role in regulating the expression of *ilvA* and *ilvE*. Moreover, considering the specificity of the expression location of *ilvA* and *ilvE* genes, we hypothesized that the closer distance to *Buchnera* may be more convenient for the synthesis and transport of essential amino acids regulated by aphids between bacteriocytes and hemocoel.

To further study the function of *ilvA* in aphid, the RNAi experiment was performed. Unlike the *ilvE* gene, the indices of mortality decreased slightly, but were not significantly different, after feeding dsilvA 72 and 96 hs (Figure 7B). However, the weight and production of aphids decreased significantly (Figures 7C, D). Recent studies have shown that common ancestor of Hymenoptera lose all key genes in the valine, leucine and isoleucine synthesis pathway, but parasitoids are able to control related pathways in their host insect, providing them with missing essential nutrients (Ye et al., 2022). Compared with the commensalism relationship between parasitoids and host insects, aphids form a long-term stable mutualistic relationship with their primary symbiont *Buchnera*. The relay synthesis process in the nutrient synthesis pathway is important evidence of coevolution. Therefore, the destruction of synthetic relay chain may be the reason for the negative impact on the growth and development of *S. miscanthi* after knocking down the expression of *ilvA* and *ilvE*. However, there are also relevant study showed that the *Buchnera* protein HisC could functionally replace the missing *ilvE*, catalyzing the terminal reaction in these pathways (Shigenobu et al., 2000). It is worth noting that the *ilvA* gene is the upstream gene of the pathway, which is different from the downstream gene *ilvE* in the synthesis pathway. Therefore, whether reducing the expression of *ilvA*

will cause functional complementation or expression response of some genes in the downstream pathway is still needs further exploration. At the same time, reduced expression of the *ilvE* gene significantly inhibited Leu, Ile and Val production in aphids (Li et al., 2022). Although in this study, we did not quantify isoleucine production in aphids after *ilvA* interference, but as a result of our previous studies, we speculated that the decrease in aphid growth fitness may be potentially associated with amino acid production, meanwhile, the decrease in the production of single one essential amino acid may also have a much smaller negative effect on aphids than the three essential amino acids. Such speculation also provides an explanation for why silencing the *ilvA* gene does not result in a significant increase in mortality.

Moreover, secondary symbiont in insect also has potential functions in compensating for the lack of amino acids (Gómez-Valero et al., 2004; Ju et al., 2017). Whether secondary symbiont rescue the negative effects on aphid growth and development caused by RNA interference remains unknown. It is worth noting that *ilvE* and *ilvA* are highly conserved in different aphids, so whether the RNAi targeting them has broad consistency is worthy of further study, which will also provide a theoretical basis for screening broad-spectrum RNAi target sites.

Numerous reports have indicated that almost all insects contain various types of endosymbionts (Baumann, 2005). However, so far, a large number of insect endosymbionts have not been cultured *in vitro*, making the study of their function dependent on host insects (Moran and Mira, 2001). Moreover, RNAi technology is not available for prokaryotic endosymbiont-associated genes, making it difficult to realize the strategy of using symbionts to control insects, necessitating new ideas. In this study, based on our previous studies, we identified another highly conserved isoleucine synthesis pathway upstream gene *ilvA* that is absent in the *Buchenra* genome but is present in the aphid genome, which plays an essential role in influencing the body weight and reproduction of aphids. With the growing popularity of genome sequencing, an increasing number of data resources on the genomes of insects and their endosymbionts have been deciphered. Our study may provide a future direction for targeting important junctions in the endosymbiont-insect metabolic relay process to control agricultural pests.

Data availability statement

The data presented in the study are deposited in the NCBI repository, accession number PRJNA908645.

Author contributions

QL, JF and JC conceived and designed the experiments. QL and YC performed the experiments. QL analyzed the data. QL and YC wrote the paper. All of the authors read and approved the final version of the manuscript. All authors contributed to the article and approved the submitted version.

Funding

The authors are thankful for the financial support provided by the National Natural Science Foundation of China (32001900), the China Postdoctoral Science Foundation (2020M680786), the National Key R & D Plan of China (2017YFD0201700), the Earmarked fund for China Agriculture Research System (CARS-22) and China's Donation to the CABI Development Fund (IVM10051).

Acknowledgments

We would like to thank Ms. Yanxia Liu for aphid rearing.

Conflict of interest

The authors declare that the research was conducted in the absence of any commercial or financial relationships that could be construed as a potential conflict of interest.

Publisher's note

Supplementary material

The Supplementary Material for this article can be found online at: https://www.frontiersin.org/articles/10.3389/fpls.2022.1092638/full#supplementary-material

References

Baumann, P. (2005). Biology bacteriocyte-associated endosymbionts of plant sap-sucking insects. *Annu. Rev. Microbiol.* 59, 155–189. doi: 10.1146/annurev.micro.59.030804.121041

Bautista, M. A. M., Miyata, T., Miura, K., and Tanaka, T. (2009). RNA Interference-mediated knockdown of a cytochrome P450, CYP6BG1, from the diamondback moth, *Plutella xylostella*, reduces larval resistance to permethrin. *Insect Biochem. Mol. Biol.* 39, 38–46. doi: 10.1016/j.ibmb.2008.09.005

Belles, X. (2010). Beyond drosophila: RNAi *in vivo* and functional genomics in insects. *Annu. Rev. Entomol.* 55, 111–128. doi: 10.1146/annurev-ento-112408

Chen, C. J., Chen, H., Zhang, Y., Thomas, H. R., and Xia, R. (2020). Tbtools: an integrative toolkit developed for interactive analyses of big biological data. *Mol. Plant* 13, 1194–1202. doi: 10.1016/j.molp.2020.06.009

Chen, W., Shakir, S., Bigham, M., Richter, A., Fei, Z. J., and Jander, G. (2019). Genome sequence of the corn leaf aphid (*Rhopalosiphum maidis* Fitch). *Gigascience.* 8, 1–12. doi: 10.1093/gigascience/giz033

Clark, M. A., Moran, N. A, Baumann, P., and Wernegreen, J. J. (2000). Cospeciation between bacterial endosymbionts (*Buchnera*) and a recent radiation of aphids (Uroleucon) and pitfalls of testing for phylogenetic congruence. *Evolution.* 54, 517–525. doi: 10.1111/j.0014-3820.2000.tb00054.x

De Clerck, C., Fujiwara, A., Joncour, P., Leonard, S., Felix, M. L., Francis, F., et al. (2015). A metagenomic approach from aphid's hemolymph sheds light on the potential roles of co-existing endosymbionts. *Microbiome.* 3, 63. doi: 10.1186/s40168-015-0130-5

Gómez-Valero, L., Soriano-Navarro, M., Perez-Brocal, V., Heddi, A., Moya, A., Garcia-Verdugo, J. M., et al. (2004). Coexistence of wolbachia with *Buchnera aphidicola* and a secondary symbiont in the aphid *Cinara cedri*. *J. Bacteriol.* 186, 6626–6633. doi: 10.1128/JB.186.19.6626-6633.2004

Guo, S. K., Gong, Y. J., Chen, J. C., Shi, P., Cao, L. J., Yang, Q., et al. (2020). Increased density of endosymbiotic *Buchnera* related to pesticide resistance in yellow morph of melon aphid. *J. Pest Sci.* 93, 1281–1294. doi: 10.1007/s10340-020-01248-0

Jaquiery, J., Peccoud, J., Ouisse, T., Legeai, F., Prunier-Leterme, N., Gouin, A., et al. (2018). Disentangling the causes for faster-X evolution in aphids. *Genome. Biol. Evol.* 10, 507–520. doi: 10.1093/gbe/evy015

Jiang, X., Zhang, Q., Qin, Y. G., Yin, H., Zhang, S. Y., Li, Q., et al. (2019). A chromosome-level draft genome of the grain aphid *Sitobion miscanthi*. *GigaScience.* 8, 1–8. doi: 10.1093/gigascience/giz101

Ju, J. F., Hoffmann, A. A., Zhang, Y. K., Duan, X. Z., Guo, Y., Gong, J. T., et al. (2017). *Wolbachia*-induced loss of male fertility is likely related to branch chain amino acid biosynthesis and *ilvE* in *Laodelphax striatellus*. *Insect. Biochem. Mol. Biol.* 85, 11–20. doi: 10.1016/j.ibmb.2017.04.002

Li, Q., Fan, J., Cheng, Y., Hou, M. L., and Chen, J. L. (2022). *ilvE* as a potential RNAi target to inhibit amino acid synthesis to control the wheat aphid *Sitobion miscanthi*. *Entomol. Gen*. doi: 10.1127/entomologia/2022/1528

Li, Q., Fan, J., Sun, J. X., Wang, M. Q., and Chen, J. L. (2018). Effect of the secondary symbiont *Hamiltonella defensa* on fitness and relative abundance of *Buchnera aphidicola* of wheat aphid, *Sitobion miscanthi*. *Front. Microbiol.* 9, 582. doi: 10.3389/fmicb.2018.00582

Li, Q., Sun, J. X., Qin, Y. G., Fan, J., Zhang, Y., Tan, X. L., et al. (2021). Reduced insecticide sensitivity of the wheat aphid *Sitobion miscanthi* after infection by the secondary bacterial symbiont *Hamiltonella defensa*. *Pest Manag Sci.* 77, 1936–1944. doi: 10.1002/ps.6221

Li, Y. Y., Zhang, B., and Moran, N. A. (2020). The aphid X chromosome is a dangerous place for functionally important genes: diverse evolution of hemipteran genomes based on chromosome-level assemblies. *Mol. Biol. Evol.* 8, 2357–2368. doi: 10.1093/molbev/msaa095

Liu, S. S., Jaouannet, M., Dempsey, D. M. A., Christine, J. I., Coustau, C., and Kogel, K. H. (2020). RNA-Based technologies for insect control in plant production. *Biotechnol. Adv.* 39, 107463. doi: 10.1016/j.biotechadv.2019.107463

Manzano-Marín, A., Simon, J. C., and Latorre, A. (2016). Reinventing the wheel and making it round again: evolutionary convergence in *Buchnera-Serratia* symbiotic consortia between the distantly related lachninae aphids *Tuberolachnus salignus* and *Cinara cedri*. *Genome Biol. Evol.* 8, 1440–1458. doi: 10.1093/gbe/evw085

Moran, N. A., and Mira, A. (2001). The process of genome shrinkage in the obligate symbiont, *Buchnera* aphidicola. *Genome. Biol.* 2, research0054.1-research 0054.12. doi: 10.1186/gb-2001-2-12-research0054

Nabholz, B., Ellegren, H., and Wolf, J. (2013). High levels of gene expression explain the strong evolutionary constraint of mitochondrial protein-coding genes. *Mol. Biol. Evol.* 30, 272–284. doi: 10.1093/molbev/mss238

Perreau, J., Zhang, B., Maeda, G. P., Kirkpatrick, M., and Moran, N. A. (2021). Strong within-host selection in a maternally inherited obligate symbiont: *Buchnera* and aphids. *Proc. Nati. Acad. Sci. U. S. A.* 118, 1–8. doi: 10.1073/pnas.2102467118

Roberto, B., Archana, S., Cindayniah, J. G., Felicidad, F. F., Sam, T. M., Glen, P., et al. (2020). A chromosome-level genome assembly of the woolly apple aphid, *Eriosoma lanigerum* hausmann (Hemiptera: Aphididae). *Mol. Ecol. Resour.* 21, 316–326. doi: 10.1111/1755-0998.13258

Kim,D., Langmead,B., and Salzberg, S. L. (2015). HISAT: a fast spliced aligner with low memory requirements. *Nat. Methods* 12, 357–360. doi: 10.1038/nmeth.3317

Shigenobu, S., Watanabe, H., Hattori, M., Sakaki, Y., and Ishikawa, H. (2000). Genome sequence of the endocellular bacterial symbiont of aphids *Buchnera* sp aps. *Nature.* 407, 81–86. doi: 10.1038/35024074

Wang, Y. P., Tang, H. B., DeBarry, J. D., Tan, X., Li, J. P., Wang, X. Y., et al. (2012). MCScanX: a toolkit for detection and evolutionary analysis of gene synteny and collinearity. *Nucleic. Acids Res.* 40, e49. doi: 10.1093/nar/gkr1293

Wilson, A. C.C., Ashton, P. D., Calevro, F., Charles, F., Colella, S., Febvay, G., et al. (2010). Genomic insight into the amino acid relations of the pea aphid, *Acyrthosiphon pisum*, with its symbiotic bacterium *Buchnera aphidicola*. *Nucleic. Acids Res.* 19, 249-258. doi: 10.1111/j.1365-2583.2009.00942.x

Wuriyanghan, H., Rosa, C., and Falk, B. W. (2011). Oral delivery of double-stranded RNAs and siRNAs induces RNAi effects in the potato/tomato psyllid, *Bactericerca cockerelli*. *PloS One* 6, e27736. doi: 10.1371/journal.pone.0027736

Ye, X., Xiong, S. J., Teng, Z. W., Yang, Y., Wang, J. L., Yu, K. L., et al. (2022). Genome of the parasitoid wasp *Cotesia chilonis* sheds light on amino acid resource exploitation. *BMC Biology.* 20, 118. doi: 10.1186/s12915-022-01313-3

Zhang, S., Gao, X. K., Wang, L., Jiang, W. L., Su, H. H., Jing, T. X., et al. (2021). Chromosome-level genome assemblies of two cotton-melon aphid *Aphis gossypii* biotypes unveil mechanisms of host adaption. *Mol. Ecol. Resour.* 00, 1–15. doi: 10.1111/1755-0998.13521

Zhang, B., Leonard, S. P., Li, Y. Y., and Moran, N. A. (2019). Obligate bacterial endosymbionts limit thermal tolerance of insect host species. *Proc. Nati. Acad. Sci. U. S. A.* 116, 24712–24718. doi: 10.1073/pnas.1915307116

Zhang, S. Y., Zhang, Q., Jiang, X., Li, Q., Qin, Y. G., Wang, W. K., et al. (2021). Novel temporal expression patterns of EBF-binding proteins in wing morphs of the grain aphid sitobion miscanthi. *Front. Physiol.* 12. doi: 10.3389/fphys.2021.732578

frontiers | Frontiers in Physiology

TYPE Original Research
PUBLISHED 06 February 2023
DOI 10.3389/fphys.2023.1097317

OPEN ACCESS

EDITED BY
Julian Chen,
Institute of Plant Protection (CAAS), China

REVIEWED BY
Qiu-Ning Liu,
Yancheng Teachers University, China
Tong-Xian Liu,
Guizhou University, China

*CORRESPONDENCE
Zixiang Yang,
zxyang@caf.ac.cn

SPECIALTY SECTION
This article was submitted to Invertebrate Physiology,
a section of the journal
Frontiers in Physiology

RECEIVED 15 November 2022
ACCEPTED 19 January 2023
PUBLISHED 06 February 2023

CITATION
Wei H, Xu X, Feng G, Shao S, Chen X and Yang Z (2023), Candidate genes potentially involved in molting and body size reduction in the male of the horned gall aphid, *Schlechtendalia chinensis*. *Front. Physiol.* 14:1097317.
doi: 10.3389/fphys.2023.1097317

Candidate genes potentially involved in molting and body size reduction in the male of the horned gall aphid, *Schlechtendalia chinensis*

Hongyuan Wei, Xin Xu, Guorui Feng, Shuxia Shao, Xiaoming Chen and Zixiang Yang*

Key Laboratory of Cultivation and Utilization of Resource Insects, Institute of Highland Forest Science, Chinese Academy of Forestry, National Forestry and Grassland Administration, Kunming, China

In general, insects grow (increase in body size) through molting. To the opposite, the body size of the males of the horned gall aphid, *Schlechtendalia chinensis*, gets smaller after molting and as they age. To understand the molecular bases of this rare phenomenon, transcriptomes were generated from 1–5 days old male and the data were analyzed *via* a weighted gene co-expression network analysis (WGCNA). A total of 15 partitioned modules with different topological overlaps were obtained, and four modules were identified as highly significant for male body length ($p < 0.05$). Kyoto Encyclopedia of Genes and Genomes (KEGG) enrichment analysis suggested that a portion of genes in the four modules are likely involved in autophagy and apoptosis. In addition, a total of 40 hub genes were obtained in the four modules, and among them eight genes were highly expressed in males compared to individuals of other generations of *S. chinensis*. These eight genes were associated with autophagy and apoptosis. Our results reveal the unique negative growth phenomenon in male *S. chinensis* after molting, and also suggest that the male *S. chinensis* with no ability to feed probably decompose their own substances *via* autophagy and apoptosis to provide energy for life activities such as germ cell development.

KEYWORDS

***Schlechtendalia chinensis*, horned gall aphid, molt, negative growth, weighted gene co-expression network analysis (WGCNA), hub gene**

Introduction

All insects molt (cast off their exoskeleton) in order to grow and develop. The molting processing costs energy and nutrients. Most insects increase their body size and experience morphological development after molting. However, there are examples on the contrary. Oviparous female aphids belong to Eriosomatinae showed decreasing body size through molts while having no functional mouthparts (Lambers, 1966). This unique phenomenon in some insects were briefly reported, but the molecular basis and the biology advantage of such a phenomenon are unclear.

Aphids are important model organisms in evolutionary biology and ecology because they exhibit unique features such as complex life cycles, sexual and asexual reproduction strategies and alternation of host plants required for normal development (Stern, 2008; Eterovic and Vilcinskas, 2016). The horned gall aphid, *Schlechtendalia chinensis* (Hemiptera: Aphididae: Eriosomatinae), is an economically important insect as it induces horned gall formations, which

are valuable for the Chinese medicine and chemical industry (Zhang et al., 1999; Blackman and Eastop, 2020; Chen et al., 2020). The life cycle of *S. chinensis* comprises a single sexual generation and five asexual generations as well as a host switch from the Chinese sumac in the summer and autumn to moss plants in the winter. Both males and females are live outside the galls (Zhang et al., 1999; Yang et al., 2010). It was reported that the newborn nymphs of males and females reach the sex mature by molting 4 days after birth. As instars progress through development, their body size decreases, resulting in negative growth (Zhang and Tang, 1987). All instars of both sexes lack functional mouthparts, meaning they cannot access to nutrition through feeding. This raises an interesting question as to why and how can they maintain normal life activities such as molting, roaming, mating and reproducing without food intake? And related to this, what are the energy and material resources used instead? Tackling these questions with transcriptomics is now possible since the genome of *S. chinensis* has been sequenced recently (Wei et al., 2022). The weighted gene co-expression network analysis (WGCNA) is a powerful method to identify co-expressed groups of genes from large heterogeneous messenger RNA expression data sets (Clarke et al., 2013). It has been successfully used for insect transcriptome analysis, to effectively mine genes of interest, and to predict gene functions (Ding et al., 2022).

In this study, we investigated the transcriptional changes over time during the sexual stages of *S. chinensis*. We generated transcriptomes of males aged from 1 to 5-day-old and clustered genes with similar expression patterns. Using WGCNA, we performed a correlation analysis between phenotypic traits and hub genes. The current study not only identified a likely mechanism by which aphids fuel their developmental processes without feeding, but also provides a foundation for further studies on the physiology and molecular biology of aphid development.

Material and methods

Insect sample collection

Spring migrants (sexuparae) of *S. chinensis* from mosses were collected in the field in Yanjin County (28°06′N, 104°22′E, 980 m elev.), Yunnan Province, China. The offspring (males and females) of the collected sexuparae were cultivated to obtain aphid samples of different ages, from 1 to 5-day-old for the study, 150 individuals in total which were immediately frozen in liquid nitrogen and stored at −80°C for further RNA analysis.

Morphological observations and measurements

Fresh aphids were cleaned gently by a tiny brush under a stereo microscope (SZ61, Olympus, Japan), then were dehydrated with a graded ethanol series (70%, 80%, 90%, 95%, and 100%) and coated with gold in a JS-1600 ion sputter coater (Saintins, Nanjing, China), and observed and photographed under a TM3000 scanning electron microscope (Hitachi, Japan). Measurements were taken using a VHX-1000 digital microscope (Keyence, Japan). Three biological replicates (ten aphid individuals per replicate) were measured for each sample. All measurements are in micrometers (μm). Data were analyzed using SPSS 20.0. The differences among samples were examined using post-hoctest on linear mixed-effects model.

High throughput transcriptome sequencing

Transcriptomes were generated from RNA samples extracted from male samples with three biological replicates (10 aphid individuals per replication). RNA amount, purity and integrity were determined on a NanoPhotometer N60 (Implen GmbH, Munich, Germany) and an Agilent 2,100 Bioanalyzer (Agilent Tech. CA, United States). cDNA libraries were initially quantified by a Qubit™ 2.0 Fluorometer (Thermo Fisher Scientific Inc. MA, United States) and diluted to 1.5 ng/μL. Later, different libraries were pooled according to the requirements of effective concentration and target data volume. RNA was sequenced using Illumina's high throughput sequencing platform NovaSeq 6,000 (Illumina, Inc. CA, United States). In order to obtain putative transcripts, clean reads were mapped to *S. chinensis* genome assembly using Hisat2 (version 2.1.0.5) (Kim et al., 2015; Wei et al., 2022). The low-quality alignments were filtered with Sequence Alignment/Map tools (SAMtools) (Li et al., 2009). Transcripts per million (TPM) expression values were calculated using featureCounts (Yang et al., 2014) and StringTie (Pertea et al., 2015) for transcripts. Transcriptomes of other generations of *S. chinensis*, autumn migrant, fundatrix, fundatrigenia, overwinter nymph, female and spring migrant (sexuparae) came from the previous research (Wei et al., 2022).

WGCNA data input and preprocessing

Three data sets, including the fragments per kilobase of exon per million mapped fragments (FPKM) value of all aphid samples, the mean body length values of each biological replicate of samples, and the gene annotation were used for WGCNA analysis (Supplementary Materials S1–S3). After FPKM values were calculated, genes which expression levels equaled to 0 were removed. The median absolute deviation (MAD) for each gene was calculated and sorted by the values. Unqualified genes were removed, and the resulting data was used for cluster analysis. The top 75% of these genes (based on a MAD value > 0.01) were used to perform a cluster analysis based on Euclidean distance of samples to construct a hierarchical clustering dendrogram. Outliers of the cluster tree were removed by manual check. We then proceeded by excluding these three samples from the data, and the data from the remaining 12 samples to construct a hierarchical clustering dendrogram based on Euclidean distance too.

Gene network construction and module identification

All analyses were conducted using the R software package WGCNA 1.71 (Langfelder and Horvath, 2008). RStudio 4.2.1 was selected for code writing and execution. All language source codes of the calculation process are shown in Supplementary Material S4. The network topology for various soft-thresholding powers were detected using a "*pickSoftThreshold()*" function and an appropriate soft-thresholding power β was selected through the scale-free fit index in the WGCNA software package. The automatic block-wise network construction and module detection were performed using a "*blockwiseModules()*" function with β as a parameter.

10.3389/fphys.2023.1097317

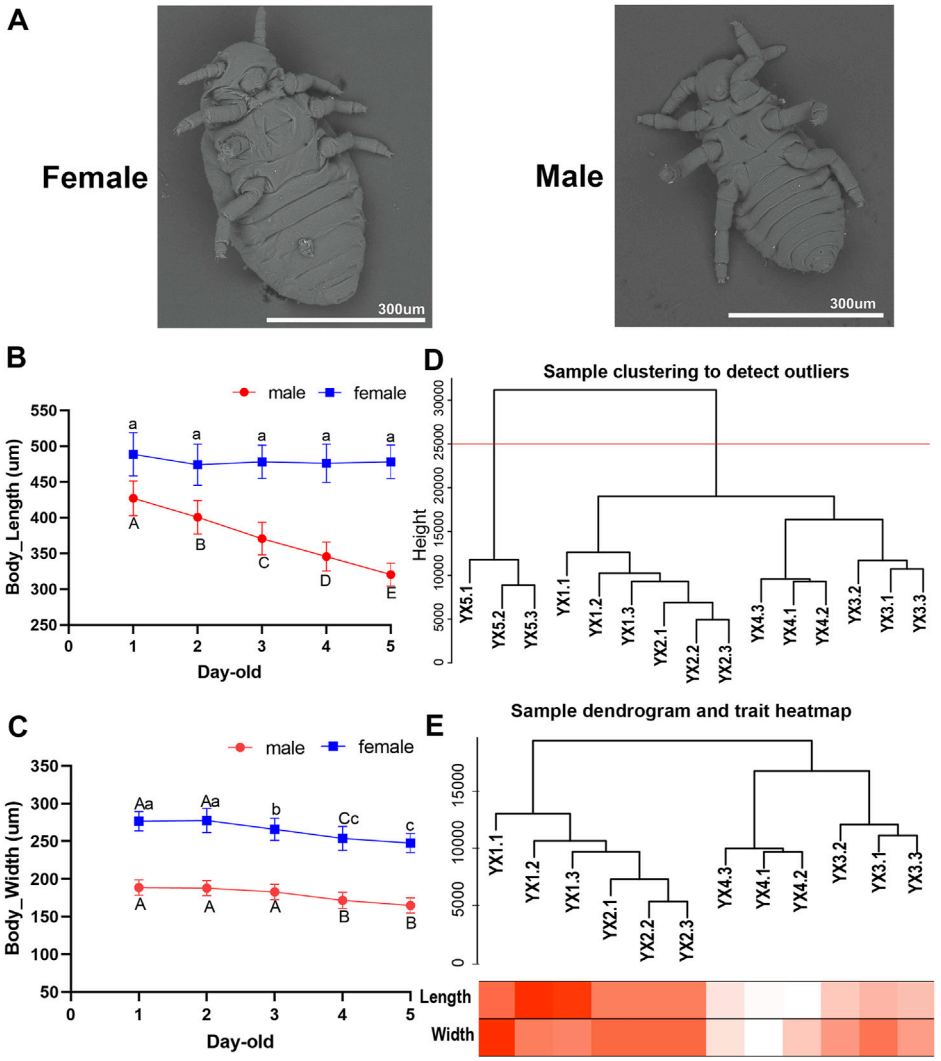

FIGURE 1
Characteristics and transcriptome analysis of male aphid, *Schlechtendalia chinensis* at different age. **(A)** Scanning electron microscope (SEM) image of females and males. **(B)** and **(C)** The body length and body width of 1–5 days old males and females (Different lower case letters and upper case letters indicate significant differences at 0.05 and 0.01 levels, respectively). **(D)** Dendrogram of samples based on their Euclidean distance. YX1, YX2, YX3, YX4, YX5 in the figure represent 1–5 days old males, respectively. The last digit of 1, 2, and 3 represents the three biological repetitions of the sample. The red horizontal division line represents the abscissa at 25,000 in the figure. **(E)** Sample dendrogram and trait heatmap of males. The darker the color, the stronger the correlation.

The network construction procedure included the following main steps: 1) Select the appropriate soft threshold (weighting coefficient) and define the similarity matrix; 2) the similarity matrix was converted into an adjacency matrix using a power adjacency function; 3) the adjacency matrix was transform into a topological overlap matrix (TOM); 4) the hierarchical clustering tree was obtained by performing hierarchical clustering for TOM-based dissimilarity (dissTOM); 5) modules were identified as branches of the hierarchical cluster tree using the dynamic tree cut method while the module eigengene (ME) which represents the overall expression level of each module was calculated; 6) the Pearson correlation coefficients between MEs of all modules were calculated, and the 1-Pearson correlation coefficient was defined as the average distance between MEs of all modules; and 7) the modules with high similarity were merged to obtain the co-expression network.

Identification of body length significant modules

The correlation between modules and morphologic trait data (body length) were calculated using the "*cor()*" function in R. The Student asymptotic *p*-value of the correlation was calculated and the module-trait association heatmap was generated by the "*corPvalueStudent()*" function. Finally, modules with high weight correlations ($p < 0.05$) were selected to draw a scatter plot of gene significance and module membership.

Network visualization and hub gene selection

Modules with $p < 0.05$ from the topological overlap results were screened. The edge and node data files were analyzed using Cytoscape

3.9.1 (Shannon et al., 2003) software by "*exportNetworkToCytoscape()*" function. First, we calculated the degree of each node, then sorted node values from large to small. In this manner, we produced a list of the top-scoping 100 genes. Then, using the Cytoscape software, the 100 nodes and their corresponding edges were used to create a network diagram. CytoNCA, the Cytoscape plug-in unit 2.1.6 (Tang et al., 2015), was used to analyze the new network diagram. We then checked the "with weight" option when calculating and setting the weight parameter in the 'Edges attributes' panel. From the analysis results of CytoNCA, the top 10% of genes, ranking from large to small, were selected as hub genes. GO and KEGG enrichment were analyzed, and ridgeline plots were made using Omicshare CloudTools with default parameters (http://www.omicshare.com/).

Results

Morphological characteristics: Observations and measurements

Utilizing SEM on both male and female *S. chinensis* specimens, we found that both lack functional mouthparts before and after molting. The body size of males is smaller than that of females (Figure 1A). With the increase of age, the body size of males and females gradually decreased, and showed negative growth through a number of molts (Supplementary Material S6). The average body lengths of 1–5 day-old males were 427.02, 400.65, 370.70, 345.59, and 320.25 μm, respectively, which represented a significant decrease as development progressed ($p < 0.05$) (Figure 1B). The average body widths observed in 1–5 days old specimens were 188.71, 187.85, 182.86, 171.55, and 164.86 μm, respectively which showed a significant reduction from day 3 to day 4 ($p < 0.05$) (Figure 1C). The average body widths of females showed a significant reduction in 3-, 4- and 5-day-old, while no significant difference in body lengths ($p > 0.05$) (Figures 1B, C).

Transcriptome sequencing result and data preprocessing

We obtained 357,765,304 bp raw data and 47,497,144 bp cleaned-up data. The alignment rate between reference genome and transcriptome assembly varied in the range of 77.20%–86.42% (Supplementary Material S7).

A total of 14,089 genes in the *S. chinensis* genome were annotated in the male transcriptome. Of these, 716 genes registered an expression level of 0 in all 15 male aphid samples (5 age groups of three replicates each). The data derived from the three replicates of 5-day-old samples, YX5.1, YX5.2 and YX5.3, were abnormal and could not be clustered with other samples. The cluster tree of the remaining 12 samples and the corresponding traits were showed in Figures 1D, E.

Network topology analysis

An appropriate soft threshold power β value is essential for constructing a weighted gene network and to calculate adjacency by the co-expression similarity. Co-expression gene networks have the characteristics of scale-free networks. A scale free topology analysis of multiple β was performed using the "*pickSoftThreshold()*" function. The results showed that the lowest flattening of scale-free topological fitting exponential curve when it reaches a β high value of 7 (the scale free topological model is supposed to be 0.85) (Figure 2A). Therefore, we selected 7 as the β for subsequent network construction.

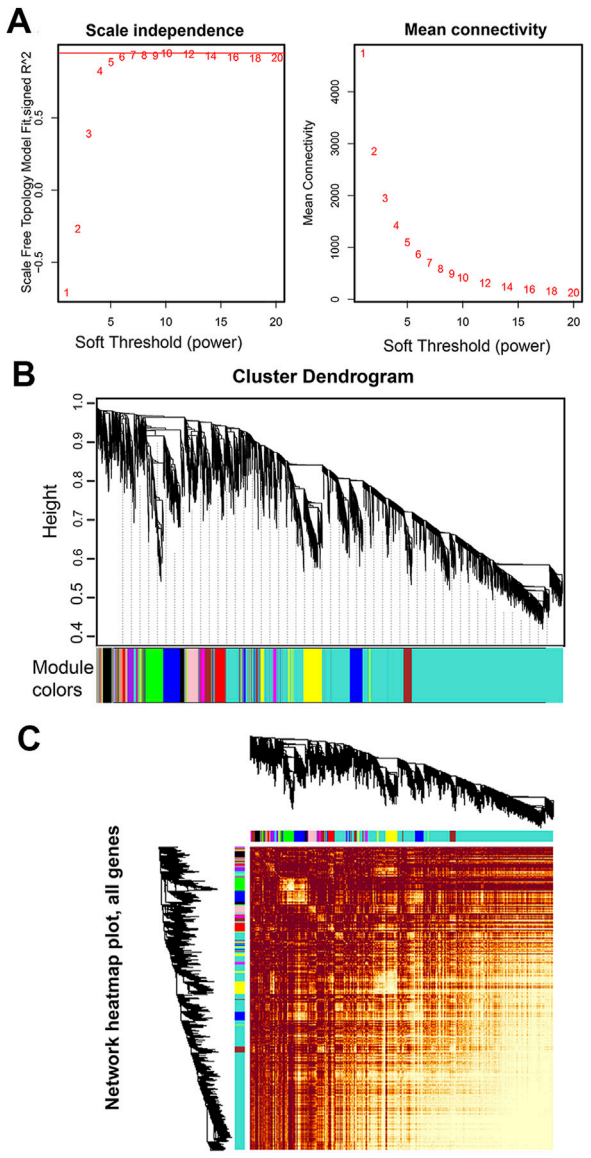

FIGURE 2
Network analysis of RNA-seq expression data in male *S. chinensis*. **(A)** Analysis of network topology for various soft-thresholding powers. Left panel: The scale free fit index (*y*-axis) as a function of the soft-thresholding power (*x*-axis); right panel: The mean connectivity (degree, *y*-axis) as a function of the soft-thresholding power (*x*-axis). The number crossed by the red horizontal line ('7' in the figure) is the lowest power that the scale-free topology fitting index curve flattens when it reaches a high value. **(B)** Dendrogram based on hierarchical clustering of genes, with dissimilarity based on the topological overlap, together with assigned module colors. **(C)** Network heatmap pot of all genes. The lighter the color, the stronger the correlation between genes.

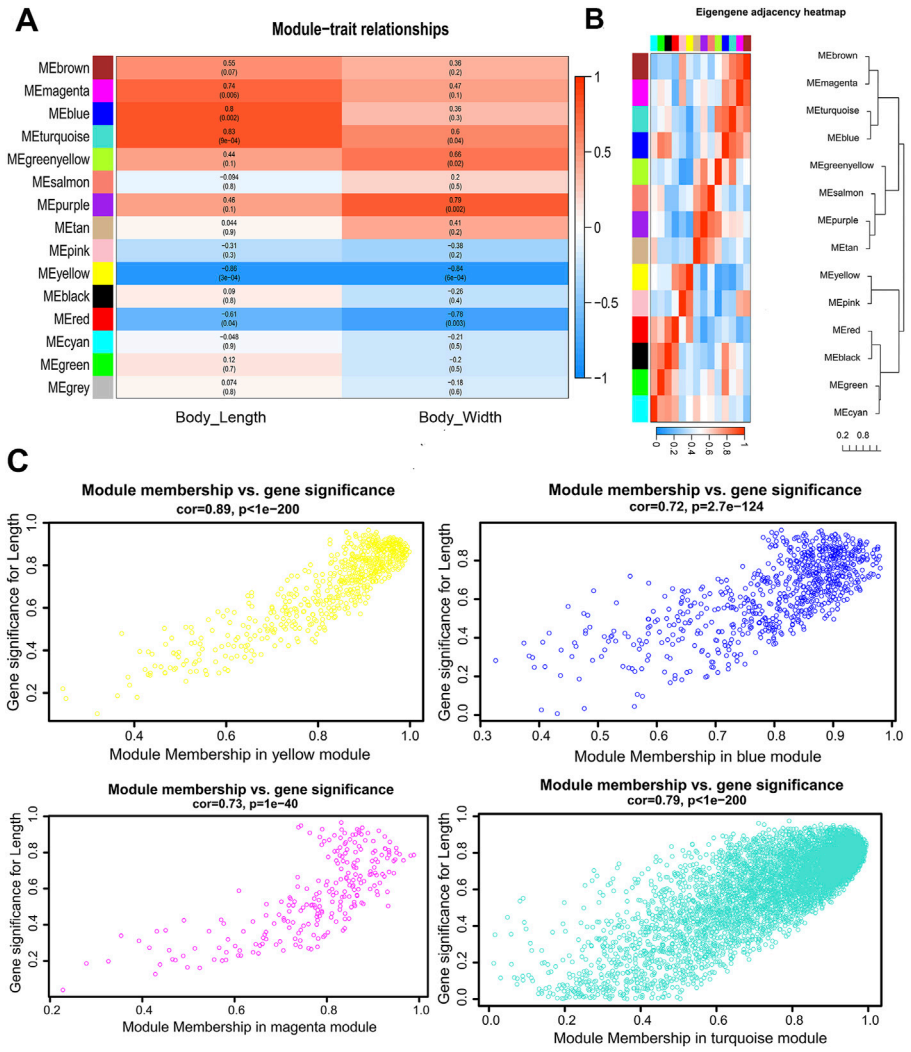

FIGURE 3
Visualization of the relationship between modules and body size traits of male *S. chinensis* **(A)** The relationship of module and trait. Each row corresponds to a module eigengene, each column corresponds to a trait, and each cell contains the corresponding correlation and *p*-value. **(B)** Hierarchical clustering dendrogram and the heatmap of the eigengenes. **(C)** Scatter plots of gene significance (GS) for male body length vs. module membership (MM) in the yellow, blue, magenta and turquoise modules.

Network construction and module detection

A co-expression network was constructed based on the optimal soft threshold of β = 7 to obtain a dissTOM of all genes (Figure 2C). The dissTOM algorithm generated a hierarchical clustering tree in which genes and gene modules were in the upper and lower parts, respectively (Figure 2B). The minimum gene number of each module was defined as 30, and 15 modules were divided according to the difference in the topological overlay, which were distinguished by different colors.

Gene co-expression modules correlated with body size traits

Gene significance (GS) is defined as the correlation (absolute value) between genes and traits to quantify the contribution of a single gene to a trait (male body length). For each module, a quantitative measure of module membership (MM) is defined as the correlation of the module eigengene with gene expression characteristics. This allows us to quantify the degree of similarity for all genes of every module on the array. Gene modules that show high significance to male body length and module members with high correlation modules of interest were identified through calculating the GS and MM. The results were used to draw a color-coded table (Figure 3A) and a summary of network (Supplementary Material S5). Four modules with magenta, blue, turquoise and yellow coding have the highest association ($p < 0.05$) with male body length (Figure 3A). The hierarchical clustering tree of modules and the adjacency heatmap of each module revealed that the turquoise and blue modules have the highest correction (Figure 3B). The scatter plot of GS and MM showed a highly significant correlation between GS and MM in the four selected modules (Figure 3C).

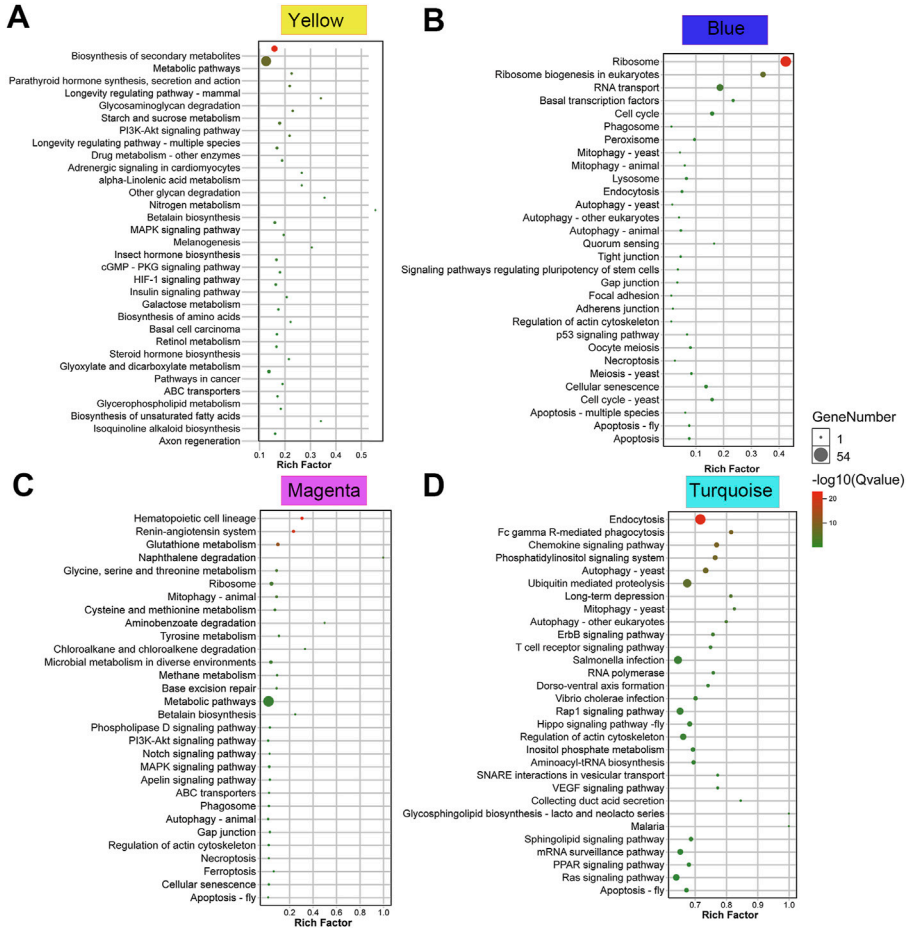

FIGURE 4
(A–D) KEGG enrichment analysis of magenta, blue, turquoise and yellow module of male *S. chinensis*.

Module analysis using KEGG enrichment

To explore the biological functions of the modules related to male body length, the four selected modules, in magenta, blue, turquoise and yellow were analyzed using KEGG enrichment pathway. In the top 30 pathways, mitophagy, autophagy and apoptosis appeared in enrichment pathway of magenta, blue, and turquoise modules (Figures 4B–D). At the same time, a large number of pathways known to regulate body size were also found in the module enrichment data. For example, P13K-Akt, Notch and MAPK were presented in the magenta module (Figure 4C). P53 linked to the blue module. Hippo, PPAR and Ras were associated with the turquoise module (Figure 4D). P13K-Akt, Insulin and MAPK were a part of the yellow module (Figure 4A).

Hub gene analysis

Through the "*exportNetworkToCytoscape()*" function of WGCNA software, the topology network calculated earlier was exported as a network file that can be recognized by the Cytoscape software. In this study, the hub genes were screened based on the degree of each gene (called nodes in the network). The degree is a connection between one node and another. The larger the degree value of a node, the more connections the node has, which means that the gene connected with the most genes and was defined as a hub gene. The top 10 genes in the magenta, blue, turquoise and yellow modules were obtained using the CytoNAC weighted calculation, with a total of 40 genes (Figure 5A). Nr annotation was performed for 40 hub genes, and 11 of them that were predicted to act in autophagy and apoptosis were selected, including Sc.chr02.0667, Sc.chr04.0038, Sc.chr06.0408, Sc.chr09.400, Sc.chr06.0991, Sc.chr09.457, Sc.chr06.0284, Sc.chr08.364, Sc.chr07.236, Sc.chr03.0629, and Sc.chr03.173. From the ridgeline plots that show the expression levels of these 11 genes for each generation of *S. chinensis*, including autumn migrant, fundatrix, fundatrigenia, overwinter nymph, female, spring migrant (sexuparae) and male. We found eight of these genes had significant higher expression levels in males than those *S. chinensis* of other generations. These eight genes encode the heat shock protein 70 B2, poly(rC)-binding protein 3-like isoform X1, ubiquitin conjugation factor E4 A, E3 SUMO-protein ligase RanBP2-like, MOB kinase activator-like 3, phosphatidylinositol 4,5-bisphosphate 3-kinase catalytic subunit delta isoform, ribosomal L1 domain-containing protein CG13096-like and myosin-IB-like. Genes of Sc.chr09.457, Sc.chr06.0284, Sc.chr08.364, and Sc.chr07.236 in females also had higher expression levels than in other generations (Figure 5B).

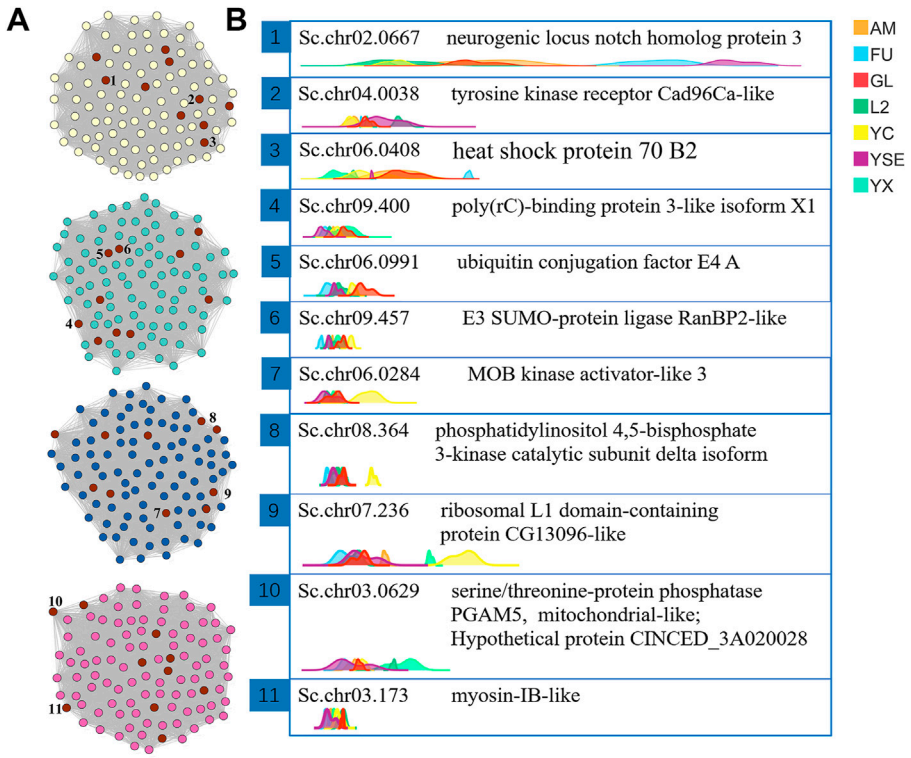

FIGURE 5
The visual network structure diagram and ridgeline plots of the screened hub genes related to body length of male *S. chinensis* **(A)** Visualization of network connections between the top 100 genes with the most connections in the yellow, turquoise, blue and magenta modules that were generated by the Cytoscape software. The nodes marked in red are the 10 most highly ranked nodes (genes) with the largest degree calculated by the CytoNAC plugin. The 1 to 10 numbers marked by the nodes are the selected hub genes. **(B)** Ridgeline plots of the expression levels of the selected hub genes in each sample showing gene ids and the protein functions annotated by NR. Abbreviations in the top right-hand corner represent different generations of *S. chinensis*. Abbreviations: AM, autumn migrant; FU, fundatrix; GL, fundatrigenia; L2, overwinter nymph; YC, female; YSE, spring migrant (sexuparae); YX, male.

Discussion

The main purposes of WGCNA analysis of RNA sequence data are to identify gene modules and explore relationships between different modules and hub genes related to a specific trait (here: Male body length). In our study, four gene modules which appeared to be correlated with the body size changes in male of *S. chinensis* were identified using WGCNA analysis. Interestingly, most pathways identified in the four modules by KEGG analysis are associated with autophagy and apoptosis, suggesting that these pathways may be critical during this sexual phase of *S. chinensis* development. For example, IIS and TOR signals regulate autophagy in fat body of *Drosophila melanogaster* (Ryan et al., 2004). The PI3K signaling pathway is necessary for autophagy to promote survival during starvation in *Cryptococcus neoformans* (Hu et al., 2008). The mTOR kinase is a key element for autophagy induction. Pathways that activate mTOR, such as Akt, and MAPK signal pathways, inhibit autophagy. Pathways that inhibit mTOR, such as AMPK, and p53 signal pathways, promote autophagy (Neufeld, 2010; Alers et al., 2012; Russell et al., 2014). Thus, we conclude that the body size of male *S. chinensis* decreases after molting without feeding is probably related to autophagy and apoptosis.

Four topological centricities including degree centrality (DC), closeness centrality (CC), between centrality (BC) and eigenvector centrality (EC) are used to measure the closeness degree of nodes to the center of the network. In our study, the weighted DC index was used to sort the nodes in the network and screen for hub genes (Ding et al., 2022). Eleven of the identified hub genes were linked to autophagy and apoptosis. For example, the Sc.chr04.0038 gene encodes the tyrosine kinase receptor Cad96Ca, which probably functions in autophagy (Lampada et al., 2017). The Sc.chr02.0108 gene encodes an XK-related protein that has significant similarity to the ced-8 gene of *Caenorhabditis elegans* and this protein controls apoptosis timing (Stanfield and Horvitz, 2000). The Sc.chr06.0408 and Sc.chr04.0212 genes encode the heat shock proteins (HSP) 70 B2 and 75 KDa. These HSPs may directly affect apoptosis by intervening in the signal transduction pathway of apoptosis and they play an important role in the regulation of apoptosis (Ikwegbue et al., 2017). They also affect autophagy (Dokladny et al., 2015). Furthermore, we identified eight genes related to autophagy and apoptosis that have higher expression levels in males of the sexual generation compared to other asexual generations. In addition, we also found that these eight genes were highly expressed in females as well, especially Sc.chr09.457, Sc.chr06.0284, Sc.chr08.364, and Sc.chr07.236 (data not reported here). Female's body size does not change significantly result from the volume of egg in female's abdomen increased along with the increase of the age (Zhang and Tang, 1987). We speculate that it may have the same metabolism, autophagy and apoptosis processes as male, and the identified eight genes may play an important role for autophagy and apoptosis in both sexes.

Autophagy is a cellular response to starvation that generates autophagosomes to carry long-lived proteins and cellular organelles to lysosomes for degradation (Miklos, 2008). During autophagy, amino acids and other nutrients are recycled from long live proteins, organelles and other components in the cytoplasm to provide nutrients for necessary life activities (Tracy and Baehrecke, 2013). Autophagy is essential for balancing sources of energy at critical times in development and an effective response to nutrient stress and many other adverse stimulates in many animals including insects (Glick et al., 2010). Mobilization of stored nutrients from the larval fat body of *D. melanogaster*, can be induced by nutrient starvation (Ryan et al., 2004). When starvation stress occurs, the size of fat body cells of *D. melanogaster* larvae decreases by 90%, and at the same time, a large number of autophagy appears (Butterworth et al., 1965; Shi and Tong, 2022). Autophagy also occurred in the ovaries of *D. melanogaster* under nutritional stress and it is crucial for egg formation (Barth et al., 2011). Hibernation is a natural starvation period. No surprise, the autophagic activity of *Troglophilus neglectus* gradually increased in the early, middle and late overwintering (hibernation) stages (Lipovšek and Novak, 2016). Nutrient levels also modulate apoptosis in special cells, such as cartilage endplate stem cells, nucleus pulposus, gastric and colon cancer cells (Matthews et al., 2006; He et al., 2017; Liu et al., 2017). Both autophagy and apoptosis are parts of programmed cell death, while autophagy can control apoptosis by increasing or decreasing the possibility of apoptosis. Conversely, apoptotic processes can increase or decrease autophagy as well (Jacob and Andrew, 2011). Autophagy and apoptosis may inhibit each other through multiple pathways or can be independently regulated by co-occurring signals. For *S. chinensis*, both male and female of the only sexual generation in its life cycle have no functional mouthparts and cannot ingest food. It makes sense that genes associated with autophagy and apoptosis were identified in the current study with *S. chinensis*, especially in males in which body size reduction was observed as they age. In order to achieve sexual maturity and mating without feeding, male aphids (and females as well) may utilize autophagy and apoptosis to provide energy and components for developmental processes.

Data availability statement

The datasets presented in this study can be found in online repositories. The names of the repository/repositories and accession number(s) can be found in the article/Supplementary Material

Author contributions

ZY and XC designed the experiments. HW, XX, and GF collected the samples and carried out the experiment. HW and SS analyzed the RNA sequencing raw data. HW and ZY wrote the manuscript. All authors contributed to the article and approved the submission of this manuscript.

Funding

This study was financially supported by the National Natural Science Foundation of China (31872305); the basic research program of Yunnan Province (202001AT070016); and the grant for Fundamental Research Funds of CAF (CAFYBB2022SY038).

Acknowledgments

We appreciate Prof. Kirst King-Jones (University of Alberta) and Prof. Ming-Shun Chen (Kansas State University) for their helpful comments.

Conflict of interest

The authors declare that the research was conducted in the absence of any commercial or financial relationships that could be construed as a potential conflict of interest.

Publisher's note

Supplementary material

The Supplementary Material for this article can be found online at: https://www.frontiersin.org/articles/10.3389/fphys.2023.1097317/full#supplementary-material

References

Alers, S., Löffler, A. S., Wesselborg, S., and Stork, B. (2012). Role of AMPK-mTOR-ulk1/2 in the regulation of autophagy: Cross talk, shortcuts, and feedbacks. *Mol. Cell Biol.* 32 (1), 2–11. doi:10.1128/MCB.06159-11

Barth, J., Szabad, J., Hafen, E., and Kohler, K. (2011). Autophagy in *Drosophila* ovaries is induced by starvation and is required for oogenesis. *Cell Death Differ.* 18, 915–924. doi:10.1038/cdd.2010.157

Blackman, R. L., and Eastop, V. F. (2020). *Aphids on the world's plants: An online identification and information guide*. United States: John Wiley & Sons.

Butterworth, F. M., Bodenstein, D., and King, R. C. (1965). Adipose tissue of *Drosophila melanogaster*. I. An experimental study of larval fat body. *J. Exp. Zool.* 158, 141–153. doi:10.1002/jez.1401580203

Chen, X. M., Yang, Z. X., Chen, H., Qi, Q., Liu, J., Wang, C., et al. (2020). A complex nutrient exchange between a gall-forming aphid and its plant host. *Front. Plant Sci.* 11, 811. doi:10.3389/fpls.2020.00811

Clarke, C., Madden, S. F., Doolan, P., Aherne, S. T., Joyce, H., O'Driscoll, L., et al. (2013). Correlating transcriptional networks to breast cancer survival: A large-scale coexpression analysis. *Carcinogenesis* 34 (10), 2300–2308. doi:10.1093/carcin/bgt208

Ding, W. F., Ling, X. F., Lu, Q., Wang, W. W., Zhang, X., Feng, Y., et al. (2022). Identification of the key pathways and genes involved in the wax biosynthesis of the Chinese white wax scale insect (*Ericerus pela* Chavannes) by integrated weighted gene coexpression network analysis. *Genes* 13 (8), 1364. doi:10.3390/genes13081364

Dokladny, K., Myers, O. B., and Moseley, P. L. (2015). Heat shock response and autophagy--cooperation and control. *Autophagy* 11 (2), 200–213. doi:10.1080/15548627.2015.1009776

Eterovic, M., and Vilcinskas, A. (2016). *Biology and ecology of aphids*. Boca Raton, Florida, United States: CRC Press Taylor & Francis Group.

Glick, D., Barth, S., and Macleod, K. F. (2010). Autophagy: Cellular and molecular mechanisms. *J. Pathol.* 221 (1), 3–12. doi:10.1002/path.2697

He, Z., Pu, L., Yuan, C., Jia, M., and Wang, J. (2017). Nutrition deficiency promotes apoptosis of cartilage endplate stem cells in a caspase-independent manner partially through upregulating BNIP3. *Acta Biochim. Biophys. Sin.* 49 (1), 25–32. doi:10.1093/abbs/gmw111

Hu, G., Hacham, M., Waterman, S. R., Panepinto, J., Shin, S., Liu, X., et al. (2008). PI3K signaling of autophagy is required for starvation tolerance and virulence of *Cryptococcus neoformans*. *J. Clin. Invest.* 118 (3), 1186–1197. doi:10.1172/JCI32053

Ikwegbue, P. C., Masamba, P., Oyinloye, B. E., and Kappo, A. P. (2017). Roles of heat shock proteins in apoptosis, oxidative stress, human inflammatory diseases, and cancer. *Pharmaceuticals* 11 (1), 2. doi:10.3390/ph11010002

Jacob, M. G., and Andrew, T. (2011). Autophagy and apoptosis: What is the connection? *Trends Cell. Biol.* 21 (7), 387–392. doi:10.1016/j.tcb.2011.03.007

Kim, D., Landmead, B., and Salzberg, S. L. (2015). Hisat: A fast spliced aligner with low memory requirements. *Nat. Methods.* 12 (4), 357–360. doi:10.1038/nmeth.3317

Lambers, D. H. R. (1966). Polymorphism in Aphididae. *Annu. Rev. Entomol.* 11 (1), 47–78. doi:10.1146/annurev.en.11.010166.000403

Lampada, A., O'Prey, J., Szabadkai, G., Ryan, K. M., Hochhauser, D., and Salomoni, P. (2017). mTORC1-independent autophagy regulates receptor tyrosine kinase phosphorylation in colorectal cancer cells via an mTORC2-mediated mechanism. *Cell Death Differ.* 24 (6), 1045–1062. doi:10.1038/cdd.2017.41

Langfelder, P., and Horvath, S. (2008). Wgcna: An R package for weighted correlation network analysis. *BMC Bioinform* 9, 559. doi:10.1186/1471-2105-9-559

Li, H., Handsaker, B., Wysoker, A., Fennell, T., Ruan, J., Homer, N., et al. (2009). The sequence alignment/map format and SAMtools. *Bioinformatics* 25, 2078–2079. doi:10.1093/bioinformatics/btp352

Lipovšek, S., and Novak, T. (2016). Autophagy in the fat body cells of the cave cricket *Troglophilus neglectus* Krauss, 1878 (Rhaphidophoridae, Saltatoria) during overwintering. *Protoplasma* 253, 457–466. doi:10.1007/s00709-015-0824-3

Liu, J., Yuan, C., Pu, L., and Wang, J. (2017). Nutrient deprivation induces apoptosis of nucleus pulposus cells via activation of the BNIP3/AIF signalling pathway. *Mol. Med. Rep.* 16 (5), 7253–7260. doi:10.3892/mmr.2017.7550

Matthews, G. M., Howarth, G. S., and Butler, R. N. (2006). Nutrient and antioxidant modulation of apoptosis in gastric and colon cancer cells. *Cancer Biol. Ther.* 5 (6), 569–572. doi:10.4161/cbt.5.6.2868

Miklos, S. (2008). Autophagy research on insects. *Autophagy* 4 (3), 265–267. doi:10.4161/auto.5787

Neufeld, T. P. (2010). TOR-Dependent control of autophagy: Biting the hand that feeds. *Curr. Opin. Cell Bio.* 22 (2), 157–168. doi:10.1016/j.ceb.2009.11.005

Pertea, M., Pertea, G. M., Antonescu, C. M., Chang, T. C., Mendell, J. T., and Salzberg, S. L. (2015). StringTie enables improved reconstruction of a transcriptome from RNA-seq reads. *Nat. Biotechnol.* 33, 290–295. doi:10.1038/nbt.3122

Russell, R. C., Yuan, H. X., and Guan, K. L. (2014). Autophagy regulation by nutrient signaling. *Cell Res.* 24 (1), 42–57. doi:10.1038/cr.2013.166

Ryan, C. S., Oren, S., and Thomas, P. N. (2004). Role and regulation of starvation-induced autophagy in the *Drosophila* fat body. *Dev. Cell.* 7 (2), 167–178. doi:10.1016/j.devcel.2004.07.009

Shannon, P., Markiel, A., Ozier, O., Baliga, N. S., Wang, J. T., Ramage, D., et al. (2003). Cytoscape: A software environment for integrated models of biomolecular interaction networks. *Genome Res.* 13 (11), 2498–2504. doi:10.1101/gr.1239303

Shi, K., and Tong, C. (2022). Analyzing starvation-induced autophagy in the *Drosophila melanogaster* larval fat body. *J. Vis. Exp.* 186. doi:10.3791/64282

Stanfield, G. M., and Horvitz, H. R. (2000). The ced-8 gene controls the timing of programmed cell deaths in *C. elegans*. *Mol. Cell.* 5 (3), 423–433. doi:10.1016/s1097-2765(00)80437-2

Stern, D. L. (2008). Aphids. *Curr. Biol.* 18 (12), R504–R505. doi:10.1016/j.cub.2008.03.034

Tang, Y., Li, M., Wang, J. X., Pan, Y., and Wu, F. X. (2015). CytoNCA: A cytoscape plugin for centrality analysis and evaluation of protein interaction networks. *BioSyst* 127, 67–72. doi:10.1016/j.biosystems.2014.11.005

Tracy, K., and Baehrecke, E. H. (2013). The role of autophagy in D*rosophila metamorphosis*. *Curr. Top. Dev. Biol.* 103, 101–125. doi:10.1016/B978-0-12-385979-2.00004-6

Wei, H. Y., Ye, Y. X., Huang, H. J., Chen, M. S., Yang, Z. X., Chen, X. M., et al. (2022). Chromosome-level genome assembly for the horned-gall aphid provides insights into interactions between gall-making insect and its host plant. *Ecol. Evol.* 12 (4), e8815. doi:10.1002/ece3.8815

Yang, L., Gordon, K. S., and Wei, S. (2014). featureCounts: An efficient general purpose program for assigning sequence reads to genomic features. *Bioinformatics* 30, 923–930. doi:10.1093/bioinformatics/btt656

Yang, Z. X., Chen, X. M., Nathan, H., and Feng, Y. (2010). Phylogeny of *Rhus* gall aphids (Hemiptera: Pemphigidae) based on combined molecular analysis of nuclear EF1a and mitochondrial COII genes. *Entomol. Sci.* 13, 351e357. doi:10.1111/j.1479-8298.2010.00391.x

Zhang, C. X., and Tang, J. (1987). Study on biology of the sexuales of Chinese horned gall aphid, *Schlechtendalia chinensis* (Bell), Postembryonic development and reproductive type. *J. Zhejiang Agric. Univ.* 13 (3), 267–273.

Zhang, G. X., Qiao, G. X., Zhong, T. S., and Zhang, W. Y. (1999). *Fauna sinica, insecta*. Switzerland: Sci. Press.

frontiers | Frontiers in Plant Science

TYPE Original Research
PUBLISHED 09 February 2023
DOI 10.3389/fpls.2023.1103236

OPEN ACCESS

EDITED BY
Julian Chen,
Institute of Plant Protection (CAAS), China

REVIEWED BY
Xiangfeng Jing,
Northwest A&F University, China
Xun Zhu,
Institute of Plant Protection (CAAS), China

*CORRESPONDENCE
Yuqing Wu
yuqingwu36@hotmail.com
Chuantao Lu
chuantaolu@qq.com

SPECIALTY SECTION
This article was submitted to Sustainable and Intelligent Phytoprotection, a section of the journal Frontiers in Plant Science

RECEIVED 20 November 2022
ACCEPTED 27 January 2023
PUBLISHED 09 February 2023

CITATION
Li T, Yang G, Li Q, Jiang Y, Kang D, Fan Z, Gong Z, Lu R, Zhou G, Wu Y and Lu C (2023) Population dynamics of migrant wheat aphids in China's main wheat production region and their interactions with bacterial symbionts.
Front. Plant Sci. 14:1103236.
doi: 10.3389/fpls.2023.1103236

Population dynamics of migrant wheat aphids in China's main wheat production region and their interactions with bacterial symbionts

Tong Li[1], Gongqiang Yang[1], Qian Li[2], Yueli Jiang[1], Dongmei Kang[1], Zhiye Fan[3], Zhongjun Gong[1], Ruijie Lu[1], Guotao Zhou[4], Yuqing Wu[1]* and Chuantao Lu[1]*

[1]Institute of Plant Protection/Henan Key Laboratory of Crop Pest Control/Key Laboratory of Integrated Pest Management on Crops in Southern Region of North China, Henan Academy of Agricultural Sciences, Zhengzhou, China, [2]College of Bioscience and Resource Environment/Key Laboratory of Urban Agriculture (North China), Ministry of Agriculture and Rural Affairs of the People's Republic of China, Beijing University of Agriculture, Beijing, China, [3]Institute of Plant Protection, Luohe Institute of Agricultural Sciences, Luohe, China, [4]Henan Yunfei Technology Development Co., Ltd, Zhengzhou, China

Sitobion miscanthi, *Rhopalosiphum padi*, and *Schizaphis graminum* are the three main pests in Chinese wheat-producing regions. In 2020, they are classified into the Chinese Class I list of agricultural diseases and pests, due to their severe harm to wheat plantings. *S. miscanthi*, *R. padi*, and *S. graminum* are migrant pests, and understanding their migration patterns and simulating their migration trajectories would improve forecasting and controlling them. Furthermore, the bacterial community of the migrant wheat aphid is also less known. In this study, we employed a suction trap to uncover the migration patterns of the three wheat aphid species in Yuanyang county, Henan province, during 2018 to 2020. And then the migration trajectories of *S. miscanthi* and *R. padi* were simulated using the NOAA HYSPLIT model. The interactions between wheat aphids and bacteria were further revealed by specific PCR and 16S rRNA amplicon sequencing. The results showed that the population dynamics of migrant wheat aphids was varied. Most of the trapped samples were identified to be *R. padi*, and *S. graminum* was the least collected sample. Typically, *R. padi* had two migration peaks in the 3 years, whereas *S. miscanthi* and *S. graminum* only exhibited one migration peak in 2018 and 2019. Moreover, the aphid migration trajectories varied over the years. Generally, the aphids originated from the south and migrated to the north. Herein, the infections of three main aphid facultative bacterial symbionts, *Serratia symbiotica*, *Hamiltonella defensa*, and *Regiella insercticola*, were detected in *S. miscanthi* and *R. padi* with specific PCR. *Rickettsiella*, *Arsenophonus*, *Rickettsia*, and *Wolbachia* were further identified with 16S rRNA amplicon sequencing. Biomarker searching indicated that *Arsenophonus* was significantly enriched in *R. padi*. Furthermore, diversity analyses showed that the bacterial community of *R.*

padi had a higher richness and evenness than that of *S. miscanthi*. In conclusion, this study expands our knowledge about the migration patterns of aphids in the main wheat plant region of China and reveals the interactions between bacterial symbionts and migrant aphids.

KEYWORDS

wheat aphid, aphid symbionts, insect migration, *Sitobion miscanthi*, *Rhopalosiphum padi*, *Schizaphis graminum*

Introduction

Wheat (*Triticum aestivum* L.) is the third major grain crop plant in China. The most common pest on wheat is the wheat aphid, which not only feeds on the grain but also spreads plant viruses like the barley yellow dwarf virus (BYDV). Studies have reported that approximately 10–15 million hectares of wheat fields in China are affected by aphid infestations, resulting in 10% yield losses annually (Hu et al., 2016; Gong et al., 2021). Indian grain aphid *Sitobion miscanthi*, Bird cherry-oat aphid *Rhopalosiphum padi* (Linnaeus), and greenbug *Schizaphis graminum* are three main wheat aphids in China. In 2020, due to their severe harm to wheat plantings, the three wheat aphids are classified into the Chinese Class I list of agricultural diseases and pests (http://www.zzys.moa.gov.cn/gzdt/202006/t20200604_6345940.htm). It is well known that wheat aphids can perform long-distance migration by air (Sun et al., 2022); hence, uncovering their seasonal migration patterns would improve forecasting and controlling them.

The insect marking–release–recapture technique (Hagler and Jackson, 2001) and trapping aerial insect samples using the sticky nets attached to the balloons and airplanes (Florio et al., 2020) have been used to track the migration of insects, but these strategies are labor-intensive. To date, the economical searchlight trap and high effective radar are widely employed to investigate insect migrations. However, the searchlight trap is mostly used to uncover the migrations of lepidopterous pests with large bodies (Guo et al., 2020; Zhou et al., 2021; Guo et al., 2022; Wang et al., 2022b), and the commonly used centimeter-wave vertical-looking radar is unsuitable for monitoring small insects, such as aphids, and a more expensive radar with a shorter wavelength is required (Chapman et al., 2003; Chapman et al., 2004; Feng et al., 2009). Suction traps have been used to monitor the aerial movement of aphids since 1964 (Macaulay et al., 1988), which probably filled the gap in the investigation of aphid migrations. Suction trap networks have been established in the United Kingdom and the United States to monitor seasonal distribution and abundance of diverse aphid species for a few decades (Bell et al., 2015; Lagos-Kutz et al., 2020). In Spain, suction traps are useful for monitoring the flight of damson-hop aphid (*Phorodon humuli*) at the start of spring (Pérez et al., 2006). In 2011, to investigate the migrations of soybean and wheat aphids, a Chinese aphid suction trap network was constructed (Qiao et al., 2011).

It is well known that aphids and bacteria share intimate relationships. In recent years, the 16S ribosomal RNA (rRNA) gene amplicon high-throughput sequencing has been applied to explore the aphid bacterial community (Xu et al., 2020; Xu et al., 2021a; Xu et al., 2021b). However, these bacterial surveys have mainly been performed in the field-collected samples; the interactions between migrant aphids and bacterial symbionts are less studied. In this study, which employed a suction trap, we uncovered the occurrence and migration patterns of the three main wheat aphids in Yuanyang county from 2018 to 2020 and simulated their migration trajectories. Furthermore, using specific PCR and 16S amplicon sequencing, we uncovered the bacterial composition in the migrant *S. miscanthi* and *R. padi*.

Materials and methods

Flying wheat aphid collection and identification

Henan province in China, which contributes a quarter of China's annual wheat harvest, is the core wheat production area. Notably, the first suction trap in Henan was constructed in Yuanyang county, Xinxiang city (35.01 N, 113.69 E). The suction trap is 8.8 m tall and collected the tiny flying insects weekly from April to June 2018–2020. Morphological characteristics were used to identify the three main wheat aphids, *S. miscanthi*, *R. padi*, and *S. graminum*, among the trapped samples. All samples were deposited in the Institute of Plant Protection, Henan Academy of Agricultural Sciences, Zhengzhou, China. They were stored in 75% ethanol and maintained under −20°C until DNA extraction.

Wheat aphid migration pattern and trajectory analysis

The population dynamics of migration wheat aphids was summarized, and their migrating peaks were revealed. The HYSPLIT (HYbrid Single-Particle Lagrangian Integrated Trajectory) model is designed to simulate the trajectory of substances transported and dispersed through atmosphere using gridded meteorological data (Stein et al., 2015; Rolph et al., 2017). It is widely used to simulate the global dust distribution, volcanic ash dispersion, and pollutant transport (Stein et al., 2007; Stunder et al., 2007; Wang et al., 2011). Tiny insects like aphids have limited flight capacity. The flight speed of aphids is approximately 0.9 m s^{-1}

(Robert, 1987), and the aphid flights are controlled by the wind when they move above at approximately 1 m from the ground (Parry, 2013). Hence, the HYSPLIT model is also suitable to calculate the migration trajectory of tiny insects with meteorological data.

In this study, the migration trajectories of *S. miscanthi* and *R. padi* were simulated with the online HYSPLIT model (https://www.ready.noaa.gov/HYSPLIT_traj.php). In these analyses, the meteorological data were obtained with the one-degree GDAS (Global Data Assimilation System) model, the model calculated star times were set on the 02:00 UTC time (10 a.m. in Beijing time) on the aphid migration peak days, and the flight heights were chosen as 10, 50, and 100 m AGL (above ground level). The aphid migration trajectories were simulated in 24 h.

DNA extraction, bacterial symbiont detections, and phylogenetic analysis

In this study, the infections of three main aphid bacterial symbionts, *Serratia symbiotica*, *Hamiltonella defensa*, *Regiella insercticola*, and one common insect bacterial symbiont, *Wolbachia*, were detected in *S. miscanthi* and *R. padi* with specific primers listed in Table S1. In these specific amplifications, aphid total DNA was extracted from a single aphid using an Ezup Column Animal Genomic DNA Purification Kit (Sangon Biotech, Shanghai), following the manufacturer's recommendations. Before DNA extraction, every aphid was washed with 70% ethanol and sterile water several times to remove surface contamination. Aphid *elongation factor-1α* gene was used as a reference to evaluate the extracted DNA quality, and the low-quality ones were excluded in the bacterial symbiont detections. The 16S rRNA sequences of the known aphid bacterial symbiont strains were retrieved to uncover the phylogenetic positions of the identified bacterial symbiont strains of *S. miscanthi* and *R. padi*. The sequences were aligned using the MUSCLE program in MEGA 7.0 (Kumar et al., 2016). Phylogenetic analysis was performed in IQ-TREE 1.6.12 (Nguyen et al., 2015). The support for each node was assessed by resampling 5,000 ultrafast bootstraps (Hoang et al., 2018). The best substitution model was selected by Bayesian information criterion in ModelFinder (Kalyaanamoorthy et al., 2017). The phylogenetic tree was visualized in Figtree 1.4.2 (http://tree.bio.ed.ac.uk/software/figtree/).

Bacterial 16S rRNA amplicon amplification and sequencing

Herein, the bacterial composition of *S. miscanthi* and *R. padi* was further uncovered by amplicon sequencing. We randomly selected 15 individuals of *S. miscanthi* and *R. padi* collected in the same year and divided them into five replicates. The genomic DNA of the pooled aphids in each replicate was extracted using the DNeasy Blood and Tissue Kit (QIAGEN, Germany) according to the manufacturer's instructions. The possible surface contamination was removed as described above. An approximately 460-bp fragment of the bacterial 16S rRNA V3–V4 region was amplified with primers 341F: CCTACGGGNGGCWGCAG and 806R: GGACTACHVGGGTATCTAAT (Qin et al., 2021). The PCR reactions were performed in triplicate in a 50-μl mixture containing 5 μl of 10 × KOD Buffer, 5 μl of 2 mM dNTPs, 3 μl of 25 mM $MgSO_4$, 1.5 μl of each primer (10 μM), 1 μl of KOD Polymerase, and 100 ng of template DNA. PCR amplifications were carried out with the following program: 94°C for 2 min, followed by 30 cycles at 98°C for 10 s, 62°C for 30 s, and 68°C for 30 s and a final extension at 68°C for 5 min. The amplicons were further purified using the AxyPrep DNA Gel Extraction Kit (Axygen Biosciences, Union City, CA, USA) according to the manufacturer's instructions. Subsequently, the purified amplicons were quantified using the ABI StepOnePlus Real-Time PCR System (Life Technologies, Foster City, USA), pooled in equimolar and generated the sequencing libraries. The next sequencing was performed by the Gene Denovo Biotechnology Co. (Guangzhou, China) on an Illumina HiSeq 2500 platform with a 2×250-bp paired-end method according to the standard protocols.

Bioinformatics analyses

The reads were trimmed using Btrim with the cutoff for average quality scores higher than 20 over a 5-bp window size and a minimum length of 180 bp (Kong, 2011). The reads ranging from 242 bp to 244 bp were employed in the following analyses with QIIME2 (version 2022.11) (Bolyen et al., 2019). Primers and adaptor sequences were removed by cutadapt plugin (Martin, 2011). ASVs (amplicon sequence variants) were obtained by merging the sequences and removing chimera with the DADA2 plugin (Callahan et al., 2016). The taxonomic assignment of representative sequences was carried out using the feature-classifier plugin against the SILVA database (silva-138-99). Four alpha diversity indexes, ACE (abundance-based coverage estimator), Chao1, Shannon, and Simpson, were calculated in QIIME2; Bray–Curtis distance matrix was calculated in QIIME2, and then PCoA (principal coordinates analysis) and NMDS (non-metric multi-dimensional scaling) were visualized with Bray–Curtis distances and plotted in the ggplot2 package. The relative abundance of the top 10 bacterial taxa among the samples and the cladogram of the differential species were analyzed and visualized by the MicrobiotaProcess package (https://github.com/YuLab-SMU/MicrobiotaProcess), with the feature table and taxonomy table obtained in QIIME2.

Results

Annual migration patterns of three wheat aphids

In this study, most of the migrant wheat aphids were trapped in 2018 (4,051 samples), and 2020 had the least number of trapped migrant wheat aphids (737 samples). In 2019, 1,271 migrant wheat aphids were trapped (Figure 1A). *R. padi* was predominant among the samples of trapped wheat aphids, whereas *S. miscanthi* and *S. graminum* were less common. However, among the three aphid species, the number of trapped aphids was not significantly divergent (ANOVA test, $F = 2.334$, $p = 0.1778$). In addition,

10.3389/fpls.2023.1103236

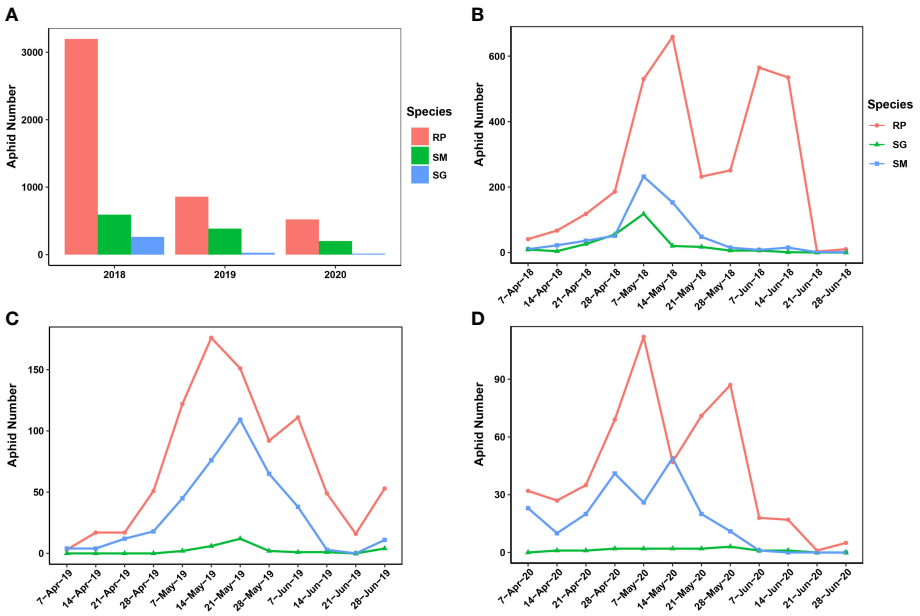

FIGURE 1
Population dynamics and migration patterns of the wheat aphids uncovered by a suction trap in Yuanyang country from 2018 to 2020. **(A)** The population dynamics of the three wheat aphids during 2018–2020. **(B–D)** The migration pattern of the three wheat aphids was revealed during 2018–2020. SM, *Sitobion miscanthi*; RR, *Rhopalosiphum padi*; SG, *Schizaphis graminum*.

different patterns of wheat aphid migration were discovered over the years (Figures 1B–D). The results indicated that the migrations of *R. padi* had two distinct peaks during 2018–2020. Specifically, in 2018 and 2019, the first *R. padi* migration peak occurred in the second week of May, and the second peak occurred in the first week of June. However, in 2020, the two *R. padi* migration peaks happened 1 week earlier than that of 2018 and 2019. In contrast, only one peak was observed in the migration of *S. graminum* and *S. miscanthi* in 2018 and 2019, which occurred in the first and third weeks of May, respectively. The *S. miscanthi* migration experienced two adjacent peaks in 2020, which occurred in the fourth week of April and the second week of May, respectively. However, no obvious peak was revealed in *S. graminum* migration in 2020, since at most three samples were trapped in the weeks and a total of 15 samples were collected.

Here, the meteorological data reflecting the local climate conditions near the suction trap (thereafter named Yuangyang), as well as those reflecting the climate conditions of a wider area, such as Xinxiang city, were involved in the statistical analyses to comprehensively uncover the underlying roles of temperature and humidity on the migrations of wheat aphids. The results indicated that there was no significant difference in the temperatures of April and May during 2018–2020, in either the Yuanyang or Xinxiang region (ANOVA test, $p > 0.05$) (Figures 2A, B). However, a significant difference in their relative humidity was observed (ANOVA test, $p < 0.05$) (Figures 2C, D). Furthermore, the multiple comparisons using Tukey's test revealed that the relative humidity of April 2018 was significantly different with that of 2020 either in the Yuanyang or Xinxiang region. However, the relative humidity of May 2018 was significantly different from that of 2019 and 2020 in the Yuanyang region, and in the Xinxiang region, the relative humidity of May 2018 was significantly different from that of 2019.

Aphid migration trajectory analyses

To identify the origin of the migrating aphids, we simulated the backward migration trajectories of immigrations. On the other hand, the forward migration trajectories of emigrations were simulated to uncover the destinations of the flying aphids. The results demonstrated similar migration trajectories at the three layers: 10 m, 50 m, and 100 m AGL (Figures 3, 4). Most *S. miscanthi* migrations on 7 May 2018 and 28 April 2020 originated from the west and southeast of Yuanyang county, respectively (Figures 3A, B). In addition, on 21 May 2019 and 14 May 2020, *S. miscanthi* migrated to the northeast and northwest of Yuanyang county, respectively (Figures 3C, D). The migration trajectories of *R. padi* are summarized in Figure 4. The results indicated that most *R. padi* migrations on 14 May 2018 originated north of Yuanyang country (Figure 4A). However, most of the migrating *R. padi* on 14 May 2019 and 7 May 2020 originated northeast of Yuanyang country (Figures 4B, C). According to the simulation of forward migration trajectories, most *R. padi* would migrate to the south and east of Yuanyang county on 7 June 2018 (Figure 4D). On the contrary, most *R. padi* would migrate to the northeast and north of Yuanyang county on 7 June 2019 and 28 May 2020, respectively (Figures 4E, F).

Specific aphid facultative symbiont detection

In this study, a total of 237 and 350 samples of *S. miscanthi* and *R. padi* were subjected to the specific bacterial symbiont detections, respectively (Table 1). *S. symbiotica*, *H. defensa*, and *R. insercticola* were detected in the aphids; however, no infection of *Wolbachia* was identified. In *S. miscanthi*, infection rates of *S. symbiotica* and

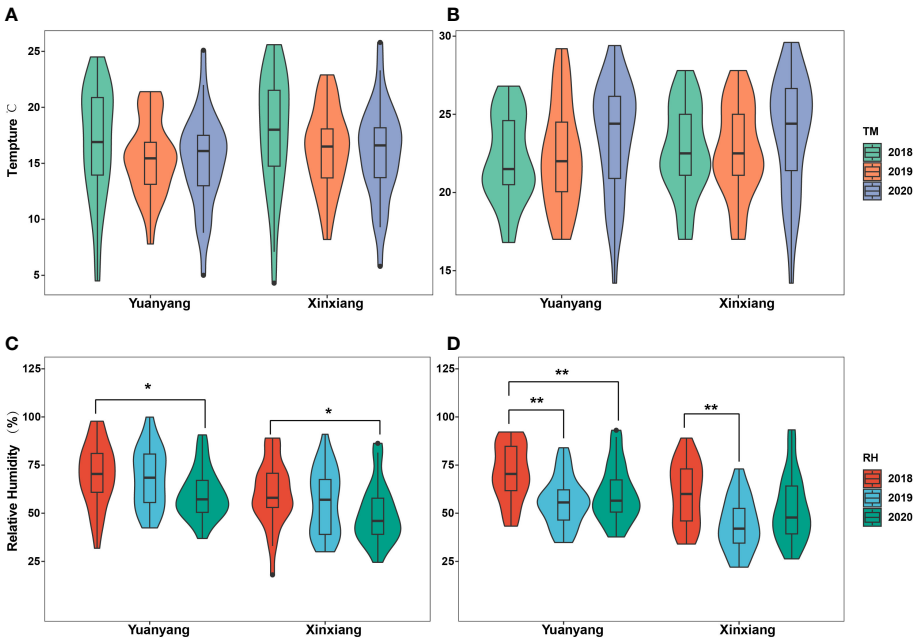

FIGURE 2
Statistical analysis of temperature and relative humidity among years in Yuanyang and Xinxiang regions. **(A, B)** Analysis with the April and May temperature obtained in Yuanyang and Xinxiang regions, respectively. **(C, D)** Analysis with the April and May relative humidity in Yuanyang and Xinxiang regions, respectively. *, indicating significant ($p<0.05$); **, indicating very significant ($p<0.01$).

H. defensa were 12.23% (29/237) and 1.27% (3/237), respectively. On the other side, in *R. padi*, infection rates of *S. symbiotica* and *H. defensa* were 7.71% (27/350) and 1.42% (5/350), respectively. The infection rates of *R. insercticola* in *S. miscanthi* and *R. padi* were 2.95% (7/237) and 4.29 (15/350), respectively. However, between *S. miscanthi* and *R. padi*, no significant difference was observed in the infections of *S. symbiotica* ($\chi^2 = 2.28$, $p = 0.13$), *H. defensa* ($\chi^2 = 0.027$, $p = 0.86$), and *R. insercticola* ($\chi^2 = 0.69$, $p = 0.40$). In the phylogenetic tree (Figure 5), the monophyly of *S. symbiotica*, *H. defensa*, and *R. insercticola* was robustly supported. In these symbiont clades, the strains identified in *S. miscanthi* and *R. padi* shared close relationships with that isolated in other aphid species, which further verified their infections.

Analyses of 16S rRNA amplicon sequencing

In this study, a total of 3,874,860 raw reads (average 129,162 reads per sample) were yielded in the 16S rRNA V3–V4 amplicon sequencing. After trimming, denoising, and chimera removal, 8,518 representative ASVs were obtained, and their taxonomic positions were identified against the SILVA database. The relative abundance of the top 10 bacterial taxa among the samples was revealed at four taxonomic levels (Figure 6). The results showed that compositions of bacterial community harbored in the *S. miscanthi* 2018 population was different from that of the remaining aphid populations. For instance, at the phylum level, in the 2018 *S. miscanthi* population, Firmicutes was dominant with 79.60% relative abundance and Proteobacteria was the second main taxon with 8.46% relative abundance. However, in the remaining aphid populations, Proteobacteria was dominant with a relative abundance ranging from 34.49% in the 2018 *R. padi* population to 78.47% in the 2019 *R. padi* population. A similar divergence was also observed at the order and family level. At the genus level, *Buchnera* was identified in all samples with an average relative abundance of 11.26%. Furthermore, two aphid facultative symbionts belonging to *Serratia* and *Rickettsiella* and three common insect bacterial symbionts, *Arsenophonus*, *Rickettsia*, and *Wolbachia*, were identified. In *S. miscanthi*, *Serratia* was the dominant aphid facultative symbiont with an average abundance of 8.41%. On the other side, *Arsenophonus* was the dominant aphid facultative symbiont in *R. padi* with an average abundance of 23.30%. In *S. miscanthi*, the average abundance of *Rickettsiella* was 10.11% much higher than that of *R. padi*, which had only 0.13% average abundance. *Rickettsia* was mainly identified in the 2019 *S. miscanthi* population with a 9.49% abundance. *Wolbachia* was only identified in the 2019 *R. padi* population with a 0.05% abundance. The results of biomarker discovery indicated that *Arsenophonus* was the most differentially abundant bacterial taxon in *R. padi* (Figure S1). Additionally, within *S. miscanthi* and *R. padi*, the abundance of *Rickettsiella*, *Arsenophonus*, and *Serratia* was varied among the years. Their lowest relative abundance was observed in the 2018 aphid populations (Figure S2). In *S. miscanthi*, the relative abundance of *Rickettsiella* in the 2018 and 2019 aphid populations was significantly different. A similar result was also observed in *Serratia* (Figure S2A). In *R. padi*, the relative abundance of *Arsenophonus* in the 2018 aphid population was significantly different from that in the 2019 and 2020 aphid populations (Figure S2B).

In this study, the alpha diversity among the samples was varied (Figure S3A). Furthermore, it was found that *R. padi* had a relatively higher richness and evenness than *S. miscanthi* (Figure S3B). In beta diversity analyses, both PCoA and NMDS analyses indicated that the

10.3389/fpls.2023.1103236

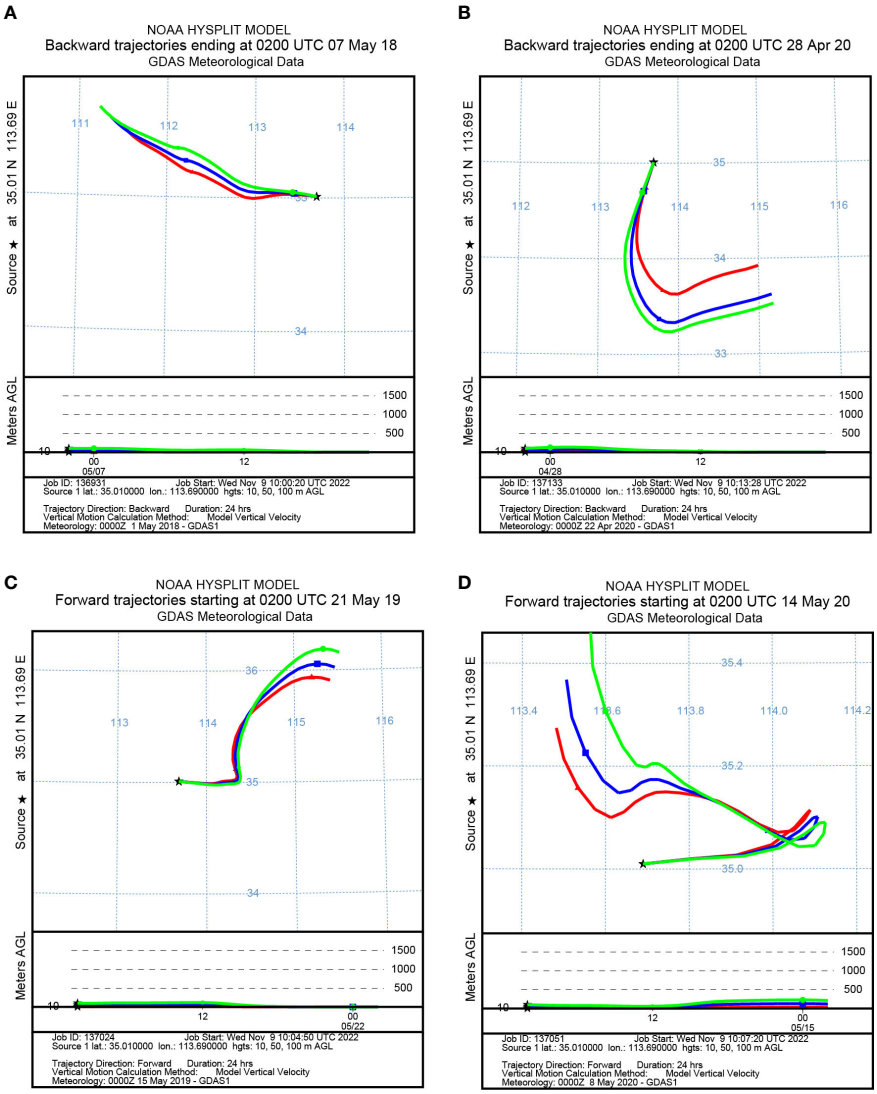

FIGURE 3
The migration trajectories of *Sitobion miscanthi* simulated by HYSPLIT. **(A, B)** Simulation of the backward trajectories on 7 May 2018 and 28 April 2020, respectively. **(C, D)** Simulation of the forward trajectories on 21 May 2019 and 14 May 2020, respectively.

bacterial community of the 2018 *S. miscanthi* population was distinct from the other samples (Figure S4). The samples of *S. miscanthi* trapped in 2019 and 2020 had similar bacterial communities. In *R. padi*, the bacterial communities were separated by years in PCoA. However, in the NMDS analysis, bacterial communities of the *R. padi* samples trapped in 2018 and 2020 and that of *S. miscanthi* samples trapped in 2019 and 2020 were not well separated.

Discussion

Population dynamics of wheat migrant wheat aphids

In this study, the amount of migration wheat aphids varied among years. Previous studies indicated that temperature and humidity are the key environmental factors influencing aphid flights (Parry, 2013). Herein, we analyzed the underlying influences of temperature and humidity on the wheat aphid migrations with two types of meteorological data. The results showed that the difference in relative humidity among the years was significant, indicating that relative humidity probably influenced the wheat aphid flight. We also found that the migrating populations of the three wheat aphids varied from each other. *R. padi* was the most abundant among the identified migrating aphids, followed by *S. miscanthi*, and *S. graminum* was the least abundant. This result was consistent with the findings of our aphid surveying in the wheat field (data not shown). In Yuanyang country, *R. padi* was the dominant wheat aphid species, particularly in the late wheat development stages characterized by higher temperatures. Previous studies demonstrated that *R. padi* performed better in high-temperature habitats (Asin and Pons, 2001) and showed greater ecological plasticity when exposed to harsh environments (Zhu et al., 2021). We hypothesize that the *R. padi* population would proliferate faster with a temperature increase than other wheat aphids; thus, more winged *R. padi* would be induced due to the low host plant quality and crowding.

10.3389/fpls.2023.1103236

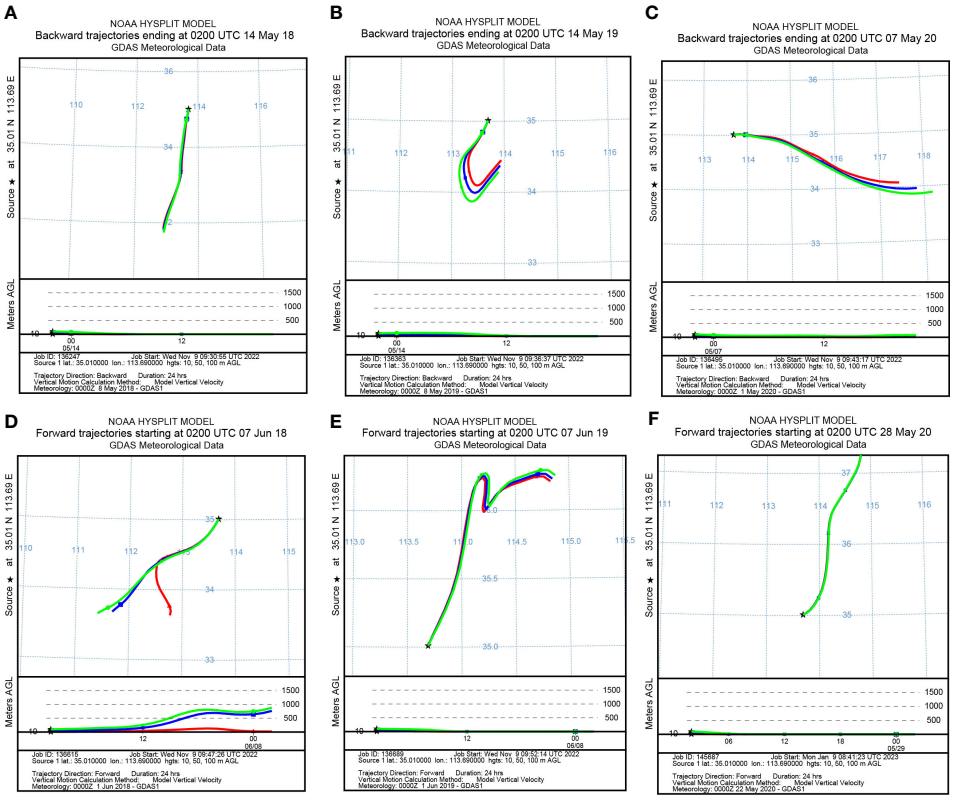

FIGURE 4
The migration trajectories of *Rhopalosiphum padi* simulated by HYSPLIT. **(A, B)** Simulation of the backward trajectories on 14 May 2018 and 14 May 2019, respectively. **(C)** Simulation of the backward trajectories on 7 May 2020. **(D, E)** Simulation of the forward trajectories on 7 June 2018 and 7 June 2019, respectively. **(F)** Simulation of the forward trajectories on 28 May 2020.

TABLE 1 Detection of bacterial symbionts in *Sitobion miscanthi* and *Rhopalosiphum padi* with specific primers.

Year	Number of aphids[a]	*Serratia symbiotica*[b]	*Hamiltonella defensa*[c]	*Regiella insercticola*[d]	*Wolbachia*[e]
2018	60/150	2/8	-/-	-/5	-/-
2019	90/100	15/10	3/-	2/3	-/-
2020	87/100	12/9	-/5	5/7	-/-

a, The number of *Sitobion miscanthi/Rhopalosiphum padi* used in the detection. b–e, The number of positive samples of *Sitobion miscanthi/Rhopalosiphum padi* in the detection. -, No positive sample was detected in the aphids.

Migration patterns and simulated trajectories of wheat aphids

A previous study indicated that in Chinese northern winter wheat plant regions, aphids would probably migrate into wheat fields during the wheat heading to flowering stages, and then migrate out in the wheat milk-ripe stage (Li et al., 2014a). In the Yuanyang country, the periods of wheat heading to flowering stages ranged from around late April to early May, and the milk-ripe stage of wheat ranged from around late May to early June. Hence, in this study, we roughly used the half of May as the threshold to distinguish the types of aphid migrations; those that occurred earlier were categorized as immigrations, while those that occurred later were categorized as emigrations. Although alate aphids will undertake appetitive flight in short distances (Loxdale et al., 1993), long-distance migrations are also observed in various aphid species (Kring, 1972). This study found that *R. padi* and *S. miscanthi* had different migration patterns. Specifically, two migration peaks were observed in *R. padi*, identified as immigrations and emigrations. However, in *S. miscanthi*, the migration patterns varied over the years. Only immigrations were observed in 2018, whereas only emigrations were observed in 2019. In 2020, two adjacent migration peaks were uncovered. These results suggest that the field population of *S. miscanthi* in Yuanyang county in 2018 likely included the migrated aphids, but few *S. miscanthi* migrated out in late June. However, in 2019, most *S. miscanthi* field specimens might have been overwintering individuals that migrated out in late May.

Wind speed and direction are the key factors influencing the initiation, path, speed, distance, and duration of aphid flight (Parry, 2013). HYSPLIT is widely used to simulate the migration trajectories of insects, such as *Helicoverpa armigera* (Feng et al., 2009), *Spodoptera frugiperda* (Westbrook et al., 2016), *Pantala flavescens* (Cao et al., 2018), and *Anopheles* mosquitos (Huestis et al., 2019). Herein, HYSPLIT was used to simulate the trajectories of *R. padi* and *S. miscanthi* on their peak migration days. The results indicated that the immigrations typically originated from the south, whereas the north was the primary destination

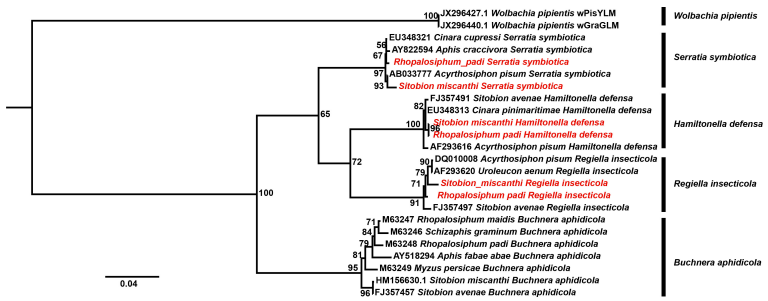

FIGURE 5
The phylogenetic analysis of aphid bacterial symbionts. The strains identified herein were highlighted with red.

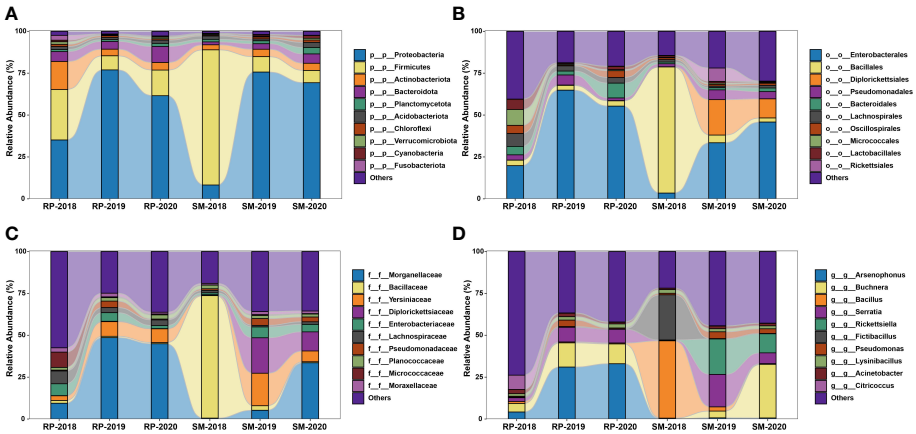

FIGURE 6
Stacked bar plot showing the relative abundance of the top 10 bacterial taxa identified in *Sitobion miscanthi* and *Rhopalosiphum padi* samples at four taxonomic levels. **(A)**, phylum; **(B)**, order; **(C)**, family; and **(D)**, genus.

of the emigrations. These findings were consistent with the previous conclusions that wheat aphid migration trajectories in Chinese wheat fields were typically from south to north in line with the monsoons (Li et al., 2014a). However, there were also some exceptions. In 2018, it was predicted that the *S. miscanthi* would migrate from the west, whereas the predicted direction of the *R. padi* in emigrations was south.

Bacterial composition of wheat aphids

Previously, using specific PCR, *H. defensa* and *R. insercticola* have been detected in *S. miscanthi* (Li et al., 2014b). Recently, the bacterial communities of *S. miscanthi* are investigated with 16S amplicon sequencing (Wang et al., 2022a). However, the examined aphids in these studies are collected in wheat fields; the bacterial community of the migrant wheat aphids is less known. In this study, using specific PCR and phylogenetic analysis, the infections of *S. symbiotica*, *H. defensa*, and *R. insercticola* were identified in *S. miscanthi* and *R. padi* migrants. However, no significant difference was observed in their infection rates. Amplicon sequencing indicated that Proteobacteria and Firmicutes were the dominant bacterial taxa in the wheat aphid migrants. Moreover, we identified two aphid facultative symbionts (*S. symbiotica* and *R. viridis*), and three common insect bacterial symbionts (*Arsenophonus*, *Rickettsia*, and *Wolbachia*). *Arsenophonus* has been detected in diverse aphid groups (Jousselin et al., 2012), whereas *R. viridis* has been identified in pea aphid (Tsuchida et al., 2010). To our knowledge, it is the first report of them in *S. miscanthi* and *R. padi*. Furthermore, *Arsenophonus* was identified to be the most differentially abundant bacterial taxon in *R. padi*. Additionally, to uncover the potential interactions between the infections of bacterial symbionts and aphid flight, the relative abundance of *Rickettsiella*, *Arsenophonus*, and *Serratia*, was used in the statistical analyses. In both *S. miscanthi* and *R. padi*, the lowest relative abundance of the bacterial symbionts was observed in the 2018 aphid populations. Furthermore, the specific PCR results revealed that the 2018 populations of *S. miscanthi* and *R. padi* had the lowest rates of bacterial symbiont infection. Since most of the aphid migrants were trapped in 2018, it indicated that aphid bacterial symbionts did not probably promote the wheat aphid migrations. However, this hypothesis needs to be further verified by comparing the aphid flight capabilities of bacterial symbiont infected and uninfected populations.

In conclusion, in this study, we used the data obtained from the Yuanyang suction trap site, uncovered the population dynamics of migrant wheat aphids in the main wheat planting region in China, and simulated their migration trajectories. Furthermore, we revealed the potential roles of

climate conditions on the aphid migrations. Additionally, the interactions between wheat aphid migrants and bacteria were investigated with specific PCR and amplicon sequencing.

Data availability statement

The original contributions presented in the study are publicly available. This data can be found here: NCBI, PRJNA898692.

Author contributions

TL, YW, and CL conceived the study. TL, GY, QL, and YJ drafted the manuscript. DK, ZF, RL, and GZ collected and identified the aphid species.TL prepared the figures. TL, YW, and QL revised the manuscript. TL, YW, and CL designed the whole study and revised the manuscript. All authors contributed to the article and approved the submitted version.

Funding

This work was supported by the China Agriculture Research System of MOF and 342 MARA (CARS-03), the Henan Provincial Science and Technology R&D Program Joint Fund (grant no. 222301420107), the Special Fund for Agro-Scientific Research in the Public Interest of China (grant no. 201103022), and the Major Public Welfare Scientific Research Project of Henan Province (grant no. 201300111600).

Acknowledgments

We thank Gangqi Fang from CAS Key Laboratory of Insect Developmental and Evolutionary Biology, Chinese Academy of Sciences, Shanghai, China, for providing help in the data analyses.

Conflict of interest

Author GZ is employed by Henan Yunfei Technology Development Co., Ltd.

The remaining authors declare that the research was conducted in the absence of any commercial or financial relationships that could be construed as a potential conflict of interest.

The handling editor JC declared a past collaboration with the authors QL, YW.

Publisher's note

Supplementary material

The Supplementary Material for this article can be found online at: https://www.frontiersin.org/articles/10.3389/fpls.2023.1103236/full#supplementary-material

SUPPLEMENTARY FIGURE 1
The cladogram and abundance of differential species. **(A)** A cladogram showing the significant differentially abundant taxa in *Sitobion miscanthi* and *Rhopalosiphum padi*. Significant differentially abundant taxa were identified by the Kruskal-Wallis test ($p < 0.05$). **(B)** The abundance and LDA effect size of differential taxa in *Sitobion miscanthi* and *Rhopalosiphum padi*.

SUPPLEMENTARY FIGURE 2
Statistic analysis of the relative abundance of *Rickettsiella*, *Arsenophonus*, and *Serratia* among years. **(A)** Analysis performed in *Sitobion miscanthi*. **(B)** Analysis performed in *Rhopalosiphum padi*.

SUPPLEMENTARY FIGURE 3
The boxplots of alpha diversity indexes. **(A)** The ACE, Chao1, Shannon and Simpson indexes of bacterial communities in the *Sitobion miscanthi* and *Rhopalosiphum padi* populations trapped during 2018-2020. **(B)** The ACE, Chao1, Shannon and Simpson indexes of bacterial communities of the entire *Sitobion miscanthi* and *Rhopalosiphum padi* samples. SM, *Sitobion miscanthi*; RR, *Rhopalosiphum padi*.

SUPPLEMENTARY FIGURE 4
The results of beta diversity analyses. **(A)** The PCoA analyses among the *Sitobion miscanthi* and *Rhopalosiphum padi* samples. **(B)** The NMDS analyses among the *Sitobion miscanthi* and *Rhopalosiphum padi* samples.

References

Asin, L., and Pons, X. (2001). Effect of High Temperature on the Growth and Reproduction of Corn Aphids (Homoptera: Aphididae) and Implications for Their Population Dynamics on the Northeastern Iberian Peninsula. *Environ. Entomol.* 30 (6), 1127–1134. doi: 10.1603/0046-225X-30.6.1127

Bell, J. R., Alderson, L., Izera, D., Kruger, T., Parker, S., Pickup, J., et al. (2015). Long-term phenological trends, species accumulation rates, aphid traits and climate: Five decades of change in migrating aphids. *J. Anim. Ecol.* 84 (1), 21–34. doi: 10.1111/1365-2656.12282

Bolyen, E., Rideout, J. R., Dillon, M. R., Bokulich, N. A., Abnet, C. C., Al-Ghalith, G. A., et al. (2019). Reproducible, interactive, scalable and extensible microbiome data science using qiime 2. *Nat. Biotechnol.* 37 (8), 852–857. doi: 10.1038/s41587-019-0209-9

Callahan, B. J., McMurdie, P. J., Rosen, M. J., Han, A. W., Johnson, A. J., and Holmes, S. P. (2016). Dada2: High-resolution sample inference from illumina amplicon data. *Nat. Methods* 13 (7), 581–583. doi: 10.1038/nmeth.3869

Cao, L. Z., Fu, X. W., Hu, C. X., and Wu, K. M. (2018). Seasonal migration of *Pantala flavescens* across the bohai strait in northern China. *Environ. Entomol.* 47 (2), 264–270. doi: 10.1093/ee/nvy017

Chapman, J. W., Reynolds, D. R., and Smith, A. D. (2003). Vertical-looking radar: A new tool for monitoring high-altitude insect migration. *BioScience* 53 (5), 503–511. doi: 10.1641/0006-3568(2003)053[0503:VRANTF]2.0.CO;2

Chapman, J., Reynolds, D., and Smith, A. (2004). Migratory and foraging movements in beneficial insects: A review of radar monitoring and tracking methods. *Int. J. Pest Manage.* 50 (3), 225–232. doi: 10.1080/09670870410001731961

Feng, H., Wu, X., Wu, B., and Wu, K. (2009). Seasonal migration of *Helicoverpa armigera* (Lepidoptera: Noctuidae) over the bohai Sea. *J. Econ. Entomol.* 102 (1), 95–104. doi: 10.1603/029.102.0114

Florio, J., Veru, L. M., Dao, A., Yaro, A. S., Diallo, M., Sanogo, Z. L., et al. (2020). Diversity, dynamics, direction, and magnitude of high-altitude migrating insects in the sahel. *Sci. Rep.* 10 (1), 20523. doi: 10.1038/s41598-020-77196-7

Gong, P., Li, X., Gao, H., Wang, C., Li, M., Zhang, Y., et al. (2021). Field evolved resistance to pyrethroids, neonicotinoids, organophosphates and macrolides in *Rhopalosiphum padi* (Linnaeus) and *Sitobion avenae* (Fabricius) from China. *Chemosphere* 269, 128747. doi: 10.1016/j.chemosphere.2020.128747

Guo, J. L., Fu, X. W., Zhao, S. Y., Shen, X. J., Wyckhuys, K. A. G., and Wu, K. M. (2020). Long-term shifts in abundance of (Migratory) crop-feeding and beneficial insect species in northeastern Asia. *J. Pest Sci.* 93, 583–594. doi: 10.1007/s10340-019-01191-9

Guo, J., Yang, F., Zhang, H., Lin, P., Zhai, B., Lu, Z., et al. (2022). Reproduction does not impede the stopover departure to ensure a potent migration in *Cnaphalocrocis medinalis* moths. *Insect Sci.* 29 (6), 1672–1684. doi: 10.1111/1744-7917.13020

Hagler, J. R., and Jackson, C. G. (2001). Methods for marking insects: Current techniques and future prospects. *Annu. Rev. Entomol.* 46, 511–543. doi: 10.1146/annurev.ento.46.1.511

Hoang, D. T., Chernomor, O., von Haeseler, A., Minh, B. Q., and Vinh, L. S. (2018). Ufboot2: Improving the ultrafast bootstrap approximation. *Mol. Biol. Evol.* 35 (2), 518–522. doi: 10.1093/molbev/msx281

Hu, X. S., Liu, Y. J., Wang, Y. H., Wang, Z., Yu, X. L., Wang, B., et al. (2016). Resistance of wheat accessions to the English grain aphid *Sitobion avenae*. *PLoS One* 11 (6), e0156158. doi: 10.1371/journal.pone.0156158

Huestis, D. L., Dao, A., Diallo, M., Sanogo, Z. L., Samake, D., Yaro, A. S., et al. (2019). Windborne long-distance migration of malaria mosquitoes in the sahel. *Nature* 574 (7778), 404–408. doi: 10.1038/s41586-019-1622-4

Jousselin, E., Coeur d'Acier, A., Vanlerberghe-Masutti, F., and Duron, O. (2012). Evolution and diversity of *Arsenophonus* endosymbionts in aphids. *Mol. Ecol.* 22 (1), 260–270. doi: 10.1111/mec.12092

Kalyaanamoorthy, S., Minh, B. Q., Wong, T. K. F., von Haeseler, A., and Jermiin, L. S. (2017). Modelfinder: Fast model selection for accurate phylogenetic estimates. *Nat. Methods* 14 (6), 587–589. doi: 10.1038/nmeth.4285

Kong, Y. (2011). Btrim: A fast, lightweight adapter and quality trimming program for next-generation sequencing technologies. *Genomics* 98 (2), 152–153. doi: 10.1016/j.ygeno.2011.05.009

Kring, J. B. (1972). Flight behaviour of aphids. *Annu. Rev. Entomol.* 17, 461–492. doi: 10.1146/annurev.en.17.010172.002333

Kumar, S., Stecher, G., and Tamura, K. (2016). Mega7: Molecular evolutionary genetics analysis version 7.0 for bigger datasets. *Mol. Biol. Evol.* 33 (7), 1870–1874. doi: 10.1093/molbev/msw054

Lagos-Kutz, D., Voegtlin, D. J., Onstad, D., Hogg, D., Ragsdale, D., Tilmon, K., et al. (2020). The soybean aphid suction trap network: Sampling the aerobiological "Soup". *Am. Entomol.* 66, 48–55. doi: 10.1093/ae/tmaa009

Li, K. B., Du, G. Q., Yin, J., Zhang, S., and Cao, Y. Z. (2014a). Monitoring the migration of *Sitobion avenae* (Fabricius) bySuction trapping (in Chinese). *Chin. J. Entomol.* 51 (6), 1504–1515. doi: 10.7679/j.issn.2095–1353.2014.175

Li, T., Xiao, J. H., Wu, Y. Q., and Huang, D. W. (2014b). Diversity of bacterial symbionts in populations of *Sitobion miscanthi* (Hemiptera: Aphididae) in China. *Environ. Entomol.* 43, 605–611. doi: 10.1603/EN13229

Loxdale, H. D., Hardie, J., Halbert, S., Foottit, R., Kidd, N. A. C., and Carter, C. I. (1993). The relative importance of short- and long-range movement of flying aphids. *Biol. Rev.* 68, 291–311. doi: 10.1111/j.1469-185X.1993.tb00998.x

Macaulay, E. D. M., Tatchell, G. M., and Taylor, L. R. (1988). The rothamsted insect survey '12-metre' suction trap. *Bull. Ent. Res.* 78, 121—129. doi: 10.1017/S0007485300016126

Martin, M. (2011). Cutadapt removes adapter sequences from high-throughput sequencing reads. *EMBnet* 17 (1), 10–12. doi: 10.14806/ej.17.1.200

Nguyen, L. T., Schmidt, H. A., von Haeseler, A., and Minh, B. Q. (2015). Iq-tree: A fast and effective stochastic algorithm for estimating maximum-likelihood phylogenies. *Mol. Biol. Evol.* 32 (1), 268–274. doi: 10.1093/molbev/msu300

Parry, H. R. (2013). Cereal aphid movement: General principles and simulation modelling. *Mov. Ecol.* 1 (1), 14. doi: 10.1186/2051-3933-1-14

Pérez, N., Seco, M. V., Valenciano, J. B., and Lorenzana, A. (2006). Use of suction-trap and moericke traps for monitoring the migration of damson-hop aphid (*Phorodon humuli*) (Hemiptera, aphididae). *New Zeal. J. Crop Hortic.* 35, 455–461. doi: 10.1080/01140670709510214

Qiao, G. X., Qin, Q. L., Liang, H. B., Cao, Y. Z., Xu, G. Q., CAO, Z. L., et al. (2011). A new aphid-monitoring network system based on suction trapping and development of "Green techniques" for aphid management (in Chinese). *Chin. J. Appl. Entomol.* 48 (6), 1596–1601.

Qin, M., Chen, J., Xu, S., Jiang, L., and Qiao, G. (2021). Microbiota associated with *Mollitrichosiphum* aphids (Hemiptera: Aphididae: Greenideinae): Diversity, host species specificity and phylosymbiosis. *Environ. Microbiol.* 23 (4), 2184–2198. doi: 10.1111/1462-2920.15391

Robert, Y. (1987). "Aphids and their environment: Dispersion and migration," in *Aphids: Their biology, natural enemies and control*. Eds. A. K. Minks and P. Harrewijn (Amsterdam: Elsevier), 299–313.

Rolph, G., Stein, A., and Stunder, B. (2017). Real-time environmental applications and display system: Ready. *Environ. Model. Software* 95, 210–228. doi: 10.1016/j.envsoft.2017.06.025

Stein, A. F., Draxler, R. R., Rolph, G. D., Stunder, B. J. B., Cohen, M. D., and Ngan, F. (2015). Noaa's hysplit atmospheric transport and dispersion modeling system. *Bull. Amer. Meteor. Soc* 96, 2059–2077. doi: 10.1175/BAMS-D-14-00110.1

Stein, A. F., Isakov, V., Godowitch, J., and Draxler, R. R. (2007). A hybrid modeling approach to resolve pollutant concentrations in an urban area. *Atmo. Environ.* 41 (40), 9410–9426. doi: 10.1016/j.atmosenv.2007.09.004

Stunder, B. J. B., Heffter, J. L., and Draxler, R. R. (2007). Airborne volcanic ash forecast area reliability. *Weather Forecast* 22 (5), 1132–1139. doi: 10.1175/WAF1042.1

Sun, J. J., Li, Q., Tan, X. L., Fan, J., Zhang, Y., Qin, Y. G., et al. (2022). Population genetic structure of *Sitobion miscanthi* in China. *J. Integr. Agric.* 21 (1), 178–187. doi: 10.1016/S2095-3119(20)63445-1

Tsuchida, T., Koga, R., Horikawa, M., Tsunoda, T., Maoka, T., Matsumoto, S., et al. (2010). Symbiotic bacterium modifies aphid body color. *Science* 330 (6007), 1102–1104. doi: 10.1126/science.1195463

Wang, C., Li, X., Jin, D., Gong, P., Li, Q., Zhang, Y., et al. (2022a). Implications of environmentally shaped microbial communities for insecticide resistance in *Sitobion miscanthi*. *Environ. Res.* 215 (Pt 2), 114409. doi: 10.1016/j.envres.2022.114409

Wang, X., Yang, X., Zhou, L., Wyckhuys, K. A., Jiang, S., Van Liem, N., et al. (2022b). Population genetics unveils Large-scale migration dynamics and population turnover of *Spodoptera exigua*. *Pest. Manage. Sci.* 78 (2), 612–625. doi: 10.1002/ps.6670

Wang, Y., Stein, A. F., Draxler, R. R., Rosa, J. D. D. L., and Zhang, X. (2011). Global sand and dust storms in 2008: Observation and hysplit model verification. *Atmo. Environ.* 45 (35), 6368–6381. doi: 10.1016/j.atmosenv.2011.08.035

Westbrook, J. K., Nagoshi, R. N., Meagher, R. L., Fleischer, S. J., and Jairam, S. (2016). Modeling seasonal migration of fall armyworm moths. *Int. J. Biometeorol.* 60 (2), 255–267. doi: 10.1007/s00484-015-1022-x

Xu, S., Jiang, L., Qiao, G., and Chen, J. (2020). The bacterial flora associated with the polyphagous aphid *Aphis gossypii* glover (Hemiptera: Aphididae) is strongly affected by host plants. *Microb. Ecol.* 79 (4), 971–984. doi: 10.1007/s00248-019-01435-2

Xu, S., Jiang, L., Qiao, G., and Chen, J. (2021a). Diversity of bacterial symbionts associated with *Myzus persicae* (Sulzer) (Hemiptera: Aphididae: Aphidinae) revealed by 16s rRNA illumina sequencing. *Microb. Ecol.* 81 (3), 784–794. doi: 10.1007/s00248-020-01622-6

Xu, T. T., Chen, J., Jiang, L. Y., and Qiao, G. X. (2021b). Diversity of bacteria associated with hormaphidinae aphids (Hemiptera: Aphididae). *Insect Sci.* 28 (1), 165–179. doi: 10.1111/1744-7917.12746

Zhou, X. Y., Wu, Q. L., JIA, H. R., and Wu, K. M. (2021). Searchlight trapping reveals seasonal cross-ocean migration of fall armyworm over the south China Sea. *J. Integr. Agric.* 20, 673–684. doi: 10.1016/S2095-3119(20)63588-2

Zhu, A. A., Li, S. M., and Ma, C. S. (2021a). Extreme Climate Shifts Pest Dominance Hierarchy through Thermal Evolution and Transgenerational Plasticity. *Funct. Ecol.* 35 (7), 1524–1537. doi: 10.1111/1365-2435.13774

frontiers | Frontiers in Plant Science

TYPE Review
PUBLISHED 19 July 2023
DOI 10.3389/fpls.2023.1150748

OPEN ACCESS

EDITED BY
Leonardo Abdiel Crespo Herrera,
International Maize and Wheat Improvement Center, Mexico

REVIEWED BY
Munir Ahmad,
Pir Mehr Ali Shah Arid Agriculture University, Pakistan
Loris Nanni,
University of Padua, Italy

*CORRESPONDENCE
Torsten Will
torsten.will@julius-kuehn.de

RECEIVED 24 January 2023
ACCEPTED 26 June 2023
PUBLISHED 19 July 2023

CITATION
Batz P, Will T, Thiel S, Ziesche TM and Joachim C (2023) From identification to forecasting: the potential of image recognition and artificial intelligence for aphid pest monitoring.
Front. Plant Sci. 14:1150748.
doi: 10.3389/fpls.2023.1150748

From identification to forecasting: the potential of image recognition and artificial intelligence for aphid pest monitoring

Philipp Batz[1], Torsten Will[2*], Sebastian Thiel[1], Tim Mark Ziesche[2] and Christoph Joachim[3]

[1]ALM – Adaptiv Lernende Maschinen – Gesellschaft mit beschränkter Haftung (GmbH), Nisterau, Germany, [2]Institute for Resistance Research and Stress Tolerance, Julius Kühn-Institute, Federal Research Centre for Cultivated Plants, Quedlinburg, Germany, [3]Institute for Plant Protection in Field Crops and Grassland, Julius Kühn-Institute, Federal Research Centre for Cultivated Plants, Braunschweig, Germany

Insect monitoring has gained global public attention in recent years in the context of insect decline and biodiversity loss. Monitoring methods that can collect samples over a long period of time and independently of human influences are of particular importance. While these passive collection methods, e.g. suction traps, provide standardized and comparable data sets, the time required to analyze the large number of samples and trapped specimens is high. Another challenge is the necessary high level of taxonomic expertise required for accurate specimen processing. These factors create a bottleneck in specimen processing. In this context, machine learning, image recognition and artificial intelligence have emerged as promising tools to address the shortcomings of manual identification and quantification in the analysis of such trap catches. Aphids are important agricultural pests that pose a significant risk to several important crops and cause high economic losses through feeding damage and transmission of plant viruses. It has been shown that long-term monitoring of migrating aphids using suction traps can be used to make, adjust and improve predictions of their abundance so that the risk of plant viruses spreading through aphids can be more accurately predicted. With the increasing demand for alternatives to conventional pesticide use in crop protection, the need for predictive models is growing, e.g. as a basis for resistance development and as a measure for resistance management. In this context, advancing climate change has a strong influence on the total abundance of migrating aphids as well as on the peak occurrences of aphids within a year. Using aphids as a model organism, we demonstrate the possibilities of systematic monitoring of insect pests and the potential of future technical developments in the subsequent automated identification of individuals through to the use of case data for intelligent forecasting models. Using aphids as an example, we show the potential for systematic monitoring of insect pests

through technical developments in the automated identification of individuals from static images (i.e. advances in image recognition software). We discuss the potential applications with regard to the automatic processing of insect case data and the development of intelligent prediction models.

KEYWORDS

deep learning, convolutional neural network, integrated pest management, decision support systems, image based identification, applied entomology, transformer models

1 Introduction

Aphids (Hemiptera: Aphidoidea) are among the most important insect pests of arable and horticultural crops. These soft-bodied, phytophagous insects mostly feed on phloem sap of plants using a piercing-sucking stylet (Dixon, 2012). There are more than 5,500 aphid species worldwide with approximately 250 species considered as economically relevant pest species (Blackman and Eastop, 2006; Favret, 2018). On a local scale, only a limited number of species are monitored regularly, whereas the composition and number of species collected within a year varies significantly between successive years with a trend of an increase in species numbers, as demonstrated for Great Britain and France between 1978 and 2000 (Hullé et al., 2010).

Migrating aphids are of special interest for agriculture in spring and fall, when they form initial infestation sites in fields, which can lead to crop yield losses by direct feeding damage due to nutrient withdrawal or through secretion of saliva as well accompanied by the transmission of phytopathogenic viruses (Robert et al., 2000; Girousse et al., 2005; Giordanengo et al., 2010). Direct feeding damage has been shown for e.g. the Bird cherry-oat aphid, *Rhopalosiphum padi*, in spring wheat with yield reduction of up to 20% (Voss et al., 1997) and Black bean aphids *Aphis fabae* in sugar beets can cause up to 50% reduction in root dry weight (Hurej and van der Werf, 1993). Average percentage losses have been estimated between 4% and 46% for potatoes and field beans, respectively (Tatchell, 1989). However, estimations of economic losses by direct feeding damage as a consequence of aphid infestation in the field are scarce.

Furthermore, aphids transmit viruses that can cause serious plant diseases (Stevens and Lacomme, 2017). Many phytopathogenic viruses use aphids as vectors, such as *Barley yellow dwarf virus* (BYDV) in e.g. barley and wheat, *Turnip yellows virus* in e.g. winter oilseed rape, *Potato virus Y* in potato and *Beet yellows virus* in sugar beet. In total, approximately 275 different viruses are vectored by 192 different aphid species (Nault, 1997) not including the recently described group of nanoviruses, which are transmitted by the pea aphid *Acyrthosiphon pisum* and infect legumes (Gaafar and Ziebell, 2020; Lal et al., 2020). Although many viruses have the potential to cause significant crop losses, a high percentage of economic losses are most likely to be attributed to individual fields or limited spatial areas. Regarding BYDV, a more recent estimation by an expert assessment estimates the economic losses of a BYDV infection for NW-Europe to be 3.26% per year (Savary et al., 2019).

In 2013, the European Union (EU) decided on a ban of three insecticides from the group of neonicotinoids for seed coating (clothianidin, imidacloprid and thiamethoxam) which hitherto was one of the most efficient and economic options to protect seedlings and young plants against early infestation by phytophagous insect pests, such as aphids, and insect-transmitted viruses (Verheggen et al., 2022). While exemptions for seed and soil treatment in certain cereals were possible between 2013 and 2018, since then the use of the mentioned neonicotinods is restricted to greenhouse uses only (European Union, 2018). In addition, the EU decided not to renew the authorization of thiacloprid, a commonly used insecticide of the same group, from the beginning of 2021 (Commission Implementing Regulation (EU) 2020/23, 2020). Due to the lack of equivalent alternatives, the control of insect pests and pest associated pathogens became more difficult. As a consequence, the pressure on agricultural yield stability is increasing as resistance to insecticides, e.g. pirimicarb belonging to the group of carbamates and pyrethroids, has been observed for several years in Germany, other European countries (Nauen and Elbert, 2003) as well as on a worldwide scale (Edwards et al., 2008). Studies on the Green peach aphid, *Myzus persicae*, in France indicate that the expansion of monocultures and the intensification of insecticide use lead to the selection for resistance against organophosphates and pyrethroids in the field (Zamoum et al., 2005). Selection of individual biotypes has also been observed in the English grain aphid *Sitobion avenae* in Great Britain (Llewellyn et al., 2003). Occasional prophylactic, large-scale or non-targeted insecticide applications are drivers of emerging resistance in a number of different aphid species (Bhatia et al., 2011), but also with the number of approved insecticidal active substances decreasing the risk of resistance development against the remaining substances increases (Després et al., 2007).

It becomes evident that this development, i.e. the reduction of available active ingredients in plant protection products in combination with increasing insect resistance against remaining insecticides, increases the potential of aphid induced yield losses in agricultural production systems. To counteract these losses, continuous monitoring of aphids in agricultural landscapes will become essential for yield stability, since aphid abundances and diversity as well as viral load of aphids are factors that may affect crop growth and plant virus transmission. A high temporal resolution of the crops' pest pressure is of great economic

importance to farmers. Additionally, monitoring data will improve the understanding of the impact of climate change on pest development and migration, hence building a basis to improve forecasting models. This kind of monitoring could be achieved by comprehensive mass trapping using yellow pan traps at local and suction traps at regional scales (e.g. Harrington et al., 2007; Kirchner et al., 2013). The biggest constraints for the utilization of such traps are, however, the limited availability of expert knowledge for species identification and the time-consuming manual identification process.

Recent advantages in artificial intelligence (AI) enabled the development of automated solutions for insect identification and classification. By efficiently processing large amounts of images without human intervention, these methods offer a possible solution in the context of time sensitive analysis and the shortage of adequate expertise mentioned above. In this review, we use aphids as a model organism to evaluate the potential of image recognition and AI in agricultural pest monitoring. We give an overview of the current methods of insect monitoring, possibilities of species identification and demonstrate how image recognition could support the identification process of high sample quantities from mass trap catches. We conclude by showing how data generated this way could be utilized for forecasting models.

2 Aphid monitoring

2.1 Aphid sampling

For targeted protection of agricultural field crops, it is mandatory to assess the temporal and spatial occurrence of harmful organisms (Barzman et al., 2015), i.e. insect monitoring is fundamental for the development of control strategies following the guidelines of integrated pest management. This way, prophylactic applications of plant protection products can be avoided, since beside ecological aspects, prophylactic applications do not guarantee a reduction in pest pressure and can be economically questionable, as aphid occurrence can vary greatly from year to year, with seasonal and regional variations in composition and abundance (e.g. Dixon, 2012; Luquet et al., 2019; Bell et al., 2020). Recent data also indicate that regional synchrony between aphid populations will decrease as a consequence of climate change (Sheppard et al., 2016), making small scale monitoring even more important for addressing regional fluctuations in pest occurrence.

For agricultural monitoring purposes, a wide range of active or passive sampling techniques enables aphid monitoring either on the crop or *via* aerial sampling (Harrington and Hullé, 2017). In order to assess the potential benefits of AI on samples from these methods, knowledge of the common methods used to monitor aphids is essential and is provided below:

Crop sampling is best suited to determine aphid infestation rates and aphid abundance at a field scale. Although this sampling method is outside the focus of this review, we give a brief summary for the sake of completeness. In everyday agricultural practice, visual aphid observation or *in-situ* aphid counts on plants or plant parts are carried out by an on-site human observer and allow farmers, advisors and growers to directly assess local, economic relevant thresholds and apply control strategies according to them. These strategies can, however, only be adequately applied on fields where the aphid pest pressure has been assessed, since crop sampling is limited by poor spatial and temporal resolution (Preti et al., 2021). General conclusion on aphid infestation on a wider, regional scale cannot be drawn from individual fields, since aphid infestation levels can vary considerably between fields within a region (Holland et al., 2021).

Aerial sampling, in contrast, relies on flying aphids. These sampling methods can disclose information about the (first) flight activity, the immigration of aphids into and emigration out of the crops as well as the duration of the flight period not only on the local, but also on regional scale (Bell et al., 2015; Harrington and Hullé, 2017). Thus, aphid monitoring by aerial sampling is crucial for monitoring aphid vectors of plant viruses and managing plant virus spread (Krüger and van der Waals, 2020). Here, yellow pan traps and suction traps are the most commonly used autonomous and technically standardized trapping devices to assess aphids in arable crops by farmers, agronomists and scientists.

Pan traps, are (colored) trays filled with liquid that attract and trap flying insects by inducing their landing behavior (Moericke, 1951). An overview for insect monitoring using pan traps has recently been provided by Montgomery et al. (2021). In brief, pan traps are typically placed in open areas, e.g. directly into the crop, with a respective distance to the field margins with the trapping height adjusted to the vegetation level, i.e. initially on the soil between crop plants and later elevated above the crop canopy. Depending on the intended species or group to be monitored, traps of different colors can be utilized. For monitoring aphids, yellow pan traps have shown the greatest trapping efficiency, especially when placed on a high contrast background, e.g. on dark soil (Döring and Chittka, 2007; Döring, 2014). Although selective for certain aphid species (Karl, 1991), over 90 aphid species have been described to be frequently caught in yellow pan traps in Central Europe, among them around 35 species with agricultural relevance (Müller, 1975; Dubnik, 1991; Basky, 1993). Due to their good trapping ability, pan traps are used in a wide range of arable crops, including e.g. sugar beet, legumes and cereals, to assess the initial flight activity and generally monitor migrating aphids on a local scale. Here, vector monitoring in seed potatoes is of particular importance worldwide (Boiteau and Parry, 1985; Harrington et al., 2009; Vučetić et al., 2013; Kim and Kwon, 2019). As an alternative to pan traps, also colored sticky traps can be used to obtain relative measurements of insect populations (Heinz et al., 1992). Instead of being caught in a liquid, here, individuals stick to an adhesive, colored surface of variable size. While catch rates differ depending on traps size and vertical or horizontal orientation (Heathcote, 1957), for some aphid species sticky traps possess better catch rates than pan traps (O'Loughlin, 1963). Since the animals are trapped on the sticky surface, regular visual checks are mandatory to avoid overfull traps where animals overlap. Only this way, an evaluation and identification of the catches is possible.

Suction traps are suitable for regional monitoring, which can be extended to a national and multi-national level (Cavalloro, 1987;

Bell et al., 2015; Lagos-Kutz et al., 2020; Ziesche et al., 2020). There are different types of suction traps, with varying technical specifications such as differences in heights, ranging from 1.6 to 12.2 m, leading to a different spatial operating capability (cf. Teulon and Scott, 2006). Even though most of the suction traps present today were installed several decades ago (Macaulay et al., 1988; e.g. Shortall et al., 2009) this approach to monitoring insect pests is far from outdated. In 2001 a dense network of suction traps was established in the Midwest of the USA (Lagos-Kutz et al., 2020) shortly after a first report of the Soybean aphid, *Aphis glycines*, in the year 2000 (Hartman et al., 2001). The suction trap network enabled researchers to observe the rapid spread of *A. glycines* during subsequent years (Ragsdale et al., 2011; Lagos-Kutz et al., 2020). Suction traps have also been used to monitor the spread of the aphid species *Diuraphis noxia* across the USA (Pike et al., 2012).

In Europe, the Rothamsted type suction trap, with a height of 12.2 m, represents the standard trap type for large scale monitoring of migrating aphids in agricultural landscapes, but also collects other flying or drifting arthropod species. Independent of subjective factors, the Rothamsted suction trap can provide technically standardized daily records during the main aphid migration season between April and December (Ziesche et al., 2020). It provides the capability for an absolute population measurement for which insect abundances can be sampled more precisely in comparison to all other methods of aerial catches (Bell et al., 2015). In temperate regions, the life cycle of several aphid species involves host alternation, e.g. between a weed or tree species in winter and an annual crop during summer. Consequently, in these periods, increased numbers of migrating winged aphids can be recorded in suction traps. Additionally, these traps have been proven to provide representative results for monitoring certain aphid populations up to a 30 km perimeter (Starý and Lukášová, 2000). Suction traps conduct sampling with a high degree of temporal resolution over many years and demonstrate their value for arthropod monitoring over large areas (Shortall et al., 2009).

Despite the high potential for agriculture and, for example, the study of climate change effects on species composition, abundance and flight activity of aphids, the operation of a suction trap network requires a lot of work, which is also accompanied by a considerable financial outlay. As a result, networks with a high number of suction traps had to be reduced in size with regard to the number of traps or completely shut down after a few years, as shown for the Soybean Aphid Suction Trap Network in the USA (Lagos-Kutz et al., 2020) and the EURAPHID trap network of the European Community (Cavalloro, 1987). This poses a risk to the collection of long-term data, which is important not only for the study of ecological aspects, but also for the validation, improvement and maintenance of forecasting models.

2.2 Identification methods

The disadvantage of all aerial sampling devices mentioned above is their limited selectivity. Besides aphids, a variety of other winged or wind-borne arthropods can be found in such aerial samples. In order to draw any conclusions from the trap catches for a specific target species or group, the taxa of interest must be identified and distinguished from unwanted bycatch.

Traditionally, taxonomic identification of insects is based on different morphological traits. Currently, this is still the method of choice for identifying insects in field monitoring, e.g. when surveying agricultural pest insects. Specimens are identified by eye either directly on the plant, from traps or collected and brought to the laboratory for closer examination. Based on the target taxa, this method of species identification can be very complex, requires a high degree of taxonomic expertise and well-trained personnel. For many insect groups, there are only a few experts worldwide, and the number of well-trained expert taxonomists is constantly decreasing (Engel et al., 2021). Despite the restrictions of this traditional identification method, it still represents a foundation for biodiversity research and integrated pest management programs. When alternative identification methods are developed, the accuracy of these methods should be compared with manual taxonomic identification. These alternative methods should be comparable with, or exceed, the accuracy of standard taxonomic methods. Here, we give a short overview of emerging and promising technologies with focus on the identification of arable pest insects, but not for standardized monitoring, although the listed methods may possess the ability to provide both.

Environmental metabarcoding enables rapid, accurate and cost-effective identification of known species. Taxonomic species identification is performed by means of a species-specific sequence on the mitochondrial cytochrome-c-oxidase I subunit gene (Hebert et al., 2003) and comparing the sequence to a reference database in private or public archives, such as BOLD (Ratnasingham and Hebert, 2007) or GenBank (Benson et al., 2013). Sequences of about eight million insects worldwide have been deposited in BOLD, including nearly 2000 aphid species. Unfortunately, this standardized method only provides presence/absence data or, as recent studies for quantitative barcoding demonstrate, promising results for estimating relative species abundance for (mixed) bulk samples (Liu et al., 2020). Still, metabarcoding does not allow conclusions to be drawn about the exact number of individuals. This is, however, of great interest when assessing insect abundance, including the presence of virus transmitting aphid species, and the severity of immigration flights for pest management actions.

Entomological radar is a remote sensing method that has recently been reviewed by Noskov et al. (2021): With radar, insects can be identified down to species level based on wing beat frequency or size. The identification of larger insects has already been demonstrated a few decades ago (Moore et al., 1986) and mass occurrences of smaller insects including biomass can be detected (Leskinen et al., 2011) but new technologies furthermore show promising results for the differentiation of smaller insects (Wang et al., 2017). Thus, there is a perspective for species and individual identification using entomological radar (Hu et al., 2020). While entomological radar provides the opportunity for a standardized identification and monitoring of flying insects at broad spatial and temporal scales, the identification of many animals in short time intervals, comparable to the catch rate of suction traps, is currently not possible using classical radar technologies. In contrast,

entomological laser radar, such as light detection and ranging (LIDAR), enables high sample rates, even for small insects, but currently possess limited identification capabilities (Brydegaard et al., 2021).

Infrared sensors (IR) are capable of detecting flying insect activity by using near-infrared LED lights and high-speed photodetectors (Rydhmer et al., 2022): Different parameters such as the wing beat frequency, melanization and wing to body ratio can be recorded in the field, automatically uploaded to a cloud database, and processed via machine learning (ML) and AI. So, the characteristic morphology of different insect groups can be specified, allowing a remote classification of insects to different taxonomic levels.

Image recognition can be utilized by a wide range of applications related to optic detection of insects enabling remote and non-destructive environmental monitoring (Preti et al., 2021). Previous studies on image recognition of insect pests have been limited to feasibility studies (Wäldchen and Mäder, 2018), and image analysis on natural backgrounds (Cheng et al., 2017; Xia et al., 2018; Patel and Bhatt, 2019). Only a few studies addressed insect identification from mass catches (e.g. Valan et al., 2019). First applications for identifying pests in arable crops using image recognition are close to marketability, e.g. yellow pan trap analysis by Xarvio field manager (BASF Digital Farming GmbH) or MagicScout/MagicTrap (Bayer AG). These apps, however, are often tailored to end users and do not allow species identification at a scientific level with the necessary scientific accuracy. Nevertheless, the fast technological process in the field of image recognition, especially in combination with AI (as explained below), and the possibility of a non-destructive identification makes this method one of the most promising tools of species identification and biodiversity research.

3 Image recognition based upon artificial intelligence

3.1 Artificial Intelligence methods

In recent years, AI methods have found applications in various fields of science and engineering (Sarker, 2021). The technical possibilities due to increasing computing capacity allow efficient automated evaluations of very large, high-dimensional data such as images and videos. Foremost, deep learning (DL) methods have led to a significant improvement in the quality of results, compared to traditional ML methods (LeCun et al., 2015). In contrast to a manual evaluation of repetitive tasks, such as object recognition and classification, automated solutions offer numerous advantages: they are inexpensive, very efficient, scale well with increasing amounts of data and deliver precise and reproducible decisions. Additionally, various open source implementations allow for a quick empirical data evaluation and comparisons between alternative technical approaches. Programming libraries such as TensorFlow, Keras and PyTorch provide a large number of different models and implementations of various methods (some of which are already pre-trained) from DL with a programming environment for an adaption of tools to the specific application at hand.

As a result, automated DL solutions are widely used in various application areas in biology, agricultural sciences, and ecology (Kamilaris and Prenafeta-Boldú, 2018). Due to the repetitive nature of insect identification, these methods appear to be a suitable tool for the sample analysis of insect mass catches from pan and suction traps (see above).

3.2 Machine learning/Image recognition

Many authors, reporting success stories in their disciplines employing AI, use the terms artificial intelligence, machine learning and deep learning almost interchangeably. However, in technical literature, these terms refer to slightly different subject matters (Goodfellow et al., 2016).

AI is the umbrella term for any computer program that can learn from its environment and make decisions based on what it has learned. Specifically, AI encompasses the fields of ML as well as DL, but also includes approaches such as symbolic AI, which relies on a set of given symbolic rules in order to execute its tasks.

ML on the other hand refers to a subset of AI that uses algorithms to learn from data, rather than relying on explicit programming. Based on a set of data, an underlying model is being trained such that the relevant rules for predicting and explaining new data are automatically learned instead of given a priori.

One specific sub-field of ML is DL, which uses a cascade of multiple layers in order to learn increasingly complex representations in the data. The complexity of a representation is defined by the non-linearity and intricacy of the function it can produce given its parameters. DL is based on neural networks, which use a biologically inspired network of interconnected nodes for learning. Each node in the network is connected to other nodes, and the connections between nodes are weighted to represent the strength of the relationship between them. The nodes in the network are organized into layers, with each layer representing a different level of abstraction. The depth of the model is denoted by its number of layers, where in practice, DL networks with up to hundreds of layers are being used.

In ML and DL, model evaluation is typically achieved by dividing the data into a training set and a test set. The model is trained on the training set and its performance is evaluated on the test set. Sometimes, an additional evaluation dataset, known as a validation set, is used during the model development and hyperparameter tuning process in order to assess the model's performance, while the test dataset is only applied in the final evaluation of the learned model. Here, the idea is to allow for a better estimate of the generalization error of the model by avoiding overfitting to the test set during the learning process.

As evaluation metrics, *accuracy*, i.e. the proportion of correct predictions to total predictions, *precision*, i.e. the proportion of true positive predictions to all positive predictions, and *recall*, i.e. the proportion of true positive predictions to all actual positive

instances, are commonly used. These metrics measure the model's ability to generalize to new data and make accurate predictions.

For image recognition applications DL methods are the most common. The most popular type of DL algorithms are Convolutional neural networks (CNNs). CNNs use a combination of convolutional layers, pooling layers, and fully connected layers to identify and classify objects in an image (O'Shea and Nash, 2015). The convolutional layers extract features from an image, such as edges, shapes, and textures, while the pooling layers reduce the size of the feature maps image, while maintaining the relevant information. Fully connected layers, i.e. types of layers that connect every neuron in one layer to every neuron in another layer, are then used to make predictions based on the extracted features. The successive layers start by capturing small scale patterns and progressively move to representations of larger image sections (Figure 1).

Recently, so called Vision Transformers (ViTs) have gained popularity in the computer vision community due to their competitive performance to the current state-of-the art CNNs in a number of image classification tasks (Dosovitskiy et al., 2020). While both, CNNs and ViTs, belong to the class of DL methods, they exhibit distinct architectural differences. CNNs process image data in a hierarchical manner, extracting local features that gradually combine to form global representations. In contrast, ViTs divide images into patches, on which a method called self-attention is being applied in order to capture both, local and long-range dependencies, within the patches. By attending to all patches and considering their relationships, ViTs can capture contextual information and understand the global structure of an image. Capturing long-ranging dependencies leads to better contextual understanding and the spatial nature of the self-attention mechanism of ViTs to a better interpretability of results.These abilities offer an advantage of ViTs over CNN models. ViTs are, however, challenging regarding their application as they require a high demand of computational and memory resources as well as larger training sets in order to adequately generalize and overcome sensitivity to variations in input data.

In contrast to DL methods, there are the classic approaches of ML, which employ a data representation by means of only one or two layers. This class of methods such as kernel learning or Bayesian methods (sometimes called shallow learning in the literature in contrast to DL) were the dominant approaches before the breakthrough of DL in recent years (Bishop, 2009).

Usually, when using classical ML methods, the data representation is not learned, but manually annotated instead. Ideally, handcrafted feature selection should transform the original data into a much lower dimensional space while retaining the information necessary for identification. In practice this process turns out to be time consuming and requires deep understanding of the data and the specific task at hand. Hence, the ease of automatically learning data representation in tandem with their good scalability and performance on big data sets have made DL a much more attractive alternative to the classical approaches especially in image recognition tasks.

One way to gain better interpretability and intuitive insight into the learned DL model is by creating synthetic data with the help of Generative Adversarial Networks (GANs) and subsequently comparing the generated images with real world input (Goodfellow et al., 2014). Also, Grad-CAM (Gradient-weighted Class Activation Mapping) is a technique used to provide interpretability in neural networks by visualizing which regions of an image are most important for a given identification or classification task (Selvaraju et al., 2020).

The need for large data sets to train DL models successfully is a well-known problem, especially in applications where additional data is unavailable or can only be gathered with significant costs and efforts. This is frequently the case in challenging image recognition tasks, such as insect identification, which often require hundreds of examples for each species but where specimens of rare species are hard to come by (Borowiec et al., 2022). Fortunately, the use of

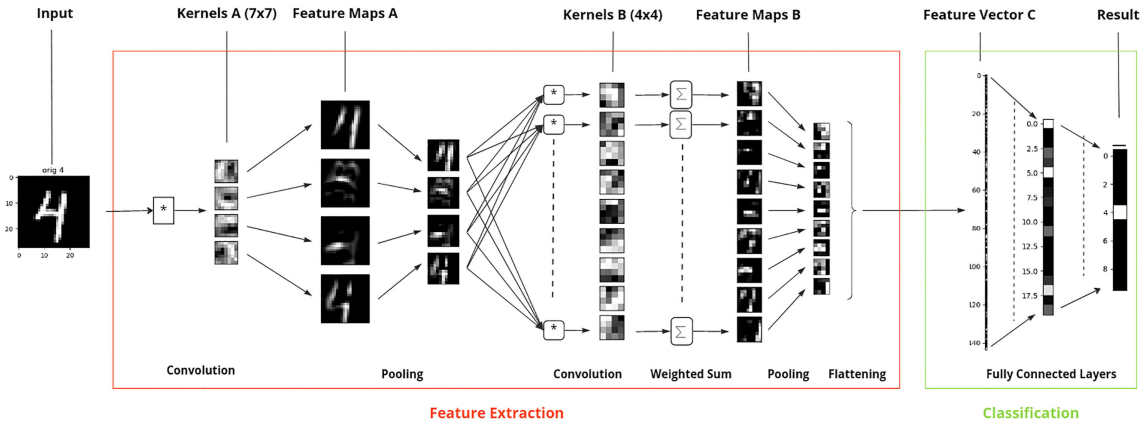

FIGURE 1
Example of image recognition, here digit identification (range 0 to 9), by convolutional neural networks based on the MNIST database. Starting from left to right, the input image ("4"), the image features are first extracted (red box) and then the image representation based on this feature vector is used for classification (green box). The underlying CNN consists of - six layers, where the first two pairs of convolutional and pooling layers are used for extracting relevant feature information from the image for digit identification and the remaining two layers for classifying the image into one of the ten digit classes. Here, the digit "4" is correctly classified to its true label.

transfer learning techniques in cases of sparse data availability have achieved surprisingly good results in a number of different applications in practice, even in cases of highly specific image recognition tasks. Instead of learning a new model from scratch, transfer learning is a technique that allows a trained model to leverage the features learned from the original task and use them to improve performance on the new task. This technique is useful when the new task has a similar data distribution to the original task. The weights of the pre-trained model are used as the starting point for the new task and the model is then fine-tuned on the new data to improve its accuracy. In addition to reducing the amount of training data needed for successful training the time required in order to train the model can often be reduced by using transfer learning (Tan et al., 2018; Wang and Deng, 2018; Zhuang et al., 2021).

Image recognition tasks commonly use a number of different transfer learning architectures, with ResNet, Inception, VGG and YOLO being the most popular. Transfer learning models are pre-trained on large datasets such as ImageNet and COCO (Common Objects in Context). COCO is an image recognition dataset designed for object detection, segmentation, and captioning with 330,000 images and 80 object categories, while ImageNet refers to a dataset containing over 14 million images and 1,000 object categories, which include common objects and concepts such as animals, vehicles, and everyday items. The YOLO architecture (Bochkovskiy et al., 2020*)* was pre-trained on the COCO data, while ResNet (He et al., 2016), Inception *(*Szegedy et al., 2015*)* and VGG (Simonyan and Zisserman, 2015) used ImageNet for pre-training.

3.3 Segmentation, classification and instance segmentation

Most applications in image recognition involve segmentation or classification tasks. Image segmentation refers to the subdivision of an image into multiple segments or regions. This includes both a delimitation of the objects from non-relevant image areas ('background') as well as the differentiation of relevant objects from each other ('instances'). Image classification describes the assignment of an entire image to one of the possible specified classes.

However, in many practical classification scenarios like insect or plant identification, the images to be analyzed frequently contain a number of different instances, each of which must first be identified and isolated in the image before the classification of each individual instance can take place. This combination of image segmentation and classification, which is referred to as instance segmentation in the literature, poses a challenge in many entomological applications: Images from mass trap catches, for instance, usually contain a great number of individuals, comprised not only of different target species but also non relevant by-catch and impurities (Cesaro Júnior et al., 2022), and can possess a high sample density, where individual animals and/or impurities may touch or overlap each other (Borowiec et al., 2022).

There are a number of different approaches to solve the instance segmentation problem- the most popular is Mask R-CNN, a two-stage CNN that first detects and subsequently segments objects in an image (He et al., 2017). The first stage uses a fully convolutional network to generate object proposals and classify those proposals. The second stage generates masks for each object proposal, indicating the area in an image where a relevant object could be located. The masks are then merged, and the resulting segmentation is used to generate the final output.

Several methods are described for the task of classification (Bishop, 2009; Goodfellow et al., 2016). In the context of DL, a softmax classifier, consisting of a fully connected layer followed by a softmax activation function is typically used as the output layer for CNNs as well as ViTs. The softmax function produces a probability distribution over the predefined classes, and the class with the highest probability is considered as the prediction for that input. Further popular choices, used in ML as well as in DL, are support vector machines classifiers, decision trees and random forests, where the latter are an ensemble method of decision trees, combining the results of multiple trees for the final prediction (Wilf et al., 2016; Segev et al., 2017; Wei et al., 2017; Zhang and Zhu, 2018).

3.4 Overview: Image classification in entomology

In recent years, there has been a growing interest in applying segmentation and classification techniques to automated insect identification (Martineau et al., 2017; Xia et al., 2018; Zhong et al., 2018). Due to the many challenging tasks of image based expert level identification, fully automatic solutions without the need for manually designed features used in ML only became feasible recently, following the development of DL algorithms. Here, expert level identification means a taxonomic identification of morphologically similar specimen with a high level of accuracy. In many cases, these identification tasks can be challenging even for a human with expert knowledge, e.g. when a species determination is based on small morphological features as in many aphids (cf. Thieme, 1989).

Up to now, publications in the field of insect identification on a species level with a high degree of morphological similarity using AI methods are scarce. In practice, the bottleneck is often the lack of available high quality training data labeled by a human expert, which is, in turn, required for solving complex classification problems. Here, the application of transfer learning methods offers a convenient approach, with good to great performance for a number of different image based classification problems (Borowiec et al., 2022). Next, we will provide a short literature overview of DL based insect identification on data with a high degree of morphological similarity. We note that the approaches discussed below are supervised methods which are unable to detect species that are not included in the training data set. In the field of entomology, very few publications discussing unsupervised techniques for identifying insect instances of an undescribed

species exist at the moment. Hitherto, the approaches discussed mainly demonstrate the viability of unsupervised insect identification and are not applicable to real world scenarios, especially with respect to more challenging tasks involving morphological similarity (Badirli et al., 2021).

One recent study was done by Valan et al. (2019), who examined two data sets with a limited number of training data. The first analysis concerns the identification of three closely related species of the Coleoptera genus *Oxythyrea* (339 images), the second example involved nine species of Plecoptera larvae (3,845 images). For both tasks DL based classification achieved better results than manual identification with 97% accuracy on the *Oxythyrea* data set and 98.6% on the Plecoptera data. The images of both datasets were not recorded within a natural setting, but rather possess a monochrome background with slight variations in lighting conditions.

For both experiments, a transfer learning based on the CNN architecture VGG16, a convolutional neural network with 16 layers pre-trained on the ImageNet dataset, in conjunction with a linear support vector machine (SVM) classifier was used.

Transfer learning has also been successfully used in challenging identification problems for non-biting midges (Milošević et al., 2020) and adult mosquitos (Motta et al., 2020). Milošević et al. (2020) used a dataset of 1,846 specimens from 10 morphologically very similar species, achieving over 98% accuracy on test data with a CNN architecture ResNet-50, a 50 layered network and therefore significantly deeper than the 16 layer of the VGG16 model used by Valan et al. (2019). Although more complex than VGG16, this model could be reliably trained with under 200 examples per class on average. One reason for the high accuracy is the lab based image acquisition protocol used, which ensured a fixed object position, camera view and angle for each midge from the test data. By closely limiting the variability of the images being used the task complexity implied by the learned feature representation can be significantly reduced, therefore requiring only a modest amount of data. In many applied applications such an intense preprocessing of data for instance in the case of mass trap images is impractical. Instead, one would rather try to learn variable orientations of animals by including relevant images in the training data or alternatively by using preprocessing tools such as automatic rotation and positioning to a reference position (Figure 2).

In an additional example, presented by Motta et al. (2020), different transfer learning models were trained to separate mosquitoes from other insects, as well as to classify mosquitoes of genus *Aedes* in comparison to *Culex*. Using a training set of 7,561 mosquito and 1,187 images of beetles, spiders and bees labeled as "other", identification accuracies of 93% and 97% were achieved. The images used are captured in different resolutions and show the specimens in various positions to the camera together with differing background structure and color distribution. Still, the transfer learning models used in conjunction with an optimization of learning parameters are able to reliably identify the relevant specimens.

The work by Hansen et al. (2020) represents an example of insect identification with a large number of species. Here, an image library of 65,841 museum specimens containing 361 carabid beetle species was used. All images were scanned according to an imaging protocol that defined light intensity, exposure time and orientation of the specimens. By using a pre-trained Inception-v-3 CNN transfer learning approach, accuracies of 51.9% and 74.9% were achieved for species and genus level, respectively, for the test data. Here, the underlying complexity of the problem due to a large variability of many different species together with subtle morphological differences for some cases leads to a significant amount of misclassifications.

A challenging identification task at a genera level was discussed by Marques et al. (2018), where 44,806 ant specimens from the online database AntWeb comprising 57 different ant genera were used for identification. For each specimen, on average 3.35 images in different orientations were available, in particular head, profile and dorsal views, depicting relevant morphological structures for identification. For identification, two different CNN models were trained: one CNN over all images and views and one ensemble of three CNNs with one neural network for each of the three orientations together with a classifier combining the three answers. In the experiments, the ensemble model (accuracy > 90%) significantly outperforms the standard model (accuracy > 80%), showing that separation into distinct sub-models helps to better preserve morphological information relevant for identification, which in turn leads to better classification.

Nanni et al. (2022) presented an empirical comparison using different transfer learning architectures on three benchmark pest data sets Deng, D0 and IP102. The data sets range from 563 images divided into ten insect classes (Deng) over 4,508 images divided in 40 insect classes (D0) and 75,222 images divided into 102 classes of pests categorized into a hierarchical taxonomy (IP102). Classification of pest data is usually complex, since images collected in the field contain not only the relevant pest objects but also the surrounding environment. Here, the object often constitutes only a small portion of the image. Therefore, fine grained analysis is necessary to differentiate the insect classes, while variability in the images is often high due to variable environmental conditions. As CNNs in this study, six different models (ResNet50, GoogleNet, ShuffleNet, MobileNetv2, DenseNet201, and EfficientNetB0) are being used, where these nets are being evaluated as combinations of models in an ensemble. For the optimization, the authors apply different versions of Adam, a variant of stochastic gradient descent methods. The results show that ensemble methods increase the accuracy in comparison to stand-alone CNNs, with 95.52% accuracy compared to 94.64% (ResNet50) on Deng and 74.11% compared to 73.12% (EfficientNetB0) on IP102. For the D0, an accuracy for the ensemble method of 99.81% is reported. For the Deng dataset a study of six human experts shows accuracy rates between 82% and 96%, so the model exhibits comparable accuracy rates to the most accomplished human experts.

The potential of ViT models in pest classification have been evaluated by Xia et al. (2022). The authors use ResNet50, MMAINet, DNVT and an ensemble learner combining the predictions of these three models in a final classification vote. MMAINet uses an attention mechanism identifying discriminatory image regions, on which fine grained CNN based classification models in different resolutions are being trained. DNVT is a hybrid architecture that combines a DenseNet CNN

FIGURE 2
Example for variable orientations of winged morphs (alatae) of the Green peach aphid, *Myzus persicae*, in a sample basin filled with ethanol (70%). The image contains five aphids in different orientation, ventral **(A)**, dorsal **(B–D)** and lateral view **(E)**. Automatic image segmentation and subsequent rotation of the specimens can be used as a first step to simplify further data analysis (right a-e). Pictures are captured with a Leica Emspira 3 digital microscope.

with the self-attention mechanisms of ViTs, which enables effective feature extraction together global context modeling. The empirical part reports results from the two pest datasets D0 and IP102. On both data sets, the best accuracy is achieved by the ensemble method (99.89% on D0 and 74.20% on IP102). However, a comparison of the accuracy for the individual models ResNet50, MMAINet and DNVT shows that the ResNet50 model performs best for both data sets (99.37% on DO and 71.71% on IP102). Here, the decision between the ensemble method and the ResNet50 for the user is one of accuracy versus computational efficiency, since the latter is computationally significantly less costly than the ensemble method.

Also Liu H. et al. (2022) propose a ViT classification model, which uses two preprocessing techniques for performance improvement. Since ViT models require a substantial amount of training data which cannot be provided by pest data sets, the authors employ a pre-training method to generate suitable training data and subsequently learn discriminative features. Specifically, a FRCF algorithm filters from the ImageNet dataset commonly used in transfer learning techniques a relevant subset, which is similar to the pest data to be classified. Then a ViT based LSMAE model is trained, which extracts a discriminatory feature representation from the semantic information in the image patches. The pest datasets are then used to fine tune the classifier. The evaluation is based on pest data sets IP102, CPB and PlantVillage, where CPB contains 10,816 images of six different mite species and a class of non-mite, while PlantVillage is a plant dataset containing 54,305 images from 14 plant species. The results report state-of-the-art accuracy on all three datasets 74.69% on IP102, 76.99% on CPB and 99.93% on PlantVillage.

In all cases of expert level classification models, deep transfer learning performs superior in terms of prediction accuracy compared to reference study models, indicating that this is the current state of the art approach for image classification in entomology, including aphid identification. The choice of the best model for a certain problem depends on several factors, in particular the number of images of individuals and the image quality of the training dataset, as well as the complexity of the underlying identification problem. The availability of a large number of transfer learning models as open-source software implementations allows for a relatively simple empirical comparison of different approaches.

3.5 Overview: Applications towards aphid identification

Several studies address the identification and classification of aphids. For each of these, the complexity of the respective task varies considerably and depends on factors such as image quality, sample purity and complexity of the samples. The challenges are determined by various factors:

1. Image capturing conditions: Is it possible to create a training set under standardized settings (exposure, image quality, background, body orientation) or does variability have to be created? This requires information from the sample and the future imaging conditions of the samples to be analyzed.
2. Image composition: What sample density is expected for the test set? Animals in dense samples may touch or even overlap each other. When arthropods other than aphids appear in a sample, as is the case for pan and suction trap catches, other taxonomic groups must be considered for classification.
3. Classification: Should aphids only be counted or should a distinction be made into species or species “types”, respectively? How many species should be distinguished, how big are the morphological differences and furthermore, are specimens present in different morphs and developmental stages (nymphs, wingless, winged) and states of conservation? In case that samples from pan and suction traps are analyzed, only winged adult aphids are expected.

3.6 Classical machine learning

Xuesong et al. (2017) used data from sticky boards as a basis for identifying and counting aphids. Statistical methods of classical ML were used as recognition algorithms. Here accuracies of over 90% are reported for both, in the greenhouse and outdoors, where the accuracy in the field experiments turned out to be slightly lower due to differences in diurnal lighting conditions. A distinction between aphids and other insect taxa was based on a simple size measurement, which, however, will not enable a robust differentiation in many practical applications, since several Hymenopteran and Dipteran species possess a comparable body size to aphids.

3.7 Deep learning

A method to analyze and classify populations of *R. padi*, using DL methods was developed by Lins et al. (2020). By segmenting 30,000 individual specimens, the model is capable to distinguish three different developmental stages (nymphs, winged adults, unwinged adults) as well as a differentiation of impurities. Standard image recognition methods were used for segmentation from the sample images, while the classification of the segmented specimens was carried out using CNN Inception-V3. A comparison with a manually performed classification shows a better recognition rate for all three aphid classes, which is quantified by the number of specimens found. The solution of a relatively simple classification problem based on large data processed in the laboratory can thus be readily solved using already available DL procedures.

Another approach is discussed by Hayashi et al. (2019), where the neural architecture search (NAS) tool of Google AutoML Vision is used to identify three aphid species (*Aphis craccivora, A. pisum, Megoura crassicauda*) from plant images. In order to evaluate the influence of the size of the training dataset, different models with a fixed number of training images per species, ranging from 20 to 400 images, were trained. One hundred training images per species were required for an accuracy of over 90% and with 400 images per species an accuracy of over 96% was achieved. However, since the species used in this study are easy to distinguish by the non expert in terms of size and color, the model does not capture the complexities of identifying morphologically similar aphid species.

The presence of aphids on images taken from lemon tree plants in the field, which feature natural background variability and changes in lighting conditions, was solved by Parraga-Alava et al. (2021).To do so, 150 images of plants were taken as training data (70 images of healthy plants, 80 images of plants infested with aphids) and a transfer learning approach with a VGG-16 network architecture was used. The authors report a classification of infested and uninfested plants with rates between 81% and 97% on lemon tree plant images of the test data set. While the objective in this experiment only involved detection of aphids, the variability induced by images taken under changing conditions in conjunction with a small sized training data set made the task more challenging.

Regarding network architecture, an almost comparable approach was used for segmentation and counting of *M. persicae* nymphs and a classification of nymphs and adults on leaves using a transfer learning system with a VGG-13 architecture (Chen et al., 2018). Here, 68 images of different plant leaves, with up to a hundred nymphs per leaf, were used for model training. In the evaluation of the aphid count on the corresponding test images, the model achieved a precision of 95.6% - and a recall of 96.5% respectively. The sample complexity can be considered as low, with no by-catches and only one aphid species and just a distinction into nymphs and adult aphids.

These studies can be regarded as interesting applications for aphid detection adapted either to a specific type of application or to a simplified modeling environment. Hence, their direct applicability in more complex practical scenarios of a wider scope involving many different aphid species of high morphological similarity seems rather limited.

3.8 Deep learning on images from mass trap catches

Cesaro Júnior et al. (2022) introduced a system for insect detection from actual field trap images (yellow pan traps), and studied the performance of an AI approach for samples of different insect density with the aim to develop an online AI tool for integrated pest management. Sample images were complex, containing hundreds of winged insects, including aphids, parasitoids, flies and thrips, all in different orientations and/or partly overlapping. Additional segmentation and identification challenges included the occurrence of contamination (dust and other small particles) as well as specimens in various states of conservation. The latter in particular seems to be of great importance for the analysis of images: While training sets often consist of intact and freshly prepared animals to perform initial learning under optimal conditions, samples from field collections may contain a considerable amount of insect fragments and contaminants. Additionally, trapping aphids in conservation liquid under field conditions can also lead to color change, and with regard to gray-scale images as used by Cesaro Júnior et al. (2022) to changing gray values, but also to a change of body shape due to inflation. The authors used a dataset of 17,908 labeled insects, comprising 9,783 aphids and 8,125 parasitoids. The automated identification and counting of the aphid and parasitoid populations was carried out with a Mask R-CNN algorithm.

To evaluate the method, the computed numbers of aphids and parasitoids were compared with the manual counts of a human expert. Here, equivalent values for precision (85%) and recall (41%) were determined for the examined test images for parasitoids and aphids. Thus, on average, significantly less than half of the relevant specimens (determined by manual counting) could be identified. This shows that the proportion of discovered specimens decreases noticeably with increasing density of animals in the image. As reasons, the authors state the high degree of contamination, the morphological similarity of the bycatch and the target aphids for identification as well as the pose variations. In practice this means that a dilution of the sample could be necessary in samples comprising a high insect density.

Although state-of-the-art methods are used here, the performance is significantly lower than that of comparable entomological studies

dealing with insect counting. The authors attribute this to the complications of pollution, (partial) overlapping of insect bodies and the presence of by-catch as listed above. These interfering factors did not occur in the data sets of the other studies described. This once again illustrates the challenges that have to be taken into account, especially with regard to the acquisition and processing of the images to be examined in an adequate manner in order to facilitate good identification results. The work of Cesaro Júnior et al. (2022) illustrates, that a system that aims to perfectly assign the segmented images to the respective species falls short of a manual evaluation at the current time if a significant proportion of the aphids are not separated from the by-catch beforehand as part of sample processing.

A table with all publicly available datasets discussed in sections 3.4 - 3.8 is provided (Table 1).

3.9 Difference in testing protocols

The papers discussed vary significantly in terms of test setup and data type. Theoretical studies typically assess methods using benchmark datasets, while applied studies address the challenges of practical implementation. These challenges encompass diverse aspects, such as integrating different data sources, like cloud-based solutions, accounting for variable weather conditions affecting field recordings, and managing bycatch and contamination in large-scale captures. Consequently, the test protocols in these experiments are tailored to address specific questions. For instance, they may involve preselecting training and test images or adjusting recording conditions, which distinguishes them from the typically randomized test protocols used in theoretical investigations. Consequently, despite sharing common target values, such as accuracy, the direct comparability of results is often limited in practice.

3.10 Towards expert level identification of aphid species by AI as basis for an automated agricultural pest monitoring (limitations and constraints)

Based on previous studies, the most promising tools for expert level identification of agricultural relevant aphid species by image recognition can be found in the field of DL with the use of CNNs. However, the development of an automated system to record, segment and classify aphids from mass trap catches faces a number of different challenges:

- The sampling method must be suitable for image recognition. Sticky traps, for instance, can have the disadvantage that specimen are partly covered by glue remnants, bycatch or other airborne particles. It is important that the sampling method or sample preparation are adjusted to the needs of ideal image recording and subsequent AI analysis.
- The recorded sample images must be segmented into individual specimens; individuals other than aphids as well as any contamination has to be detected and filtered out during AI analysis.
- Individual specimen are recorded in different orientations to the camera (caudal, lateral, dorsal, ventral, cranial) and may be in contact or overlapping with other insect bodies.
- Depending on the sampling intervals (emptying trap containers) and temperature conditions, aphid individuals may occur in different conservation stages, i.e. the longer aphids stay in the trapping solution the higher the degree of color change and the change of body shape (bloating) in contrast to freshly caught aphids. Furthermore, wax deposits

TABLE 1 Publicly available datasets from different publications that have been discussed in sections 3.4 - 3.8.

Authors	Year	Title	Link
Valan, M., Makonyi, K., Maki, A., Vondráček, D., and Ronquist, F. (Valan et al., 2019)	2019	Automated taxonomic identification of insects with expert-level accuracy using effective feature transfer from convolutional networks	https://datadryad.org/stash/dataset/doi:10.5061/dryad.20ch6p5
Hansen, O. L. P., Svenning, J.-C., Olsen, K., Dupont, S., Garner, B. H., Iosifidis, A., et al. (Hansen et al., 2020)	2020	Species-level image classification with convolutional neural network enables insect identification from habitus images	https://zenodo.org/record/3549369
Marques, A. C. R., M Raimundo, M., B Cavalheiro, E. M., F P Salles, L., Lyra, C., and J Von Zuben, F. (Marques et al., 2018)	2018	Ant genera identification using an ensemble of convolutional neural networks	https://zenodo.org/record/1134690
Wu, X., Zhan, C., Lai, Y., Cheng, M., & Yang, J.	2019	Insect Pest Dataset (IP102)	https://github.com/xpwu95/IP102
Bollis, E., Pedrini, H., & Avila, S.	2020	Citrus Pest Benchmark (CPD)	https://github.com/edsonbollis/Citrus-Pest-Benchmark
Hughes, D.P., & Salathé, M.	2015	Plant Village Dataset	https://www.kaggle.com/datasets/emmarex/plantdisease
Xie, C., Wang, R., Zhang, J., Chen, P., Dong, W., Li, R., Chen, T., & Chen, H.	2018	Xie2 (D0) Dataset	http://www.dlearningapp.com/web/DLFautoinsects.htm

on the cuticule, e.g. typical for different aphid species, may disappear. Regarding the described effects, significant intraspecific differences may appear, with strong effects for some species while for others only slight morphological changes are expected depending e.g. on the color of a species and the melanization of cuticular components. On a more abstract level, this corresponds to the challenging class of classification problems with a high intra-class variance and small inter-class variance. Consequently, these kind of problems require classification methods that are able to model a high degree of complexity, which in turn require a larger number of relevant training examples for reliable and robust classification results.

- Potential morphological difference in-between aphid species must be ruled out or accounted for, when collecting training data.
- Aphid species abundance and species composition can show strong regional variation, possibly also leading to the presence of aphid species with exotic host plants depending upon the location of a trap and the surrounding plant community (Bell et al., 2015). In addition, a spatio-temporal morphological variability has to be taken into account in the training data, as shown for seasonal variation in *M. persicae* (Taylor and Robert, 1984).
- To avoid overfitting of strongly represented classes, it is mandatory to homogenize the training datasets of the classifier for each species.
- High-quality sample data validated by human experts is essential for a precise training of the algorithm. A focus on economically important pest species may help to reduce the complexity of a training data set as rearing of animals in the greenhouse may improve its quality due to a high number of images of the training data set.

Hitherto, to the best of our knowledge, no study presented an adequate solution for AI based expert level aphid identification from mass catches. However, promising models in the broader field of insect identification, demonstrating remarkable results for a variety of different insect species, could be applicable to this specific context.

4 Modeling and forecasting

4.1 State of aphid forecasting

In agriculture, monitoring of, and forecasting models for pest insects, are by their nature related, as forecasting models almost always rely, at least partly, on data derived from monitoring activities. Monitoring and forecasting are conducted and developed, respectively, with the aim to ensure crop protection by continuous improvement of cultivation methods. Measures may include the adjustment of the sowing time to minimize aphid infestation at early crop stages, to plan crop rotation to control pest emergence or diseases spread, and finding the right timing for plant protection measures such as the application of insecticides (Dedryver et al., 2010) in the sense of integrated pest management. This makes it even more important to time the use of crop protection products according to pest infestation. Here, forecasting models can aid the decision making process.

To establish a forecasting model for an insect pest, knowledge about the biology and life history traits of the pest species is mandatory. Additionally, a basic understanding of the development of insect pests in context with environmental conditions, such as weather or climate, is vitally important for the development and improvement of such models. Here long-term monitoring networks, such as the suction trap networks (e.g. Tilman et al., 2006) are designed to study the impact of climatic or environmental changes on population dynamics and effects on the diversity of species on a spatio-temporal scale (Bell et al., 2015).

In the last forty to fifty years, several aphid forecasting models have been developed using a wide variety of modelling approaches, with the aim being to predict the occurrence and population dynamics of different aphid species in arable crops. A table listing the most important studies and aphid models for different crops is included in the Supplementary Material (SM1). A number of the existing models focus on the phenology of a herbivore and its host in relation to abiotic factors, which has proven to achieve significant prediction at a regional level by using monitoring data (Harrington and Hullé, 2017). In addition, models that can predict the migratory behavior of aphids, including arrival time, are of significant interest as these models will identify periods with high migration risk where in-field monitoring efforts could be targeted. Furthermore, as soon as certain aphid pest species occur in e.g. suction or pan traps, subsequent field observations might be necessary to assess aphid abundance on the plant level.

For the holistic evaluation of cropping systems and the further development of alternative crop production strategies, generally model-based methods are used. For aphid pests, these are generally invasion warnings when winged aphids start flying from their overwintering hosts into crops or, with warming winters, when they increasingly survive in the field. Modeling approaches have been developed for numerous important crops and pests such as the simulation model “GTLAUS01”, which modes the population dynamics of three important aphid species in cereals (Gosselke et al., 2001), or “SIMLAUS”, which allows predictions either for a specific crop or for a specific region and aims at forecasting possible outbreaks of BYDV by calculating the probabilities of reproduction and survival of three cereal aphid species (Klueken et al., 2009).

As a practice applied prediction method, near real-time pest incidence data coupled with remote sensing data and GIS tools facilitate early warning of impending pest build-up in space-time resolution, whereat the measure of weather data from pest-affected areas is still an essential input for models (Prasad and Prabhakar, 2012). As insect development is mainly influenced by weather factors, temperature and precipitation data are directly tied to the success of predicting population dynamics in a particular region (Dent and Binks, 2020).

Forecast models are available for potatoes predicting the spread of a Potato virus Y in the current season using trap data of aphid flights (Steinger et al., 2015) to optimize virus control in seed potato production. Qi et al. (2004) review the procedure and decision

making process for controlling *M. persicae* and predicting outbreaks of virus yellows disease in sugar beet in the UK. While surveys began in 1946 and a first virus yellows spray warning scheme was introduced in 1959, the forecasting model has been continuously developed since.

Models often simulate one or a few species and rely on the most complete information possible on the auto-ecological demands of the developmental stages which respond to the prevailing environmental conditions. Still, successful forecasting techniques are those that are as simple as possible and that are based on very precise knowledge of the biology and ecology of the pests concerned (Prasad and Prabhakar, 2012), such as the first flight activity or the survival rate of overwintering aphids in temperate regions.

Thus, forecast models are used as decision-making aids to optimize the temporal and spatial planning of infestation surveys, to estimate the need for control and the scheduling of control measures (Dedryver et al., 2010). Effective decision support tools are required in order to provide agricultural practitioners with advice regarding appropriate and economic pest management strategies (Duffy et al., 2017) and to complement recent changes regarding pesticide regulations in the European Union aimed at a general reduction of pesticide applications (Lechenet et al., 2017).

In practice, however, successful decision making depends upon the availability of integrated, high quality information (Harrington and Hullé, 2017) and the information-base should be ensured continuously and in high resolution by extensive monitoring. Generally and with changing conditions during climate change in particular, forecast models of aphids need to be compared and validated regularly for a wide-scale use in crop protection (Klueken et al., 2009; Zeng et al., 2020).

4.2 Utilization of AI in aphid forecasting

AI could be utilized to assist and enhance aphid pest forecasting in several ways, by 1) automated identification of insects, whether from suction/pan traps or camera-equipped traps, based on image recognition and DL, 2) development of new forecasting models based on ML or neural networks (e.g. Jarošová et al., 2019), and 3) optimizing the monitoring infrastructure to improve predictive models (Bourhis et al., 2021). Due to the objective of this review, we take a closer look at the potential of AI based, automated identification based on image recognition.

Almost all current models use different aspects of the occurrence or abundance of aphid pests in correlation with weather data (SM1). While abiotic factors, such as temperature or precipitation, can be assessed easily over a large spatial scale, and are often provided by meteorological services, the spatial resolution of monitoring locations is often limited. Monitoring networks, with a representative number of monitoring locations (e.g. traps), are often missing, although highly desirable, because to gain robustness in forecasting accuracy, it is mandatory to capture significant spatio-temporal variations in pest insect abundance in suitable numbers over multiple seasons, so subsequent generalized predictions by forecasting models are meaningful (Bourhis et al., 2021). In turn, operating a monitoring network requires at least some sort of pest insect identification, as explained before. This is often the limiting factor for spatially explicit monitoring.

Here, an AI-based automated identification of aphid pests from mass trap catches, but also other traps that require an image based identification, such as camera-equipped traps using image recognition, has a high potential to overcome the current limitations in monitoring insect pests. Benefits are: 1) the handling time (sorting, identification) of catches could be reduced, allowing large catch volumes to be processed in relatively short time and data to be available on a daily basis, 2) the identification is independent of a human expert, with standardized results, as individual person error is eliminated, 3) an AI based identification application can be used at multiple sites or as a cloud application, thus enabling standardized monitoring of aphids within a large monitoring network with high spatio-temporal resolution, 4) thanks to prompt sample processing, invasive insect pests and associated plant diseases can be detected more quickly with a higher success rate.

This way, future forecasting models could be set on a profound basis. Monitoring data, such as aphid flight data, collected over a wide area enables the creation and verification of more accurate models (Bell et al., 2019). This facilitates complex analyses including the interaction of climate change, land use, cultivation methods, and the occurrence of insect pests, but also allows for the optimization of cultivation systems with regard to pest infestation and virus transmission or the influence of global warming on the abundance and distribution of insect pests. In the long term, this would allow for a continuous assessment of the pest potential of individual species.

That these goals are already within reach is shown by a recent study concerning insect pests in cotton fields in China. Liu C. et al. (2022) developed an autonomous pest monitoring and forecasting device that is capable of capturing and transmitting images of phototactic insects caught in a modified light trap. The insect images are subsequently identified on a local server by methods of DL algorithms. Unfortunately, details on species identification were not yet addressed by the authors, since their main focus was to compare different DL methods for background removal to optimize the image for classification. Nevertheless, it clearly demonstrates the potential of automated, AI-based monitoring and outlines the current state of the art.

5 Conclusion and prospects

Information on insect occurrence serves a number of purposes, including research on current scientific questions about changes in biodiversity and species abundance. But also the implementation of important and more applied agricultural tasks such as monitoring the spread of (new) vector-transmitted plant diseases, reducing the use of chemical pesticides as part of the European Green Deal, and the early development of resistant crops in case of the emergence of new pest insects, relies on a profound understanding of the distribution and abundance of insects. This knowledge, however, requires a great amount of insect related data with an adequate temporal and spatial resolution, as was planned to acquire, for example, within the EURAPHIS network.

An automated identification of insect pests, supported by AI as outlined above, could be a promising tool to enable a timely processing of a large number of samples from mass trap catches, which subsequently can lead to timely and highly specific insect pest warnings. The decoupling of the identification process from a human expert and the associated relatively low costs for operation and data analysis could form the basis for comprehensive long-term monitoring activities, not only in Europe, but also in other regions. This form of monitoring is already used at a regional level for biodiversity research. At least for biodiversity research, the importance of such has already been clearly demonstrated at regional level (e.g. Seibold et al., 2019).

The provision of data from mass trap catches in cloud-based databases would allow a large number of research groups to utilize and evaluate the data for various research questions, such as the adaptation of forecast models in connection with climate data and data on regional crop production by AI-based models.

Research activities in image based identification, but also other identification disciplines, will be essential for future biodiversity, and consequently pest insect monitoring.

Author contributions

CJ and TW conceived the idea of this review. PB, TW and CJ wrote the original draft of the manuscript. TZ and ST wrote sections of this manuscript. PB, TW, CJ critically edited the manuscript. ST prepared and revised the figures. All authors contributed to manuscript revision, read, and approved the submitted version. All authors contributed to the article and approved the submitted version.

Funding

The project is supported by funds of the Federal Ministry of Food and Agriculture (BMEL) based on a decision of the Parliament of the Federal Republic of Germany. The Federal Office for Agriculture and Food (BLE) provides coordinating support for artificial intelligence (AI) in agriculture as funding organization, grant number 28DK106A20/28DK106B20.

Acknowledgments

The authors thank Daniel Leybourne for his critical review of the manuscript and valuable comments.

Conflict of interest

Author PB and ST are employed by ALM – Adaptiv Lernende Maschinen – GmbH.

The remaining authors declare that the research was conducted in the absence of any commercial or financial relationships that could be construed as a potential conflict of interest.

Publisher's note

Supplementary material

The Supplementary Material for this article can be found online at: https://www.frontiersin.org/articles/10.3389/fpls.2023.1150748/full#supplementary-material

References

Badirli, S., Picard, C. J., Mohler, G., Akata, Z., and Dundar, M. (2021). Classifying the unknown: identification of insects by deep open-set Bayesian learning. *BioRxiv*, 460492. doi: 10.1101/2021.09.15.460492

Barzman, M., Bàrberi, P., Birch, A. N. E., Boonekamp, P., Dachbrodt-Saaydeh, S., Graf, B., et al. (2015). Eight principles of integrated pest management. *Agron. Sustain. Dev.* 35, 1199–1215. doi: 10.1007/s13593-015-0327-9

Basky, Z. (1993). Identification key for alate aphids caught in yellow pan traps. *Acta Phytopathol. Entomol. Hung.* 28, 71–121.

Bell, J. R., Alderson, L., Izera, D., Kruger, T., Parker, S., Pickup, J., et al. (2015). Long-term phenological trends, species accumulation rates, aphid traits and climate: five decades of change in migrating aphids. *J. Anim. Ecol.* 84, 21–34. doi: 10.1111/1365-2656.12282

Bell, J. R., Blumgart, D., and Shortall, C. R. (2020). Are insects declining and at what rate? an analysis of standardised, systematic catches of aphid and moth abundances across great Britain. *Insect Conserv. Divers.* 13, 115–126. doi: 10.1111/icad.12412

Bell, J. R., Botham, M. S., Henrys, P. A., Leech, D. I., Pearce-Higgins, J. W., Shortall, C. R., et al. (2019). Spatial and habitat variation in aphid, butterfly, moth and bird phenologies over the last half century. *Global Change Biol.* 25, 1982–1994. doi: 10.1111/gcb.14592

Benson, D. A., Cavanaugh, M., Clark, K., Karsch-Mizrachi, I., Lipman, D. J., Ostell, J., et al. (2013). GenBank. *Nucleic. Acids Res.* 41, D36–D42. doi: 10.1093/nar/gks1195

Bhatia, V., Uniyal, P. L., and Bhattacharya, R. (2011). Aphid resistance in *Brassica* crops: challenges, biotechnological progress and emerging possibilities. *Biotechnol. Adv.* 29, 879–888. doi: 10.1016/j.biotechadv.2011.07.005

Bishop, C. M. (2009). *Pattern recognition and machine learning* (New York, NY: Springer).

Blackman, R. L., and Eastop, V. F. (2006). *Aphids on the world's herbaceous plants and shrubs: volume 1: host lists and keys and volume 2: the aphids* (London: John Wiley & Sons Ltd).

Bochkovskiy, A., Wang, C., and Liao, H. M. (2020). YOLOv4: optimal speed and accuracy of object detection. *arXiv [Preprint]*. doi: 10.48550/arXiv.2004.10934

Boiteau, G., and Parry, R. H. (1985). Monitoring of inflights of green peach aphids, *Myzus persicae* (Sulzer), in new Brunswick potato fields by yellow pans from 1974 to 1983: results and degree-day simulation. *Am. Potato. J.* 62, 489–496. doi: 10.1007/BF02854522

Borowiec, M. L., Dikow, R. B., Frandsen, P. B., McKeeken, A., Valentini, G., and White, A. E. (2022). Deep learning as a tool for ecology and evolution. *Methods Ecol. Evol.* 13, 1640–1660. doi: 10.1111/2041-210X.13901

Bourhis, Y., Bell, J. R., van den Bosch, F., and Milne, A. E. (2021). Artificial neural networks for monitoring network optimisation - a practical example using a national insect survey. *Environ. Model. Software* 135, 104925. doi: 10.1016/j.envsoft.2020.104925

Brydegaard, M., Kouakou, B., Jansson, S., Rydell, J., and Zoueu, J. (2021). High dynamic range in entomological scheimpflug lidars. *IEEE J. Sel. Top. Quantum Electron.* 27, 1–11. doi: 10.1109/JSTQE.2021.3062088

Cavalloro, R. (1987). *Aphid migration and forecasting "Euraphid" systems in European community countries* (Luxembourg).

Cesaro Júnior, T., Rieder, R., Di Domênico, J. R., and Lau, D. (2022). InsectCV: a system for insect detection in the lab from trap images. *Ecol. Inform.* 67, 101516. doi: 10.1016/j.ecoinf.2021.101516

Chen, J., Fan, Y., Wang, T., Zhang, C., Qiu, Z., and He, Y. (2018). Automatic segmentation and counting of aphid nymphs on leaves using convolutional neural networks. *Agronomy* 8, 129. doi: 10.3390/agronomy8080129

Cheng, X., Zhang, Y., Chen, Y., Wu, Y., and Yue, Y. (2017). Pest identification *via* deep residual learning in complex background. *Comput. Electron. Agric.* 141, 351–356. doi: 10.1016/j.compag.2017.08.005

Commission Implementing Regulation (EU) 2020/23 (2020). Commission implementing regulation (EU) 2020/23 of 13 January 2020 concerning the non-renewal of the approval of the active substance thiacloprid, in accordance with regulation (EC) no 1107/2009 of the European parliament and of the council concerning the placing of plant protection products on the market, and amending the annex to commission implementing regulation (EU) no 540/2011 (Text with EEA relevance). *O. J.*, 8–11.

Dedryver, C.-A., Le Ralec, A., and Fabre, F. (2010). The conflicting relationships between aphids and men: a review of aphid damage and control strategies. *C. R. Biol.* 333, 539–553. doi: 10.1016/j.crvi.2010.03.009

Dent, D., and Binks, R. H. (2020). "Sampling, monitoring and forecasting," in *Insect pest management*. Eds. D. Dent and R. H. Binks (Boston, MA: CAB International), 12–38.

Després, L., David, J.-P., and Gallet, C. (2007). The evolutionary ecology of insect resistance to plant chemicals. *Trends. Ecol. Evol.* 22, 298–307. doi: 10.1016/j.tree.2007.02.010

Dixon, A. F. G. (2012). *Aphid ecology: an optimization approach* (Dordrecht: Springer Netherlands).

Döring, T. F. (2014). How aphids find their host plants, and how they don't. *Ann. Appl. Biol.* 165, 3–26. doi: 10.1111/aab.12142

Döring, T. F., and Chittka, L. (2007). Visual ecology of aphids - a critical review on the role of colours in host finding. *Arthropod Plant Interact.* 1, 3–16. doi: 10.1007/s11829-006-9000-1

Dosovitskiy, A., Beyer, L., Kolesnikov, A., Weissenborn, D., Zhai, X., Unterthiner, T., et al. (2020). An image is worth 16x16 words: transformers for image recognition at scale. *ArXiv [Preprint]* 11929. doi: 10.48550/arXiv.2010.11929

Dubnik, H. (1991). *Blattläuse: artenbestimmung - biologie - bekämpfung* (Gelsenkirchen-Buer: Mann).

Duffy, C., Fealy, R., and Fealy, R. M. (2017). An improved simulation model to describe the temperature-dependent population dynamics of the grain aphid, *Sitobion avenae*. *Ecol. Modell.* 354, 140–171. doi: 10.1016/j.ecolmodel.2017.03.011

Edwards, O. R., Franzmann, B., Thackray, D., and Micic, S. (2008). Insecticide resistance and implications for future aphid management in Australian grains and pastures: a review. *Aust. J. Exp. Agric.* 48, 1523. doi: 10.1071/EA07426

Engel, M. S., Ceríaco, L. M. P., Daniel, G. M., Dellapé, P. M., Löbl, I., Marinov, M., et al. (2021). The taxonomic impediment: a shortage of taxonomists, not the lack of technical approaches. *Zool. J. Linn. Soc* 193, 381–387. doi: 10.1093/zoolinnean/zlab072

European Union (2018). Consolidated text: commission implementing regulation (EU) no 485/2013 of 24 May 2013 amending implementing regulation (EU) no 540/2011, as regards the conditions of approval of the active substances clothianidin, thiamethoxam and imidacloprid, and prohibiting the use and sale of seeds treated with plant protection products containing those active substances (Text with EEA relevance). ELI. Available at: http://data.europa.eu/eli/r.

Favret, C. (2018) *Aphid species file*. Available at: http://Aphid.SpeciesFile.org (Accessed 5 December 2022).

Gaafar, Y. Z. A., and Ziebell, H. (2020). Aphid transmission of nanoviruses. *Arch. Insect. Biochem. Physiol.* 104, e21668. doi: 10.1002/arch.21668

Giordanengo, P., Brunissen, L., Rusterucci, C., Vincent, C., van Bel, A., Dinant, S., et al. (2010). Compatible plant-aphid interactions: how aphids manipulate plant responses. *C. R. Biol.* 333, 516–523. doi: 10.1016/j.crvi.2010.03.007

Girousse, C., Moulia, B., Silk, W., and Bonnemain, J.-L. (2005). Aphid infestation causes different changes in carbon and nitrogen allocation in alfalfa stems as well as different inhibitions of longitudinal and radial expansion. *Plant Physiol.* 137, 1474–1484. doi: 10.1104/pp.104.057430

Goodfellow, I., Bengio, Y., and Courville, A. (2016). *Deep learning* (Cambridge, Massachusetts, London, England: MIT Press).

Goodfellow, I., Pouget-Abadie, J., Mirza, M., Xu, B., Warde-Farley, D., Ozair, S., et al. (2014). Generative adversarial networks. *arXiv* 2661. doi: 10.48550/arXiv.1406.2661

Gosselke, U., Triltsch, H., Roßberg, D., and Freier, B. (2001). GETLAUS01–the latest version of a model for simulating aphid population dynamics in dependence on antagonists in wheat. *Ecol. Modell.* 145, 143–157. doi: 10.1016/S0304-3800(01)00386-6

Hansen, O. L. P., Svenning, J.-C., Olsen, K., Dupont, S., Garner, B. H., Iosifidis, A., et al. (2020). Species-level image classification with convolutional neural network enables insect identification from habitus images. *Ecol. Evol.* 10, 737–747. doi: 10.1002/ece3.5921

Harrington, R., Clark, S. J., Welham, S. J., Verrier, P. J., DENHOLM, C. H., Hullé, M., et al. (2007). Environmental change and the phenology of European aphids. *Global Change Biol.* 13, 1550–1564. doi: 10.1111/j.1365-2486.2007.01394.x

Harrington, R., and Hullé, M. (2017). "16 monitoring and forecasting," in *Aphids as crop pests*. Eds. H. F. van Emden and R. Harrington (Wallingford Oxfordshire UK, Boston MA: CABI), 362–381.

Harrington, R., Stevens, M., Alderson, L. J., Cox, D., Denholm, I., Foster, S. P., et al. (2009). Complementary methods for monitoring sugar beet aphids to improve risk management of virus yellows. *Redia* 92, 215–217.

Hartman, G. L., Domier, L. L., Wax, L. M., Helm, C. G., Onstad, D. W., Shaw, J. T., et al. (2001). Occurrence and distribution of aphis glycines on soybeans in Illinois in 2000 and its potential control. *Plant Health Prog.* 2. doi: 10.1094/PHP-2001-0205-01-HN

Hayashi, M., Tamai, K., Owashi, Y., and Miura, K. (2019). Automated machine learning for identification of pest aphid species (Hemiptera: aphididae). *Appl. Entomol. Zool.* 54, 487–490. doi: 10.1007/s13355-019-00642-0

He, K., Gkioxari, G., Dollar, P., and Girshick, R. (2017). "Mask r-CNN," in *Proceedings of the IEEE international conference on computer vision*. 2961–2969.

He, K., Zhang, X., Ren, S., and Sun, J. (2016). Deep residual learning for image recognition. *IEEE Conf. Comput. Vision Pattern Recogn. (CVPR)* 770–778. doi: 10.1109/CVPR.2016.90

Heathcote, G. D. (1957). The optimum size of sticky aphid traps. *Plant Pathol.* 6, 104–107. doi: 10.1111/j.1365-3059.1957.tb00788.x

Hebert, P. D. N., Cywinska, A., Ball, S. L., and deWaard, J. R. (2003). Biological identifications through DNA barcodes. *Proc. Biol. Sci.* 270, 313–321. doi: 10.1098/rspb.2002.2218

Heinz, K., Parrella, M. P., and Newman, J. P. (1992). Time-efficient use of yellow sticky traps in monitoring insect populations. *J. Econ. Entomol.* 85, 2263–2269. doi: 10.1093/jee/85.6.2263

Holland, J. M., McHugh, N. M., and Salinari, F. (2021). Field specific monitoring of cereal yellow dwarf virus aphid vectors and factors influencing their immigration within fields. *Pest Manage. Sci.* 77, 4100–4108. doi: 10.1002/ps.6435

Hu, C., Kong, S., Wang, R., Zhang, F., and Wang, L. (2020). Insect mass estimation based on radar cross section parameters and support vector regression algorithm. *Remote Sens.* 12, 1903. doi: 10.3390/rs12111903

Hullé, M., Coeur d'Acier, A., Bankhead-Dronnet, S., and Harrington, R. (2010). Aphids in the face of global changes. *C. R. Biol.* 333, 497–503. doi: 10.1016/j.crvi.2010.03.005

Hurej, M., and van der Werf, W. (1993). The influence of black bean aphid, *Aphis fabae* scop., and its honeydew on leaf growth and dry matter production of sugar beet. *Ann. Appl. Biol.* 122, 201–214. doi: 10.1111/j.1744-7348.1993.tb04027.x

Jarošová, J., Żelazny, W. R., and Kundu, J. K. (2019). Patterns and predictions of barley yellow dwarf virus vector migrations in central Europe. *Plant Dis.* 103, 2057–2064. doi: 10.1094/PDIS-11-18-1999-RE

Kamilaris, A., and Prenafeta-Boldú, F. X. (2018). Deep learning in agriculture: a survey. *Comput. Electron. Agric.* 147, 70–90. doi: 10.1016/j.compag.2018.02.016

Karl, E. (1991). Einsatz einer saugfalle zur Überwachung der flugaktivität von getreideblattläusen (Homoptera: aphidinea: aphididae). *Entomol. Gen.* 16, 161–166. doi: 10.1127/entom.gen/16/1991/161

Kim, J., and Kwon, M. (2019). Population dynamics of aphid species in Korean seed potato cultivation area over four decades. *Entomol Res.* 49, 179–184. doi: 10.1111/1748-5967.12348

Kirchner, S. M., Hiltunen, L., Döring, T. F., Virtanen, E., Palohuhta, J. P., and Valkonen, J. P. T. (2013). Seasonal phenology and species composition of the aphid fauna in a northern crop production area. *PloS One* 8, e71030. doi: 10.1371/journal.pone.0071030

Klueken, A. M., Hau, B., Freier, B., Friesland, H., Kleinhenz, B., and Poehling, H.-M. (2009). Comparison and validation of population models for cereal aphids. *J. Plant Dis. Prot.* 116, 129–140. doi: 10.1007/BF03356299

Krüger, K., and van der Waals, J. E. (2020). Potato virus y and potato leafroll virus management under climate change in sub-Saharan Africa. *S. Afr. J. Sci.* 116. doi: 10.17159/sajs.2020/8579

Lagos-Kutz, D., Voegtlin, D. J., Onstad, D., Hogg, D., Ragsdale, D. W., Tilmon, K., et al. (2020). The soybean aphid suction trap network: sampling the aerobiological "soup". *Am. Entomol.* 66, 48–55. doi: 10.1093/ae/tmaa009

Lal, A., Vo, T. T. B., Sanjaya, I. G. N. P. W., Ho, P. T., Kim, J.-K., Kil, E.-J., et al. (2020). Nanovirus disease complexes: an emerging threat in the modern era. *Front. Plant Sci.* 11. doi: 10.3389/fpls.2020.558403

Lechenet, M., Dessaint, F., Py, G., Makowski, D., and Munier-Jolain, N. (2017). Reducing pesticide use while preserving crop productivity and profitability on arable farms. *Nat. Plants* 3, 17008. doi: 10.1038/nplants.2017.8

LeCun, Y., Bengio, Y., and Hinton, G. (2015). Deep learning. *Nature* 521, 436–444. doi: 10.1038/nature14539

Leskinen, M., Markkula, I., Koistinen, J., Pylkkö, P., Ooperi, S., Siljamo, P., et al. (2011). Pest insect immigration warning by an atmospheric dispersion model, weather radars and traps. *J. Appl. Entomol.* 135, 55–67. doi: 10.1111/j.1439-0418.2009.01480.x

Lins, E. A., Rodriguez, J. P. M., Scoloski, S. I., Pivato, J., Lima, M. B., Fernandes, J. M. C., et al. (2020). A method for counting and classifying aphids using computer vision. *Comput. Electron. Agric.* 169, 105200. doi: 10.1016/j.compag.2019.105200

Liu, M., Clarke, L. J., Baker, S. C., Jordan, G. J., and Burridge, C. P. (2020). A practical guide to DNA metabarcoding for entomological ecologists. *Ecol. Entomol.* 45, 373–385. doi: 10.1111/een.12831

Liu, C., Zhai, Z., Zhang, R., Bai, J., and Zhang, M. (2022). Field pest monitoring and forecasting system for pest control. *Front. Plant Sci.* 13, 990965. doi: 10.3389/fpls.2022.990965

Liu, H., Zhan, Y., Xia, H., Mao, Q., and Tan, Y. (2022). Self-supervised transformer-based pre-training method using latent semantic masking auto-encoder for pest and disease classification. *Comput. Electron. Agric.* 203, 107448. doi: 10.1016/j.compag.2022.107448

Llewellyn, K. S., Loxdale, H. D., Harrington, R., Brookes, C. P., Clark, S. J., and Sunnucks, P. (2003). Migration and genetic structure of the grain aphid (*Sitobion avenae*) in Britain related to climate and clonal fluctuation as revealed using microsatellites. *Mol. Ecol.* 12, 21–34. doi: 10.1046/j.1365-294X.2003.01703.x

Luquet, M., Hullé, M., Simon, J.-C., Parisey, N., Buchard, C., and Jaloux, B. (2019). Relative importance of long-term changes in climate and land-use on the phenology and abundance of legume crop specialist and generalist aphids. *Insect Sci.* 26, 881–896. doi: 10.1111/1744-7917.12585

Macaulay, E. D. M., Tatchell, G. M., and Taylor, L. R. (1988). The rothamsted insect survey '12-metre' suction trap. *Bull. Entomol. Res.* 78, 121–128. doi: 10.1017/S0007485300016126

Marques, A. C. R., Raimundo, M., M., B., Cavalheiro, E. M., Salles, L. F. P., Lyra, C., et al. (2018). Ant genera identification using an ensemble of convolutional neural networks. *PloS One* 13, e0192011. doi: 10.1371/journal.pone.0192011

Martineau, M., Conte, D., Raveaux, R., Arnault, I., Munier, D., and Venturini, G. (2017). A survey on image-based insect classification. *Pattern Recognit.* 65, 273–284. doi: 10.1016/j.patcog.2016.12.020

Milošević, D., Milosavljević, A., Predić, B., Medeiros, A. S., Savić-Zdravković, D., Stojković Piperac, M., et al. (2020). Application of deep learning in aquatic bioassessment: towards automated identification of non-biting midges. *Sci. Total Environ.* 711, 135160. doi: 10.1016/j.scitotenv.2019.135160

Moericke, V. (1951). Eine farbfalle zur kontrolle des fluges von blattläusen, insbesondere der pfirsichblattlaus, *Myzodes persicae* (Sulz). *Nachr. Dtsch. Pflanzenschutzd.* 3, 23–24.

Montgomery, G. A., Belitz, M. W., Guralnick, R. P., and Tingley, M. W. (2021). Standards and best practices for monitoring and benchmarking insects. *Front. Ecol. Evol.* 8. doi: 10.3389/fevo.2020.579193

Moore, A., Miller, J. R., Tabashnik, B. E., and Gage, S. H. (1986). Automated identification of flying insects by analysis of wingbeat frequencies. *J. Econ. Entomol.* 79, 1703–1706. doi: 10.1093/jee/79.6.1703

Motta, D., Santos, A. Á. B., Machado, B. A. S., Ribeiro-Filho, O. G. V., Camargo, L. O. A., Valdenegro-Toro, M. A., et al. (2020). Optimization of convolutional neural network hyperparameters for automatic classification of adult mosquitoes. *PloS One* 15, e0234959. doi: 10.1371/journal.pone.0234959

Müller, F. P. (1975). Bestimmungsschlüssel für geflügelte blattläuse in gelbschalen. *Arch. Phytopathol. Plant Prot.* 11, 49–77. doi: 10.1080/03235407509431157

Nanni, L., Manfe, A., Maguolo, G., Lumini, A., and Brahnam, S. (2022). High performing ensemble of convolutional neural networks for insect pest image detection. *Ecol. Inform.* 67, 101515. doi: 10.1016/j.ecoinf.2021.101515

Nauen, R., and Elbert, A. (2003). European Monitoring of resistance to insecticides in *Myzus persicae* and *Aphis gossypii* (Hemiptera: aphididae) with special reference to imidacloprid. *Bull. Entomol. Res.* 93, 47–54. doi: 10.1079/BER2002215

Nault, L. R. (1997). Arthropod transmission of plant viruses: a new synthesis. *Ann. Entom. Soc Amer.* 90, 521–541. doi: 10.1093/aesa/90.5.521

Noskov, A., Bendix, J., and Friess, N. (2021). A review of insect monitoring approaches with special reference to radar techniques. *Sensors* 21. doi: 10.3390/s21041474

O'Loughlin, G. T. (1963). Aphid trapping in Victoria. I. The seasonal occurrence of aphids in three localities and a comparision of two trapping methods. *Aust. J. Agric. Res.* 14, 61. doi: 10.1071/AR9630061

O'Shea, K., and Nash, R. (2015). An introduction to convolutional neural networks, arXiv. *arXiv* .08458. doi: 10.48550/arXiv.1511.08458

Parraga-Alava, J., Alcivar-Cevallos, R., Riascos, J. A., and Becerra, M. A. (2021). "Aphids detection on lemons leaf image using convolutional neural networks," in *Systems and information sciences: proceedings of ICCIS 2020*. Ed. M. Botto-Tobar (Cham: Springer International Publishing AG), 16–27.

Patel, D. J., and Bhatt, N. (2019). Insect identification among deep learning's meta-architectures using TensorFlow. *Int. J. Eng. Adv. Technol.* 9, 1910–1914. doi: 10.35940/ijeat.A1031.109119

Pike, K. S., Allison, D., Boydston, L., Qualset, C. O., Vogt, H. E., and Summers, C. G. (2012). Suction trap reveals 60 wheat aphid species, including Russian wheat aphid. *Calif. Agric.* 43, 22–24.

Prasad, Y. G., and Prabhakar, M. (2012). "Pest monitoring and forecasting," in *Integrated pest management: principles and practice*. Ed. D. P. Abrol (Wallingford: CABI), 41–57.

Preti, M., Verheggen, F., and Angeli, S. (2021). Insect pest monitoring with camera-equipped traps: strengths and limitations. *J. Pest Sci.* 94, 203–217. doi: 10.1007/s10340-020-01309-4

Qi, A., Dewar, A. M., and Harrington, R. (2004). Decision making in controlling virus yellows of sugar beet in the UK. *Pest Manage. Sci.* 60, 727–732. doi: 10.1002/ps.871

Ragsdale, D. W., Landis, D. A., Brodeur, J., Heimpel, G. E., and Desneux, N. (2011). Ecology and management of the soybean aphid in north America. *Annu. Rev. Entomol.* 56, 375–399. doi: 10.1146/annurev-ento-120709-144755

Ratnasingham, S., and Hebert, P. D. N. (2007). Bold: the barcode of life data system (http://www.barcodinglife.org). *Mol. Ecol. Notes* 7, 355–364. doi: 10.1111/j.1471-8286.2007.01678.x

Robert, Y., Woodford, J. A., and Ducray-Bourdin, D. G. (2000). Some epidemiological approaches to the control of aphid-borne virus diseases in seed potato crops in northern Europe. *Virus Res.* 71, 33–47. doi: 10.1016/S0168-1702(00)00186-6

Rydhmer, K., Bick, E., Still, L., Strand, A., Luciano, R., Helmreich, S., et al. (2022). Automating insect monitoring using unsupervised near-infrared sensors. *Sci. Rep.* 12, 2603. doi: 10.1038/s41598-022-06439-6

Sarker, I. H. (2021). Machine learning: algorithms, real-world applications and research directions. *SN Comput. Sci.* 2, 160. doi: 10.1007/s42979-021-00592-x

Savary, S., Willocquet, L., Pethybridge, S. J., Esker, P., McRoberts, N., and Nelson, A. (2019). The global burden of pathogens and pests on major food crops. *Nat. Ecol. Evol.* 3, 430–439. doi: 10.1038/s41559-018-0793-y

Segev, N., Harel, M., Mannor, S., Crammer, K., and El-Yaniv, R. (2017). Learn on source, refine on target: a model transfer learning framework with random forests. *IEEE Trans. Pattern Anal. Mach. Intell.* 39, 1811–1824. doi: 10.1109/TPAMI.2016.2618118

Seibold, S., Gossner, M. M., Simons, N. K., Blüthgen, N., Müller, J., Ambarlı, D., et al. (2019). Arthropod decline in grasslands and forests is associated with landscape-level drivers. *Nature* 574, 671–674. doi: 10.1038/s41586-019-1684-3

Selvaraju, R. R., Cogswell, M., Das, A., Vedantam, R., Parikh, D., and Batra, D. (2020). Grad-CAM: visual explanations from deep networks *via* gradient-based localization. *Int. J. Comput. Vis.* 128, 336–359. doi: 10.1007/s11263-019-01228-7

Sheppard, L. W., Bell, J. R., Harrington, R., and Reuman, D. C. (2016). Changes in large-scale climate alter spatial synchrony of aphid pests. *Nat. Clim. Change* 6, 610–613. doi: 10.1038/nclimate2881

Shortall, C. R., Moore, A., Smith, E., Hall, M. J., Woiwod, I. P., and Harrington, R. (2009). Long-term changes in the abundance of flying insects. *Insect Conserv. Divers.* 2, 251–260. doi: 10.1111/j.1752-4598.2009.00062.x

Simonyan, K., and Zisserman, A. (2015). Very deep convolutional networks for Large-scale image recognition. *arXiv [Preprint]*, 1409.1556v6. doi: 10.48550/arXiv.1409.1556

Starý, P., and Lukášová, H. (2000). Suction air traps vs. crops in monitoring Russian wheat aphid, *Diuraphis noxia* (Kurdj.) in central Europe (Hom., aphididae). *Anz. Schadlingskd.* 73, 49–54. doi: 10.1046/j.1439-0280.2000.00049.x

Steinger, T., Goy, G., Gilliand, H., Hebeisen, T., and Derron, J. (2015). Forecasting virus disease in seed potatoes using flight activity data of aphid vectors. *Ann. Appl. Biol.* 166, 410–419. doi: 10.1111/aab.12190

Stevens, M., and Lacomme, C. (2017). "15 transmission of plant viruses," in *Aphids as crop pests*. Eds. H. F. van Emden and R. Harrington (Wallingford Oxfordshire UK, Boston MA: CABI), 323–361.

Szegedy, C., Vanhoucke, V., Ioffe, S., Shlens, J., and Wojna, Z. (2015). "Rethinking the inception architecture for computer vision," in *2016 IEEE Conference on Computer Vision and Pattern Recognition (CVPR)*. 2818–2826.

Tan, C., Sun, F., Kong, T., Zhang, W., Yang, C., and Liu, C. (2018). "A survey on deep transfer learning," in *International Conference on Artificial Neural Networks (ICANN) 2018*. (Springer International Publishing). 270–279. doi: 10.1007/978-3-030-01424-7_27

Tatchell, G. M. (1989). An estimate of the potential economic losses to some crops due to aphids in Britain. *Crop Prot.* 8, 25–29. doi: 10.1016/0261-2194(89)90095-1

Taylor, L. R., and Robert, Y. (1984). *A handbook for aphid identification* (Harpenden, Hertfordshire, England: Rothamsted Experimental Station).

Teulon, D., and Scott, I. (2006). The use of suction traps for detection of unwanted invasive insects and other invertebrates. *N. Z. Plant Prot.* 59, 125–131. doi: 10.30843/nzpp.2006.59.4446

Thieme, T. (1989). Zur biologie und morphologie von *Aphis armata* hausmann 1802 (Horn., aphididae). *J. Appl. Entomol.* 107, 113–117. doi: 10.1111/j.1439-0418.1989.tb00237.x

Tilman, D., Reich, P. B., and Knops, J. M. H. (2006). Biodiversity and ecosystem stability in a decade-long grassland experiment. *Nature* 441, 629–632. doi: 10.1038/nature04742

Valan, M., Makonyi, K., Maki, A., Vondráček, D., and Ronquist, F. (2019). Automated taxonomic identification of insects with expert-level accuracy using effective feature transfer from convolutional networks. *Syst. Biol.* 68, 876–895. doi: 10.1093/sysbio/syz014

Verheggen, F., Barrès, B., Bonafos, R., Desneux, N., Escobar-Gutiérrez, A. J., Gachet, E., et al. (2022). Producing sugar beets without neonicotinoids: an evaluation of alternatives for the management of viruses-transmitting aphids. *Entomol. Gen.* 42, 491–498. doi: 10.1127/entomologia/2022/1511

Voss, T. S., Kieckhefer, R. W., Fuller, B. W., McLeod, M. J., and Beck, D. A. (1997). Yield losses in maturing spring wheat caused by cereal aphids (Homoptera: aphididae) under laboratory conditions. *J. Econ. Entomol.* 90, 1346–1350. doi: 10.1093/jee/90.5.1346

Vučetić, A., Vukov, T., Jovičić, I., and Petrović-Obradović, O. (2013). Monitoring of aphid flight activities in seed potato crops in Serbia. *Zookeys* 319, 333–346. doi: 10.3897/zookeys.319.4315

Wäldchen, J., and Mäder, P. (2018). Machine learning for image based species identification. *Methods Ecol. Evol.* 9, 2216–2225. doi: 10.1111/2041-210X.13075

Wang, M., and Deng, D. (2018). Deep visual domain adaptation: a survey. *Neurocomputing* 312, 135–153. doi: 10.1016/j.neucom.2018.05.083

Wang, R., Hu, C., Fu, X., Long, T., and Zeng, T. (2017). Micro-Doppler measurement of insect wing-beat frequencies with W-band coherent radar. *Sci. Rep.* 7, 1396. doi: 10.1038/s41598-017-01616-4

Wei, X.-S., Luo, J.-H., Wu, J., and Zhou, Z.-H. (2017). Selective convolutional descriptor aggregation for fine-grained image retrieval. *IEEE Trans. Image Process.* 26, 2868–2881. doi: 10.1109/TIP.2017.2688133

Wilf, P., Zhang, S., Chikkerur, S., Little, S. A., Wing, S. L., and Serre, T. (2016). Computer vision cracks the leaf code. *Proc. Natl. Acad. Sci. U.S.A.* 113, 3305–3310. doi: 10.1073/pnas.1524473113

Xia, D., Chen, P., Wang, B., Zhang, J., and Xie, C. (2018). Insect detection and classification based on an improved convolutional neural network. *Sensors* 18, 4169. doi: 10.3390/s18124169

Xia, W., Han, D., Li, D., Wu, Z., Han, B., and Wang, J. (2022). An ensemble learning integration of multiple CNN with improved vision transformer models for pest classification. *Ann. Appl. Biol.* 182, 144–158. doi: 10.1111/aab.12804

Xuesong, S., Zi, L., Lei, S., Jiao, W., and Yang, Z. (2017). Aphid identification and counting based on smartphone and machine vision. *J. Sens.* 2017, 1–7. doi: 10.1155/2017/3964376

Zamoum, T., Simon, J.-C., Crochard, D., Ballanger, Y., Lapchin, L., Vanlerberghe-Masutti, F., et al. (2005). Does insecticide resistance alone account for the low genetic variability of asexually reproducing populations of the peach-potato aphid *Myzus persicae*? *Heredity* 94, 630–639. doi: 10.1038/sj.hdy.6800673

Zeng, J., Liu, Y., Zhang, H., Liu, J., Jiang, Y., Wyckhuys, K. A. G., et al. (2020). Global warming modifies long-distance migration of an agricultural insect pest. *J. Pest Sci.* 93, 569–581. doi: 10.1007/s10340-019-01187-5

Zhang, Q., and Zhu, S.-C. (2018). Visual interpretability for deep learning: a survey. *Front. Inf. Technol. Electron. Eng.* 19, 27–39. doi: 10.1631/FITEE.1700808

Zhong, Y., Gao, J., Lei, Q., and Zhou, Y. (2018). A vision-based counting and recognition system for flying insects in intelligent agriculture. *Sensors* 18, 1489. doi: 10.3390/s18051489

Zhuang, F., Qi, Z., Duan, K., Xi, D., Zhu, Y., Zhu, H., et al. (2021). A comprehensive survey on transfer learning. *Proc. IEEE* 109, 43–76. doi: 10.1109/JPROC.2020.3004555

Ziesche, T. M., Bell, J. R., Ordon, F., Schliephake, E., and Will, T. (2020). Long-term monitoring of insects in agricultural landscapes. *Mitt. Dtsch. Ges. Allg. Angew. Entomol.* 22, 101–106.

Frontiers in
Plant Science

Cultivates the science of plant biology and its applications

The most cited plant science journal, which advances our understanding of plant biology for sustainable food security, functional ecosystems and human health.

Discover the latest Research Topics

See more →

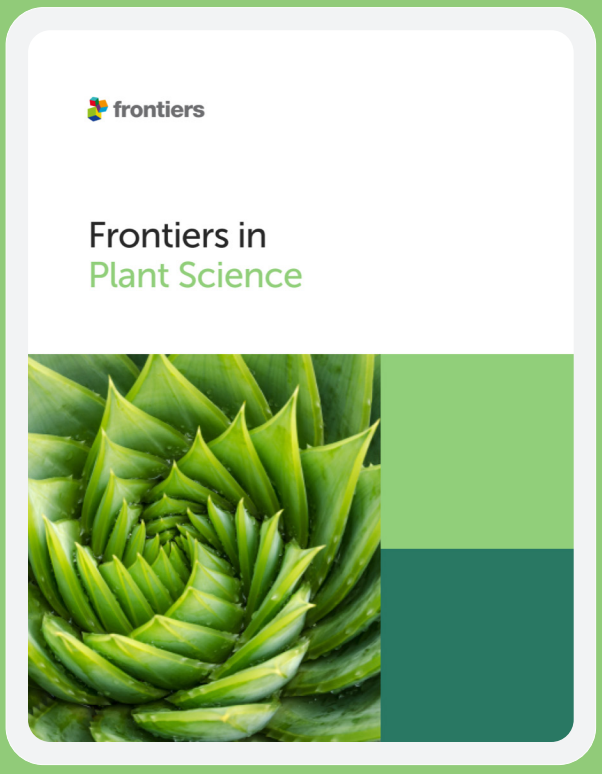

Frontiers

Avenue du Tribunal-Fédéral 34
1005 Lausanne, Switzerland
frontiersin.org

Contact us

+41 (0)21 510 17 00
frontiersin.org/about/contact